INTERNATIONAL DOCTORAL
SCHOOL OF THE USC

José Manuel
Otero Mato

PhD Thesis

Theoretical and computational study of nanostructures dispersion on ionic liquids and its mixtures

Santiago de Compostela, 2022

Doctoral Programme in Materials Science

USC
UNIVERSIDADE
DE SANTIAGO
DE COMPOSTELA

TESIS DE DOCTORADO

THEORETICAL AND COMPUTATIONAL STUDY OF NANOSTRUCTURES DISPERSION ON IONIC LIQUIDS AND ITS MIXTURES.

José Manuel Otero Mato

ESCUELA DE DOCTORADO INTERNACIONAL DE LA UNIVERSIDAD DE SANTIAGO DE COMPOSTELA

PROGRAMA DE DOCTORADO EN CIENCIA DE MATERIALES

SANTIAGO DE COMPOSTELA

2022

USC
UNIVERSIDADE
DE SANTIAGO
DE COMPOSTELA

DECLARACIÓN DEL AUTOR/A DE LA TESIS

D./Dña. **José Manuel Otero Mato**

Título de la tesis: **Theoretical and computational study of nanostructures dispersion on ionic liquids and its mixtures.**

Presento mi tesis, siguiendo el procedimiento adecuado al Reglamento y declaro que:

1) La tesis abarca los resultados de la elaboración de mi trabajo.
2) De ser el caso, en la tesis se hace referencia a las colaboraciones que tuvo este trabajo.
3) Confirmo que la tesis no incurre en ningún tipo de plagio de otros autores ni de trabajos presentados por mí para la obtención de otros títulos.
4) La tesis es la versión definitiva presentada para su defensa y coincide la versión impresa con la presentada en formato electrónico.

Y me comprometo a presentar el Compromiso Documental de Supervisión en el caso que el original no esté depositado en la Escuela.

En **Santiago de Compostela**, **1 de julio de 2022**.

Firma electrónica

USC
UNIVERSIDADE
DE SANTIAGO
DE COMPOSTELA

AUTORIZACIÓN DEL DIRECTOR / TUTOR DE LA TESIS

Theoretical and computational study of nanostructures dispersion on ionic liquids and its mixtures.

D. Luis Miguel Varela Cabo, catedrático del área de Física da Materia Condensada, del Departamento de Física de Partículas de la Universidade de Santiago de Compostela,

INFORMA:

Que la presente tesis, se corresponde con el trabajo realizado por D. José Manuel Otero Mato, bajo mi dirección/tutorización, y autorizo su presentación, considerando que reúne los requisitos exigidos en el Reglamento de Estudios de Doctorado de la USC, y que como director de esta no incurre en las causas de abstención establecidas en la Ley 40/2015.

De acuerdo con lo indicado en el Reglamento de Estudios de Doctorado, declara también que la presente tesis doctoral es idónea para ser defendida en base a la modalidad de COMPENDIO DE PUBLICACIONES, en los que la participación del doctorando/a fue decisiva para su elaboración y las publicaciones se ajustan al Plan de Investigación.

En Santiago de Compostela, 1 de julio de 2022

USC
UNIVERSIDADE
DE SANTIAGO
DE COMPOSTELA

Resumo

Esta tese propón como obxectivo presentar un estudo exhaustivo das propiedades dos líquidos iónicos (LIs) e as súas mesturas con outros disolventes en presenza de solutos con diferentes tamaños e propiedades. Os LIs son materiais formados unicamente por anións e catións que, polas súas xeometrías, conseguen ter unha temperatura de fusión baixa (menos de 100 °C é o máis aceptado pola comunidade). Noutras palabras, estariamos a falar de sales fundidos a temperatura ambiente. Debido xustamente á constitución puramente iónica, os LIs presentan unha serie de propiedades moi interesantes que non se atopan noutros líquidos, como poden ser: baixa volatilidade, ampla ventá electroquímica, altas condutividades, alta viscosidade, alta estabilidade térmica e boas capacidades de solvatación, entre outras. Esta serie de propiedades impulsou a aplicación destes compostos iónicos nun amplo abanico de campos, como por exemplo: lubricantes, disolventes para case calquera composto, medios catalizadores, en supercondensadores, baterías, industria nuclear ou en procesos de extracción e separación. Ademais, están considerados como disolventes de deseño, xa que escollendo coidadosamente os anións e catións que conforman un LI podemos axustar as súas propiedades para un determinado propósito. Isto fai que exista unha cantidade enorme de potenciais LIs. E non só iso, senón que mesturando distintos LIs tamén podemos axustar estas propiedades, incrementando aínda máis as opcións.

Unha das principais razóns pola que os LIs posúen temperaturas de fusión tan baixas é a asimetría que existe entre os anións e catións que os constitúen. Xeralmente, os anións posúen formas moleculares simples e con certas simetrías, mentres que os catións, están formados maioritariamente por moléculas máis grandes cunha zona onde se concentra a carga e outra na que predominan grupos moleculares orgánicos. Aínda que esta é a tendencia xeral dos LIs máis empregados, estes papeis pódense intercambiar. Esta estrutura molecular dos constituíntes dos LIs axuda a entender o por que das súas boas propiedades de solvatación.

USC
UNIVERSIDADE DE SANTIAGO DE COMPOSTELA

Como se sabe, xeralmente *similia similibus solvuntur*. No caso dos LIs temos un disolvente que presenta tanto unha parte polar (centrada normalmente nos centros de carga dos ións) e unha orgánica. Por iso, ao levar a cabo unha disolución nestes compostos, os ións dispoñeranse de forma que orienten a súa parte polar ou orgánica cara ao soluto en función da natureza deste. Se consideramos solutos cargados habemos de esperar que os constituíntes dos LIs con carga oposta se distribúan ao redor para apantallar a carga creando así complexos de coordinación e unha serie de capas de solvatación onde a carga destas iríase alternando. Este escenario sería o equivalente á disolución de sales en LIs. Por poñer un exemplo, poderiamos considerar unha disolución dun sal de litio cuxo anión sexa o mesmo que o do LI que usemos para a disolución. Este tipo de sistemas son de gran interese con vistas á súa aplicación en dispositivos electroquímicos como poden ser baterías. Coñecer como os LIs solvatan estes sales implica coñecer os mecanismos de difusión dentro do fluído e por tanto como se transporta a carga nestes sistemas. Todos estes detalles sobre diferentes aspectos dos LIs serán obxecto de discusión na parte introdutoria desta tese.

Doutra banda, consideraremos o efecto do aumento do tamaño de dito soluto. Ata tal punto que, en boa aproximación, podemos estudar as proximidades do soluto como unha superficie plana en contacto cun LI. Nesta situación, do mesmo xeito que tiñamos oscilacións de carga nas proximidades dos solutos esféricos, aquí terá lugar un fenómeno similar pero agora coa xeometría plana inducida pola interfase. En función da densidade de carga da superficie, a súa composición e xeometría, o LI dispoñerase dunha forma ou outra. Esta aproximación non só é interesante para entender a solvatación de partículas moi grandes nestes fluídos, senón que ademais, novamente, comprender ben este escenario é moi importante para unha boa descrición do que ocorre nunha batería ou un supercondensador, onde teremos unha interfase cargada en presenza dun electrolito LI. Folga dicir que vivimos tempos nos que estes dispositivos electroquímicos están cada vez máis presentes no noso día a día e un bo coñecemento dos fundamentos do seu funcionamento é crucial para poder seguir innovando e progresando no campo. Finalmente,

USC
UNIVERSIDADE DE SANTIAGO DE COMPOSTELA

o escenario onde temos nanoestructuras de tamaños intermedios dispersas en LIs é tamén de gran interese para a súa aplicación, por exemplo, en dispositivos fotónicos con dispersións de nanopartículas metálicas onde a presenza do LI modifique a resposta dos plasmones de superficie; en dispersións de nanoestructuras para catalizar reaccións ou en presenza de nanoestructuras porosas para dar soporte mecánico mentres se preservan as propiedades dos LIs.

Na presente tese lévase a cabo o estudo dos sistemas mencionados mediante simulacións moleculares. Isto vainos a permitir acceder a información sobre a estrutura e dinámica destes sistemas, con resolución atómica que, en ocasións, será complementada con resultados experimentais. Entre as principais técnicas de simulación empregadas cabe destacar as simulacións de dinámica molecular (DM) e os cálculos de teoría do funcional densidade (DFT). Coa primeira obtemos información da traxectoria dun conxunto de átomos dentro dunha caixa de simulación nunhas condicións que nos poidan interesar (presión, temperatura, presenza de interfases...). Esta traxectoria obtense integrando as ecuacións clásicas do movemento de cada átomo calculando as interaccións entre eles cun campo de forzas. Na maior parte das simulacións levadas a cabo nesta tese o campo de forzas utilizado é un coñecido como OPLS-AA o cal está optimizado para a simulación de líquidos. Usouse a suite de simulación GROMACS para levar a cabo estas simulacións. Doutra banda, os cálculos DFT permítennos obter a densidade electrónica correspondente ao estado de mínima enerxía dun sistema mediante a resolución das ecuacións de Kohn–Sham. Isto resulta moi conveniente á hora de calcular as cargas parciais de cada átomo (que son utilizadas polos campos de forzas usados en DM) ou as configuracións de equilibrio de sistemas de interese. Ademais de para isto, usáronse cálculos DFT nesta tese para o estudo da transferencia protónica entre especies iónicas. O software usado para estes cálculos foi o programa Gaussian 16 co funcional de intercambio e correlación B3LYP. Os detalles en relación ás ferramentas usadas para o desenvolvemento desta tese serán introducidas en detalle no Capítulo 2.

Unha das primeiras cuestións que se propuxo na presente tese foi

USC
UNIVERSIDADE DE SANTIAGO DE COMPOSTELA

que, aínda que se comezase o estudo das dispersións de nanoestructuras en LIs caracterizando a solvatación de solutos pequenos ou LIs en presenza de interfases planas, nalgún momento afrontaríase o labor de levar a cabo simulacións con nanoestructuras con tamaños da orde das decenas de nanómetros. Realizar simulacións de DM con caixas de simulación o suficientemente grandes como para conter as devanditas estruturas cos campos de forzas convencionais, é unha tarefa moi custosa que require grandes tempos de cálculo, mesmo nos maiores supercomputadores. Para reducir estes tempos de cómputo, unha solución é utilizar o que se coñecen como campos de forza "coarse grained" (CG). Estes, en lugar de describir as moléculas como o conxunto real dos seus átomos constituíntes, traballan cunha serie de esferas conectadas que, *grosso modo*, representan a morfoloxía da molécula que se quere simular. Isto permite reducir considerablemente o número de interaccións que hai que calcular durante a simulación e por tanto, reduce considerablemente os tempos. O problema das simulacións con estes campos de forzas é que se perden os detalles a nivel atómico, o cal escurece o obxectivo de describir a física ao redor destas nanoestructuras. A estratexia ideal é levar a cabo simulacións longas cun campo de forzas CG para obter a configuración de equilibrio dun determinado sistema e despois substituír as moléculas CG polos seus equivalentes en resolución atómica. Feita esta transformación, poderíase estender a simulación partindo dunha configuración moi próxima ao equilibrio termodinámico e, en pouco tempo, obter unha imaxe detallada con resolución atómica dos sistemas. En vistas a ter unha ferramenta que permitise de maneira automática intercambiar entre distintos campos de forza independentemente do tipo de molécula que se estivese utilizando, desenvolveuse e implementou o algoritmo Gaddle Maps. No Capítulo 4 desta tese introdúcese esta ferramenta así como algúns sistemas de exemplo onde o seu uso resulta de gran utilidade.

Centrando o foco na investigación das propiedades de solvatación dos LIs, no Capítulo 5 preséntase un estudo onde se caracteriza mediante simulacións de DM a estrutura e dinámica dunha partícula modelo esférica no seo dun LI con auga. Este traballo naceu como a continua-

USC
UNIVERSIDADE DE SANTIAGO DE COMPOSTELA

ción dun previo levado a cabo por colegas da universidade de Stuttgart onde estudaban o mesmo sistema pero en ausencia de auga. Sempre que se levan a cabo investigacións con LIs, é moi importante ter claro como pode afectar a presenza dun disolvente molecular ás súas propiedades, máis concretamente, a auga. Sábese que pequenas cantidades de disolvente no seo dun LI (o que se coñece como límite "water in salt") inducen grandes cambios na dinámica do fluído o que se pode reflectir nun aumento importante da condutividade ou unha diminución da viscosidade. Ademais, unha gran parte dos LIs son higroscópicos, o que fai que, salvo que se sexa extremadamente coidadoso na súa manipulación, sempre se atopen restos de auga no seu interior. Neste traballo utilizouse o acetato de 1-etil-3-metilimidazolio ([EMIM][ACE]) como LI e unha fracción molar de auga igual ao 5 % que pretende simular a mencionada auga residual. A partícula modelo ao redor da cal se estuda a estrutura e dinámica, consiste nunha esfera de van der Waals de 3.4 Å de radio efectivo e que pretende ser un modelo CG dun soluto xenérico. Ademais, para ter unha imaxe da solvatación de distintos tipos de soluto, estúdanse os casos onde a partícula ten carga positiva, negativa ou neutra. As conclusións principais deste traballo son que a presenza de auga non cambia significativamente a estrutura das capas de solvatación ao redor dos solutos, pero si se observa unha adsorción preferente de moléculas de auga na primeira e segunda capas ao redor das esferas negativa e positiva respectivamente. Tamén se atopa unha correlación forte entre a orientación destas moléculas de auga e o campo eléctrico nas proximidades dos solutos, vendo como se aliña o momento dipolar da auga con este. Finalmente, vese como, aínda que a presenza de auga non altere significativamente a contorna dos solutos así como a presenza dos solutos non altera a dinámica da auga, a mobilidade das esferas increméntase en máis dunha orde de magnitude. Isto reflicte que, aínda tratándose de cantidades de auga consideradas a miúdo como "residuais", as propiedades dinámicas do LI poden cambiar drasticamente.

Seguindo con esta liña, analizamos que ocorre cando cambiamos o tamaño e a carga desta partícula solvatada mediante unha caracterización de disolucións de diferentes sales alcalinas e alcalinotérreas nun

USC
UNIVERSIDADE DE SANTIAGO DE COMPOSTELA

LI prótico como é o nitrato de etilamonio (EAN). Este traballo, o cal se detallará no Capítulo 6, combina técnicas teórico-computacionales con medidas experimentais. Nunha primeira parte deste estudo móstranse as medidas experimentais das entalpías de solvatación dos distintos sales, atopando unha correlación moi importante entre estes valores e as densidades iónicas dos sales na súa fase cristalina. Doutra banda, estes valores da entalpía de solvatación dos distintos catións en EAN son moi similares aos que presentan para disolucións con auga, poñendo de manifesto as similitudes entre ambos os fluídos como medios disolventes. Unha comparativa entre os resultados experimentais e os calculados a partir de simulacións de DM suxire que as simulacións son o suficientemente precisas como para servir de soporte para dar explicación á física detrás destes procesos. Ademais, mediante as simulacións, podemos acceder ao estudo da solvatación de certos sales pouco solubles que non son accesibles experimentalmente debido ás limitacións dos distintos instrumentos de medida. A partir dos resultados destas simulacións preséntase unha caracterización detallada da estrutura ao redor dos diferentes catións. Ademais, atópase unha correlación moi forte entre as propiedades de cada sistema e o campo eléctrico presente na superficie de cada catión, o cal está determinado polo seu tamaño e carga. A partir desta correlación conseguimos desenvolver unha ferramenta que permite interpolar as diferentes magnitudes para distintos solutos en función destes parámetros. En resumo, as conclusións principais deste traballo son, por unha banda, que as propiedades de solvatación destes sistemas están principalmente gobernadas polas interaccións electrostáticas, xogando as interaccións de van der Waals un papel moi secundario, e doutra banda, que as capas de solvatación ao redor dos catións son moi similares en EAN e en auga.

Como último traballo nesta tese tratando partículas con simetría esférica, no Capítulo 7, preséntanse os resultados froito da colaboración con colegas experimentais onde se estuda a estrutura e o transporte de carga nun novo sal hidratado obtido a partir dunha reacción ácido-base que involucra ao ácido 12-tungstenofosfórico e ao imidazol. Este tipo de materiais, que presentan unha condutividade protónica importante

USC
UNIVERSIDADE DE SANTIAGO DE COMPOSTELA

mesmo a temperatura ambiente, son clave para o desenvolvemento de novas membranas para mellorar de rendemento de distintos dispositivos electroquímicos, como por exemplo celas de combustible. O principal obxectivo deste traballo era ver como cambiando a concentración de moléculas de auga no sistema pódese pasar dunha condutividade protónica típica de sistemas acuosos a unha máis característica de sistemas baseados en LIs (coas vantaxes xa mencionadas dunha boa estabilidade térmica e electroquímica). O obxectivo do doutorando neste traballo foi o de ofrecer unha visión microscópica detallada que completase os experimentos levados a cabo. Para iso usáronse todos os coñecementos e ferramentas desenvolvidas nos traballos previamente mencionados, xa que o sistema en cuestión, desde o punto de vista computacional, pódese tratar como un LI en presenza de auga onde os anións están constituídos por partículas con simetría esférica cun radio ao redor dos 5.2 Å. Vemos como este traballo xa supón o estudo de estruturas con tamaños máis grandes. Por unha banda, mediante simulacións de DM obtívose información estrutural destes sistemas vendo como esta cambiaba coa cantidade de auga. Observouse que existen 4 puntos de adsorción preferente para a auga ao redor de cada anión así como a súa orientación máis probable, onde un dos hidróxenos oriéntase cara ao centro de devandito anión. Ademais, a distribución das diferentes orientacións dos catións imidazolio ao redor dos anións, a cal mostra dúas poboacións (unha correspondente aos catións orientados co anel paralelo á superficie do anión e outra perpendicular), coincide perfectamente coas observacións experimentais. Doutra banda, leváronse a cabo cálculos DFT para esclarecer cal é a ruta de transferencia protónica óptima nestes sistemas. Os resultados destes cálculos suxiren que os protóns se moven a través dos catións imidazolio e a auga e que a presenza dos anións, que condiciona a orientación de ambas as especies, diminúe a barreira enerxética da transferencia por este camiño.

Paralelamente á liña de investigación relativa a partículas esféricas, leváronse a cabo traballos onde se estuda o límite de partículas moi grandes, é dicir, como se comporta o LI e as súas mesturas nas proximidades de interfases planas. No primeiro traballo dentro desta liña que

USC
UNIVERSIDADE DE SANTIAGO DE COMPOSTELA

se presenta nesta tese (Capítulo 8) estúdase a estrutura tridimensional da dobre capa eléctrica. Esta dobre capa non é máis que unha organización inhomoxénea dos anións e catións dun LI ou unha disolución electrolítica ao redor dunha superficie que se caracteriza por presentar oscilacións amortecidas de carga. Por poñer un exemplo simple, supoñamos que temos unha interfase cunha densidade de carga positiva en presenza dun LI. Os anións do LI tenderán a acumularse na interfase para apantallar a carga desta. Isto fará que unha segunda capa de catións se acumúle a continuación para apantallar a carga de exceso xerada pola primeira capa de anións e así sucesivamente ata entrar nunha rexión en ausencia de campo eléctrico. Esta fenomenoloxía xa estaba estudada con anterioridade na literatura. A novidade do traballo aquí presente é a imaxe detallada non só da estrutura da dobre capa eléctrica na dirección perpendicular á interfase, senón que ademais, como os anións e catións se distribúen no plano paralelo á devandita interfase. Neste estudo lévanse a cabo simulacións de DM con tetrafluoroborato de 1-butil-3-metilimidazolio ([BMIM][BF_4]) tanto puro como mesturado con disolventes moleculares como auga, metanol e etanol confinados entre dúas paredes de grafeno con densidades de carga opostas ($\pm 1 e/nm^2$). Nunha primeira parte deste traballo faise unha análise exhaustiva da estrutura axial dos compoñentes dos sistemas nas proximidades de ambas as interfases vendo como a presenza dos disolventes moleculares afectan ás primeiras capas. Do mesmo xeito que se fixo para as simulacións con esferas modelo, atopouse unha correlación entre a orientación das moléculas de disolvente e o campo eléctrico nas súas proximidades. Nunha segunda parte do traballo analízase e caracterízase a distribución da adsorción nas interfases de todas as especies, verificando que a adición dos distintos disolventes inducía cambios nesta. Ademais, comprobouse que este patrón de adsorción non se restrinxe só á primeira capa nas proximidades da interfase, senón que se propaga cara ao seo do fluído a medida que se vai difuminando. Vese tamén que o patrón formado non está determinado pola morfoloxía da interfase, senón que vén dado principalmente pola densidade de carga da capa adsorbida podendo esta ser modificada cambiando a carga das interfases ou engadindo disolventes.

USC
UNIVERSIDADE DE SANTIAGO DE COMPOSTELA

Continuando coa investigación de LIs en presenza de interfases planas, no Capítulo 9 preséntase un traballo no que nos centramos no efecto do nanoconfinamento na estrutura axial de LIs deixando de lado a estrutura lateral estudada previamente. Concretamente, o obxectivo principal é analizar a aparición de capas iónicas a medida que a distancia entre paredes planas se increménta, así como o rango de alcance destas nas propiedades estruturais do líquido. Para iso, leváronse a cabo simulacións de DM empregando EAN como LI confinado entre dúas interfases planas implícitas, é dicir, obxectos matemáticos que emulan a interacción do LI cunha parede de grafeno pero sen presenza física da devandita parede. Os resultados mostran como aparece unha correlación moi interesante entre as propiedades dinámicas e as estruturais coa separación entre paredes. Con todas as simulacións levadas a cabo para varias separacións, conseguimos expresar as propiedades dun novo sistema cunha distancia entre paredes moi grande como a superposición dun sistema nanoconfinado cun determinado tamaño de fenda máis un sistema en ausencia de paredes. Para o LI estudado, o tamaño óptimo necesario para describir este sistema máis grande resultou ser de 2.7 nm, indicando que o efecto das interfases se propaga dentro do líquido uns 1.35 nm. O formalismo teórico aplicado aquí é extrapolable a outros sistemas e permite ter unha estimación do efecto das interfases en sistemas nanoconfinados. Por tanto, isto pode ser de gran utilidade á hora de desenvolver dispositivos baseados en materiais nanoporosos ou nanoestructuras con cavidades de certos tamaños.

Nestes estudos relativos á caracterización de nanoestructuras nos límites de pequenos e grandes tamaños, o foco estaba posto nas propiedades estruturais do medio e, en especial, en como as diferentes especies moleculares se reordean ao redor destas estruturas. Noutras palabras, as propiedades dinámicas deixáronse un pouco de lado. Isto principalmente é debido á falta de datos experimentais cos que validar os resultados das simulacións, os cales poden desviarse significativamente da realidade ao non estar a usar campos de forzas optimizados para o estudo destas propiedades dinámicas. Con todo, para ter unha visión completa do comportamento destes medios iónicos densos como soporte para dis-

USC
UNIVERSIDADE DE SANTIAGO DE COMPOSTELA

tintas estruturas, é crucial comprender de maneira fundamental as súas propiedades de transporte. Para encher esta falta de coñecemento, levouse a cabo un traballo onde se estudaban mesturas binarias de LIs con etanol mediante simulacións de DM. Ademais, para o estudo da condutividade iónica, comparáronse os datos extraídos das simulacións con medidas experimentais dos mesmos sistemas. O obxectivo principal deste traballo (o cal se presentará en detalle no Capítulo 10) é a comprobación da solidez dun formalismo teórico previamente desenvolto no grupo de investigación. Este formalismo, trata de describir os fenómenos de transporte en sistemas iónicos como saltos das especies cargadas entre celas de distinta mobilidade dentro do seo do fluído. Por unha banda, unha comparativa con traballos previamente publicados para sistemas similares con auga, mostra diferenzas significativas na forma de solvatación do cosolvente molecular, o que se traduce nunha diminución da mobilidade iónica cando a auga é substituída por un alcol. Con todo, a achega máis importante do traballo é a demostración da capacidade do modelo teórico para describir a dependencia das condutividades destes sistemas a medida que cambia a concentración de cosolvente. Non só iso, senón que ademais, mostramos que as frecuencias dos saltos antes mencionados calculados cos parámetros dos axustes á conductividade (magnitude macroscópica) coinciden coas calculadas directamente das simulacións (parámetros microscópicos), poñendo de manifesto a solidez dos cimentos sobre os que se constrúe a teoría. Esta validación desta teoría facilita enormemente a elección de compostos e concentracións para unha determinada aplicación ao reducir considerablemente o número necesario de experimentos ou simulacións. Ademais, coñecer as propiedades dinámicas do medio implica coñecer en gran medida as propiedades dinámicas de dispersións de nanoestructuras. O seguinte paso para avanzar na liña marcada por esta tese sería a do estudo completo da solvatación e transporte de nanoestructuras con tamaños da orde das decenas de nanómetros. Isto será o obxectivo principal de futuras investigacións xa fora do marco da presente tese por falta de tempo.

No Capítulo 11 enuméranse as principais conclusións e as futuras liñas de traballo derivadas deste traballo. Preséntase tamén unha listaxe

USC
UNIVERSIDADE DE SANTIAGO DE COMPOSTELA

de publicacións relacionadas pero non contidas nesta tese.

USC
UNIVERSIDADE DE SANTIAGO DE COMPOSTELA

USC
UNIVERSIDADE
DE SANTIAGO
DE COMPOSTELA

Resumen

Esta tesis plantea como objetivo presentar un estudio exhaustivo de las propiedades de los líquidos iónicos (LIs) y sus mezclas con otros disolventes en presencia de solutos con diferentes tamaños y propiedades. Los LIs son materiales formados únicamente por aniones y cationes que, por sus geometrías, consiguen tener una temperatura de fusión baja (menos de 100 °C es lo más aceptado por la comunidad). En otras palabras, estaríamos hablando de sales fundidas a temperatura ambiente. Debido justamente a la constitución puramente iónica, los LIs presentan una serie de propiedades muy interesantes que no se encuentran en otros líquidos, como pueden ser: baja volatilidad, amplia ventana electroquímica, alta conductividad, alta viscosidad, alta estabilidad térmica y buenas capacidades de solvatación, entre otras. Esta serie de propiedades ha impulsado la aplicación de estos compuestos iónicos en un amplio abanico de campos, como por ejemplo: lubricantes, disolventes para casi cualquier compuesto, medios catalizadores, en supercondensadores, baterías, industria nuclear o en procesos de extracción y separación. Además, están considerados como disolventes de diseño, ya que escogiendo cuidadosamente los aniones y cationes que conforman un LI podemos ajustar sus propiedades para un determinado propósito. Esto hace que exista una cantidad enorme de potenciales LIs. Y no solo eso, sino que mezclando distintos LIs también podemos ajustar estas propiedades, incrementando aún más las opciones.

Una de las principales razones por la que los LIs poseen temperaturas de fusión tan bajas es la asimetría que existe entre los aniones y cationes que los constituyen. Generalmente, los aniones poseen formas moleculares simples incluso con ciertas simetrías, mientras que los cationes, están formados mayoritariamente por moléculas más grandes con una zona donde se concentra la carga y otra en la que predominan grupos moleculares orgánicos. Aunque esta es la tendencia general de los LIs más empleados, estos papeles se pueden intercambiar. Esta estructura molecular de los constituyentes de los LIs ayuda a entender el

USC
UNIVERSIDADE DE SANTIAGO DE COMPOSTELA

por qué de sus buenas propiedades de solvatación. Como se sabe, generalmente *similia similibus solvuntur*. En el caso de los LIs tenemos un disolvente que presenta tanto una parte polar (centrada normalmente en los centros de carga de los iones) y una orgánica. Por ello, al llevar a cabo una disolución en estos compuestos, los iones se dispondrán de forma que orienten su parte polar u orgánica hacia el soluto en función de la naturaleza de este. Si consideramos solutos cargados hemos de esperar que los constituyentes de los LIs con carga opuesta se distribuyan alrededor para apantallar la carga creando así complejos de coordinación y una serie de capas de solvatación donde la carga de estas se iría alternando. Este escenario sería el equivalente a la disolución de sales en LIs. Por poner un ejemplo, podríamos considerar una disolución de una sal de litio cuyo anión sea el mismo que el del LI que usemos para la disolución. Este tipo de sistemas son de gran interés con vistas a su aplicación en dispositivos electroquímicos como pueden ser baterías. Conocer cómo los LIs solvatan estas sales implica conocer los mecanismos de difusión dentro del fluido y por tanto cómo se transporta la carga en estos sistemas. Todos estos detalles sobre diferentes aspectos de los LIs serán objeto de discusión en la parte introductoria de esta tesis.

Por otro lado, consideraremos el efecto del aumento del tamaño de dicho soluto. Hasta tal punto que, en buena aproximación, podremos estudiar las proximidades del soluto como una superficie plana en contacto con un LI. En esta situación, al igual que teníamos oscilaciones de carga en las proximidades de los solutos esféricos, aquí tendrá lugar un fenómeno similar pero ahora con la geometría plana inducida por la interfase. En función de la densidad de carga de la superficie, su composición y geometría, el LI se dispondrá de una forma u otra. Esta aproximación no solo es interesante para entender la solvatación de partículas muy grandes en estos fluidos, sino que además, nuevamente, comprender bien este escenario es muy importante para una buena descripción de lo que ocurre en una batería o un supercondensador, donde tendremos una interfase cargada en presencia de un electrolito LI. Huelga decir que vivimos tiempos en los que estos dispositivos electroquímicos están cada vez más presentes en nuestro día a día y un buen conocimiento de los

USC
UNIVERSIDADE DE SANTIAGO DE COMPOSTELA

fundamentos de su funcionamiento es crucial para poder seguir innovando y progresando en el campo. Finalmente, el escenario donde tenemos nanoestructuras de tamaños intermedios dispersas en LIs es también de gran interés para su aplicación, por ejemplo, en dispositivos fotónicos con dispersiones de nanopartículas metálicas donde la presencia del LI modifique la respuesta de los plasmones de superficie; en dispersiones de nanoestructuras para catalizar reacciones o en presencia de nanoestructuras porosas para dar soporte mecánico mientras se preservan las propiedades de los LIs.

En la presente tesis se lleva a cabo el estudio de los sistemas mencionados mediante simulaciones moleculares. Esto nos va a permitir acceder a información sobre la estructura y dinámica de estos sistemas, con resolución atómica que, en ocasiones, será complementada con resultados experimentales. Entre las principales técnicas de simulación empleadas cabe destacar las simulaciones de dinámica molecular (DM) y los cálculos de teoría del funcional densidad (DFT). Con la primera obtenemos información de la trayectoria de un conjunto de átomos dentro de una caja de simulación en unas condiciones que nos puedan interesar (presión, temperatura, presencia de interfases...). Esta trayectoria se obtiene integrando las ecuaciones clásicas del movimiento de cada átomo calculando las interacciones entre ellos con un campo de fuerzas. En la mayor parte de las simulaciones llevadas a cabo en esta tesis el campo de fuerzas utilizado es el denominado OPLS-AA, el cual está optimizado para la simulación de líquidos. Se ha usado la suite de simulación GROMACS para llevar a cabo estas simulaciones. Por otro lado, los cálculos DFT nos permiten obtener la densidad electrónica correspondiente al estado de mínima energía de un sistema mediante la resolución de las ecuaciones de Kohn–Sham. Esto resulta muy conveniente a la hora de calcular las cargas parciales de cada átomo (que son utilizadas por los campos de fuerzas usados en DM) o las configuraciones de equilibrio de sistemas de interés. Además de para esto, se han usado cálculos DFT en esta tesis para el estudio de la transferencia protónica entre especies iónicas. El software usado para estos cálculos fue el programa Gaussian 16 con el funcional de intercambio y correlación B3LYP. Los detalles en

USC
UNIVERSIDADE DE SANTIAGO DE COMPOSTELA

relación a las herramientas usadas para el desarrollo de esta tesis serán introducidas en detalle en el Capítulo 2.

Una de las primeras cuestiones que se planteó en la presente tesis fue que, aunque se comenzara el estudio de las dispersiones de nanoestructuras en LIs caracterizando la solvatación de solutos pequeños o LIs en presencia de interfases planas, en algún momento se afrontaría la labor de llevar a cabo simulaciones con nanoestructuras con tamaños del orden de las decenas de nanómetros. Realizar simulaciones de DM con cajas de simulación lo suficientemente grandes como para contener dichas estructuras con los campos de fuerzas convencionales, es una tarea muy costosa que requiere grandes tiempos de cálculo, incluso en los mayores superordenadores. Para reducir estos tiempos de cómputo, una solución es utilizar lo que se conocen como campos de fuerza "coarse grained" (CG). Estos, en lugar de describir las moléculas como el conjunto real de sus átomos constituyentes, trabajan con una serie de esferas conectadas que, *grosso modo*, representan la morfología de la molécula que se quiere simular. Esto permite reducir considerablemente el número de interacciones que hay que calcular durante la simulación y por tanto, reduce considerablemente los tiempos. El problema de las simulaciones con estos campos de fuerzas es que se pierden los detalles a nivel atómico, lo cual oscurece el objetivo de describir la física en torno a estas nanoestructuras. La estrategia ideal es llevar a cabo simulaciones largas con un campo de fuerzas CG para obtener la configuración de equilibrio de un determinado sistema y después reemplazar las moléculas CG por sus equivalentes en resolución atómica. Hecha esta transformación, se podría extender la simulación partiendo de una configuración muy próxima al equilibrio termodinámico y, en poco tiempo, obtener una imagen detallada con resolución atómica de los sistemas. En vistas a tener una herramienta que permitiese de manera automática intercambiar entre distintos campos de fuerza independientemente del tipo de molécula que se estuviese utilizando, se desarrolló e implementó el algoritmo Gaddle Maps. En el Capítulo 4 de esta tesis se introduce esta herramienta así como algunos sistemas de ejemplo donde su uso resulta de gran utilidad.

USC
UNIVERSIDADE DE SANTIAGO DE COMPOSTELA

Centrando el foco en la investigación de las propiedades de solvatación de los LIs, en el Capítulo 5 se presenta un estudio donde se caracteriza mediante simulaciones de DM la estructura y dinámica de una partícula modelo esférica en el seno de un LI con agua. Este trabajo nació como la continuación de uno previo llevado a cabo por colegas de la universidad de Stuttgart donde estudiaban el mismo sistema pero en ausencia de agua. Siempre que se llevan a cabo investigaciones con LIs, es muy importante tener claro cómo puede afectar la presencia de un disolvente molecular a sus propiedades, más concretamente, el agua. Se sabe que pequeñas cantidades de disolvente en el seno de un LI (lo que se conoce como límite "water in salt") inducen grandes cambios en la dinámica del fluido lo que se puede reflejar en un aumento importante de la conductividad o una disminución de la viscosidad. Además, una gran parte de los LIs son higroscópicos, lo que hace que, salvo que se sea extremadamente cuidadoso en su manipulación, siempre se encuentren restos de agua en su interior. En este trabajo se utilizó el acetato de 1-etil-3-metilimidazolio ([EMIM][ACE]) como LI y una fracción molar de agua igual al 5 % que pretende simular la mencionada agua residual. La partícula modelo en torno a la cual se estudia la estructura y dinámica, consiste en una esfera de van der Waals de 3.4 Å de radio efectivo y que pretende ser un modelo CG de un soluto genérico. Además, para tener una imagen de la solvatación de distintos tipos de soluto, se estudian los casos donde la partícula tiene carga positiva, negativa o neutra. Las conclusiones principales de este trabajo son que la presencia de agua no cambia significativamente la estructura de las capas de solvatación en torno a los solutos, pero sí se observa una adsorción preferencial de moléculas de agua en la primera y segunda capas en torno a las esferas negativa y positiva respectivamente. También se encuentra una correlación fuerte entre la orientación de estas moléculas de agua y el campo eléctrico en las cercanías de los solutos, viendo cómo se alinea el momento dipolar del agua con este. Finalmente, se ve cómo, aunque la presencia de agua no altere significativamente el entorno de los solutos así como la presencia de los solutos no altera la dinámica del agua, la movilidad de las esferas se incrementa en más de un orden de magnitud. Esto refleja que, aún tratándose de cantidades de agua consi-

USC UNIVERSIDADE DE SANTIAGO DE COMPOSTELA

deradas a menudo como "residuales", las propiedades dinámicas del LI pueden cambiar drásticamente.

Siguiendo con esta línea, analizamos qué ocurre cuando cambiamos el tamaño y la carga de esta partícula solvatada mediante una caracterización de disoluciones de diferentes sales alcalinas y alcalinotérreas en un LI prótico como es el nitrato de etilamonio (EAN). Este trabajo, el cual se detallará en el Capítulo 6, combina técnicas teórico-computacionales con medidas experimentales. En una primera parte de este estudio se muestran las medidas experimentales de las entalpías de solvatación de las distintas sales, encontrando una correlación muy importante entre estos valores y las densidades iónicas de las sales en su fase cristalina. Por otro lado, estos valores de la entalpía de solvatación de los distintos cationes en EAN son muy similares a los que presentan para disoluciones con agua, poniendo de manifiesto las similitudes entre ambos fluidos como medios disolventes. Una comparativa entre los resultados experimentales y los calculados a partir de simulaciones de DM sugiere que las simulaciones son lo suficientemente precisas como para servir de soporte para dar explicación a la física detrás de estos procesos. Además, mediante las simulaciones, podemos acceder al estudio de la solvatación de ciertas sales poco solubles que no son accesibles experimentalmente debido a las limitaciones de los distintos instrumentos de medida. A partir de los resultados de estas simulaciones se presenta una caracterización detallada de la estructura en torno a los diferentes cationes. Además, se encuentra una correlación muy fuerte entre las propiedades de cada sistema y el campo eléctrico presente en la superficie de cada catión, el cual está determinado por su tamaño y carga. A partir de esta correlación conseguimos desarrollar una herramienta que permite interpolar las diferentes magnitudes para distintos solutos en función de estos parámetros. En resumen, las conclusiones principales de este trabajo son, por un lado, que las propiedades de solvatación de estos sistemas están principalmente gobernadas por las interacciones electrostáticas, jugando las interacciones de van der Waals un papel muy secundario, y por otro lado, que las capas de solvatación en torno a los cationes son muy similares en EAN y en agua.

USC
UNIVERSIDADE DE SANTIAGO DE COMPOSTELA

Como último trabajo en esta tesis tratando partículas con simetría esférica, en el Capítulo 7, se presentan los resultados fruto de la colaboración con colegas experimentales donde se estudia la estructura y el transporte de carga en una novedosa sal hidratada obtenida a partir de una reacción ácido-base que involucra al ácido 12-tungstenofosfórico y al imidazol. Este tipo de materiales, que presentan una conductividad protónica importante incluso a temperatura ambiente, son clave para el desarrollo de nuevas membranas para mejorar de rendimiento de distintos dispositivos electroquímicos, como por ejemplo celdas de combustible. El principal objetivo de este trabajo era ver cómo cambiando la concentración de moléculas de agua en el sistema se puede pasar de una conductividad protónica típica de sistemas acuosos a una más característica de sistemas basados en LIs (con las ventajas ya mencionadas de una buena estabilidad térmica y electroquímica). El objetivo del doctorando en este trabajo fue el de ofrecer una visión microscópica detallada que completase los experimentos llevados a cabo. Para ello se usaron todos los conocimientos y herramientas desarrolladas en los trabajos previamente mencionados, ya que el sistema en cuestión, desde el punto de vista computacional, se puede tratar como un LI en presencia de agua donde los aniones están constituidos por partículas con simetría esférica con un radio en torno a los 5.2 Å. Vemos como este trabajo ya supone el estudio de estructuras con tamaños más grandes. Por un lado, mediante simulaciones de DM se obtuvo información estructural de estos sistemas viendo cómo esta cambiaba con la cantidad de agua. Se observó que existen 4 puntos de adsorción preferencial para el agua en torno a cada anión así como su orientación más probable, donde uno de los hidrógenos se orienta hacia el centro de dicho anión. Además, la distribución de las diferentes orientaciones de los cationes imidazolio en torno a los aniones, la cual muestra dos poblaciones (una correspondiente a los cationes orientados con el anillo paralelo a la superficie del anión y otra perpendicular), coincide perfectamente con las observaciones experimentales. Por otro lado, se llevaron a cabo cálculos DFT para esclarecer cuál es la ruta de transferencia protónica óptima en estos sistemas. Los resultados de estos cálculos sugieren que los protones se mueven a través de los cationes imidazolio y las moléculas de agua.

USC UNIVERSIDADE DE SANTIAGO DE COMPOSTELA

Además, la presencia de los aniones, que condiciona la orientación de ambas especies, disminuye la barrera energética de la transferencia por esta ruta.

Paralelamente a la línea de investigación relativa a partículas esféricas, se llevaron a cabo trabajos donde se estudia el límite de partículas muy grandes, es decir, cómo se comporta el LI y sus mezclas en las proximidades de interfases planas. En el primer trabajo dentro de esta línea que se presenta en esta tesis (Capítulo 8) se estudia la estructura tridimensional de la doble capa eléctrica. Esta doble capa no es más que una organización inhomogénea de los aniones y cationes de un LI o una disolución electrolítica en torno a una superficie que se caracteriza por presentar oscilaciones amortiguadas de carga. Por poner un ejemplo simple, supongamos que tenemos una interfase con una densidad de carga positiva en presencia de un LI. Los aniones del LI tenderán a acumularse en la interfase para apantallar la carga de esta. Esto hará que una segunda capa de cationes se acumule a continuación para apantallar la carga de exceso generada por la primera capa de aniones y así sucesivamente hasta entrar en una región en ausencia de campo eléctrico. Esta fenomenología ya estaba estudiada con anterioridad en la literatura. Lo novedoso del trabajo aquí presente es la imagen detallada no solo de la estructura de la doble capa eléctrica en la dirección perpendicular a la interfase, sino que además, cómo los aniones y cationes se distribuyen en el plano paralelo a dicha interfase. En este estudio se llevan a cabo simulaciones de DM con tetrafluoroborato de 1-butil-3-metilimidazolio ([BMIM][BF_4]) tanto puro como mezclado con disolventes moleculares como agua, metanol y etanol confinados entre dos paredes de grafeno con densidades de carga opuestas ($\pm 1 e/nm^2$). En una primera parte de este trabajo se hace un análisis exhaustivo de la estructura axial de los componentes de los sistemas en las proximidades de ambas interfases viendo cómo la presencia de los disolventes moleculares afectan a las primeras capas. Al igual que se hizo para las simulaciones con esferas modelo, se encontró una correlación entre la orientación de las moléculas de disolvente y el campo eléctrico en sus proximidades. En una segunda parte del trabajo se analiza y caracteriza la distribución de la

USC
UNIVERSIDADE DE SANTIAGO DE COMPOSTELA

adsorción en las interfases de todas las especies, verificando que la adición de los distintos disolventes inducía cambios en esta. Además, se comprobó que este patrón de adsorción no se restringe solo a la primera capa en las proximidades de la interfase, sino que se propaga hacia el seno del fluido a medida que se va difuminando. Se ve también que el patrón formado no está determinado por la morfología de la interfase, sino que viene dado principalmente por la densidad de carga de la capa adsorbida pudiendo esta ser modificada cambiando la carga de las interfases o añadiendo distintos disolventes.

Continuando con la investigación de LIs en presencia de interfases planas, en el Capítulo 9 se presenta un trabajo en el que nos centramos en el efecto del nanoconfinamiento en la estructura axial de LIs dejando de lado la estructura lateral estudiada previamente. Concretamente, el objetivo principal es analizar la aparición de capas iónicas a medida que la distancia entre paredes planas se incrementa, así como el rango de alcance de estas en las propiedades estructurales del líquido. Para ello, se llevaron a cabo simulaciones de DM usando EAN como LI confinado entre dos interfases planas implícitas, es decir, objetos matemáticos que emulan la interacción del LI con una pared de grafeno pero sin presencia física de dicha pared. Los resultados muestran cómo aparece una correlación muy interesante entre las propiedades dinámicas y las estructurales con el tamaño de la rendija simulada. Con todas las simulaciones llevadas a cabo para varios tamaños de rendija, conseguimos expresar las propiedades de un nuevo sistema con una distancia entre paredes muy grande como la superposición de un sistema nanoconfinado con un determinado tamaño de rendija más un sistema en ausencia de paredes. Para el LI estudiado, el tamaño óptimo de la rendija necesaria para describir este sistema más grande resultó ser de 2.7 nm, indicando que el efecto de las interfases se propaga dentro del líquido unos 1.35 nm. El formalismo teórico aplicado aquí es extrapolable a otros sistemas y permite tener una estimación del efecto de las interfases en sistemas nanoconfinados. Por tanto, esto puede ser de gran utilidad a la hora de desarrollar dispositivos basados en materiales nanoporosos o nanoestructuras con cavidades de ciertos tamaños.

USC
UNIVERSIDADE DE SANTIAGO DE COMPOSTELA

En estos estudios relativos a la caracterización de nanoestructuras en los límites de pequeños y grandes tamaños, el foco estaba puesto en las propiedades estructurales del medio y, en especial, en cómo las diferentes especies moleculares se reordenan en torno a estas estructuras. En otras palabras, las propiedades dinámicas se dejaron un poco de lado. Esto principalmente es debido a la falta de datos experimentales con los que validar los resultados de las simulaciones, los cuales pueden desviarse significativamente de la realidad al no estar usando campos de fuerzas optimizados para el estudio de estas propiedades dinámicas. Sin embargo, para tener una visión completa del comportamiento de estos medios iónicos densos como soporte para distintas estructuras, es crucial comprender de manera fundamental sus propiedades de transporte. Para llenar esta falta de conocimiento, se llevó a cabo un trabajo donde se estudiaban mezclas binarias de LIs con etanol mediante simulaciones de DM. Además, para el estudio de la conductividad iónica, se compararon los datos extraídos de las simulaciones con medidas experimentales de los mismos sistemas. El objetivo principal de este trabajo (el cual se presentará en detalle en el Capítulo 10) es la comprobación de la solidez de un formalismo teórico previamente desarrollado en el grupo de investigación. Este formalismo, trata de describir los fenómenos de transporte en sistemas iónicos como saltos de las especies cargadas entre celdas de distinta movilidad dentro del seno del fluido. Por un lado, una comparativa con trabajos previamente publicados para sistemas similares con agua, muestra diferencias significativas en la forma de solvatación del cosolvente molecular, lo que se traduce en una disminución de la movilidad iónica cuando el agua es reemplazada por un alcohol. Sin embargo, la aportación más importante del trabajo es la demostración de la capacidad del modelo teórico para describir la dependencia de las conductividades de estos sistemas a medida que cambia la concentración de cosolvente. No solo eso, sino que además, mostramos que las frecuencias de los saltos antes mencionados calculados con los parámetros de los ajustes a la conductividad (magnitud macroscópica) coinciden con las calculadas directamente de las simulaciones (parámetros microscópicos), poniendo de manifiesto la solidez de los cimientos sobre los que se construye la teoría. Esta validación facilita enormemente la elección

USC UNIVERSIDADE DE SANTIAGO DE COMPOSTELA

de compuestos y concentraciones para una determinada aplicación al reducir considerablemente el número necesario de experimentos o simulaciones. Además, conocer las propiedades dinámicas del medio implica conocer en gran medida las propiedades dinámicas de dispersiones de nanoestructuras. El siguiente paso para avanzar en la línea marcada por esta tesis sería la del estudio completo de la solvatación y transporte de nanoestructuras con tamaños del orden de las decenas de nanómetros. Esto será el objetivo principal de futuras investigaciones ya fuera del marco de la presente tesis por falta de tiempo.

Finalmente, en el Capítulo 11 se enumeran las principales conclusiones de esta tesis así como futuras líneas de trabajo derivadas la misma. Se presenta también un listado de publicaciones relacionadas pero no contenidas en esta tesis.

USC
UNIVERSIDADE DE SANTIAGO DE COMPOSTELA

USC
UNIVERSIDADE
DE SANTIAGO
DE COMPOSTELA

Summary

This thesis aims to present an exhaustive study of the properties of ionic liquids (ILs) and their mixtures with other solvents in the presence of solutes with different sizes and properties. ILs are materials formed solely by anions and cations that, due to their geometries, have low melting temperatures (less than 100 °C is the most accepted by the community). In other words, they can be thought as molten salts at room temperature. Due to this purely ionic constitution, ILs present a series of very interesting properties that are not found in other liquids, such as: low volatility, wide electrochemical window, high conductivity, high viscosity, high thermal stability and good solvation capacities, among others. This series of properties has promoted the application of these ionic compounds in a wide variety of fields such as: lubricants, solvents for almost any compound, catalyst media, in supercapacitors, batteries, nuclear industry or in extraction and separation processes. In addition, they are considered designer solvents, since by carefully choosing the anions and cations that make up an IL, their properties can be adjusted for a certain purpose. This means that there is an enormous number of potential ILs. And not only that, but by mixing different ILs we can also adjust these properties, further increasing the options.

One of the main reasons why ILs have such low melting temperatures is the asymmetry that exists between the anions and cations that constitute them. Generally, anions have simple molecular topologies even with certain symmetries, while cations are formed mainly by larger molecules with one part where the charge is concentrated at and another in which organic molecular groups predominate. Although this is the general trend for the most widely used ILs, these roles can be interchanged. This molecular structure of the ILs constituents helps to understand the reason for their good solvation properties. As is known, generally *similia similibus solvuntur*. In the case of ILs, we have a solvent that has both a polar part (usually placed on the charge centres of the ions) and an organic part. Therefore, when carrying out a solu-

USC
UNIVERSIDADE DE SANTIAGO DE COMPOSTELA

tion in these compounds, the ions will be arranged in such a way that they orient their polar or organic part towards the solute, depending on its nature. If we consider charged solutes, we expect the constituents of the ILs with opposite charge to be distributed around to screen that charge, thus creating coordination complexes and a series of solvation shells with charge alternation. This scenario would be the equivalent to the solvation of salts in ILs. To give an example, we could consider a solution of a lithium salt whose anion is the same as that of the IL that we use for the solution. These types of systems are of great interest for their applications in electrochemical devices such as batteries. Knowing how ILs solvate these salts implies knowing the diffusion mechanisms within the fluid and therefore how charge is transported in these systems. All these details about different aspects of ILs will be discussed in the introductory part of this thesis.

On the other hand, we will consider the effect of increasing the size of the solute. Up to a size that, to a good approximation, we can study the vicinity of the solute as a flat surface in contact with an IL. In this situation, just as we had charge oscillations in the vicinity of spherical solutes, a similar phenomenon will take place here but now with the planar geometry induced by the interface. Depending on the charge density of the surface, its composition and geometry, the IL will be arranged in one way or another. This approximation is not only interesting to understand the solvation of very large particles in these fluids, but also, again, for having a good description of what happens in a battery or a supercapacitor, where we will have an interface charged in the presence of an IL electrolyte. It goes without saying that we are living times in which the importance of these electrochemical devices in our daily lives is increasing so, a good understanding of the fundamentals of their operation is crucial in order to continue innovating and progressing in the field. Finally, the scenario where we have nanostructures of intermediate sizes dispersed in ILs is also of great interest for application, for example, in photonic devices with metallic nanoparticle dispersions where the presence of IL modifies the response of surface plasmons; nanostructure dispersions as to catalyse reactions, or in the presence of

USC
UNIVERSIDADE DE SANTIAGO DE COMPOSTELA

porous nanostructures to provide mechanical support while preserving the properties of the ILs.

In this thesis, the study of the aforementioned systems is carried out by means of molecular simulations. This will allow us to access information about the structure and dynamics of these systems with atomic resolution that, in some cases, will be complemented with experimental results. Among the main simulation techniques used, it is worth highlighting molecular dynamics (MD) simulations and density functional theory (DFT) calculations. With the first, we obtain information on the trajectory of a set of atoms inside a simulation box under certain conditions of interest (pressure, temperature, presence of interfaces...). This trajectory is obtained by integrating the classical equations of motion of each atom calculating the interactions between them with a force field. In most of the simulations carried out, the employed force field is the one known as OPLS-AA, which is optimized for simulations with liquids. The GROMACS simulation suite has been used to carry out these simulations. On the other hand, DFT calculations allow us to obtain the electron density corresponding to the ground energy state of a system by solving the Kohn–Sham equations. This is very convenient when calculating the partial charges of each atom (which are used by the force fields used in MD) or the equilibrium configurations of systems of interest. In addition to this, DFT calculations have been used in this thesis for the study of proton transfer between ionic species. The software used for these calculations was the Gaussian 16 program with the B3LYP exchange-correlation functional. All the details regarding the tools used in the development of this thesis will be introduced in Chapter 2.

One of the first questions raised in this thesis was that, although the study of dispersions of nanostructures in ILs would begin characterizing the solvation of small solutes or ILs in the presence of planar interfaces, at some point, the task of carrying out simulations with nanostructures with sizes of the order of tens of nanometres would be faced. Performing MD simulations with simulation boxes large enough to contain such structures with conventional force fields is a very expensive task that

USC
UNIVERSIDADE DE SANTIAGO DE COMPOSTELA

requires long computational times even on the largest supercomputers. To reduce these times, one solution is to use what are known as "coarse grained" (CG) force fields. These, instead of describing the molecules as the real set of their constituent atoms, work with a series of connected spheres that, roughly, represent the morphology of the molecule to be simulated. This makes it possible to considerably reduce the number of interactions that must be calculated during the simulation and, therefore, considerably reduces the times. The problem with simulations with these force fields is that details at the atomic level are lost, which obscures the goal of describing the physics around these nanostructures. The ideal strategy is to carry out long simulations with a CG force field to obtain the equilibrium configuration of a given system and then, replace the CG molecules with their equivalents in atomic resolution. Once this transformation is done, the simulation could be extended starting from a configuration very close to thermodynamic equilibrium and, in a short time, obtain a detailed image of the system with atomic resolution. In order to have a tool that allow the automatic exchange between different force fields regardless of the type of molecule being used, the Gaddle Maps algorithm was developed and implemented. In Chapter 4 of this thesis this tool is introduced as well as some example systems where its application is very useful.

Focusing on the investigation of the solvation properties of ILs, a study where the structure and dynamics of a spherical model particle within a mixture of IL and water is presented in Chapter 5. This work was born as the continuation of a previous one carried out by colleagues from the University of Stuttgart where they studied the same system but in the absence of water. Whenever a research involving ILs is carried out, it is very important to have a good understanding about how the presence of a molecular solvent can affect its properties, more specifically, water. It is known that small amounts of solvent within an IL (what is known as the "water in salt" limit) induce large changes in the dynamics of the fluid, which can be reflected in a significant increase in conductivity or a decrease of the viscosity. In addition, a lot of ILs are hygroscopic, which means that, unless being extremely careful in

USC
UNIVERSIDADE DE SANTIAGO DE COMPOSTELA

their handling, there would be always traces of water. In this work, 1-ethyl-3-methylimidazolium acetate ([EMIM][ACE]) was used as IL and a molar fraction of water equal to 5% was employed to emulate the aforementioned residual water. The model particle around which the structure and dynamics are studied consists of a van der Waals sphere with an effective radius of 3.4 Å, which is intended to be a CG model of a generic solute. In addition, to have an insight of the solvation of different types of solute, situations where the particle has a positive, negative or neutral charge are studied. The main conclusions of this work are that the presence of water does not significantly change the structure of the solvation layers around the solutes while a preferential adsorption of water molecules is observed in the first and second layers around the negative and positive spheres, respectively. A strong correlation is also found between the orientation of these water molecules and the electric field in the vicinity of the solutes, seeing how the dipole moment of water aligns with it. Finally, it is seen how, although the presence of water does not significantly alter the environment of the solutes and the presence of solutes does not alter the dynamics of water, the mobility of the spheres increases by more than one order of magnitude. This reflects that, even when dealing with water concentrations often considered as "residual", the dynamic properties of the IL can change drastically.

Following this line, we analyse what happens when we change the size and charge of this solvated particle by characterizing solutions of different alkali salts in a protic IL such as the ethylammonium nitrate (EAN). This work, which will be detailed in Chapter 6, combines theoretical and computational techniques with experimental measurements. In the first part of this study, the experimental measurements of the solvation enthalpies of the different salts are shown, finding a very important correlation between these values and the ionic densities of the salts in their crystalline phase. On the other hand, the values of the solvation enthalpy of the different cations in EAN are very similar to those for solutions with water, highlighting the similarities between both fluids as solvent media. A comparison between the experimental results and those calculated from MD simulations suggests that the simulations are

USC
UNIVERSIDADE DE SANTIAGO DE COMPOSTELA

accurate enough to support the explanation of the physics behind these processes. In addition, through simulations, we can access the study of the solvation of certain poorly soluble salts that are not experimentally accessible due to the limitations of some measurement instruments. From the results of these simulations, a detailed characterization of the structure around the different cations is presented. In addition, a very strong correlation is found between the properties of each system and the electric field present on the surface of each cation, which is determined by its size and charge. From this correlation we managed to develop a tool that allows us to interpolate the different magnitudes for different solutes based on these parameters. In summary, the main conclusions of this work are, on the one hand, that the solvation properties of these systems are mainly governed by electrostatic interactions, with van der Waals interactions playing a very minor role, and on the other hand, that the solvation shells around cations are very similar in EAN and water.

As the last work in this thesis dealing with particles with spherical symmetry, in Chapter 7, the results from a collaboration with experimental colleagues are presented. In this work we study the structure and charge transport in a novel hydrated salt obtained from an acid-base reaction involving 12-tungstenophosphoric acid and imidazole. These types of materials, which have a significant proton conductivity even at room temperature, are very important for the development of new membranes to improve the performance of different electrochemical devices such as fuel cells. The main objective of this work was to see how, by changing the concentration of water molecules in the system, it is possible to go from a protonic conductivity typical of aqueous systems to one more characteristic of IL-based systems (with the aforementioned advantages of good thermal and electrochemical stability). Our contribution to this work was to offer a detailed microscopic picture that complete the experiments carried out. For this, all the knowledge and tools developed in the previously mentioned works were used, since these systems, from the computational point of view, can be treated as an IL in the presence of water, where the anions are made up of particles with spherical symmetry with a radius around 5.2 Å. This supposed a step for-

USC UNIVERSIDADE DE SANTIAGO DE COMPOSTELA

ward in this line of this thesis as it involves the study of structures with larger sizes. On the one hand, by means of MD simulations, structural information of these systems was obtained by studying how it changed with the amount of water. It was observed that there are 4 preferential adsorption sites for water around each anion as well as that it is more probable to find these water molecules with one of their hydrogens oriented towards the centre of the anion. In addition, the distribution of the different orientations of the imidazolium cations around the anions, which shows two populations (one corresponding to the cations oriented with the ring parallel to the surface of the anion and another perpendicular), agrees perfectly with the experimental measurements. On the other hand, DFT calculations were carried out to clarify which is the optimal proton transfer path in these systems. The results of these calculations suggest that the protons move through the imidazolium cations and water molecules. Moreover, the presence of the anions, which conditions the orientation of both species, lowers the energy barrier of the transfer through this path.

Parallel to this research line regarding spherical particles, work was carried out to study the limit of very large particles, i.e., how IL and its mixtures behave in the vicinity of flat interfaces. In the first work within this line that is presented in this thesis (Chapter 8) the three-dimensional structure of the electrical double layer is studied. This electric double layer is nothing more than an inhomogeneous organization of the anions and cations of an IL or an electrolytic solution around a surface that is characterized by presenting damped oscillations of charge. To give a simple example, suppose we have an interface with a positive charge density in the presence of an IL. The anions of the IL will tend to accumulate at the interface to screen its charge. This will cause a second layer of cations to accumulate next to the anions to screen the excess of charge generated by them and so on until entering a region with no electric field. This phenomenology had already been studied previously in the literature. The novelty of the work presented here is the detailed picture not only of the structure of the electric double layer in the direction perpendicular to the interface, but also how the anions and

USC
UNIVERSIDADE DE SANTIAGO DE COMPOSTELA

cations are distributed in the parallel direction. In this study, MD simulations were carried out with 1-butyl-3-methylimidazolium tetrafluoroborate ([BMIM][BF_4]) both pure and mixed with molecular cosolvents such as water, methanol and ethanol confined between two graphene walls with opposite charge densities ($\pm 1\ e/nm^2$). In the first part of this work, an exhaustive analysis of the axial structure of the components of the systems in the vicinity of both interfaces is made to see how the presence of molecular cosolvents affects the first layers. As in simulations with model spheres, a correlation was found between the orientation of the solvent molecules and the electric field in their neighbourhoods. In a second part of the work, the adsorption distribution in the interfaces of all the species is analysed and characterized, verifying that the addition of the different solvents induced changes in it. Moreover, it was found that this adsorption pattern is not restricted only to the first layer in the vicinity of the interface, but that it spreads towards the bulk of the fluid as it diffuses. It is also seen that the pattern formed is not determined by the morphology of the interface, but rather is given mainly by the charge density of the adsorbed layer, which can be modified by changing the charge of the interfaces or adding different cosolvents.

Continuing with the investigation of ILs in the presence of planar interfaces, in Chapter 9 a work in which we focus on the effect of nanoconfinement on the axial structure of ILs is presented, leaving aside the previously studied lateral structure. Specifically, the main objective is to analyse the appearance of ionic layers as the distance between flat walls increases and also characterize the range of their effect in the structural properties of the liquid. For this, MD simulations were carried out using EAN as IL confined between two implicit flat interfaces, that is, mathematical objects that emulate the interaction of the IL with a graphene wall but without the physical presence of the wall. The results show a very interesting correlation between the dynamic and structural properties with the size of the simulated slit. With all the simulations carried out for various slit sizes, we manage to express the properties of a new system with a very large distance between walls as the superposition of a nanoconfined system with a given slit size plus a bulk system. For the

USC
UNIVERSIDADE DE SANTIAGO DE COMPOSTELA

studied IL, the optimal size of the slit necessary to describe this larger system turned out to be 2.7 nm, indicating that the effect of the interfaces propagates within the liquid at about 1.35 nm. The theoretical formalism applied here can be extrapolated to other systems and allows estimating the effect of interfaces in nanoconfined systems. Therefore, this can be very useful when developing devices based on nanoporous materials or nanostructures with cavities of certain sizes.

In all the aforementioned studies related to the characterization of nanostructures in the limits of small and large sizes, the focus was on the structural properties of the medium and, in particular, how the different molecular species rearrange themselves around these structures. In other words, the dynamic properties were left out a bit. This is mainly due to the lack of experimental data with which to validate the simulation results, which can deviate significantly from reality when optimized force fields for the study of these dynamic properties are not used. However, to gain a complete insight into the behaviour of these dense ionic media as support for different structures, a fundamental understanding of their transport properties is crucial. To fill this lack of knowledge, a work was carried out where binary mixtures of ILs with ethanol were studied by means of MD simulations. In addition, for the study of ionic conductivity, the data extracted from the simulations were compared with experimental measurements of the same systems. The main objective of this work (which will be presented in detail in Chapter 10) is to check the soundness of the theoretical formalism previously developed in the research group that tries to describe the transport phenomena in ionic systems as jumps of the charged species between cells with different mobilities. On the one hand, a comparison with previously published works for similar systems with water shows significant differences in the solvation of the molecular cosolvent, which translates into a decrease in the ionic mobility when water is replaced by alcohol. However, the most important contribution of the work is the demonstration of the ability of the theoretical model to describe the dependence of the conductivities of these systems with the cosolvent concentration. Not only that, but also, we show that the frequencies of the aforemen-

USC
UNIVERSIDADE DE SANTIAGO DE COMPOSTELA

tioned jumps calculated with the parameters coming from the fit to the conductivities (macroscopic magnitude) match those calculated directly from the simulations (microscopic parameters), highlighting the solidity of the foundations on which the theory is constructed. The validation of this theory makes the choice of compounds and concentrations for a given application much easier by considerably reducing the number of required experiments or simulations. In addition, knowing the dynamic properties of the medium implies knowing to a great extent the dynamic properties of dispersions of nanostructures. The next step to advance in the line marked by this thesis would be the complete study of the solvation and transport of nanostructures with sizes of the order of tens of nanometers. This will be the main aim of future research, outside the contents of this thesis due to lack of time.

Finally, in Chapter 11 the main conclusions of this thesis are listed, as well as future lines of work derived from it. A list of related publications but not contained in this thesis is also presented.

USC
UNIVERSIDADE DE SANTIAGO DE COMPOSTELA

A Xabi, que marca el final de una etapa
y el inicio de otra...

USC
UNIVERSIDADE
DE SANTIAGO
DE COMPOSTELA

USC
UNIVERSIDADE
DE SANTIAGO
DE COMPOSTELA

Agradecimientos

Esta tesis es el fruto del arduo trabajo llevado a cabo durante los últimos cinco años. En este viaje ha habido momentos buenos y momentos no tan buenos, entre los cuales cabe destacar una pandemia que puso al mundo patas arriba. Es sobre todo en los momentos más duros cuando uno necesita sentir el apoyo de la gente que lo rodea y, en mi caso, puedo decir que me siento afortunado de haber tenido los mejores compañeros de viaje. Por este motivo, me gustaría dedicar unas palabras de agradecimiento a todas estas personas y en especial:

- A mi familia, en concreto: A mis padres, por educarme como lo han hecho e inculcarme los valores que hacen que sea quien soy; a mi hermano, quien, pese a la distancia, ha sido siempre un gran apoyo; y a mi tía Marina, que ha estado muy presente durante esta etapa y me ha ayudado en todo lo que estaba de su mano.

- A Pkecha, la persona con la que comparto todo, por la paciencia que ha tenido hasta ahora para aguantar mis manías y mis cosas de físico. Espero que no se canse nunca.

- A Luis Miguel, por ser el mejor director de tesis que alguien puede tener. Gracias a él, este período ha sido un camino de rosas en el que nos lo hemos pasado muy bien (entre comidas, cineclubs y caminatas) y además, también hemos sacado mucho trabajo adelante.

- A Hadrián, por ser un muy buen amigo y un gancho invisible que, desde que empezamos la carrera, siempre ha tirado de mí para obligarme a no quedarme atrás y aprender algo nuevo todos los días.

- A Álex y a Víctor, con los que he compartido muchas horas de debates absurdos en el despacho y con quienes he vivido momentos muy divertidos.

USC
UNIVERSIDADE DE SANTIAGO DE COMPOSTELA

- A mis amigos, con especial mención a Unai, a Edi y a toda la kuadrilla, porque, aunque estén en la distancia o no vea tanto como me gustaría, siempre los llevo conmigo.

- Al Pedroso Team, esa segunda familia que me ha aportado esa dosis diaria de deporte que uno necesita para desconectar y con los que me lo he pasado en grande todos estos años.

- A los miembros del grupo Nafomat, especialmente a la sección computacional (Trini, Borja, Javier, Julio...) quienes, cada uno a su manera, también han formado parte de este viaje.

Además, también agradezco la financiación y recursos facilitados por las siguientes entidades que han hecho posible la realización de esta tesis: Al centro de supercompuntación de Galicia (CESGA) por los recursos computacionales a la hora de hacer ciertos cálculos; al Ministerio de Educación por su financiación a través de mi beca para la formación de profesorado universitario (FPU); a los proyectos MAT2014-57943-C3-1P, MAT-2014-57943-C3-2P, MAT2014-57943-C3-1P, MAT2014-57943-C3-2P, MAT2017-89239-C2-1P, MAT2017-89239-C2-12P, CTQ2015-65816-R, PGC2018-093745-B-I00 y FIS2012-33126 del Ministerio de Economía y Competitividad bajo el amparo de los cuales se desarrolló la tesis; a la Xunta de Galicia por la financiación a través de la red gallega de líquidos iónicos (REGALIS CN 2014/1015), AGRUP 2015/11, ED431D 2017/06, ED431E 2018/08 y GRC ED431C 2016/001; y a la Unión Europea por el apoyo a través de acciones COST (CM1206 y MP1303) y a los fondos FEDER.

USC UNIVERSIDADE DE SANTIAGO DE COMPOSTELA

Contents

List of Figures li

List of Tables lxix

List of publications included in this thesis lxxi

List of publications related to this thesis lxxiii

I Introduction and Methods 1

1 Introduction 3
1.1 Motivation and Purpose 3
1.2 General and Specific Objectives 5
1.3 Ionic Liquids 7

2 Methods 13
2.1 Molecular Dynamics 14
2.2 Density Functional Theory 32

II Results 39

3 Summary of the Results 41

USC UNIVERSIDADE DE SANTIAGO DE COMPOSTELA

4 GADDLE Maps: General Algorithm for Discrete object Deformations based on Local Exchange Maps 55
4.1 Introduction . . . 57
4.2 Theoretical and computational methods . . . 60
4.3 Results . . . 71
4.4 Conclusions and perspectives . . . 84

5 Solvation in Ionic Liquid-Water mixtures: A Computational Study 89
5.1 Introduction . . . 91
5.2 Simulation Details . . . 93
5.3 Results and Discussion . . . 95
5.4 Summary and Conclusion . . . 111

6 Enthalpy of solvation of alkali metal salts in a protic ionic liquid: Effect of cation charge and size 115
6.1 Introduction . . . 117
6.2 Materials and methods . . . 118
6.3 Results . . . 124
6.4 Conclusions . . . 143

7 A New Solid State Proton Conductor: The Salt Hydrate Based on Imidazolium and 12-Tungstophosphate 145
7.1 Introduction . . . 147
7.2 Experimental Section . . . 149
7.3 Results and discussion . . . 156
7.4 Conclusions . . . 176
7.5 Supporting Information . . . 177

8 3D Structure of the Electric Double Layer of Ionic Liquid-Alcohol Mixtures at the Electrochemical Interface 179
8.1 Introduction . . . 181
8.2 Computational Section . . . 184
8.3 Results and Discussion . . . 186
8.4 Conclusions . . . 218

USC UNIVERSIDADE DE SANTIAGO DE COMPOSTELA

9 Nanoconfined Ionic Liquids: A Computational Study 221
9.1 Introduction 223
9.2 Simulation Details 225
9.3 Results and Discussion 227
9.4 Summary and Conclusion 245

10 Structure, Dynamics and Conductivities of Ionic Liquid-Alcohol Mixtures 249
10.1 Introduction 251
10.2 Methods 252
10.3 Results and discussion 255
10.4 Conclusions 270

III Conclusions 273

11 Conclusions and Future Perspectives 275
11.1 Conclusions 275
11.2 Future Perspectives 277

A Post-Print Version of the Publications 279
A.1 GADDLE Maps: General Algorithm for Discrete object Deformations based on Local Exchange Maps 281
A.2 Solvation in Ionic Liquid-Water mixtures: A Computational Study 295
A.3 Enthalpy of solvation of alkali metal salts in a protic ionic liquid: Effect of cation charge and size 305
A.4 A New Solid State Proton Conductor: The Salt Hydrate Based on Imidazolium and 12-Tungstophosphate . . . 317
A.5 3D Structure of the Electric Double Layer of Ionic Liquid-Alcohol Mixtures at the Electrochemical Interface 331
A.6 Nanoconfined Ionic Liquids: A Computational Study . 347
A.7 Structure Dynamics and Conductivities of Ionic Liquid-Alcohol Mixtures 359

USC UNIVERSIDADE DE SANTIAGO DE COMPOSTELA

B Supplementary Information **367**
B.1 Supplementary information for: Enthalpy of solvation of alkali metal salts in a protic ionic liquid: Effect of cation charge and size 369
B.2 Supplementary information for: A New Solid State Proton Conductor: The Salt Hydrate Based on Imidazolium and 12-Tungstophosphate 381
B.3 Supplementary information for: 3D Structure of the Electric Double Layer of Ionic Liquid-Alcohol Mixtures at the Electrochemical Interface 389
B.4 Supplementary information for: Nanoconfined Ionic Liquids: A Computational Study 393
B.5 Supplementary information for: Structure Dynamics and Conductivities of Ionic Liquid-Alcohol Mixtures . 401

C Information of the publications **409**
C.1 GADDLE Maps: General Algorithm for Discrete object Deformations based on Local Exchange Maps 411
C.2 Solvation in Ionic Liquid-Water mixtures: A Computational Study 413
C.3 Enthalpy of solvation of alkali metal salts in a protic ionic liquid: Effect of cation charge and size 415
C.4 A New Solid State Proton Conductor: The Salt Hydrate Based on Imidazolium and 12-Tungstophosphate . . . 417
C.5 3D Structure of the Electric Double Layer of Ionic Liquid-Alcohol Mixtures at the Electrochemical Interface 419
C.6 Nanoconfined Ionic Liquids: A Computational Study . 421
C.7 Structure Dynamics and Conductivities of Ionic Liquid-Alcohol Mixtures 423

Bibliography **425**

USC UNIVERSIDADE DE SANTIAGO DE COMPOSTELA

List of Figures

1.1 Evolution of global population, GDP and renewable and non-renewable energy production in the last decades. . . . 4
1.2 Schematic representation of different families of complex charged fluids and their relatation with ILs. 8
1.3 Molecular structure of most common anions and cations. . 9

2.1 Different simulation techniques and their range of applicability in terms of time and spatial resolution. The acronyms stay for: quantum chemistry (GC), ab inition MD (AbMD), MD with coarse grained force fields (CG-MD) and kinetic Monte Carlo (K-MC). 14
2.2 Snapshots of two initial configurations for a simulation box with EAN obtained with a lattice distribution (left) and with a random packing using PACKMOL (right). 17
2.3 Representation of the relevant magnitudes involved in the calculation of the different terms in bonded interactions. . 20
2.4 Potential energy associated to the rotation of the dihedral angle. 20
2.5 Multiple representations of the same molecule (the POPC phospholipid) using different force fields. 21
2.6 Time evolution of the temperature of the system for a pure IL ([BMIM][BF_4]) between two graphene walls during annealing (time interval between 0 and 1 ns), and in the stabilization (time interval between 1 and 11 ns) steps. The inset shows in detail the annealing region. 27

USC UNIVERSIDADE DE SANTIAGO DE COMPOSTELA

2.7 Schematic representation of a ”real” graphene wall (left) and an implicit interface emulating a homogeneous bidimensional distribution of atoms (right). 30

2.8 Schematic representation of the proton hopping process proposed by Grotthuss. 36

4.1 Schematic workflow of the algorithm operation. First of all, the input files are used to load one molecule of each species in both AT and CG resolutions. Next, these molecules are used as inputs in the alignment engine to obtain the optimal exchange map between resolutions through a Monte Carlo simulation. Finally, these exchange maps are used to extrapolate the AT configuration to the rest of the molecules of the CG system. 61

4.2 Scheme with the possible single atom displacements for atoms with one, two or three bonds. Red beads represent the CG molecule atoms and black lines the bonds. Blue vectors indicate the possible directions to move the corresponding atom, perpendicular to the cyan lines and surface. 62

4.3 Sequence of displacements in a deformation of a CG structure. Blue spheres represent the displaced beads. Light colors represent the initial positions in the previous step. . . . 64

4.4 Average order parameters determined for the sn-1 (circles) and sn-2 (triangles) chains of 128 DPPC molecules corresponding to a lipid bilayer obtained from: the final structure of a 100-ns-long MD simulation at 323 K (left); the direct backmapping to AT level, with no equilibration, from the CG structure corresponding to the previous AT bilayer simulated for 100-ns (middle); and the equilibrated AT system with 5 ns of MD simulation after the backmapping. The bilayer structure was simulated for 15 ns more but the order parameters did not change after the first 5 ns of MD. The original bilayer was obtained from the lipidbook web site. . 73

USC UNIVERSIDADE DE SANTIAGO DE COMPOSTELA

4.5 Top: Representations of the initial and final structures of ubiquitin at CG level. Bottom: Initial and final structures of ubiquitin at AT level. The initial CG structure was obtained from the transformation of the AT structure with PDB-ID=1UBQ[106] to the MARTINI force field representation using the *martinize.py* tool. The final CG structure was obtained by 200 ns of MD simulation. The backmapping of the final CG structure to AT resolution using the GROMOS54a7 force field[92] corresponds to the initial AT structure. The final AT structure was obtained by 50 ns of MD simulation. In all snapshots water molecules were removed for clarity. 75

4.6 2D structure of the peptide with sequence RRLKRLLRR-LKRL. 76

4.7 Top: Overlapped CG and AT representations of DPPC and the CPP. Middle: Representations of the initial and final structures of the CPP in a DPPC bilayer at CG level. Bottom: Initial and final structures of the CPP in a DPPC bilayer at AT level. The initial CG structure was constructed by inserting the CPP in a preformed DPPC bilayer using the MARTINI force field. The final CG structure was obtained by 1.2 μs of MD simulation. The backmapping of the final CG structure to AT resolution using the GROMOS53a6 force field[91] corresponds to the initial AT structure. The final AT structure was obtained by 50 ns of MD simulation. In all snapshots water molecules were removed for clarity. 77

4.8 Left: 2D structure of the CP with sequence RRKWLWLW (underlining represents D-amino-acid residues). Right: schematic representation of a SCPN. 78

USC UNIVERSIDADE DE SANTIAGO DE COMPOSTELA

4.9 Top: Overlapped CG and AT representations of DPPC and the CP. Middle: Representations of the initial and final structures of the CP in a POPC bilayer at CG level. Bottom: Initial and final structures of the CP in a POPC bilayer at AT level. The initial CG structure was constructed by inserting the CP in a preformed POPC bilayer using the MARTINI force field. The final CG structure was obtained by 150 ns of MD simulation. The backmapping of the final CG structure to AT resolution using the OPLS-AA force field[35] corresponds to the initial AT structure. The final AT structure was obtained by 20 ns of MD simulation. In all snapshots water molecules were removed for clarity. . . . 79

4.10 Top: Overlapped CG and AT representations of SDS and αCD. Middle: Representations of the initial and final structures of the αCD2SDS1 complexes at CG level. Bottom: Initial and final structures of the αCD2SDS1 complexes at AT level. The initial CG structure was constructed by inserting 100 MARTINI αCD2SDS1 complexes at random locations. The final CG structure was obtained by 6 μs of MD simulation. The backmapping of the final CG structure to AT resolution using the GROMOS54a7[92] force field corresponds to the initial AT structure. The final AT structure was obtained by 10 ns of MD simulation. In all snapshots water molecules were removed for clarity. 80

4.11 2D structure of vitamin E. 81

USC UNIVERSIDADE DE SANTIAGO DE COMPOSTELA

4.12 Top: Overlapped CG and AT representations of vitamin E and the DNA chain with sequence 5'-AGGTAGTGTAATCGCCTTG-3'. Middle: Representations of the initial and final structures of the simulated system at CG level. Bottom: Initial and final structures of the vitamin E aggregate with the DNA chain partially embedded at AT level. The initial CG structure was constructed by inserting 500 MARTINI vitamin E molecules and a DNA chain at random locations. The final CG structure was obtained by 250 ns of MD simulation. The backmapping of the final CG structure to AT resolution using the AMBER/GAFF force field corresponds to the initial AT structure. The final AT structure was obtained by 10 ns of MD simulation. In all snapshots water molecules were removed for clarity. 82

4.13 Vitamin E representation before (transparent) and after (opaque) the mapping. The chiral center is enlarged to highlight chirality conservation. 83

4.14 Top: Overlapped CG and AT representations of the simulated ion pair ([BMIM][BF_4]). Bottom: Final structures at CG and AT resolution for the 500 molecules of the IL simulated. The CG structure was obtained after 500 ns of MD simulation using the MARTINI force field, starting from a $(5.4\ nm)^3$ cubic box built using *Packmol*.[32] The final AT structure was obtained after 5 ns of MD simulation using the OPLS-AA force field,[35] starting from the backmapped structure at the end of the CG-MD simulation. 84

5.1 Molecular representation of the simulated species. The orange arrows represent the vectors employed in the orientational study. 96

USC UNIVERSIDADE DE SANTIAGO DE COMPOSTELA

5.2 Two dimensional histogram of the conditional probability of finding an EMIM (top row), ACET (middle row) or water (bottom row) molecule at a certain distance with a certain orientation around the negatively (left column), neutral (middle column) and positively (right column) charged model sphere. Bright regions represents high presence probability while dark ones indicate absence of molecules. 97
5.3 Comparative between RDFs of different molecular species around the negatively (top), neutral (middle) and positively (bottom) charged central solute particle for simulated systems with (solid lines) and without (dashed lines) water. . . 100
5.4 Cumulative distribution function for water around neutral (black), positively charged (red) and negatively charged (blue) spheres. 102
5.5 Electric field around negatively charged (top), neutral (middle) and positively charged (bottom) spheres. In each subplot the corresponding 2D histogram from Fig. 5.2 for water is represented in the background with transparency. For the system with the negatively charged sphere, the most representative molecular orientation at two different distances around the sphere are represented. 103
5.6 Velocity autocorrelation function (top) and velocity density of states (bottom) of water molecules close to the negatively charged (blue), neutral (black) and positively charged (red) model spheres. The behaviour of water molecules far from the solute is represented for comparison in solid black line. 105
5.7 Mean squared displacement (top) and α coefficient from the RMSD fit (bottom) as function of time for neutral (black), positively charged (red) and negatively charged (blue) spheres. The black dashed line in the MSD plot represents the unit slope meaning that the spheres enter in the diffusive regime, while in the α representation the value of $\alpha = 0.5$ corresponds to that for which the spheres are considered to be in the diffusive regime. 107

USC UNIVERSIDADE DE SANTIAGO DE COMPOSTELA

5.8 Cage correlation functions of the cations (red) and anions (blue) around the model solutes for simulations with (solid lines) and without (dashed lines) water. 108

5.9 MSD of the cations (top) and anions (bottom) in the simulated systems with three differently charged spheres with (solid lines) and without (dashed lines) water. Black dotted lines with unitary slope are represented as a visual reference to identify the diffusive regime. 110

5.10 Probability that the model solute moves less than 0.3 nm as function of time for neutral (black), positively (red) and negatively (blue) charged spheres in the simulations with (solid lines) and without (dashed lines) water. 111

6.1 Schematic diagram of solvation of alkaline metals in EAN(l), where square represents the alkaline metal (M^+), circle the nitrate anion (NO_3^-) and triangle the ethylammonium cation ($CH_3CH_2NH_3^+$). 119

6.2 Schematically representation of the thermochemical cycle used for the determination of the heat of solution of alkali metal nitrate salts in EAN(l). The "v" subindex is equal to 1 for the monovalent salts and 2 for the divalent ones. . . 123

6.3 Linear fit of the enthalpies of solution of mixtures of EAN and salt for all the studied salts and concentrations. The obtained values of the slopes of the fit lines are shown in the legend. 128

6.4 Reaction scheme for the relation between the solution and enthalpy solvation of the alkaline metal nitrate salts in EAN(l). As introduced before and to unify notation, "v" is equal to "1" for the monovalent salts and "2" for the divalent ones. 130

6.5 Exchange of M^+ (top) or M^{2+} (bottom) for Li^+ into a solution of Li^+ in EAN(l). 132

USC UNIVERSIDADE DE SANTIAGO DE COMPOSTELA

6.6 Comparison between the solvation of the alkali metals in water ($\Delta_{\text{hyd}}H_m$)[269] and those in EAN ($\Delta_{\text{solv}}H_m$). The black dashed line represents the values where $\Delta_{\text{hyd}}H_m = \Delta_{\text{solv}}H_m$. Closed circles, experimental data; Open circles, MD results. 133

6.7 SDFs of lithium around nitrate anions in EAN (a) and around water molecules (b). The green and blue volumes represent the regions around the molecules where it is 50 and 100 times more probable to find a lithium cation compared with the homogeneous distribution respectively. Snapshots from the simulations of the solvation shells illustrating the SDFs are also presented in the right side. . 135

6.8 Enthalpy of exchange of M^+ (a) or M^{2+} (b) by Li^+ in a solution of EAN. Closed circles, experimental data; Open circles, MD results. 136

6.9 Integrands of Eq. (6.20) for all the simulated monovalent (top) and divalent (bottom) metal cations. The distance is referred to the surface of the cations. The shifted charge distributions are represented in the insets. 138

6.10 Electrostatic work of solvation of an alkali metal cation in EAN calculated according to Eq. (6.20) (circles and solid lines) and (6.21) (triangles and dashed lines), relative to the value of lithium for monovalent salts (blue) and magnesium for divalent ones (orange). 139

6.11 Radial distribution functions of nitrate anions (top) and ethylammonium cations (bottom) around the salt cations. The distances are measured to the metal surface and the colours are determined by the electric field at the cations interface. 142

USC UNIVERSIDADE DE SANTIAGO DE COMPOSTELA

7.1 Atomic structure and atom labelling of (left) the Keggin unit of the 12-tungstophosphoric acid H_3WPA and (right) imidazole in its neutral form. In the Keggin structure, a distinction is made between internal (O_i), terminal (O_t), bridging (O_b) and corner shared (O_c) oxygen atoms. On imidazole, the hydrogen atoms are at position N^1, C^2, C^4 and C^5, while N^3 is the proton acceptor site. 148

7.2 Raman spectra recorded at room temperature for H_3WPA (blue) and $Imid_3$WP (red), in the low-frequency region (A), in the mid-frequency region (B), and in the high-frequency region (C). In B and C, vertical black dashed lines indicate the position of some vibrational modes calculated (after scaling) for protonated imidazole (i.e. for the imidazolium cation) as presented in reference 299. In B, asterisks indicate vibrational modes arising from the imidazolium cation. In C, the Raman spectrum of H_3WPA has been vertically offset for clarity, together with the respective fitting components and the fit result. The fit results for both H_3WPA and $Imid_3$WP are shown as a white curve superimposed to the experimental data. 158

7.3 A: Thermogravimetric analysis of $Imid_3WP{\cdot}nH_2O$ in the temperature range 25 - 500 °C. The blue arrows indicate the temperature at which the DSC measurements has shown endothermic transitions. B: Temperature dependence of the W=O_t stretching mode measured by Raman spectroscopy. C: Comparative plot showing the mass loss event and the Raman shift change in the temperature range 25 - 145 °C. . 161

USC UNIVERSIDADE DE SANTIAGO DE COMPOSTELA

7.4 Arrhenius plot of the proton conductivity measured for the salt hydrate $Imid_3WP{\cdot}nH_2O$ (red filled circles) upon heating and subsequent cooling. The conductivity values for the reference material $H_3WPA{\cdot}nH_2O$ ($n\approx0$) measured by us in this study (yellow circles) and reported by Tjapkin et al.[276] (yellow diamonds) are also shown for comparison, as well as the conductivity values reported by Mioc et al.[279] for $MgHWPA{\cdot}nH_2O$ (n=12) (yellow triangles). Dashed lines are fits to the experimental data. 164

7.5 Most probable molecular orientations and types of hydrogen bonds that can be established between the imidazolium cation and the WP anion. 168

7.6 A: ^1H magic angle spinning (MAS) experiments performed in the solid state with spinning rates of 10 and 25 kHz. B: $^{31}P\{^1H\}$ HETCOR NMR spectra collected at 15 kHz with 800 μs of contact time. 169

7.7 XRD pattern (main) and SEM image (inset) of the $Imid_3WP$ salt hydrate. 170

7.8 Distribution of closest distances between Keggin anions (i.e. P - P distances) for all the simulated degrees of hydration (represented by the number of water molecules, *n*). The average of these distributions, along with the respective standard deviation, is shown in the inset plot. . . 172

7.9 RDFs of water molecules (A) and imidazolium cations (B) around the Keggin anions, for all the simulated degrees of hydration. 173

USC UNIVERSIDADE DE SANTIAGO DE COMPOSTELA

7.10 SDFs of water molecules around Keggin anions from two perspectives (A and B), as well as of Keggin anions around either imidazolium cations (C) or water molecules (D). The cut-off values are chosen for a better visualization and are referred to the value corresponding to a random distribution, ρ_{bulk}. In the top plots, green and blue correspond to 41.7 and 16.7 times ρ_{bulk}, while in the bottom plots green, red and blue correspond to 16.5, 12.6 and 8.9 times ρ_{bulk}, respectively. For the case of water around Keggin anions, this value is calculated assuming that water can only exist in the space not occupied by the anions. In A) and B) the O_t atoms are colored in black. 175

7.11 Schematic representation of the energy for the most relevant states along the proton transfer paths. The values of the energy are referred to the initial state which corresponds to the situation where the proton is bonded to the imidazole molecule. 176

8.1 Number density profiles for the component of the simulated mixtures in the direction perpendicular to the graphene walls. The number densities of the cossolvent molecules are scaled up by a factor of 10 for clarity. The insets in each subplot show the regions closer than 3 nm to the electrodes. 188

8.2 Radial distribution functions of cosolvent molecules (green), anions (blue) and cations (red) around water (top), methanol (middle) and ethanol (bottom) molecules. 191

8.3 Number density profiles for different atoms of $BMIM^+$. The color code for the densities is the same as the atoms in the background $BMIM^+$ cation (red for the terminal carbon of the butyl group, magenta for one of the carbon atoms of the imidazolium ring, green for the nitrogen atom bonded to the ethyl group and black for the terminal carbon of the ethyl group). 192

USC UNIVERSIDADE DE SANTIAGO DE COMPOSTELA

8.4 Orientation distribution functions for water (blue), methanol (orange) and ethanol (green) molecuels close to the anode. The inset shows the 2D histogram for the orientation and spatial distribution of the OH group of the methanol (top) and ethanol (bottom). Lighter areas represent high probabilities of finding an OH group at a distance from the graphene wall specified in the x-axis and with a given value of the cosine of the angle between the vector normal to the anode (directed towards the bulk) and the vector pointing from the oxygen to hydrogen in OH. 193
8.5 Number density profiles around the positively charged graphene wall in IL-methanol mixtures (same color code as in Fig. 8.1). The inset shows the corresponding electrostatic potential (solid blue) and the z component of the electric field (dashed red line). Regions shadowed in green represent the positions of the peaks in the density profile and the draw cosolvent molecules show the configurations with the lowest energies (i.e. those with their dipolar moment oriented in the direction of the applied electric field) in each region. 196
8.6 Number density profiles for the oxygen and carbon atoms in alcohol molecules within one nanometer from the anode. Oxygen atom density profile is plotted in green while the one relative to the carbon atom bonded to the oxygen (C1) in black and the terminal carbon of ethanol in blue. The most probable situation of the molecules are schematized with the transparent molecule representation. 197
8.7 2D anion distributions at the positively charged electrode. Each column, from left to right, represents the distributions for the pure IL and its mixtures with water, methanol and ethanol, respectively. The first, second and third rows correspond to the anion distribution in the first, second and third anionic layers, respectively. Lighter regions indicate a high probability of anion presence and dark a low probability of anion presence. 200

USC UNIVERSIDADE DE SANTIAGO DE COMPOSTELA

8.8 Left: overlaps between consecutive ionic layer density maps for anions in the pure IL; bottom, anions in the first (red) and second (green) layers; top, anions in the second and third (blue) layers. The yellow and cyan regions are a consequence of the overlapping between red and green and between green and blue, respectively. Right: snapshot of the pure IL MD simulation where the herringbone-like structure can be appreciated in the anions' distribution. Graphene carbon atoms are represented in grey. 201

8.9 Mean cluster size and eccentricity values for the clusters in the density maps of the first ionic layer for the simulated systems. 202

8.10 Polar representations of the integrals of the Fourier transformations of the anions density maps in the first ionic layer next to the anode for the simulated systems. The full Fourier transforms are shown in the top left corner for each simulated systems. 204

8.11 Mean square displacement for the anions in the first ionic layer close to the anode for the simulated systems in log-log scale. 207

8.12 Anion (blue) and cation (red) density profiles. Solid lines, graphene walls; dashed lines, implicit walls with benzene carbon atoms; dotted lines, implicit walls with silicon. . . . 208

8.13 Lateral structure of anions in the three layers closest to implicit walls of benzene carbon atoms (left column) and of silicon atoms (right column). 210

USC UNIVERSIDADE DE SANTIAGO DE COMPOSTELA

8.14 Top: theoretically predicted 2D density maps by Eq. (8.12) for the first three ionic layers closest to the anode. Bottom: charge-density profiles calculated with the ionic density profiles for the pure system between graphene walls ($\Phi_C(z)$, in solid red) and the one predicted by Eq. (8.6) with the parameters fitted to the simulation results ($\Phi(z)$, in blue). The solid blue line corresponds to the region employed for the fit, which excludes the high packing region and is delimited by the vertical dotted black line, while dotted blue line is the extrapolation. 212

9.1 Number density profiles for anions (blue) and cations (red) for the simulations performed changing the distance between interfaces. The slit size of each graph can be read in the Y axis. These profiles can not be quantitatively analyzed as they are a projection of a 3D plot so the height of the curves are scaled differently. However, they are accurate enough to compare the ionic distribution along the Z axis as the slit size changes. 228

9.2 Total number density (blue) and potential energy (red) for the simulated systems with 500 ionic pairs changing the distance between walls. 230

9.3 MSDs in log-log scale for the anions in the simulations with slit sizes of 1, 2, 3, 4, 5, 6, 8 nm and 500 ionic pairs (excluding the 8 nm simulation which was performed with 1000 ionic pairs). The MSD for the anions in bulk conditions is also represented (solid black) as well as the unit slope line (dashed black). 231

USC UNIVERSIDADE DE SANTIAGO DE COMPOSTELA

9.4 (a) Anions' MSDs for all the performed simulations with 500 ionic pairs as well as the one for the system with 1000 ionic pairs and 8 nm of distance between walls. (b) and (c) summarize the dependence of the diffusion coefficients and position fluctuations, respectively, obtained fitting the MSDs between 10 and 20 ns (shadowed region) to the Eq. (9.2). The results for bulk simulation are also represented in black dashed lines for comparison. 232

9.5 Structural descriptors for the simulations changing the number of ionic pairs with 1.7 nm of wall separation: (a) density profiles for anions and cations along the Z axis; (b) coordination number of anions around cations as a function of distance; (c) number of hydrogen bonds per molecule. The dotted black line represents the average number of hydrogen bonds per ionic pair in bulk simulations and the shadowed region covers its standard deviation. 234

9.6 (a) Anions' MSDs for the simulations with 1.7 nm of separation between walls and different number of ionic pairs. (b) and (c) represent the dependence with the inverse of the lateral simulation box size of the diffusion coefficients and position fluctuations, respectively, obtained fitting the MSDs between 10 and 20 ns (shadowed region) to the Eq. (9.2). . 235

9.7 Same representation as in Fig. 9.1, but now for simulations performed varying the distance between interfaces from 1 to 3 nm keeping the lateral simulation box size constant. . 237

9.8 (a) Total number density (blue) and potential energy per ionic pair (red); (b) number of hydrogen bonds per ionic pair for simulations with constant lateral box size. The dotted black line represents the average number of hydrogen bonds per ionic pair in bulk simulations and the shadowed region covers its standard deviation. 238

USC UNIVERSIDADE DE SANTIAGO DE COMPOSTELA

9.9 (a) Anions' MSDs for the simulations with constant lateral box size. (b) and (c) summarize the dependence of the diffusion coefficients and position fluctuations obtained in the same way as for Fig. 9.4. The results for bulk simulation are also represented in black dashed lines for comparison. . 240

9.10 Anions' VACFs for the simulations with constant lateral box size. The inset represents the dependence of the collision time with the slit size of the simulation, i.e. the intersection of VACFs with the small black line placed at around $t = 0.12$ ps. 241

9.11 Top: the MSDs for the anions in different layers in the simulation with slit size of 8 nm. Bottom: the anion's density profile with shadowed regions delimiting the anions layers. 244

9.12 Comparison between the MSD for the system with wall separation of 8 nm and those obtained from confined simulations and Eq. (9.4). Left: the whole curves for the estimated MSDs, the one calculated from the simulation (solid black) and the MSD for anions in bulk (dashed black) used in Eq. (9.4). Right: the average normalized distance between each test MSD and that calculated from the simulation between $t = 10$ ns and $t = 20$ ns. 245

10.1 Radial distribution functions (RDFs) and coordination numbers. (a) Cation-anion, (b) alcohol-anion, (c) alcohol-cation, and (d) alcohol-alcohol RDFs obtained from simulations of [BMIM][I]-alcohol mixtures with different IL molar fractions, indicated by different colours (see the colour bar on the right). The insets show coordination numbers as functions of IL molar fraction. The coordination numbers have been calculated by integrating the RDFs up to the first solvation shell, denoted by vertical black dashed lines in the main figures. 256

USC UNIVERSIDADE DE SANTIAGO DE COMPOSTELA

10.2 Spatial distribution functions (SDFs) of $[I]^-$ at $[BMIM]^+$ obtained from molecular dynamics simulations of [BMIM][I] mixed with alcohols for IL molar fractions (a) 0.1, (b) 0.5, and (c) 1. The isosurfaces represent the regions with a more than ten times higher probability of finding an anion than the probability of a homogeneous distribution determined by the anion bulk density. 257

10.3 Velocity autocorrelation functions (VACFs) and vibrational density of states (VDOS). Normalised VACFs obtained by molecular dynamics simulations are shown for different molecular species and for different IL volume fractions, as indicated by different colours (see the colour bar on the right). The insets show the corresponding VDOSs. Note that the colour code is set according to the volume fraction of IL (ϕ_{IL}), which is more convenient for further comparison with theoretical predictions (see Table S1 and S2 in the SI for the correspondence between molar and volume fractions). 259

10.4 Self-diffusion coefficients of ions. The diffusion coefficients have been calculated using Eq. (10.3) (dashed lines) and Eq. (10.2) (solid lines). 261

10.5 Ionic conductivities calculated using the Nernst-Einstein approximation with the diffusion coefficients obtained from MSDs and VACFs and by using the Green-Kubo equation for the mixtures with [BMIM][I]. 262

10.6 Comparison of the simulation and experimental results for two ionic liquids. The plots show the Bayesian regression of the experimental and computational results of the conductivities to the pseudo-lattice random-alloy model, Eq. (10.7), as a function of IL volume fraction. The white lines inside the coloured regions represent the most probable fit. The coloured regions are the result of the superposition of randomly chosen 1% of all the curves estimated by the regression. 264

USC UNIVERSIDADE DE SANTIAGO DE COMPOSTELA

10.7 Average jumping frequency $\bar{\nu}$ as a function of the ion volume fraction. The symbols show the results obtained by computing $\bar{\nu}$ directly from simulations. The solid lines show the results obtained by using Eq. (10.12) as described in the text. The top plot is for [BMIM][I] and the bottom plot for [EMIM][I] mixtures. 269

USC UNIVERSIDADE DE SANTIAGO DE COMPOSTELA

List of Tables

6.1 Values of molar solution enthalpy of EAN(l), $LiNO_3$(cr), KNO_3(cr), $RbNO_3$(cr), $CsNO_3$(cr), $Mg(NO_3)_2{\cdot}6H_2O$(cr) and $Ca(NO_3)_2{\cdot}4H_2O$(cr) in water at 298.15 K. 125

6.2 Enthalpies of formation of hydrated and non-hydrated divalent nitrate salts and water. 127

6.3 Difference between B and $\Delta_{\text{sol}}H_2$ for all the studied salts. The results for the dehydrated salts were calculated using the results from the previous section. The number of ions per unit volume in the crystal phase is presented only for the anhydrous salts. 129

6.4 Enthalpy of solution at infinite dilution in the liquid phase ($\Delta_s H_m^{\infty}(\text{M}(\text{NO}_3)_\text{v})$), enthalpy of formation of alkaline metal in the gas phase ($\Delta_f H(\text{M}^{\text{v}+})$(g)), enthalpy of formation of alkaline metal salt in the solid phase ($\Delta_f H(\text{M}(\text{NO}_3)_\text{v})$), enthalpy of formation of nitrate in the gas phase ($\Delta_f H(\text{NO}_3{}^-)$), enthalpy of solvation of alkali metal salt ($\Delta_{\text{solv}} H_m^{\infty *}(\text{M}(\text{NO}_3)_\text{v})$) and enthalpy of solvation for the exchange of Li^+ for M^{v+} in EAN solution ($\Delta_{\text{exc}} H_m^{\infty *}(\text{Li}^+ \text{ to } \text{M}^+)$). All values are in kJ mol^{-1}. 131

7.1 Observed Raman active vibrational modes and proposed assignment 156

8.1 Ratio between the probabilities of finding cosolvent molecules near the electrodes for the simulated systems and the value corresponding to the homogeneous case. 189

USC UNIVERSIDADE DE SANTIAGO DE COMPOSTELA

8.2 Values of the integral of the Fourier transformation eccentricities and χ parameter (Eq. (8.3)) for the clusters in the patterns for the first ionic layer close to the anode (see Fig. 8.9). 204
8.3 Surface area fraction of the regions occupied by the anions in the first layer density maps for every simulated system. . 205

9.1 Number of anions in each layer of the simulation with a slit size of 8 nm during the whole simulation. 243

10.1 The most probable values of the pseudo-lattice random-alloy model fit to the computational and experimental results for mixtures of [EMIM][I] and [BMIM][I] with ethanol. 266

USC UNIVERSIDADE DE SANTIAGO DE COMPOSTELA

List of publications included in this thesis

- **3D structure of the electric double layer of ionic liquid-alcohol mixtures at the electrochemical interface,** José M. Otero-Mato, Hadrián Montes-Campos, Óscar Cabeza, Diddo Diddens, Alina Ciach, Luis J. Gallego, Luis M. Varela, *Physical Chemistry Chemical Physics,* **48**(20), 30412-30427 (2018). **Journal information:** Impact factor in 2018: 3.567. Category: Physics, Atomic, Molecular & Chemical. Ranking inside category: 9/36 (Q1).

- **GADDLE Maps: General Algorithm for Discrete Object Deformations Based on Local Exchange Maps,** José M. Otero-Mato, Hadrián Montes-Campos, Martín Calvelo, Rebeca García-Fandiño, Luis J. Gallego, Ángel Piñeiro, Luis M. Varela, *Journal of chemical theory and computation,* **2**(14), 466-478 (2018). **Journal information:** Impact factor in 2018: 5.313. Category: Physics, Atomic, Molecular & Chemical. Ranking inside category: 6/36 (Q1).

- **Solvation in ionic liquid-water mixtures: A computational study,** José M. Otero-Mato, Volker Lesch, Hadrián Montes-Campos, Jens Smiatek, Diddo Diddens, Óscar Cabeza, Luis J. Gallego, Luis M. Varela, *Journal of Molecular Liquids,* **292**, 111273 (2019). **Journal information:** Impact factor in 2019: 5.065. Category: Physics, Atomic, Molecular & Chemical. Ranking inside category: 4/37 (Q1).

- **Nanoconfined ionic liquids: A computational study,** José M. Otero-Mato, Hadrián Montes-Campos, Óscar Cabeza, Luis J. Gallego, Luis M. Varela, *Journal of Molecular Liquids,* **320**, 114446 (2020). **Journal information:** Impact factor in 2020: 6.165. Category: Physics, Atomic, Molecular & Chemical. Ranking inside category: 4/37 (Q1).

- **A New Solid-State Proton Conductor: The Salt Hydrate Based on Imidazolium and 12-Tungstophosphate,** Anna

USC UNIVERSIDADE DE SANTIAGO DE COMPOSTELA

Martinelli, José M. Otero-Mato, Mounesha N. Garaga, Khalid Elamin, Seikh Mohammad Habibur Rahman, Josef W. Zwanziger, Ulrike Werner-Zwanziger, Luis M. Varela, *Journal of the American Chemical Society,* **34**(143), 13895-13907 (2021). **Journal information:** Impact factor in 2020: 15.419. Category: Chemistry, Multidisciplinary. Ranking inside category: 15/178 (Q1).

- **Structure, Dynamics and Conductivities of Ionic Liquid-Alcohol Mixtures,** José M. Otero-Mato, Hadrián Montes-Campos, Víctor Gómez-González, Martín Montoto, Óscar Cabeza, Svyatoslav Kondrat, Luis M. Varela, *Journal of Molecular Liquids,* **355**, 118955 (2022). **Journal information:** Impact factor in 2020: 6.165. Category: Physics, Atomic, Molecular & Chemical. Ranking inside category: 4/37 (Q1).

- **Enthalpy of solvation of alkali metal salts in a protic ionic liquid: Effect of cation charge and size,** Juan J. Parajó, José M. Otero-Mato, Ana I. M. C. L. Lobo Ferreira, Luis M. Varela, Luis M. N. B. F. Santos, *Journal of Molecular Liquids,* **360**, 119228 (2022). **Journal information:** Impact factor in 2020: 6.165. Category: Physics, Atomic, Molecular & Chemical. Ranking inside category: 4/37 (Q1).

USC UNIVERSIDADE DE SANTIAGO DE COMPOSTELA

List of publications related to this thesis

- **Molecular dynamics simulation of the behaviour of water in nano-confined ionic liquid-water mixtures,** Borja Docampo-Álvarez, Víctor Gómez-González, Hadrián Montes-Campos, José M. Otero-Mato, Trinidad Méndez-Morales, Óscar Cabeza, Luis J. Gallego, Ruth M. Lynden-Bell, Vladislav B. Ivaništšev, Maxim V. Fedorov, Luis M. Varela, *Journal of Physics: Condensed Matter,* **46**(28), 464001 (2016).

- **Two-dimensional pattern formation in ionic liquids confined between graphene walls,** Hadrián Montes-Campos, José M. Otero-Mato, Trinidad Méndez-Morales, Óscar Cabeza, Luis J. Gallego, Alina Ciach, Luis M. Varela, *Physical Chemistry Chemical Physics,* **36**(19), 24505-24512 (2017).

- **Nanostructured solvation in mixtures of protic ionic liquids and long-chained alcohols,** Hadrián Montes-Campos, José M. Otero-Mato, Trinidad Méndez-Morales, Elena López-Lago, Olga Russina, Óscar Cabeza, Luis J. Gallego, Luis M. Varela, *The Journal of chemical physics,* **12**(146), 124503 (2017).

- **Molecular dynamics simulations of the structure of mixtures of protic ionic liquids and monovalent and divalent salts at the electrochemical interface,** Víctor Gómez-González, Borja Docampo-Álvarez, José M. Otero-Mato, Óscar Cabeza, Luis J. Gallego, Luis M. Varela, *Physical Chemistry Chemical Physics,* **18**(20), 12767-12776 (2018).

- **Mixtures of Lithium Salts and Ionic Liquids at Defected Graphene Walls,** Hadrián Montes-Campos, José M. Otero-Mato, Roberto Carlos Longo, Óscar Cabeza, Luis J. Gallego, Luis M. Varela, *Journal of Molecular Liquids,* **289**, 111083 (2019).

USC UNIVERSIDADE DE SANTIAGO DE COMPOSTELA

- **Borophene vs. graphene interfaces: Tuning the electric double layer in ionic liquids,** Víctor Gómez-González, José M. Otero-Mato, Hadrián Montes-Campos, Xabier García-Andrade, Amador García-Fuente, Andrés Vega, Jesús Carrete, Óscar Cabeza, Luis J. Gallego, Luis M. Varela, *Journal of Molecular Liquids,* **303**, 112647 (2020).

- **Electronic and optical properties of borophene and graphene with an adsorbed ionic liquid: A density functional theory study,** Kazem Zhour, José M. Otero-Mato, Fouad El Haj Hassan, Hussein Fahs, Majid Vaezzadeh, Elena López-Lago, Luis J. Gallego, Luis M. Varela, *Journal of Molecular Liquids,* **316**, 113803 (2020).

- **Ionic liquids nanoconfined in zeolite-templated carbon: A computational study,** Hadrián Montes-Campos, Trinidad Méndez-Morales, José M. Otero-Mato, Óscar Cabeza, Luis J. Gallego, Enrique Lomba, Luis M. Varela, *Journal of Molecular Liquids,* **318**, 114264 (2020).

- **The interaction of ammonia with the protic ionic liquid ethylammonium nitrate: A simulation study,** Alejandro Rivera-Pousa, José M. Otero-Mato, Alberto Coronas, Anthony J. Stone, Ruth M. Lynden-Bell, Trinidad Méndez-Morales, Luis M. Varela, *Journal of Molecular Liquids,* **320**, 114437 (2020).

- **Tuning the hybrid borophene-/graphene-ionic liquid interface: Effect of metal cations on the electronic and photonic properties,** Kazem Zhour, José M. Otero-Mato, Fouad El Haj Hassan, Hussein Fahs, Majid Vaezzadeh, Elena López-Lago, Luis J. Gallego, Luis M. Varela, *Journal of Molecular Liquids,* **321**, 114759 (2021).

- **Computational study of the structure of ternary ionic liquid/salt/polymer electrolytes based on protic ionic liquids,**

USC UNIVERSIDADE DE SANTIAGO DE COMPOSTELA

José M. Otero-Mato, Alejandro Rivera-Pousa, Hadrián Montes-Campos, Óscar Cabeza, A. Heuer, Diddo Diddens, Luis M. Varela, *Journal of Molecular Liquids,* **333**, 115883 (2021).

USC
UNIVERSIDADE DE SANTIAGO DE COMPOSTELA

USC
UNIVERSIDADE
DE SANTIAGO
DE COMPOSTELA

Part I

Introduction and Methods

USC
UNIVERSIDADE DE SANTIAGO DE COMPOSTELA

USC
UNIVERSIDADE
DE SANTIAGO
DE COMPOSTELA

1- Introduction

1.1 Motivation and Purpose

The world population has been growing almost exponentially during the last decades and, although the annual growth rate has been decreasing since 1968 (see Fig. 1.1), the truth is that every day, the population increases in more than two hundred thousand people. During the last years, specially enhanced by the pandemic, we saw how the shortage of raw materials affected our day to day: lack of stock of electronic devices for all kind of applications (vehicles, computers, appliances...), slow supply of materials for the industry at high costs, an increase of the price of the electricity, etc. Even though the increase of the population was not the main reason for this lack of resources, the pandemic, as well as the war between Russia and Ukraine in Europe, boosted the problems. Even more, we have to add that, critical raw materials, as well as oil and gas reserves, are located in very specific regions around the world which do not always have good international relations with our countries. Taking all this into account, to maintain our current lifestyles (note in Fig. 1.1 that the GDP is directly proportional to the population), some actions need to be taken. On the one hand, the energy production must increase to face the increment of the demand using traditional energy resources in the short term but also, and more important, develop new technologies or improve the existing ones involving renewable and green energies to replace traditional non-renewable ones in the medium-long term. This replacement has been already started some years ago as it is also represented in Fig. 1.1, where it can be seen that the percentage of the consumption of energy obtained from renewable sources has being increasing. However, to reach the objectives of net-zero emissions by 2050, aimed by the European Commission, the replacement should be much faster. On the other hand, we have to become energetically

USC UNIVERSIDADE DE SANTIAGO DE COMPOSTELA

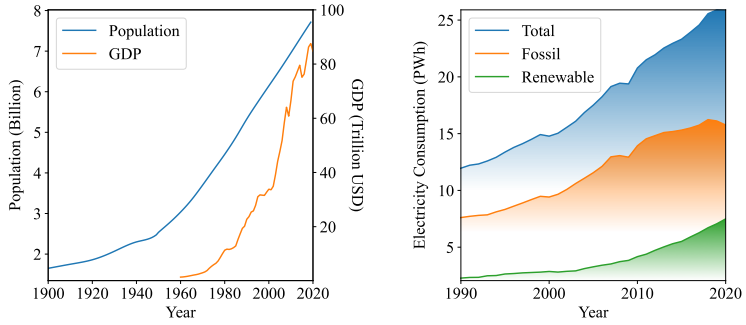

Figure 1.1: Evolution of global population, GDP and renewable and non-renewable energy production in the last decades.

more efficient and improve the recyclability of the materials, specifically of the scarce critical ones.

In terms of reducing the dependence of non-renewable energy sources, a lot of efforts are being made specially by the European Community, which plans to assign more than 1.2 trillion euros through NextGenerationEU funding for the next 7 years. These efforts are being devoted mainly to digitalization and *green* projects, most of which will be focused on the building of new infrastructure related to renewable energy sources such as photovoltaic or wind power plants. However, given the dependent nature of these energy sources on external factors, it is necessary that their development go hand in hand with the development of new technologies to store the excess energy for later reuse. In this sense, it is worth mentioning the use of batteries or the production and storage of green hydrogen. Regarding the development of new batteries, there is still a lot to do, from increasing energy storage densities to reducing the use of critical raw materials such as lithium or cobalt. With regard to hydrogen storage, there is also much to be done in this field. Currently, the most common way to store hydrogen is to pressurize it in tanks at pressures larger than 600 bar.

USC UNIVERSIDADE DE SANTIAGO DE COMPOSTELA

Working at these high pressures considerably hinders the use of this gas in certain applications, specially when the security of the tanks can not be guaranteed. One of the possible solutions to this problem is to store hydrogen in solid materials (nanoporous structures) or in liquid solutions that allow reversible adsorption and desorption of the gas. As stated, much work remains to be done to improve these technologies.

Ionic liquids (ILs) are very good candidates to be present in multiple applications in these fields. Due to their good electrochemical properties (which will be discussed in the next section), they are surely going to be part of the next generation of batteries and supercapacitors.[1] Moreover, due to their good solvation properties, they are also ideal for recyclability applications or hydrogen storage. For instance, recent investigations are using ILs for recycling cellulose from biomass[2] or, closely related with critical materials, elements with interest for electrochemical applications such as lithium, manganese, cobalt and nickel.[3] Also closely related with energy storage, ILs are also being studied for their usage as hydrogen solvents.[4] Another interesting application of ILs is to use them in conjunction with nanoparticles to be applied in catalysis, electrochemical or separation process.[5] Even more, using optical or magnetically active nanoparticles, photonic devices can be developed, opening the door to new sensor technologies which could be implemented in batteries of the future (see the BATTERY 2030+ roadmap in Ref. 6). In summary, ILs are considered very promising materials for the most important necessities of the society in the next decades. For this reason, a very deep knowledge of their properties must be achieved in order to exploit their applicability as much as possible.

1.2 General and Specific Objectives

In this context of technological development where the aforementioned fields play a key role, ILs are among the materials with a larger number of potential applications. This thesis aims to contribute to the fundamental understanding of these dense ionic fluids, focusing especially on

USC
UNIVERSIDADE DE SANTIAGO DE COMPOSTELA

the characterization of their solvation properties at a molecular level. To achieve this objective, pure ILs and their mixtures with different molecular cosolvents will be studied in presence of different structures. Particularly, the following specific objectives were addressed:

1. Development of a computational tool that allows the molecular simulation at different space/time-scales. To be able to study dispersions of different nanostructures in ILs and their mixtures using molecular simulations, it is necessary to combine the computational cost reductions given by coarse-grained force fields and the atomic resolution of conventional fully-atomistic ones. This tool will be presented in Chapter 4.

2. Characterization of the solvation of relatively small spherical particles in ILs, starting with fixed size ideal spheres with different charges (Chapter 5), continuing with the analysis of the effects of the size (Chapter 6) and finally, investigating more complex structures, where proton transference plays a key role (Chapter 7). The effects of the addition of water to the ionic systems will be also analysed.

3. Study of the behaviour of ILs and their mixtures in the presence of very large nanostructures. In this approach, we modelled the structures as planar interfaces of different materials and charges. We also analysed the effect of the nanoconfinement in these fluids, which could be useful to understand the solvation of nanostructures with nanometric pores. These studies will be detailed in Chapters 8 and 9.

4. Validation of a sound theoretical framework to describe the transport properties of ILs and their mixtures. This framework not only describes the dependence of the ionic conductivity of ILs with the cosolvent concentration or temperature, but it also relates it with microscopic magnitudes of the systems. This validation will be presented in Chapter 10 and it is crucial to understand the transport properties of dispersions of nanostructures.

USC
UNIVERSIDADE DE SANTIAGO DE COMPOSTELA

In the next section we will introduce ILs, their main properties and why they are so important in the aforementioned research areas.

1.3 Ionic Liquids

Consider we have an ionic salt such as the sodium chloride. Usually these compounds are found forming crystals with very high melting temperatures (around 800 °C for sodium chloride). The main reason behind this is that their constituents, anions with negative charge and cations with positive, have the proper size and symmetry to form a regular lattice, optimizing the electrostatic potential and forming very rigid and stable configurations. However, in ILs, the anions and cations forming the salt are changed in such way that they differ in size and geometry, e.g. a large cation with an alkyl chain and delocalized charge, and a small anion. In this scenario, although we manage to arrange the ions to minimize the electrostatic energy, this structure will be very sensitive to thermal fluctuations, which translates into low melting temperatures. When this happens and the melting temperature is below 100 °C (this limit is the most widely accepted,[7] but different values can be found in the literature) we have an IL. It was Paul Walden in 1914 who firstly introduced this term to name these materials. Specifically, he was synthesizing ethylammonium nitrate (EAN) for electric conductivity measurements,[8] an IL which is still the object of numerous studies.

From this description of ILs we can say that they can be considered as molten salts. However, ILs share a lot of similarities with almost all the families of charged complex fluids (see Fig. 1.2). For instance, ILs can be thought as electrolyte solutions in the very high ionic concentration limit. This means that the theories developed for electrolyte solutions, such as the Debye–Hückel theory or the Bahe–Varela formalism, can also be applied for mixtures of ILs with molecular cosolvents (always in the concentration range where the formalisms apply). On the other hand, ILs can also be thought as ionic surfactants with small alkyl chains, or as any other type of fluid that tends to order forming meso-

USC UNIVERSIDADE DE SANTIAGO DE COMPOSTELA

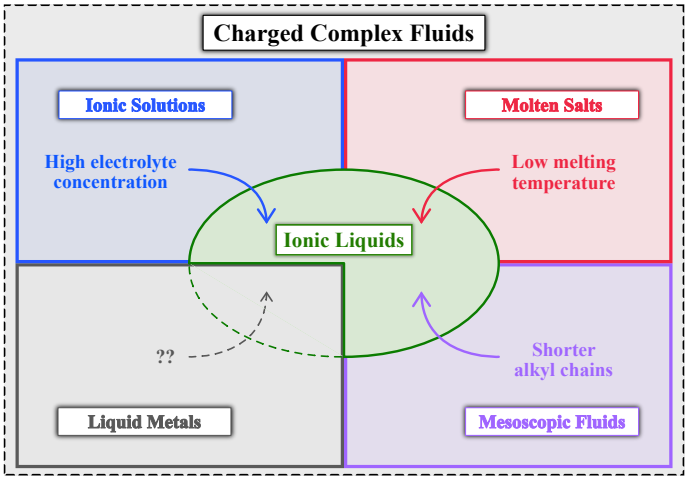

Figure 1.2: Schematic representation of different families of complex charged fluids and their relatation with ILs.

scopic structures. Indeed, there are reports of ILs being used as liquid crystals due to this mesoscopic structuring hability.[9]

Although there exists a plethora of ILs, they can be grossly classified in two big families depending on their synthesis process. On the one hand, protic ILs[10] (PILs) are those obtained from a Brønsted acid-base reaction, i.e. a proton transfer from one molecule to another:

$$A + B \longrightarrow AH^+ + B^-$$

Due to this synthesis process, PILs have a proton available to form hydrogen bonds, which makes them usually good solvents for polar compounds. For instance, the aforementioned EAN, which is a PIL, stands out from other ILs because of its similarities with water. Indeed, in Chapter 6, we present a work where these similarities are highlighted and explained from a molecular point of view. On the other hand, ILs that do not fit under this definition are called aprotic ILs (AILs). These are usually harder to synthesize, and thus, they are frequently more expensive.

USC UNIVERSIDADE DE SANTIAGO DE COMPOSTELA

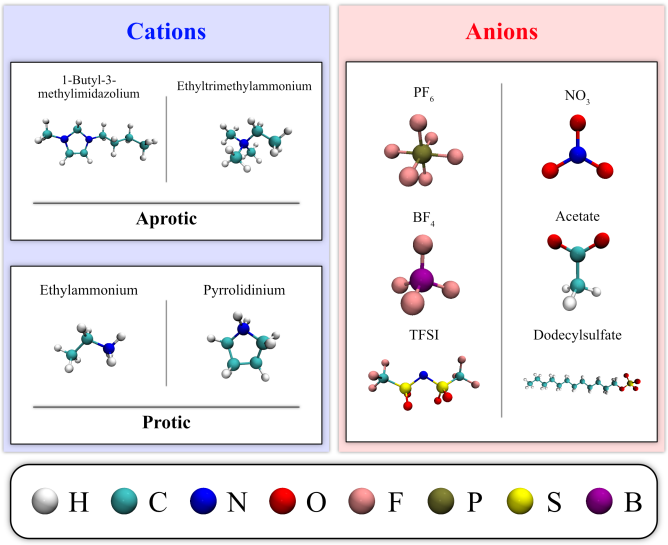

Figure 1.3: Molecular structure of most common anions and cations.

Despite this classification, all the ILs are formed by negatively charged anions and positively charged cations. Generally, the former consist of small inorganic ions (NO_3^-, PF_6^-, BF_4^-) and the latter are usually formed by different families (imidazolium, pyrrolidinium, pyridiniu, ammonium...) linked to organic alkyl chains. It is worth mentioning that there are some relevant exception to this rule. For example, the bis(trifluoromethane)sulfonimide anion (usually called TFSI) is relatively large compared with other anions and it is widely used in electrochemical applications. Some examples of commonly used anions and cations are represented in Fig. 1.3.

What makes ILs so interesting for a wide variety of applications are their properties which are closely related with the fact that these materials are formed exclusively by ions. In the following, we summarized some of their most interesting properties and some applications derived from them:

- **Tunability**: Depending on the selection of the anion and cation

USC UNIVERSIDADE DE SANTIAGO DE COMPOSTELA

forming a given IL, its properties can be adjusted to optimize a certain application. For instance, the [EMIM][TFSI] is usually a good candidate for electrochemical applications. If, for some reason, a certain application requires a similar IL but with lower ionic conductivity, one could try to increase the size of the ethyl chain of the cation, maybe replacing it with a $BMIM^+$ cation. It is well known that increasing the size of the cation decreases the ionic conductivity[11] due to a decrease of its mobility. Combining the currently known anions and cations more than one million of different ILs can be obtained. Moreover, ILs can be generated combining a cation with two different anions (or vice versa) leading to so-called ternary ILs, which exponentially increases the number of available combinations.[12]

- **Low vapour pressures and low volatility**: Due to the strength of the Coulomb interactions between the constituents of ILs, it is, energetically speaking, very hard for an anion-cation pair to escape from the liquid bulk. In other words, the cohesion energy between the ions is very large. Indeed, for various ILs the vapour pressure undetectable with currently experimental techniques. For example, the measured vapour pressure for [BMIM][TFSI] at 120 °C is 1.2 Pa, which is in the order of magnitude of other solvents with very large molecules such as polyethylene glycols.[13] For some other ILs, this magnitude can only be measured by increasing the temperature to a point where the IL constituents react and form volatile compounds.[14]

- **Thermal stability**: Very much related with the previous point, ILs do not degrade easily even at high temperatures. This means that these materials are guaranteed to maintain their properties even in extreme conditions of high temperatures and pressures. There are experiments where imidazolium based ILs did not show any sign of degradation even heating them during five hours at 300 °C.[15] On the other hand, some PILs decompose before reaching the boiling points.[10] All these make ILs perfect for being applied

USC UNIVERSIDADE DE SANTIAGO DE COMPOSTELA

in different devices such as fuel cells[1] or thermal storage.[16]

- **High viscosity**: Again, due to the strong ion-ion interactions, ILs usually show very slow dynamics leading to quite viscous systems. It is reported that increasing the alkyl chain length of the cations increases the viscosity due to an increase in the van der Waals interactions.[17] On the other hand, increasing the size of the anions induces a more delocalized charge distribution and thus weakens the hydrogen bonding, i.e. the viscosity decreases.[18] This, together with the previous mentioned good thermal properties, make ILs perfect candidates to be used as lubricants.[19] It is worth mentioning that this slow dynamics of the molecules of the ILs can be significantly enhanced with the addition of molecular cosolvents even in very low concentrations.[20] In this way, the dynamic-related properties can be easily tuned for other applications.

- **Wide electrochemical window and high ionic conductivities**: Due to the fact that ILs are generally formed by species with almost no reduction/oxidation tendency (as they are already partially ionized), they are chemically stable under relatively large voltages. This confers ILs a very good electrochemical stability, preventing them upon chemical degradation. To put some numbers, an electrochemical window of around 6 V is reported for the N-butyl-N-methylpyrrolidinium bis(trifluoromethylsulfonyl)amide IL[21] and around 4.5 V for [EMIM][BF_4].[17] It is true that similar values are also obtained in some organic solvents (values for propylene carbonate or acetonitrile ca. 4 V). However, ILs have the advantage that, due to be formed by charge carriers, present a relatively high ionic conductivity which can be increased with the addition of small amounts of solvent (such as those mentioned with relatively high electrochemical windows). This makes ILs perfect to be used as advanced electrolytes in batteries or supercapacitors.[22]

- **Good solvation properties**: Due to the wide variety of anions

USC UNIVERSIDADE DE SANTIAGO DE COMPOSTELA

and cations available to chose to form an IL, it is almost guaranteed that there is at least one IL capable to solvate a certain solute. Moreover, the polarity of the fluid can also be tuned to create hydrophilic or hydrophobic solvents or even amphiphile ones. Due to this, ILs are usually called designer solvents.[23] It is worth mentioning at this point the nanostructure solvation paradigm, which explains the solvation properties of ILs from a molecular point of view. It is well known that two different regions can be identified inside an IL looking at their polarity. On one hand, there is a polar region formed by the charge centres of the ions and their polar groups. On the other hand, the alkyl chains (generally from the cations), tend to form organic regions.[24] This segregation translates into the appearance of nano-domains with different polarities where solvents of different types can find their place. Even more, amphiphilic molecules can also be accommodated at the interface between polar and apolar regions.[25] These good solvation properties, together with their chemical stability, make ILs ideal to be used as "universal" solvents with very high reusability, being relatively easy to recover. Their usage for cellulose dissolution,[26] biomass processing,[27] antibiotics recycling[28] or extraction of critical raw materials[3] are some examples of their applications in this matter.

USC
UNIVERSIDADE DE SANTIAGO DE COMPOSTELA

2- Methods

In the following sections the main used techniques in the development of this thesis will be introduced. All of them can be classified under computational methods or computer simulations. Computer simulations facilitate the study of a system by creating a virtual copy of it. One of the main advantage of these methods is that performing small modifications in the system being studied is a very easy task which is not the case when working with real experiments. Moreover, they provide microscopic information that is usually not accessible through experiments. However, computer simulations are not a perfect method. One of their main limitations is that the size and/or time scales of a system that can be simulated is at the end limited by the computational power. In other words, the size and time resolutions are limited by the chosen simulation technique. Nowadays, there are a lot of simulation techniques that allow the study of a wide variety of systems, going from scattering experiments in nuclear physics to calculation of stress and strains in large buildings or modelling thermal conductivity of different materials. In Fig. 2.1 some of the most important techniques are enumerated according to their space/time application range.

In this thesis, the used methods fall mainly into the molecular simulation category (the ones with less than μm of spatial resolution in Fig. 2.1). This type of simulations are used for the study of materials through their characterization at atomic levels. Going to the limit of the smallest sizes accessible with this type of simulations, we have quantum chemistry or the Density Functional Theory (DFT) based techniques. With these methods, one has access to the electronic structure of crystalline structures (which gives access to the band structures of solids) or to molecular orbitals when working with isolated molecules. These techniques are very limited in terms of the number of atoms that they can simulate (in the order of tens) and, although there are some variations of these techniques that do allow it, they are limited to calculations in the ground state and at $T = 0\,\mathrm{K}$. On the other hand, slightly increasing the

USC
UNIVERSIDADE DE SANTIAGO DE COMPOSTELA

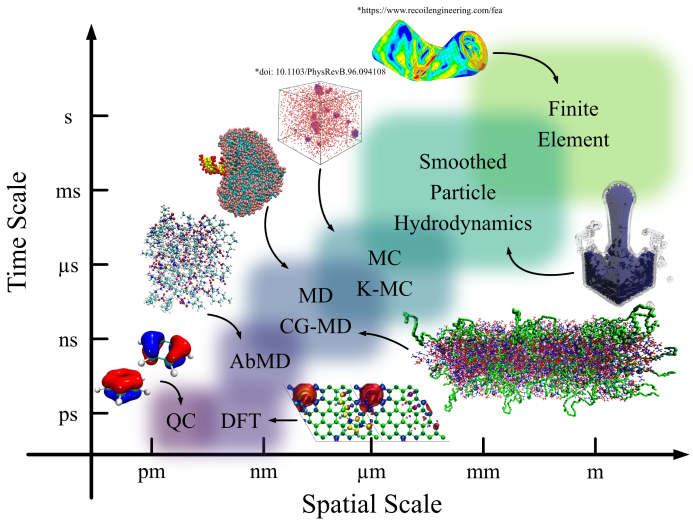

Figure 2.1: Different simulation techniques and their range of applicability in terms of time and spatial resolution. The acronyms stay for: quantum chemistry (GC), ab inition MD (AbMD), MD with coarse grained force fields (CG-MD) and kinetic Monte Carlo (K-MC).

spatial and temporal scale, we find molecular dynamics (MD) simulations. In the following sections we will explain in more detail both the DFT and the MD, detailing all those aspects that are most relevant for the development of this thesis.

2.1 Molecular Dynamics

The most used method in this thesis is, by far, that of MD simulations. MD allows us to access to the time series of the positions, velocities and forces of all the particles of a given system within a simulation box. This evolution of the positions and velocities of all the particles in the system form what is called the trajectory. The procedure to obtain the trajectory of a system is conceptually very simple. All you have to do is, given an initial configuration of the atoms in a system, calculate the forces on

USC
UNIVERSIDADE DE SANTIAGO DE COMPOSTELA

each atom using what is called the force field. With these forces and Newton's second law, the acceleration on each atom is calculated. With the acceleration and knowing the initial position and velocity, the new position and velocity after a time Δt (small enough for the integration of the equations of motion to be valid) can be calculated. By repeating this process a desired number of times, the trajectory of the system is obtained, i.e. the time series of the positions and velocities of all the particles ($\{\vec{r_k}(t), \vec{v_k}(t)\}_{k=1}^{N}$). With these magnitudes, thermodynamic averages can be calculated. For instance, the enthalpy, which plays a key role in the work presented in Chapter 6, can be calculated as the average over all the frames in the simulation:

$$H = \frac{1}{N_{\text{frames}}} \sum_{i=1}^{N_{\text{frames}}} V_i + p_i \mathcal{V}_i, \tag{2.1}$$

where V_i is the potential energy, which is calculated with the force field, p_i the pressure and $\mathcal{V}_i$ the volume of the simulation box, in each frame. Moreover, correlation functions can also be calculated, which are directly related with the transport coefficients through the Green–Kubo relations:

$$\gamma = \int_0^\infty \langle A(\vec{r}, \vec{v}, t) \cdot B(\vec{r}, \vec{v}, t') \rangle dt. \tag{2.2}$$

These relations are also used in this thesis, for instance in Chapter 10, where the ionic conductivities are calculated using the current autocorrelation function. There are a lot of programs available to perform MD simulations. For all the simulations presented in this thesis, the GROMACS[29;30] software was used. One of the main reasons to choose this software among others is that it is free, well maintained and it performs pretty well under parallelization in CPU cores, GPUs or multiple computation nodes. Moreover, it comes with a lot of extra-functionalities to post-process the simulations and to manipulate the files derived from the calculations. It is worth mentioning another software that is also widely used which is called LAMMPS.[31] This simulation suite has the advantage that allows for more flexibility in the

USC UNIVERSIDADE DE SANTIAGO DE COMPOSTELA

simulation conditions. However, GROMACS was the perfect choice for the aims of this thesis.

Although the algorithm to perform MD simulations seems quite simple, there is a whole series of details and problems that must be taken into account so that the final result is as close as possible to the analogous real system. In the following subsections we will see in detail each of the steps to be carried out to finish a simulation and what are the different problems that have to be addressed in each of these steps.

2.1.1 Initial Configuration

The first task to do to carry out a simulation is to obtain an initial configuration from which start the integration of the equations of motion. To obtain this configuration, firstly, one must calculate approximately the size of the simulation box and how many molecules must put inside it based on previous knowledge of the density of the system. Once the number of molecules is known and also is the box size, one has to decide how to distribute all the molecules inside the box. One of the most obvious (and easiest to implement) way to do that is to distribute them in a perfect lattice with the unit cell calculated to match the density requirements. However, this method, specially when working with charged molecules as those in ILs, can lead to metastable configurations where a crystalline phase is artificially created. Another option to pack the molecules is to do it randomly. Although it sounds easy, it is a hard problem to put molecules randomly inside a simulation box in a dense configuration and guarantee that there is no overlap between them. Fortunately, this problem has been already solved by Martínez *et al.*[32] providing a very useful free software called PACKMOL. This software is widely used by the community for obtaining initial configurations for MD simulations, and it was used for almost every work presented in this thesis. In Fig. 2.2 we show the resulting simulation boxes when using both methods.

USC UNIVERSIDADE DE SANTIAGO DE COMPOSTELA

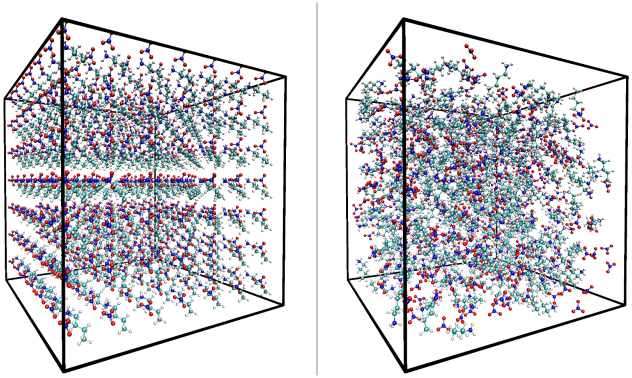

Figure 2.2: Snapshots of two initial configurations for a simulation box with EAN obtained with a lattice distribution (left) and with a random packing using PACKMOL (right).

Using this strategy to obtain the initial configurations brings another problem which is only relevant when working with very large molecules such as polymers or large atomic structures as those planned to be studied in this thesis. The problem is related with the periodic boundary conditions (pbcs). These are used to simulate infinitely large systems by replicating the simulation box in the three dimensions of space. Using this approach, when generating the initial configuration, one would expect to have large molecules going outside the limits of the box and getting into from the opposite side if pbcs are taken into account. However, PACKMOL does not contemplate this casuistic and will always place the molecules inside the box limits. This is usually not a big concern because, if the dynamics of the system is fast enough, large molecules will eventually cross the simulation box and quickly reach the equilibrium configuration. Nevertheless, as it was mentioned in the introduction, one of the major drawbacks of ILs is that they are viscous, which translates into slow molecular dynamics. In other words, very large simulation times will be required to reach the equilibrium state starting from

USC UNIVERSIDADE DE SANTIAGO DE COMPOSTELA

initial configurations that do not take pbcs into. To solve this problem, we developed a tool that, using PACKMOL at intermediate steps, is able to generate initial configurations where large molecules or structures are packed considering pbcs. This tool has already been used for simulations of mixtures with ILs and polymers[33] and is available to the community as an open source project (https://github.com/txemaotero/large-molecule-pbc-packing). Moreover, recently, the tool has been modified to allow packing with pbcs only in some directions, which is very useful in simulations with interfaces. The tool also guarantees that the large species are packked following a random homogeneous distribution. See the public repository for more information about this packing algorithm.

2.1.2 The Force Field

With the initial configuration in hand, one could start to integrate the equations of motions to obtain the trajectory of the system. However, to do that, one needs to calculate the forces acting on each atom. These forces are determined by the force field. There are a lot of available force fields, each one optimized for a certain task. Some of the most used in the literature are OPLS,[34] OPLS-AA,[35] CL&P,[36] APPLE&P,[37] GROMOS,[38] AMBER,[39] CHARMM,[40] GAFF[41] or MARTINI[42]. Although each force field comes with a set of parameters optimized for different applications, most of them share the algorithm to calculate the interactions between particles. There are two types of interactions, one between bonded atoms and one between non-bonded atoms

$$V = V_{\text{bonded}} + V_{\text{non-bonded}}. \tag{2.3}$$

To exemplify the functional form of each type, we are going to present the case the OPLS-AA as it is the most used in this thesis, although the same can be applied to other force fields. The interaction between bonded atoms has three terms, one to parametrize the force between pairs of bonded atoms, another one for triplets of atoms forming an angle

USC UNIVERSIDADE DE SANTIAGO DE COMPOSTELA

and, finally, one describing the torsion forces for groups of four atoms (dihedrals).

$$V_{\text{bonded}} = V_{\text{bonds}} + V_{\text{angles}} + V_{\text{dihedrals}}. \tag{2.4}$$

See Fig. 2.3, where a schematic representation of how these terms are related with the molecular configuration is present. The first two therms are described by harmonic oscillators with given equilibrium distances, angles and constants:

$$V_{\text{bonds}} = \sum_{\forall \text{ bonds}} K_r(r - r_{\text{eq}})^2 \tag{2.5}$$

$$V_{\text{angles}} = \sum_{\forall \text{ angles}} K_\alpha(\alpha - \alpha_{\text{eq}})^2. \tag{2.6}$$

For the dihedrals, a cosine expansion is used:

$$V_{\text{dihedrals}} = \sum_{\forall \text{ dihedrals}} \frac{V_1}{2}\left[1 + \cos(\theta + f_1)\right] + \frac{V_2}{2}\left[1 - \cos(2\theta + f_2)\right] + \frac{V_3}{2}\left[1 + \cos(3\theta + f_3)\right]. \tag{2.7}$$

This functional shape models the energy barrier that is present, for example, in polymers to go from cis to trans configurations (see Fig. 2.4).

For atoms that are separated more than 2 bonds, the non-bonded interactions are calculated as the sum of two terms: the dispersive interactions model by a Lennard–Jones (LJ) potential and the electrostatic ones calculated by the Coulomb law

$$V_{\text{non-bonded}} = \sum_{\forall\{i,j\}/i\neq j} \underbrace{4\varepsilon_{ij}\left[\left(\frac{\sigma_{ij}}{r_{ij}}\right)^{12} - \left(\frac{\sigma_{ij}}{r_{ij}}\right)^{6}\right]}_{V_{\text{LJ}}} + \underbrace{\frac{q_i q_j}{r_{ij}^2}}_{V_{\text{Coulomb}}}. \tag{2.8}$$

It has to be mentioned that these non-bonded interactions are scaled by a factor of 0.5 when the atoms are separated exactly 3 bonds. This factor, called fudge factor, is introduced to match experimental

USC UNIVERSIDADE DE SANTIAGO DE COMPOSTELA

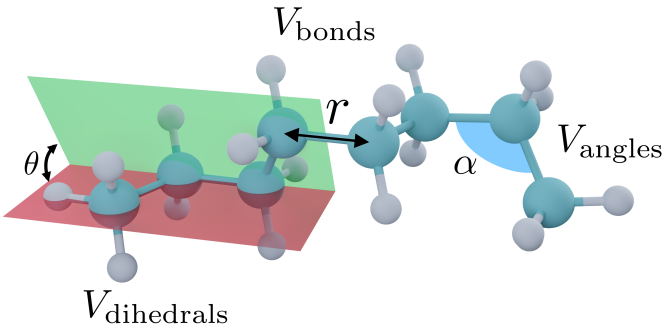

Figure 2.3: Representation of the relevant magnitudes involved in the calculation of the different terms in bonded interactions.

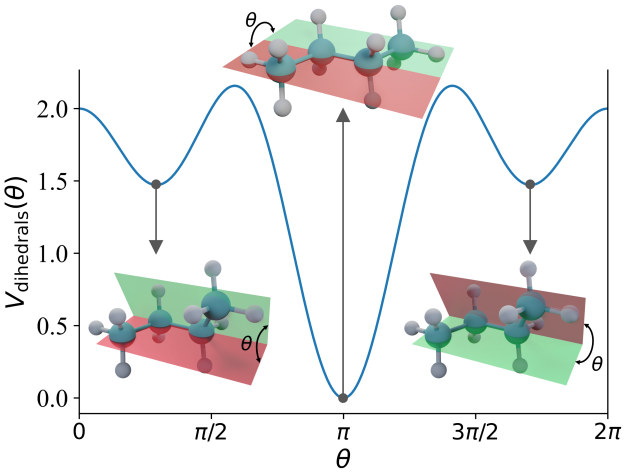

Figure 2.4: Potential energy associated to the rotation of the dihedral angle.

USC
UNIVERSIDADE DE SANTIAGO DE COMPOSTELA

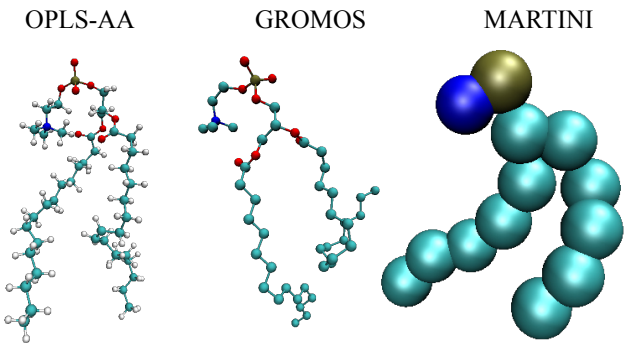

Figure 2.5: Multiple representations of the same molecule (the POPC phospholipid) using different force fields.

results and quantum mechanical calculations.[35] As it was mentioned, multiple force fields are based on small variations of this model, but the associated constant are fitted to optimize a certain application. For instance, the OPLS force field is optimized for simulating liquids and it uses a united atom model where groups of atoms are considered to be a single particle, which reduces the computational cost. Its all atom version (OPLS-AA) does take into account all the atoms. To put some other examples, AMBER is designed to accurately simulate biomolecules and CHARMM to simulate proteins. Other force fields may include additional terms to take into account other effects. For instance, the APPLE&P force field introduce many body interactions to take into account the electronic density of the atoms considering their electric dipole moments. In Fig. 2.5 some representations of the same molecule in different forcefields are presented.

It was mentioned that the original OPLS force field did not represent the molecules as the collection of all its atoms, but it assumed a united atom model. Another force field that follows this approach and plays an important role in this thesis is MARTINI.[42] This force field uses a set of

USC UNIVERSIDADE DE SANTIAGO DE COMPOSTELA

rules to convert functional groups of atoms into beads with fitted bonds between them. At the end, the number of beads representing a molecule is around five times less than the number of atoms. With this representation of the molecules, the number of operations to perform during the simulation decreases significantly. Moreover, due to the large masses of the beads, the step used to discretize the time can be increased. In summary, longer simulations of larger systems can be performed in shorter times. Of course, this is achieved by loosing information of the specific distribution of atoms. This loss of information was the motivation to develop a tool that allows the automatic conversion between force fields, which will be introduced in Chapter 4.

2.1.3 Minimization Methods

Once we have an initial configuration of the molecules inside a simulation box and we know how to calculate the forces between each particle, we need to relax the artificially generated initial configuration before starting to integrate the equations of motion. This must be done in order to avoid untrackable motions or molecular overlaps. To minimize the energy of the system, two methods were used in this thesis. For almost all the simulations, we first applied the steepest decent algorithm to the initial configuration. This algorithm basically moves iteratively all the atoms in the direction of the force acting on each of them. If we denote by $\vec{r}_n$ the position of all the atoms in the system and by $\vec{F}_n$ the force on each atom, the algorithm calculates the new positions as:

$$\vec{r}_{n+1} = \vec{r}_n + \frac{\vec{F}_n}{\max(|\vec{F}_n|)} h_n, \tag{2.9}$$

being h_n a given maximum displacement. This algorithm works very well specially with configurations far from the equilibrium. We run it for a certain number of steps and then, the output configuration is minimized using the conjugate gradient algorithm.[43] At the end, a configur-

USC UNIVERSIDADE DE SANTIAGO DE COMPOSTELA

ation with low forces on all atoms is achieved and the integration of the equations of motion can be performed to obtain an equilibrated system.

2.1.4 Integration Method

With a well minimized system, the motion of each atom can be calculated without the risk of finding very large forces that may induce molecular overlaps or other kind of artefacts. To calculate the trajectory of a system, firstly the time is discretized by a time step that should be short enough to avoid large displacements of atoms between consecutive frames. However, setting very short time steps implies to simulate more frames to reach the desired time and thus, the simulation will take longer to finish. The optimal value is usually determined by the molecular groups with the lowest masses, i.e. the fastest dynamics, which are usually those involving hydrogen atoms. A typical value of the time step, specially for the simulations performed for this thesis, where all-atom force fields are used, is around 1 or 2 fs. One trick that is usually done to increase the time step without loosing much precision, is to apply constrains to bonds and angles involving hydrogen atoms. This approximation consists on fixing the bond sizes or the angles between atoms to the equilibrium value (r_{eq} and α_{eq} in Eqs. (2.5) and (2.6)). With this, the dynamics of the most mobile species are restricted, and larger time steps can be used. In this thesis, for some works, restrictions to bonds involving hydrogen atoms were applied.

Now we have all the ingredients to start the calculation of the trajectory of all the atoms in the system. For this thesis, two algorithms where used to calculate the positions and velocities of the atoms at a time $t + \Delta t$ from the values at time t. On one hand, we used the Leap–Frog integration method. With this algorithm, the velocities of the atoms

USC
UNIVERSIDADE DE SANTIAGO DE COMPOSTELA

between two consecutive frames are used to calculate the positions:

$$\vec{v}\left(t+\frac{\Delta t}{2}\right)=\vec{v}\left(t-\frac{\Delta t}{2}\right)+\frac{\Delta t}{m}\vec{F}(t) \tag{2.10}$$

$$\vec{r}\,(t+\Delta t)=\vec{r}\,(t)+\Delta t\cdot\vec{v}\left(t+\frac{\Delta t}{2}\right). \tag{2.11}$$

Note that m is the mass of the atom and $\vec{F}(t)$ the force on that atom calculated using the force field. With this approach, velocities in the final trajectory will not correspond exactly to the same time as the positions (note the $\Delta t/2$ offset). However, this is not an issue in most cases. The other used algorithm that does not present this problem, and which was also used for some simulations in this thesis, is the velocity Verlet integrator. In it, the positions in the next frame are calculated with the positions, velocities and forces of the current one as:

$$\vec{r}\,(t+\Delta t)=\vec{r}(t)+\Delta t\cdot\vec{v}(t)+\frac{\Delta t^2}{2m}\vec{F}(t). \tag{2.12}$$

Then, using these new positions, the forces in the new frame are calculated and used to compute the velocities:

$$\vec{v}\,(t+\Delta t)=\vec{v}(t)+\frac{\Delta t}{2m}\left[\vec{F}(t)+\vec{F}(t+\Delta t)\right]. \tag{2.13}$$

Although this algorithm does not present the problem of the different times for positions and velocities, it is not implemented for all the options available in GROMACS. Moreover, this integrator performs better when the simulations are performed with temperature or pressure coupling. These couplings and some other special simulation conditions will be discussed in the next subsection.

2.1.5 Different Simulation Conditions

USC
UNIVERSIDADE DE SANTIAGO DE COMPOSTELA

The aforementioned integration methods do not introduce any modification to the energy of the system when they are repeatedly applied in each frame (apart from artificial effects when the time step is not short enough). This means that the simulations are performed in the microcanonical (or NVE) ensemble. However, to compare with experiments, it is sometimes very convenient to work at constant temperature and/or constant pressure. To emulate a contact between the system and a thermal or pressure reservoir multiple techniques are available. Regarding the thermostat, two methods were used in the development of this thesis: the Berendsen[44] and the v-rescale[45] thermostats. Both thermostats work by rescaling the velocities of all the atoms in the system by a factor, different in each method. In the Berendsen thermostat, the scaling factor is calculated to mimic a weak coupling with a thermal reservoir (at temperature T_0). By applying this thermostat, the temperature of the system evolves according to:

$$\frac{dT}{dt} = \frac{T - T_0}{\tau}. \tag{2.14}$$

In other words, the temperature will decay exponentially to T_0 with a decay time τ that is given as a simulation parameter. This is usually set to 0.1 or 0.2 ps in the simulations performed for this thesis. Regarding the v-rescale thermostat, it is based on the same principle, but it adds a term to the time evolution to reproduce the canonical distribution of the kinetic energy (K) of the system:

$$P(K)dK \propto K^{\frac{N_f}{2}-1} e^{-\beta K} dK, \tag{2.15}$$

where N_f is the number of degrees of freedom and β the Boltzman factor. For this reason, this was the most used thermostat in this thesis.

Closely related to the possibility of changing the temperature in the simulations, there is a technique that was frequently used, specially with systems between interfaces. As it was mentioned in the introduction, ILs are usually very viscous. This means that the motion of the molecules is very slow compared with other molecular cosolvents such as water or ethanol. To allow simulations with ILs to explore a wider energy

USC UNIVERSIDADE DE SANTIAGO DE COMPOSTELA

landscape to find the equilibrium configuration, we used the simulated annealing protocol. This technique is usually applied after the minimization step and consists on increasing the temperature of the system for a certain period of time. Then, simulating at that temperature for a while, and finally cooling down the system until the desired temperature is reached. With this process we prevent the total system or some molecules to be trapped in a local minimum of the energy. This happens frequently in simulations with ILs and salts between charged interfaces, where the electric double layer (EDL) is formed and some charged species may be trapped in artificial position due to the random nature of the initial configuration. The annealing prevents these edge cases. It is very important to adopt low enough heating and cool down rates to allow the system to follow the thermostat. Otherwise, the process loses its validity. In the work presented in Chapter 8, where we used this method, we checked that the chosen rates were slow enough to allow the IL temperature to follow the thermostat. We represent in Fig. 2.6 the variation of the temperature of the system with the time for the simulation with pure IL.

As well as the temperature of a simulation can be fixed, the same can be done with the pressure to work in the NpT or NpE ensemble. While the temperature is modified by applying a scale factor to the velocities of the atoms in the system, to change the pressure the position of the atoms as well as the dimension of the simulation box are scaled. With the same ideas proposed by the Berendsen and v-rescale methods for the thermostat, there are two algorithms widely used in the literature to apply a barostat: the Berendsen[44] and the Parrinello–Rahman[46] pressure coupling methods. The Berendsen barostat is essentially the same as the thermostat but changing temperature by pressure, i.e. it induces an exponential decay of the pressure of the system to a desired value with a decay time set as input parameter. On the other hand, the Parrinello–Rahman method follows a different approach. It defines an equation of motion for the simulation box vectors that depends on the difference between the pressure in the system and the target pressure. Moreover, an additional term is included in the Hamiltonian of the sys-

USC
UNIVERSIDADE DE SANTIAGO DE COMPOSTELA

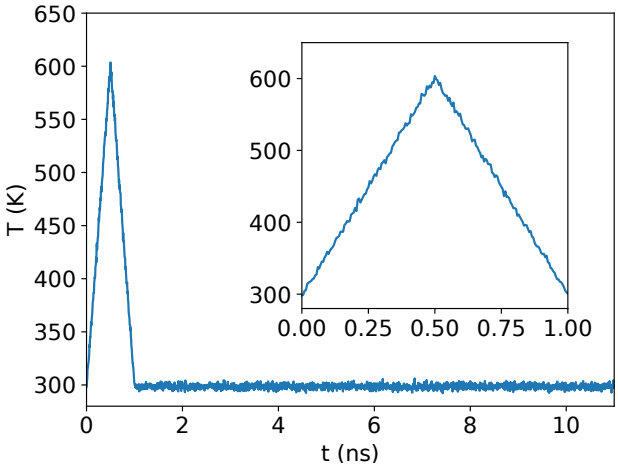

Figure 2.6: Time evolution of the temperature of the system for a pure IL ([BMIM][BF_4]) between two graphene walls during annealing (time interval between 0 and 1 ns), and in the stabilization (time interval between 1 and 11 ns) steps. The inset shows in detail the annealing region.

tem to take this into account, which translates into a new term in the equation of motion of each atom. In theory, Parrinello–Rahman barostat gives the true NpT ensemble, and, again, that is why it is the most used in the simulations performed for this thesis. It is worth mentioning that this pressure coupling method has an analogous implementation for temperature coupling which is known as the Nosé–Hoover thermostat.[47;48] We also want to point out that GROMACS allows setting different pressure coupling constants for the different components of the pressure tensor. While for most of the bulk simulations an isotropic barostat is used (same pressure coupling in the three dimensions of the space), for simulations with interfaces, as the ones presented in Chapter 8 and 9, it is interesting to allow different volume variations in the direction perpendicular to the interfaces and in the parallel ones.

To finish this section, we will introduce another simulation condition that was used in some cases, which is the possibility to simulate the

USC UNIVERSIDADE DE SANTIAGO DE COMPOSTELA

existence of an external electric field. GROMACS allows to introduce the effect of a Gaussian laser pulse in each of the three directions of the space:

$$E(t) = E_0 e^{-\frac{(t-t_0)^2}{2\sigma^2}} \cos\left[\omega(t-t_0)\right]. \tag{2.16}$$

This term induces an additional electric force on each charged atom which is introduced in the equations of motions. For the aim of this thesis, the introduction of an external electric field results very useful in simulations of ILs and its mixtures between planar interfaces. In those simulations we used a constant electric field in the direction perpendicular to the interfaces (this is achieved by setting ω, t_0 and σ to zero) to emulate the conditions of charged interfaces. Indeed, in Chapter 8, a comparison between the results obtained by applying this external field are compared with those obtained by assigning a charge to each atom in the interfaces.

2.1.6 Planar Interfaces

Up to now, we have considered the utility of annealing simulations and anisotropic barostats in simulations with interfaces, but nothing about how these interfaces are introduced has been said. For the works presented in this thesis, two methods were used. For the simulations reported in Chapter 8 two "real" graphene walls were introduced parallel to the XY-plane and in the coordinates $Z = 0$ and Z equal to the desired slit size. To determine the dimensions of the walls, one should estimate the simulation box size based on the slit size and the number of molecules to simulate. In this estimation the density of the same system in bulk conditions is used or, in case of being a mixture, the density is calculated with the density of the pure compounds supposing an ideal mixture. Of course, this assumption about the preservation of the density in the bulk and under confinement may not be very accurate. Moreover, once the section of the simulation box is calculated, the obtained val-

USC UNIVERSIDADE DE SANTIAGO DE COMPOSTELA

ues for the X and Y dimension must be adjusted to match a multiple of the graphene unit cell. All these approximations translate into a system that, once it is stabilized, does not reproduce the bulk density in the region far from the walls. To fix these deviations the distance between the walls is adjusted and then, the systems is equilibrated again. This change in the wall separation must be done manually, i.e. when using this method for simulate interfaces, no barostat can be applied to adjust the box dimensions through a NpT simulation. This is mainly because two reasons. First, in the X and Y directions, the dimensions can not change because the graphene walls have to replicate well when pbcs are applied. On the other hand, GROMACS only allow periodicity in all the directions in this kind of simulations. This means that to avoid the interactions between molecules in the real simulation box and those replicated in the Z direction, an empty space should be added in that direction. This avoids the introduction of an anisotropic barostat to fit the distance between walls as it will only reduce the Z dimension of the box to remove the artificially low pressure induced by that empty space. Not only that but, due to the parallelization algorithm, the introduction of this empty space has also a high impact on the performance of the simulation as some part of the computational resources must be dedicated to simulate that empty space. It is true that this performance issues can be improved by doing some adjustments in the parallelization method, but it is something to take into account. Despite these inconveniences, this method for simulations with interfaces has the advantage that the charges of each individual atom in the walls can be set. Even more, vacancy defects can be introduced with redistribution of charge[49] and the results derived from the solvent-interfaces interaction is fully accessible.

Another option to perform simulations with interfaces, specially when the interactions between the interface material and the fluid are not a priority in the study, is to use implicit walls. These mathematical objects emulate the existence of homogeneous distribution of atoms in a XY-plane or in a region (for example $Z < 0$) with no need to insert additional atoms in the system. Focussing on the first kind of implicit

USC
UNIVERSIDADE DE SANTIAGO DE COMPOSTELA

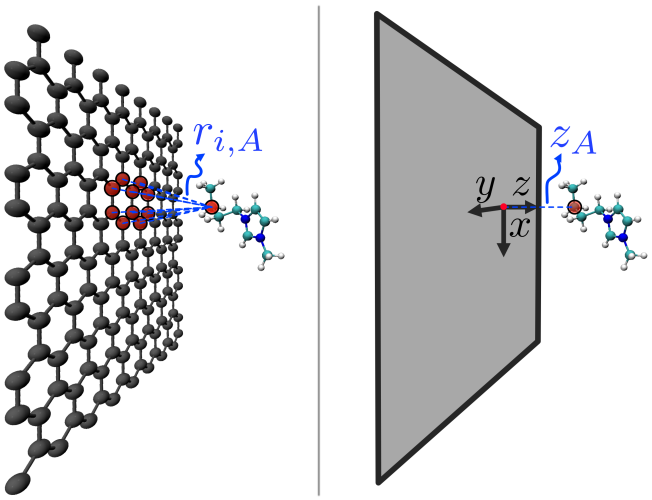

Figure 2.7: Schematic representation of a "real" graphene wall (left) and an implicit interface emulating a homogeneous bidimensional distribution of atoms (right).

walls, their interaction with the atoms of the fluid between the interfaces is calculated as a 10-4 LJ potential only dependent on the distance between the wall and the atoms. Let us try to understand the origin of this potential. For that, we will use the scheme represented in Fig. 2.7 as a guide. First, consider how the interaction between an atom of the fluid and a real graphene (although the same can be applied for any kind of interface) wall is calculated. The contribution of the wall (W) to the potential energy of the atom (A) is calculated as the sum of the interaction between the atoms of the fluid and all the atoms in the wall. If each atom pair interacts through a 12-6 LJ potential and there are n wall atoms that are closer than a given van der Waals cut-off radious to the considered atom:

$$\Phi_{W\text{-}A}(r_A) = \sum_{i=1}^{n} 4\varepsilon \left[\left(\frac{\sigma}{r_{i,A}} \right)^{12} - \left(\frac{\sigma}{r_{i,A}} \right)^{6} \right], \qquad (2.17)$$

where $r_{i,A}$ is the distance between the wall atom i and the atom of the fluid. Now, instead of having a known spatial distribution of the atoms

USC UNIVERSIDADE DE SANTIAGO DE COMPOSTELA

of the wall (e.g. graphene lattice), consider a homogeneous continuous distribution of them with a surface atomic density of $\rho_s = dN/dS$. In this scenario, to calculate the interaction between the implicit wall (I) and the fluid atom, instead of adding the interactions for all the atoms in the wall, we should integrate in all the surface of the wall. To calculate this integral, we will use polar coordinates with the axis and origin set as represented in Fig. 2.7. With these considerations, the interaction is calculated as:

$$\Phi_{I\text{-}A}(z_A) = \int_0^{2\pi} d\theta \int_0^{\infty} 4\varepsilon\rho_s \left[\left(\frac{\sigma}{\sqrt{r^2 + z_A^2}} \right)^{12} - \left(\frac{\sigma}{\sqrt{r^2 + z_A^2}} \right)^{6} \right] r dr. \tag{2.18}$$

Integrating this expression, the functional form of the 10-4 LJ potential is obtained:

$$\Phi_{I-A}(z_A) = 2\pi\sigma^2\varepsilon\rho_s \left[\frac{2}{5} \left(\frac{\sigma}{z_A} \right)^{10} - \left(\frac{\sigma}{z_A} \right)^{4} \right] \tag{2.19}$$

If we compare this expression with Eq. (2.17), we already see a high reduction in computational cost. While for implicit walls only one operation per fluid atom must be performed, when "real" interfaces are used, there are n operations to perform. Moreover, using these interfaces allows to use a barostat to perform NpT simulations, since there is no restriction in the lateral size of the box and pbcs can be applied only in the X and Y directions. This means that there is no need to introduce any empty space to avoid interactions with replicas, which, at the same time, reduces the computational costs. This method was the one used for the simulations presented in Chapter 8, where a comparison with similar systems but with "real" graphene walls is presented. All the simulations reported in Chapter 9 were also carried out with this kind of virtual interfaces.

USC UNIVERSIDADE DE SANTIAGO DE COMPOSTELA

Of course, all the advantages of using implicit walls come at the cost of losing details of the interactions with the interface. In some recent simulations that will be studied in future works, we are using a combination of both kind of simulations that allows us to recover the detailed interactions with the interface. With this combined method, we are allowed to apply pbcs only in the X and Y directions and thus, keeping a good computational performance. The process basically consists in performing a complete simulation using implicit walls until a well stabilized system is obtained. Then, "real" walls are introduced in the positions of the implicit ones and the interactions with the implicit walls are turned off (by setting σ and ε of the implicit walls to zero). There is only a minor detail to take into account in this process and it is that the lateral simulation box size must be set from the packing step to the correct size, so when the "real" walls are introduced they replicate well in the lateral directions. This is achieved by using an anisotropic barostat allowing only volume variations in the Z direction.

2.2 Density Functional Theory

Most of the works presented in this thesis are based on the results from MD simulations or theoretical analysis. However, in the results presented in Chapter 7, some results obtained with density functional theory (DFT) calculations are included. In this section we will very briefly summarize the fundamentals of this formalism, and how we implemented our simulations, paying special attention to the study of proton transference process.

We saw that MD simulations target to calculate the trajectory of the atoms in a system by calculating the potential energy of each one. In the most detailed approach, this potential is calculated using the atomic positions and partial charges and, with some forcefields, the electronic polarization is also considered. All the MD calculations, particularly those reported in this thesis, are performed using a classical approximation. With DFT, we can access to more precise results by solving the

USC
UNIVERSIDADE DE SANTIAGO DE COMPOSTELA

time-independent Schrödinger equation:

$$\hat{H}\left|\Psi\right\rangle = E\left|\Psi\right\rangle . \tag{2.20}$$

As we are dealing with electrons and atomic nuclei, the Hamiltonian must include the terms associated to the kinetic energy of all the electrons and nuclei, as well as all electrostatic interactions between all the particles in the system (electron-electron, electron-nucleus and nucleus-nucleus). To simplify this Hamiltonian, the Born-Oppenheimer approximation[50] is used. In this approximation, based on the fact that the motion of the electrons is way faster than that of the nuclei, the electronic and nuclear degrees of freedom are decoupled and treated separately. In this sense, we can average out the nuclear terms in the Hamiltonian, so it can be written as:

$$\hat{H} = -\frac{\hbar^2}{2m_e}\sum_i \nabla_i^2 + \frac{1}{4\pi\varepsilon_0}\sum_i\sum_{j>i}\frac{e^2}{|\vec{r_i}-\vec{r_j}|} - \frac{1}{4\pi\varepsilon_0}\sum_i\sum_\alpha\frac{Z_\alpha e^2}{|\vec{r_i}-\vec{r_\alpha}|}, \tag{2.21}$$

where Z_α is the atomic number of the α atom. Even though the problem is simplified with this approximation, it is still very hard to find the eigenvalues that diagonalized this Hamiltonian as it consists in a large many-body problem that scales poorly with the number of nuclei and electrons. To simplify even more the problem by turning a very complex many-body calculation into a set of easier one-body equations, the Hohenberg–Kohn theorems together with the Kohn–Sham equations are used.[51] The former theorems prove two facts. On the one hand, the total energy of a system is univocally defined by the electronic density function and, on the other hand, the electronic density that minimizes the total energy is the one corresponding to the ground state. While in MD simulations the trajectory of each atom was the target result, with DFT, we aim to obtain this electronic density ($\rho(\vec{r})$) in the ground state. These theorems by itself do not simplify the problem but, using their implications, Kohn and Sham showed that the results obtained by solving Eq.

USC UNIVERSIDADE DE SANTIAGO DE COMPOSTELA

(2.21) are equivalent to those obtained by solving a set of equations that describe the physics of hypothetical particles (quasi-electrons) under the effect of an effective potential:

$$\left(-\frac{\hbar^2}{2m_e}\nabla_i^2 + V_{\text{eff}}(\vec{r})\right)\phi_i(\vec{r}) = \epsilon_i\phi_i(\vec{r}). \tag{2.22}$$

The effective potential is a combination of three terms: the external potential, which also includes the contribution of the interactions with the nuclei, the Hartree term for the electron-electron repulsion,

$$V_H(\vec{r}) = \int \frac{e^2\rho(\vec{r'})}{\left|\vec{r} - \vec{r'}\right|}d^3\vec{r'}, \tag{2.23}$$

and the exchange correlation potential. The first two terms can be easily calculated by knowing the nuclei distribution and the electronic density (which is the magnitude that we want to calculate). However, the exchange correlation potential, which contains the rest of the non-considered many-body interactions, is completely unknown. Although we are not going into much detail here, it is worth mentioning that there are many approximations that attempt to provide an estimation of this exchange correlation term. The most used ones are the local density approximation (LDA), the generalized gradient approximation (GDA) and the hybrid functionals that are a combination of the first two. The one used for the DFT calculations presented in Chapter 7 is called B3LYP,[52] which belongs to the hybrid functionals family. The reader is referred to Ref. 53 for a detailed description of these approximations of the exchange correlation potentials.

Once the set of equations for the quasi-electrons are solved for an initial guess of the electronic density, the new electronic density predicted by the solution can be calculated as:

$$\rho(\vec{r}) = \sum_i \left|\phi_i(\vec{r})\right|^2 \tag{2.24}$$

Then, this electronic density can be used again to solve the equations to get a new one until a predefined level of convergence is achieved.

USC UNIVERSIDADE DE SANTIAGO DE COMPOSTELA

Finally, with the electronic density of the system, the total energy and other interesting magnitudes can be calculated. For the results presented in this thesis, we only used the total energy of the ground state to study proton transference process which will be discussed in the next subsection.

Before getting into more detail about proton transference, we want to say a few words about a simulation method that combines the explained DFT with MD which is usually called ab initio MD. In this method, instead of calculating the forces acting on each atom in each frame by means of analytical expressions combining multiple classical interactions (the force field), they are calculated from the derivatives of the potential energy calculated with DFT. Then the integration of the equations of motion is done in the same way as for classical MD simulations. This method has the huge advantage that the obtained dynamics reproduces more realistic system evolution. For instance, in this kind of simulations chemical reactions can take place, while it is not possible in classic MD, where the bonds between atoms are fixed during the whole simulation. However, as a DFT convergence loop has to be executed in each frame, this method is computationally very expensive and it can only be used for simulation boxes with just a few atoms. To finish, let us make a special mention to a new method developed by Montes *et al.*[54] that aims to speed up ab initio MD simulations of ILs by using a neural-network based force field (NeuralIL). This force field needs to be trained with the forces obtained from DFT calculations of similar systems to the ones that are going to be simulated. Once it is trained, the MD forces are obtained with calls to the neural-network, which are orders of magnitudes faster than performing ab initio MD simulations, while leading to equivalent results.

2.2.1 Grotthuss Mechanism

Pure water is known to be a poor electrically conducting medium.

USC UNIVERSIDADE DE SANTIAGO DE COMPOSTELA

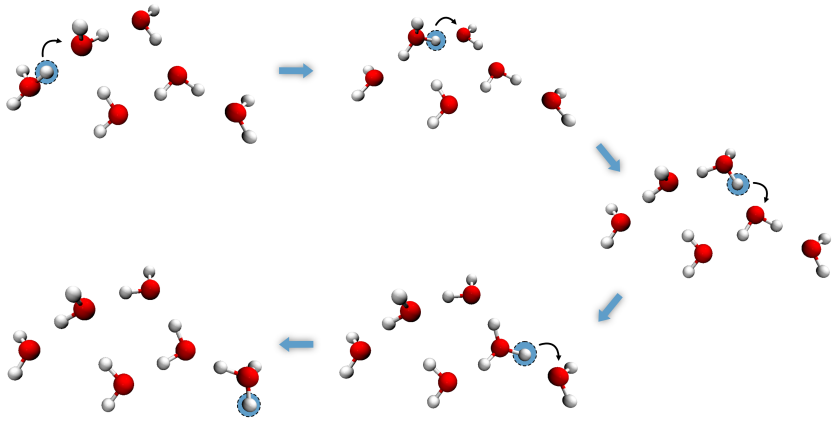

Figure 2.8: Schematic representation of the proton hopping process proposed by Grotthuss.

This is of course a consequence of its molecular nature and absence of free electrons. However, it presents an equilibrium population of protonated and deprotonated species (hydronium and hydroxide ions) which can act as charge carriers and contribute to the solvent conductivity. In 1806, Grotthuss[55] proposed a mechanism to describe the pure water conductivity as the result of a proton hopping process. A schematic representation of this process is plotted in Fig. 2.8. Note that this picture should be critically seen, as experimental and computational results suggest that the real process involves more complex ions such the Eigen and Zundel cations.[56]

This mechanism does not only show up in water but also in other solvents that present a strong hydrogen bond network, e.g. PILs or mixtures of ILs and water. This proton hopping process can be computationally studied using the aforementioned ab initio MD. There are some articles in the literature where this kind of simulations are performed for characterizing the hydrogen bond network and proton hopping in these media.[57] Another way to analyze this phenomenon is to study the lowest energy path that a proton should follow to hop from one species to an-

USC UNIVERSIDADE DE SANTIAGO DE COMPOSTELA

other. In this method, the dependence of the energy of the system with a reaction coordinate is calculated to obtain the shape of the barrier (see for instance Ref. 58 where this method is used to study proton transfer in water clusters). However, for the results presented on Chapter 7 of this thesis, due to the complexity of the studied system, and to compare with the experimental results, we characterized the proton-hopping paths in terms of the total energy of the initial, final and intermediate atomic configurations calculated with DFT. The initial and final configurations were extracted from MD simulations, while the intermediate ones were artificially generated to force the existence of a protonated species. It must be mentioned that the artificial configurations were relaxed to minimize their energy and then find the ground state of that minimized configuration. With this approach, which was already used to study proton hopping in similar systems,[59] we were able to study how the presence of a complex anion, that forms hydrogen bonds with water molecules, decreases the energy barrier present in the hopping process between water molecules and imidazolium cations (precursor of a widely used family of ILs), in very good agreement with previously reported experimental results.

USC
UNIVERSIDADE DE SANTIAGO DE COMPOSTELA

USC
UNIVERSIDADE
DE SANTIAGO
DE COMPOSTELA

Part II

Results

USC
UNIVERSIDADE
DE SANTIAGO
DE COMPOSTELA

USC
UNIVERSIDADE
DE SANTIAGO
DE COMPOSTELA

3- Summary of the Results

With the aim of contextualizing and gluing together all the results obtained during this thesis, a summary of the followed path in the past years will be presented in this chapter. We will see how, to achieve the objectives of the thesis, at some point, we had to deal with the problem of simulating very large systems while keeping reasonable computation times but without loosing structural information. Although the simulations carried out during the first steps of the thesis were not performed in this limit of large systems, we wanted to solve the problem before it arose, which conformed the first objective of this thesis. Once the tool to solve that problem (Gaddle Maps) was developed, two parallel lines were opened to reach a deep understanding of the solvation properties of ILs and its mixtures, which is crucial to characterize dispersions of nanostructures in these densely ionic solvents. On the one hand, we studied the limit of small nanostructures with spherical symmetry. In this aspect, we first characterized the effect of water addition to the IL, as well as how changing the charge of the solute affects the molecular structure of the solvation shells and in the mobility of the solutes. In this study the solute was a very generic spherical particle without internal atomic structure. Then, to analyse the effect of the solute size we studied the energetics and structure of solvation of alkaline salts in an IL by means of experiments and simulations. This gave us a very detailed understanding of the role of the electric field in the surface of the solute to determine the molecular structure of the surrounding media. Indeed, the results showed that the analysis can be extrapolated to larger particles. In the last work of this line, we characterized an ionic system where the anions were formed by complex atomic structures. This supposed a step forward with respect to the previous works as not only the size of the considered spheres increased, but also ideal spheres were replaced by real complex atomic structures. Moreover, this work supposed a challenge to learn and apply new techniques to study the proton conductivity in these systems. On the other hand, we wanted

USC
UNIVERSIDADE DE SANTIAGO DE COMPOSTELA

to know what happens in the vicinity of possible nanostructures when they are very large in comparison with the ionic medium. To answer this question, two different studies about ILs (and their mixtures with molecular cosolvents) confined between charged planar interfaces were done. In the first one, we focussed on the structure of the EDL and how it is affected when cosolvents are added or when the material at the interface changes. In the second one, we forgot about the material and charge of the interface and analysed the spatial range of the effect of the interface on the structure of the media by means of simulations of a pure IL under extremely confined conditions. After all these exhaustive studies regarding the structure, we analysed the transport properties of these fluids to have a better picture of the dynamics of dispersions of nanostructures. For this task, simulations and experiments of binary mixtures of ILs and alcohols were performed to test and validate a theoretical framework based on a pseudo-lattice random-alloy model which describes the medium conductivity as the hopping of charged species between cells with different mobilities. In the following, we will go deeper into these works, explaining the context, the motivations, the main results and the knowledge transfer of each one.

Going back to a time when no one knew what the word "COVID" meant or how a global pandemic could change our society, a young student finishes his master degree and starts his journey to becoming a PhD. I want to mention that, at that time, I had already some notions of how the scientific research world works. During the last year of my Physics degree and during the Master degree I was lucky to collaborate with the group which would end up being that where the thesis presented here would be developed. In other words, I was already familiarized with the techniques and topics treated in the group when I started the thesis which helped me a lot. Back then, the group had a lot of experience studying ILs by means of MD simulations. They had already studied these novel materials in mixtures with some small molecular cosolvents and electrochemically interesting salts. Moreover, the first works of ILs confined between planar interfaces started to appear in the group. It was in this context where the route for the current thesis was drafted.

USC
UNIVERSIDADE DE SANTIAGO DE COMPOSTELA

This thesis was born as an opportunity to extend the knowledge that the group already had in the field towards more complex systems with high interest in multiple fields (as it was already mentioned in section 1.1) but keeping the ILs as the main topic.

To address the challenge of properly characterizing more complex systems, specifically, dispersions of nanostructures in ILs and its mixtures, simulations with very large numbers of molecules needed to be performed. To contextualize, let us suppose that we want to study a dispersion of gold nanoparticles in an IL. The nanoparticles have a diameter of 7 nm. This means that to simulate a single particle in presence of the IL, and to be sure that the particle does not interact with its own replica created by the periodic boundary conditions, a simulation box with at least 14 nm of side length should be created. Note that the complexity of the MD algorithm in simulations with charged atoms is $O(N \log_2(N))$, where N is the number of atoms. Moreover, the number of atoms in a simulation box is proportional to its volume with is equal to cube of the side length if cubic boxes are considered ($V = L^3$). In other words, the computation time of a simulation scales $O(L^3 \log_2(L))$ with the box side length. Going back to the gold nanoparticle, imagine we want to simulate it in a simulation box of 15 nm of side length (to work with round numbers). Most of the bulk simulations performed for this thesis had a side length of around 5 nm and they took, in the best cases with the most powerful machine in the cluster of the group, around 3 days. We need to multiply by 3 the side of the simulation box to simulate the nanoparticle which translates into a factor of $3^3 \log_2(3) \approx 42.8$ in the computation time or, in other words, we would have to wait more than 4 months to finish just one system. Of course this time could be reduced by parallelizing the simulation in multiple computation nodes in a super-computer, but then we would have to deal with waiting times in the queues and resource limitations. The point is that another approach to simulate this kind of large system is needed.

Searching for a new strategy, we found that, in other fields more related with biology, the use of CG force fields to simulate large structures such as lipid bilayers, vesicles or large proteins was extended. With this

USC
UNIVERSIDADE DE SANTIAGO DE COMPOSTELA

kind of force fields, not only the number of "atoms" is reduced, but also the simulation time step can be increased allowing to simulate larger times with the same time steps. There were some works in the literature where this force fields were used to obtain equilibrium configurations, e.g. protein unfolding, vesicle formation, etc. and then, with specific tools, replace each molecule in the simulation box with its representation in an all-atom force field. The resulting system was then used as starting point to perform a short simulation with atomic resolution, which resulted in the one used for the final analysis. We thought that this approach was exactly what we needed to perform simulations with nanostructures and opened the door to a wide variety of possibilities to perform multiscale simulations. However, the existing tools to perform the force field exchange, i.e. replacing the molecules in a system from CG to all-atoms, were very limited. Indeed, they only worked with proteins and some biologically interesting molecules and the transformations were restricted to a very small set of force fields. So, if we wanted to use that approach in systems with complex nanostructures and different ILs and molecular cosolvents, we had to develop a more general tool than the existing ones to perform the exchange between all kind of molecules and all kind of force fields. This was how the idea for developing the Gaddle Maps algorithm came out.

Most of the existing tools manually defined the correspondence between each bead in each molecular species in the CG representation and the atoms in the all-atom force field. Then, they iterate through the molecules in the systems and apply this correspondence. This was the main source of the restrictions of those tools. The power of Gaddle Maps is that this correspondence is found automatically by searching the optimal overlapping between molecules in their different force field representations in the same way as a human would do. This idea resulted in the publication presented in Chapter 4. There, a detailed description of the algorithm as well as some examples of applications are presented. It must be mentioned that, although this tool will be used in our own investigations, it can be applied for all kind of systems and with different purposes, e.g. it can also be used to change one kind of molecule for

USC
UNIVERSIDADE DE SANTIAGO DE COMPOSTELA

another in an entire simulation. That is why we also release our implementation of the algorithm as a public repository to be accessible to the community.

Once this algorithm was developed, we move towards simulating systems which help us characterizing the solvation properties of ILs and their mixtures. The final goal is to understand systems with different nanostructures in different concentrations. This nanostructures may have a wide variety of geometries: spherical nanoparticles, nanotubes, nano-porous structures... As it was mentioned, performing simulations with these nanometric structures immersed in ILs is very time-consuming which means that simulating different scenarios, e.g. different cosolvent concentrations, different ILs, etc. becomes a big challenge. For this reason, we decided to start characterizing these systems in two limits, which allowed simulating multiple media at the same time under different conditions. On the one hand, studies of small particles with spherical symmetry were performed. This allowed us to characterize the effect of the addition of cosolvent to the IL, the effect of changing the size or the charge of the particle and even develop some intuition on how they could be extrapolated to larger particles. On the other hand, the limit of very large structures was studied by simulations of ILs and some mixtures in the presence of planar interfaces with different charges and materials allowing a full characterization of how the molecules of the medium rearrange in the neighbourhood of interfaces under different conditions. In the following, a more detailed description of the studies in each line is presented.

Starting with the study of spherical particles in ILs, during the first stages of the thesis, the opportunity to collaborate with colleagues from the Helmholtz-Institute in Münster appeared. At that, time they had published an article where the properties of solvation of pure [EMIM][ACE] were studied by means of bulk MD simulations of a spherical particle with different charges.[60] The particle was a CG model of a generic solute consisting on a simple van der Waals sphere. The next step of this work was to understand what happens in these systems when small amounts of water are present in the IL and that is what we did. Having a good

USC
UNIVERSIDADE DE SANTIAGO DE COMPOSTELA

knowledge of the effects of water addition in these dense ionic fluids is very important mainly for two reasons. On the one hand, it is well known that the addition of molecular cosolvents can drastically change their dynamic properties and, depending on its nature, also their structure. On the other hand, and maybe more importantly, most of the ILs are hygroscopic, so they tend to adsorb water from the surrounding environment. This makes it very difficult to find completely dry ILs in real applications.

To be able to directly compare with the already published results for systems without water, we simulated three systems (with neutral, positively and negatively charged solutes) following the same methodology and force field and adding a 5% of water. This amount of water is supposed to reproduce that of residual water that could be found in a real application. It is worth mentioning that, due to the slow dynamics of these systems and to have good enough statistics, the simulations were 300 ns long, which is considered a very long time when using all-atom force fields. Indeed, each of the simulations took around 1 month of computation time. A very exhaustive characterization of the molecular structure around the spherical solutes was performed. For that, the average position and orientation of the different species relative to the solute were calculated and compared with the situation in the dried homologous systems. The results showed that the water presence do not significantly change the ion distribution around the solute and it only shows a preferential coordination with the negatively charged solute. In that case, the orientation of water molecules is determined by the electric field in that region. Although the structure is almost the same, the dynamics does show drastic changes. Indeed, a huge enhance of the solute mobility is observed, particularly in the charged ones. All these results were summarized in a publication which will be presented in detail in Chapter 5.

Before continuing with the next work about spherical particles in ILs, let us make a little parenthesis to talk about a very important work related with all the published results during this thesis. It has been already introduced how the Gaddle Maps algorithm was developed

USC UNIVERSIDADE DE SANTIAGO DE COMPOSTELA

and implemented. In the study of solvation of spherical particles, the used tools for characterizing and representing different magnitudes were also mostly developed by the author of this thesis. In general, during the thesis, a wide variety of systems were simulated, and to fully understand the physics behind them, the existing analysing tools were not enough. For this reason, a very interesting set of aptitudes, usually associated to other fields (informatics, programming, data analytics, machine-learning, big-data, etc.), were adopted. Some examples could be: detection of molecular clusters, image processing for pattern recognition in density maps, optimization and parallelization of existing algorithms for analysing large systems or automatization of the process of preparing and sending simulations with different conditions. Moreover, most of the simulations carried out during the thesis were performed in the cluster of the research group, which is maintained by the members of the group, so knowledge on computer systems management was also acquired. Although the tools and knowledge derived from all these aspects are not collected in any publication, they are stored for the use of the group. For instance, all the developed tools for analysing and representing magnitudes from MD simulations or DFT calculations are collected in different code repositories (currently, more than 30 thousand lines of code). More theoretical aspects or other features related with simulations or environment setups are also well documented and preserved in different repositories. All this knowledge is available for the members of the group which showed to be incredibly useful, particularly for the new members to speed up their learning process.

Going back to spherical particles in ILs, our next step was to study the effect of the size and charge on the solvation properties. Instead of following the same approach as in our previous work, where the solute was a model CG sphere, we decided, in order to allow a comparison with real systems, to study the solvation of alkali metal nitrate salts in EAN. In these solutions, as the salts share the anion with the IL, we can focus on how the IL molecules arrange around the different metal cations which have different radius and valences. It has to be mentioned that a

USC
UNIVERSIDADE DE SANTIAGO DE COMPOSTELA

characterization of dispersions of this kind of cations in ILs has a lot of interest in fields such as electrochemistry and photonics. Moreover, the choice of using EAN as solvent opens the door to the comparison with solvation in other polar solvents such as water. To undertake this study, we employed both experimental and computational techniques. On the one hand, high precision solution-reaction calorimetry was employed to estimate the enthalpy of solvation of the different salts in EAN. With these data on hand, we found a clear correlation between them and the ionic structure of the corresponding salt crystal lattice. The comparison of the enthalpy of solvation of these salts in EAN with the same magnitude for solvation in water showed almost a one-to-one correspondence. This corroborates the well known water-like solvent properties of EAN. To shed some light on the origin of these similarities we performed MD simulations of the same systems. Firstly, we validated the accuracy of these simulations by calculating directly the enthalpies, which showed a very good correspondence with the experimental ones. Secondly, we analysed the structure of the solvation shells around the metal cations. We found that the distribution of the oxygen atoms of the nitrate anions around the metals in EAN/salt mixtures is very similar to that of the oxygens of water molecules in water/salt systems. Even more, the coordination numbers of anions and water around the alkali cations are very similar except for the caesium. All these results helped to understand from a more fundamental point of view the water-like solvation properties of EAN. On the other hand, we developed a theoretical framework that allowed estimating the contribution of the electrostatic interactions to the solvation enthalpy. We compare the results obtained from this theory and those from the simulations. We saw that the electrostatic interactions are the main contribution to the enthalpy, being the excluded volume interactions only relevant for cations with the highest electric field in their surface, i.e. magnesium. Taking all this into account, we developed a software which is able to interpolate different magnitudes such as the structure around a cation and the enthalpy of solvation given only the charge and effective radius of the solvated cation. This study will be presented in detail in Chapter 6.

USC
UNIVERSIDADE DE SANTIAGO DE COMPOSTELA

To advance in the line of spherical structures in ionic media, the next step was to work with slightly larger particles and introduce atomic details in them, leaving aside perfect van der Waals spheres. The perfect opportunity to study systems that fall under this description arose when Prof. A. Martinelli proposed us to collaborate in an experimental study they were carrying out about the characterization of a special kind of salts. The reason why these salts were so interesting for the content of this thesis was because of the shape of the anions of the salt. These anions were structures formed by 40 oxygen, 12 tungsten and 1 phosphorous atoms distributed in what is known as Keggin structure, which has spherical shape. On the other hand, for each anion there are three imidazolium cations in the salt, which are very similar to previously studied ones, such as the $EMIM^+$. It is true that this system is a bit far from the previous studies where particles in a very dilute limit were considered. However, this was an opportunity to study the opposite limit, i.e. highly concentrated dispersions of charged spherical particles in an ionic medium. Moreover, although this system was interesting for this thesis, it was even more for practical applications. Specially, for those related with electrochemical devices such as fuel cells, as it shows a very high proton conductivity, particularly when it is hydrated with small amounts of water. Our contribution to this collaboration was to provide a detailed picture in the atomic scale of these systems via MD and DFT simulations to complement the experimental results about structure and conductivity. A remarkable good agreement was found between experiments and simulations. For example, we have not only been able to confirm the two main orientations of imidazolium cations around the anions using MD simulations, but also we have been able to quantify the percentage of cations in each orientation. Even more, experimentally, it was concluded that hydration water was strongly bound to the anions and with the simulations, we could determine exactly the adsorption sites of water around the anions. We could also give some qualitative explanation of the enhancement of the protonic conductivity with the presence of water obtained experimentally by means of DFT calculations. All these results will be presented in detail in Chapter 7. It has to be mentioned that this work was very important in the formation of the author of this

USC UNIVERSIDADE DE SANTIAGO DE COMPOSTELA

thesis in terms of getting a deeper knowledge about DFT calculations and in terms of developing parameterization of new compounds for MD simulations.

Parallel to these studies regarding small spherical particles, simulations to characterize the opposite limit, i.e. very large nanostructures, were carried out. In this line, the surface of the "very large" toy structures were approximated by flat interfaces in contact with ILs and their mixtures with molecular cosolvents. In the first work related with this limit we focused on the characterization of the EDL, i.e., how the different molecular species arrange in the vicinities of the interfaces and how this structure is affected by different factors such as the charge of the interface, addition of molecular cosolvent or the material of the interfaces. For this task, a set of MD simulations of mixtures of [BMIM][BF_4] and different molecular cosolvents (water, ethanol and methanol) between two oppositely charged parallel graphene slabs were performed. The separation between the slabs was ca. 10 nm. This allowed the existence of a region far from the walls where the bulk properties of the liquid were recovered so a good comparison between bulk and interfacial properties could be done. It has to be mentioned that, although these systems were proposed as an approximation to study large nanostructures they are also a very good description of systems with interest for electrochemical devices such as supercapacitors or batteries so, part of the analysis is also focused on that direction.

The first thing that was studied in this work was the molecular distribution of the different species along the direction perpendicular to the box, focusing on the regions close to the interfaces, i.e. the EDL. Very similar to what happened in the previously introduced work about spherical particles in a mixture of IL and water, the addition of solvent does not significantly affect the ionic structure in the neighbourhood of the walls. However, in this scenario, a preferential adsorption of the cosolvent molecules is only observed at the positively charged wall, while around spherical particles water molecules were only detected close to the surroundings of the negatively charged one. The reason for this is related to the highly packed configurations of the anions around the pos-

USC UNIVERSIDADE DE SANTIAGO DE COMPOSTELA

itively charged solutes, which, due to the excluded volume interactions, prevents the presence of any other molecular specie in the first solvation shell. On the other hand, when planar positive interfaces are considered, the anions in the first layer close to it do not need to be in so highly packed configuration to screen the charge density of the wall and slightly more free volume is available for the cosolvent molecules to be adsorbed. Moreover, the calculations of the radial distribution functions in the bulk region showed a preference by all the considered cosolvents to coordinate with anions instead of cations, so it is not surprising to see more cosolvent molecules at the interface with more adsorbed anions. Regarding the cations at the negatively charged interface, they tend to be adsorbed with their alkyl chains laying at the surface and with the imidazole ring perpendicular to the wall to allow more densely packed configurations. We interestingly check also in this work that the average orientation of the adsorbed cosolvent molecules is also strongly correlated with the electric field, and thus, with the ion distribution. Once the structure in the Z direction was completely characterized, the lateral distribution of the ionic species in planes parallel to the interfaces were analysed by means of two-dimensional density maps and image processing tools. The main result in this matter was that, if the distribution of the adsorbed anions in the positively charged interfaces is analysed, highly ordered patterns can be observed. Moreover, these patterns can be tuned changing the cosolvent and they are propagated towards next ionic layers in a herringbone-like structure. We proved that this structure is not affected when the graphene slabs are replaced with implicit walls emulating different materials. We also developed a simple theory that relates the observed lateral structures only with the ionic charge distribution. This exhaustive structural study of the EDL is contained in the publication in Chapter 8.

After reaching such a detailed understanding of the behaviour of pure IL and mixtures close to charged interfaces, and to follow the same steps as for spherical particles, a description of the situation around neutral interfaces was missing. Thanks to the previous study, we knew that the material of the interface is not important for the properties of the

USC
UNIVERSIDADE DE SANTIAGO DE COMPOSTELA

media, particularly if one is not interested in the specific interaction between the liquid and the interface. With this in mind, we decided to perform a new set of simulations with EAN between planar implicit walls separated a variable distance. In the previous work we employed an aprotic IL so, to explore a wider variety of phenomenology, we decided to proceed with a protic one for this study to understand how the hydrogen bond network is affected by confinement. As we were not interested in the interface-IL interactions, we could employ implicit walls, which considerably accelerates the computational times and allowed performing a very large number of simulations considering almost a continuous range of wall separations from ultra confined situations to simulations with a clear bulk region in the middle. The main goal of these new set of simulations was, of course, to characterize the ionic layering near neutral interfaces as we did before for charged ones. However, motivated by previous works in the literature,[61–63] we wanted to check if the properties of the IL could be affected by confinement. Indeed, we end up finding a clear correlation between the ionic layering between the walls and some structural (density, hydrogen bonds or potential energy) and dynamic (ionic diffusion or short-time position fluctuation) properties. One of the most important results from these simulations is that the nanoconfined systems can be used, together with a simple theory, to have a very good estimation of the spatial range of the effect of the wall in the IL properties. This can be very useful to calculate an optimal porous size in nanoporous materials to be used together with ILs and tune their properties. All these results were collected and published in the Journal of Molecular Liquids (Chapter 9). It has to be mentioned that during the simulation process we had to deal with some problems related with how the dynamic properties are affected by the simulation box size. We tried to be very cautious with this effect and it is also discussed in this chapter.

After this work, a solid knowledge of the solvation properties and structure of ILs and their mixtures close to spherical particles and planar interface was achieved. However, mainly due to the employed force fields, the dynamic properties of the considered ionic media had been

USC
UNIVERSIDADE DE SANTIAGO DE COMPOSTELA

partially left aside. Having a good theoretical framework to model and explain the transport properties of ILs and their mixtures is crucial for a complete characterization of dispersions of nanostructures in these fluids. To solve the lack of knowledge in this matter, we performed atomistic MD simulations of binary mixtures of $BMIM^+$ iodide ([BMIM][I]) and [EMIM][I] with ethanol. We used these simulations to characterize the structure, which fell into the picture drawn by the nanostructured solvation paradigm, i.e. the alcohol molecules distribute homogeneously without forming clusters (as water does). However, these results about the structure were mainly used to understand the difference in the dynamic properties of these mixtures and those with water, which were previously reported.[64] To study the dynamic properties we calculated the ionic conductivity of the mixtures using different theoretical approaches, which led us to the conclusion that the anion-cation correlations can be very relevant in the vicinities of the conductivity maxima. To support the reliability of the conductivities calculated with simulations using non-polarizable force fields, we compared these results with conductivities measured with experiments. The comparative showed that the computational results slightly underestimates the real values (which could be solved using more computationally expensive polarizable force fields), but a very good reproduction of the shape of conductivity dome was obtained. We took this as a proof of the validity of our simulations to characterize the transport phenomenology taking place in these systems. We used the pseudo-lattice random-alloy theoretical framework previously developed in our research group to fit the obtained data. The theory describes the conductivity of a mixture (macroscopic magnitude) using the jumping frequencies of the charged species in the media between cells with different mobilities (microscopic behaviour). We not only confirm that this theory was able to fit all our data sets but also, we used the parameters of the fits to estimate the average jumping frequencies of the molecules in the mixtures and compared this estimation with the values calculated directly from the simulations. The results showed a remarkably good correspondence, which proofs the soundness of the foundations of the theory. Proving the validity of the theory helps affording expensive computations or experiments

USC UNIVERSIDADE DE SANTIAGO DE COMPOSTELA

to predict the dynamic properties of these systems, which considerable accelerates the research progress in the field and, even more important for the aim of this thesis, provides an accurate tool to understand and describe the diffusion of nanostructures dispersed in these media. This study was published in an article also reported in the Journal of Molecular Liquids and it is presented in Chapter 10.

In summary, as it was mentioned in the previous paragraphs, in the following chapters, all the parts of the story told here will be introduced and discussed in detail. At the end, a whole battery of results that make up a very detailed idea of the behaviour of ILs and their mixtures at interfaces with different geometries and under different circumstances will be presented. In addition, there will be a very well founded theory to explain the transport properties of these fluids, properly understanding the role of the cosolvent in their mixtures. The next step to take would be the characterization of intermediate sized nanostructures using all the knowledge already acquired. However, although work has been started in this regard, due to lack of time, they are not part of this thesis and will be the subject of future works.

USC
UNIVERSIDADE DE SANTIAGO DE COMPOSTELA

4- GADDLE Maps: General Algorithm for Discrete object Deformations based on Local Exchange Maps

It is true that to study dispersions of nanostructures in ILs and its mixtures firstly, one must understand how these liquids solvate small solutes and how they place in the surroundings of planar interfaces, which could be interpreted as the infinitely large particle limit. However, at some point, it will be necessary to simulate nanostructures with size in the order of tens of nanometres to have a good insight in the field. As it was mentioned before, such large simulations can not be performed in reasonable times without using CG force fields. However, although this kind of force fields are the perfect tool to obtain the equilibrium configuration of large systems, they loose the structural information at the atomic level. To be able to perform simulations with CG force fields of the self-assembly process of certain nanostructures or just to get the equilibrium configuration of nanostructure dispersions and then recover the atomic resolution, the Gaddle Maps algorithm was developed.

In this chapter, a detailed description of this algorithm is presented. This tool opens the path to a new way of performing simulations of large systems with the process mentioned above. This methodology was applied previously to systems containing some proteins or some biologically interesting lipids. However, the available tools to perform the interchange between force fields were very restrictive, being most of them focused on proteins or lipids, and with a very small set of force fields. To solve these limitations, the "General Algorithm for Discrete object Deformations based on Local Exchange Maps", or Gaddle Maps, was developed. This algorithm has no restrictions in terms of which molecules it can map or in which force field they are represented. Moreover, there is no need for the user to input additional information that is not available in the files needed for the simulations.

To perform this exchange between molecules in different force fields, the algorithm finds the optimal overlap between both represent-

USC
UNIVERSIDADE DE SANTIAGO DE COMPOSTELA

ations using a Monte Carlo sampling of the possible configurations of the molecules with fewer particles. These configurations are explored by making small changes to the molecular configurations (translations, rotations and single-atom displacements). After finding the optimal overlapping, an exchange map is generated which allows extrapolating this overlap to all the molecular configurations found in a simulation. After presenting and describing the algorithm, a wide variety of systems are used as examples of the algorithm application, e.g. systems including vesicles, ILs, DNA fragments, nano-tubes, proteins, etc. An open source implementation of the algorithm as a Python module can be found in Ref. 65.

The post-print version of this publication can be found in the appendix A.1.

The author of this thesis contributed to this publication, according to the CRediT contribution classification,[66;67] with: Conceptualization, Data curation, Formal Analysis, Investigation, Methodology, Software, Validation, Visualization, Writing - original draft, Writing - review & editing.

USC
UNIVERSIDADE DE SANTIAGO DE COMPOSTELA

JCTC Journal of Chemical Theory and Computation

Article

Cite This: J. Chem. Theory Comput. 2018, 14, 466−478

pubs.acs.org/JCTC

GADDLE Maps: General Algorithm for Discrete Object Deformations Based on Local Exchange Maps

J. Manuel Otero-Mato,[†] Hadrián Montes-Campos,[†] Martín Calvelo,[§] Rebeca García-Fandiño,[⊥] Luis J. Gallego,[†] Ángel Piñeiro,*[,∥] and Luis M. Varela*[,†]

[†]Nanomaterials, Photonics and Soft Matter Group, Departamento de Física de Partículas y Departamento de Física Aplicada, Facultade de Física, Universidade de Santiago de Compostela, Campus Vida s/n, E-15782 Santiago de Compostela, Spain

[⊥]CIQUP, Department of Chemistry and Biochemistry, Faculty of Sciences, University of Porto, R. Campo alegre, 687, P-4169-007 Porto, Portugal

[§]Department of Organic Chemistry, Center for Research in Biological Chemistry and Molecular Materials, University of Santiago de Compostela, Campus Vida s/n, E-15782 Santiago de Compostela, Spain

[∥]Soft Matter and Molecular Biophysics Group, Departamento de Física Aplicada, Facultade de Física, Universidade de Santiago de Compostela, Campus Vida s/n, E-15782 Santiago de Compostela, Spain

DOI: https://doi.org/10.1021/acs.jctc.7b00861

USC UNIVERSIDADE DE SANTIAGO DE COMPOSTELA

5- Solvation in Ionic Liquid-Water mixtures: A Computational Study

To address the challenge of characterizing dispersions of nanostructures in ILs and its mixtures, a deep understanding of the solvation properties of these media must be achieved. To focus on this aspect and to avoid effects that may be due to the nanostructure geometry, size or material, a toy model consisting on a spherical generic particle immersed on an ionic fluid was used. Following this idea, one of the first tasks carried out during this thesis was the characterization of small spherical generic particles solvated in mixtures of an IL with water by means of MD simulations.

In this chapter, the implementation and results of these simulations are presented. The chosen IL was the 1-ethyl-3-methylimidazolium acetate and water was present in a 5% concentration. The reason for this choice was to study the effect of water presence in a concentration that is usually considered as "residual", unavoidable due to the hygroscopic nature of many ILs. This comparison was done with previously reported results[60] for the same systems without water. The effects of the solute charge are also characterized by means of simulations with neutral, positively and negatively charged spheres.

The results reveal that water does not significantly perturb neither the structure of the electric double layer, nor the orientation of ions in the neighbourhood of the solute particle. Although water does not seem to play any significant role in the solvation of neutral solutes, there is an excess of water in the first and second ionic solvation shell of positively and negatively charged solutes, respectively. The correlation between the electric field around the negatively charged solute and the orientation of the dipole moment of water molecules is also studied, finding that, although the dynamic properties of water molecules are almost unaltered in the presence of the solute, and the ionic cage around the central solute particle is only slightly affected upon water addition, the mobility of the

USC UNIVERSIDADE DE SANTIAGO DE COMPOSTELA

spheres is drastically enhanced.

The post-print version of this publication can be found in the appendix A.2.

The author of this thesis contributed to this publication, according to the CRediT contribution classification,[66;67] with: Conceptualization, Data curation, Formal Analysis, Investigation, Methodology, Software, Validation, Visualization, Writing - original draft, Writing - review & editing.

USC UNIVERSIDADE DE SANTIAGO DE COMPOSTELA

Journal of Molecular Liquids 292 (2019) 111273

Contents lists available at ScienceDirect

Journal of Molecular Liquids

journal homepage: www.elsevier.com/locate/molliq

Solvation in ionic liquid-water mixtures: A computational study

José M. Otero-Mato[a], Volker Lesch[b], Hadrián Montes-Campos[a], Jens Smiatek[c,d], Diddo Diddens[d], Oscar Cabeza[e], Luis J. Gallego[a], Luis M. Varela[a,*]

[a]Grupo de Nanomateriais, Fotónica e Materia Branda, Departamento de Física de Partículas, Universidade de Santiago de Compostela, Campus Vida s/n E-15782, Santiago de Compostela, Spain
[b]Senacor Technologies AG, Joseph-Schumpeter-Allee 1, Bonn 53227, Germany
[c]Institut für Computerphysik, Universität Stuttgart, D-70569 Stuttgart, Germany
[d]Helmholtz-Institute Münster (HI MS), Ionics in Energy Storage, Forschungszentrum Jülich GmbH, Corrensstraße 46, Münster 48149, Germany
[e]Facultade de Ciencias, Universidade da Coruña, Campus A Zapateira s/n E-15008, A Coruña, Spain

ARTICLE INFO

Article history:
Received 12 April 2019
Received in revised form 6 June 2019
Accepted 30 June 2019
Available online 13 July 2019

DOI: https://doi.org/10.1016/j.molliq.2019.111273

USC UNIVERSIDADE DE SANTIAGO DE COMPOSTELA

6- Enthalpy of solvation of alkali metal salts in a protic ionic liquid: Effect of cation charge and size

Continuing with the line started with the previous work, we planned to analyse the effect of the solute size and charge (magnitude of the charge in this case instead of the sign). For this task, we decided to avoid virtual solute particles and use different alkali metal cations (mono- and divalents). With this approach, we do not only consider our own goals, but also, we tried to provide a valuable set of results for systems with interest in other fields which can be useful for the community. The chosen IL used as solvent for the salts was the model PIL, EAN. This was the chosen IL mainly because it is very accessible, but also because its solvation properties are comparable with those of another polar solvents such as water.

For this study we performed high precision solution-reaction calorimetry to obtain the heat of solvation of all the salts in EAN, which was used for the analysis of the thermodynamics. A strong correlation between the structure of the salts in the crystalline phase and its enthalpy of solvation in the IL was found. A detailed picture of the molecular environments in the solvation shells around the metal cations is provided by means of MD simulations. The analysis of the energetics and structure of solvation confirms the well-known water-like properties of EAN, showing that the solvation shells around the metal cations in both media are very similar. On the other hand, the results showed that it is energetically more favourable to solvate smaller cations with higher valence. Indeed, the simulations and a simple developed theory, showed that the long-range electrostatic interactions are the main contribution to solvation enthalpy, with the electric field at the surface of the alkali metal cations as the basic magnitude controlling it.

The post-print version of this publication can be found in the appendix A.3 and its supplementary material in the B.1.

The author of this thesis contributed to this publication, accord-

USC UNIVERSIDADE DE SANTIAGO DE COMPOSTELA

ing to the CRediT contribution classification,[66;67] with: Conceptualization, Methodology, Software, Validation, Formal Analysis, Investigation, Data Curation, Writing - Original Draft, Writing - Review & Editing, Visualization.

USC
UNIVERSIDADE DE SANTIAGO DE COMPOSTELA

Journal of Molecular Liquids 360 (2022) 119228

Contents lists available at ScienceDirect

Journal of Molecular Liquids

journal homepage: www.elsevier.com/locate/molliq

Enthalpy of solvation of alkali metal salts in a protic ionic liquid: Effect of cation charge and size

Juan J. Parajó [a,b,1], José M. Otero-Mato [b,1], Ana I.M.C. Lobo Ferreira [a], Luis M. Varela [b], Luis M.N.B.F. Santos [a,*]

[a] CIQUP, Institute of Molecular Sciences (IMS) - Departamento de Química e Bioquímica, Faculdade de Ciências da Universidade do Porto, Rua do Campo Alegre, P-4169-007 Porto, Portugal
[b] Grupo de Nanomateriais, Fotónica e Materia Branda, Departamento de Física de Partículas, Universidade de Santiago de Compostela, Campus Vida s/n E-15782, Santiago de Compostela, Spain

ARTICLE INFO

Article history:
Received 4 February 2022
Revised 18 April 2022
Accepted 21 April 2022
Available online 12 May 2022

DOI: https://doi.org/10.1016/j.molliq.2022.119228

7- A New Solid State Proton Conductor: The Salt Hydrate Based on Imidazolium and 12-Tungstophosphate

Continuing with the line of spherical particle dispersions in ILs and their mixtures, in the third year of this thesis, the opportunity to collaborate with an experimental research group to characterize a specific type of hydrated salts arose. The salt in question is obtained from an acid-base reaction via proton transfer from 12-tungstophosphoric acid to imidazolium (the same process followed to synthesize PILs). For each anion of this salt there are three imidazolium cations, which share many properties with other cations previously used in this thesis (such as $EMIM^+$, used in Chapter 5). This compound showed a very high proton conductivity even at room temperatures, making it a very good candidate for various electrochemical applications, specifically for membranes in fuel cells. On the other hand, the most interesting thing about this collaboration in relation to the content of this thesis is the structure and shape of anions. Each anion contains one phosphorous, 12 tungsten and 40 oxygen atoms distributed in a typical structure in heteropoly acids known as Keggin structure. This structure has a spherical shape and has terminal oxygens on its surface that are hydrogen bond acceptors. This work is very interesting for the development of the thesis since it not only represents a step forward in terms of considering particles with larger radius, but also introduces details in the topology of the particles, being no longer perfect spheres. In addition, to provide a complete view of the microscopic behaviour of these systems, not only molecular dynamics simulations were carried out, but also DFT calculations were used to study the phenomenology related with proton hopping in the vicinity of the anion surface.

The main objective of the collaboration was to provide a microscopic picture of the structure of these systems to support and complete the results obtained experimentally. We were also interested in characterizing how changing the salt hydration levels affected this structure.

USC
UNIVERSIDADE DE SANTIAGO DE COMPOSTELA

However, the most novel and interesting aspect of this work is that a considerably high proton conductivity appears for this type of salt at a specific degree of hydration.

The experimental results show that the proton conductivity of the salt with 4 water molecules per anion measured at truly anhydrous conditions reads $0.8 \times 10^{-6}\,\mathrm{S\,cm^{-1}}$ at 322 K, which is higher than the conductivity reported for any other related hydrated salt, despite the lower hydration. In the pseudo-anhydrous state (2 water molecules per anion), the proton conductivity is still remarkable and, judging from the low activation energy ($E_a = 0.26\,\mathrm{eV}$), attributed to structural diffusion of protons. From complementary X-ray diffraction data, vibrational spectroscopy, and solid-state NMR experiments, the local structure of this salt hydrate was resolved, with imidazolium cations preferably orienting flat on the surface of the tungstophosphate anions, thus achieving a densely packed solid material, and water molecules of hydration that establish extremely strong hydrogen bonds. Computational results confirm these structural details and also evidence that the path of the lowest energy for the proton transfer involves primarily imidazole and water molecules, while the proximate Keggin anion contributes with reducing the energy barrier for this particular pathway.

The post-print version of this publication can be found in the appendix A.4 and its supplementary material in the B.2.

The author of this thesis contributed to this publication specially with the computational part. The experiments have been carried out by the rest of the co-authors in their facilities. In terms of the CRediT contribution classification,[66;67] the author contributed to the computational part with: Data curation, Formal Analysis, Investigation, Methodology, Software, Validation, Visualization, Writing - original draft, Writing - review & editing.

USC
UNIVERSIDADE DE SANTIAGO DE COMPOSTELA

JACS
JOURNAL OF THE AMERICAN CHEMICAL SOCIETY
pubs.acs.org/JACS
Article

A New Solid-State Proton Conductor: The Salt Hydrate Based on Imidazolium and 12-Tungstophosphate

Anna Martinelli,* José M. Otero-Mato, Mounesha N. Garaga, Khalid Elamin, Seikh Mohammad Habibur Rahman, Josef W. Zwanziger, Ulrike Werner-Zwanziger, and Luis M. Varela

Cite This: *J. Am. Chem. Soc.* 2021, 143, 13895−13907

Read Online

DOI: https://doi.org/10.1021/jacs.1c06656

USC
UNIVERSIDADE DE SANTIAGO DE COMPOSTELA

8- 3D Structure of the Electric Double Layer of Ionic Liquid-Alcohol Mixtures at the Electrochemical Interface

In parallel to the research line with spherical particles, more simulations were carried out of systems where the opposite limit was considered, i.e. how the ILs and their mixtures would behave around very large particles (compared to the molecules of the medium). In this limit we can approximate the surface of the dispersed nanostructure in the IL as a flat interface in contact with the ionic fluid.

This chapter presents the results of a series of MD simulations of mixtures of 1-butyl-3-methylimidazolium tetrafluoroborate with different molecular cosolvents such as water, methanol and ethanol between two charged graphene interfaces separated by a distance of approximately 10 nm. The main aim of this set of simulations was to fully characterize the structure of the EDL in both the perpendicular and parallel direction respect to the interfaces. The adsorption of cosolvent molecules at the graphene walls is characterized as well as their distribution across the system. The results show that, due to a higher affinity of the polar groups to be close to the anions in combination with the electrostatic and excluded volume interactions, there exists a marked tendency of the OH^- groups to lie close to the anode, inducing small changes in the first cation layer. The orientation of cosolvent molecules is found to be closely related to the alignment of the molecular dipole moment with the electric field. The lateral ionic distribution in the layers close to the electrodes is also investigated, which shows a structural transition from liquid-like lamellar ordering to solid-like hexagonal patterns as the size of the cosolvent molecules increases, leading to smaller position fluctuations of the ions. The dependence of the specific patterns on the nature of the electrodes is also studied. This study strongly suggests that the ionic patterns formed in the first ionic layers next to the charged interfaces are universal since their existence does not crucially depend on the atomic composition of the interfacial material, but only on the net

USC UNIVERSIDADE DE SANTIAGO DE COMPOSTELA

charge density of the considered ionic layer, which significantly changes the ionic mobility in this region.

The post-print version of this publication can be found in the appendix A.5 and its supplementary material in the B.3.

The author of this thesis contributed to this publication, according to the CRediT contribution classification,[66;67] with: Conceptualization, Data curation, Formal Analysis, Investigation, Methodology, Software, Validation, Visualization, Writing - original draft, Writing - review & editing.

USC
UNIVERSIDADE DE SANTIAGO DE COMPOSTELA

PCCP

PAPER

Check for updates

Cite this: *Phys. Chem. Chem. Phys.*, 2018, **20**, 30412

3D structure of the electric double layer of ionic liquid–alcohol mixtures at the electrochemical interface†

José M. Otero-Mato, [a] Hadrián Montes-Campos, [a] Oscar Cabeza, [b] Diddo Diddens, [c] Alina Ciach, [d] Luis J. Gallego [a] and Luis M. Varela *[a]

DOI: https://doi.org/10.1039/C8CP05632C

USC UNIVERSIDADE DE SANTIAGO DE COMPOSTELA

9- Nanoconfined Ionic Liquids: A Computational Study

In the previous chapter the attention was focused on the 3D structure of the EDL in the vicinities of charged interfaces, as well as on how it changes with the addition of molecular cosolvents or changing the materials of the interfaces. In this chapter, the focus will be on the study of the effects of the nanoconfinament on pure ILs. For this task, the charge from the interfaces will be removed as well as their atomic details. Specifically, in this part of the thesis, how the properties of ILs change upon confinement between two walls at various nanometric distances will be studied. This is very interesting for this thesis for two reasons. On the one hand, the range of the effects of a supposed nanoparticle in the structure of the ionic medium can be determined with this kind of simulations as it will be shown. On the other hand, this provides some insights on how the structure and dynamics of an IL correlates with the pores that could be present in complex nanostructures.

Indeed, in these simulations, a correlation between the dynamic properties and the structure under extremely nanoconfined circumstances is found. For EAN IL (the one used in the simulations), the ionic structure inside the simulation boxes is a consequence of a subtle combination of ion packing, hydrogen bonding, electrostatic and van der Waals forces. It is also studied how the dynamic properties of this material change in these conditions, showing a decrease in the ionic mobility for very low slit sizes, recovering the bulk behaviour as the distance between walls increases. Moreover, when short wall separations are considered, it is shown that the ionic mobility at short times is a minimum when the hydrogen bonding is also a minimum. Finally, the effect of the interface in the long-time ion dynamics only extends to a quite small region (ca. 1.35 nm) next to the walls. It is also reported that the overall behaviour of the nanoconfined liquid in the slit pore can be described by the superposition of a bulk and a confined simulation with a fitted wall separation.

USC
UNIVERSIDADE DE SANTIAGO DE COMPOSTELA

The post-print version of this publication can be found in the appendix A.6 and its supplementary material in the B.4.

The author of this thesis contributed to this publication, according to the CRediT contribution classification,[66;67] with: Conceptualization, Data curation, Formal Analysis, Investigation, Methodology, Software, Validation, Visualization, Writing - original draft, Writing - review & editing.

USC
UNIVERSIDADE DE SANTIAGO DE COMPOSTELA

Journal of Molecular Liquids 320 (2020) 114446

Contents lists available at ScienceDirect

Journal of Molecular Liquids

journal homepage: www.elsevier.com/locate/molliq

Nanoconfined ionic liquids: A computational study

José M. Otero-Mato [a], Hadrián Montes-Campos [a], Oscar Cabeza [b], Luis J. Gallego [a], Luis M. Varela [a,*]

[a] Grupo de Nanomateriais, Fotónica e Materia Branda, Departamento de Física de Partículas, Universidade de Santiago de Compostela, Campus Vida s/n, E-15782 Santiago de Compostela, Spain
[b] Facultade de Ciencias, Universidade da Coruña, Campus A Zapateira s/n, E-15008 A Coruña, Spain

ARTICLE INFO

Article history:
Received 30 July 2020
Received in revised form 22 September 2020
Accepted 25 September 2020
Available online 3 October 2020

DOI: https://doi.org/10.1016/j.molliq.2020.114446

USC UNIVERSIDADE DE SANTIAGO DE COMPOSTELA

10- Structure, Dynamics and Conductivities of Ionic Liquid-Alcohol Mixtures

Although in the previously presented works some efforts to characterize the dynamic properties of ILs were done, the truth is that we did not pay enough attention to this topic. Having a good theoretical framework capable of describing magnitudes such us the ionic conductivity of these ionic media is crucial to have a full insight of the physics governing these systems. Even more, understanding the dynamics of mixtures of ILs with molecular cosolvents implies being able to optimize the conditions of the media in dispersions of nanostructures to obtain a desired environment for a certain application.

With this aim, we study the microscopic structure and transport properties of ions in mixtures of 1-butyl-3-methylimidazolium and 1-butyl-3-ethylimidazolium iodide with ethanol using atomistic molecular dynamics simulations and experimental conductivity measurements. The results are compared with those for the same ionic liquid in water (reported previously in the literature[64]). The comparison reveals essential differences in ionic structure that are closely related to the differences in the solubility mechanisms of both types of solvents. In particular, unlike for aqueous solutions, we find a homogeneous distribution of solvent molecules in the system, i.e. we observe no cluster formation, which agrees with the nano-structured solvation paradigm. In addition, we calculated the conductivities of these systems in the whole concentration range and compared them with experimental data. Although the simulated values slightly underestimate the experimental ones, they reproduce the shape of the experimental conductivity dome reasonably well. We also show that the pseudo-lattice random-alloy model, which is based on microscopic ion hopping frequencies, describes the conductivity data accurately. We computed the average jumping frequencies directly from simulations and found that they agree well with those obtained by fitting the simulation conductivity data. These results showed that the pseudo-lattice random-alloy model is a valuable framework to

USC
UNIVERSIDADE DE SANTIAGO DE COMPOSTELA

describe the conductivities of ionic liquid-solvent mixtures and particularly, their concentration dependence. It shall also apply to other systems, e.g. inorganic electrolytes and dispersed ionic conductors.

The post-print version of this publication can be found in the appendix A.7 and its supplementary material in the B.5.

The author of this thesis contributed to this publication, according to the CRediT contribution classification,[66;67] with: Conceptualization, Methodology, Software, Validation, Formal Analysis, Investigation, Data Curation, Writing - original draft, Writing - review & editing, Visualization.

USC
UNIVERSIDADE DE SANTIAGO DE COMPOSTELA

Journal of Molecular Liquids 355 (2022) 118955

Contents lists available at ScienceDirect

Journal of Molecular Liquids

journal homepage: www.elsevier.com/locate/molliq

Structure, dynamics and conductivities of ionic liquid-alcohol mixtures

José M. Otero-Mato [a], Hadrián Montes-Campos [a], Víctor Gómez-González [a], Martín Montoto [a], Oscar Cabeza [b], Svyatoslav Kondrat [c,d,e], Luis M. Varela [a,*]

[a] Grupo de Nanomateriais, Fotónica e Materia Branda, Departamento de Física de Partículas, Facultade de Física and Instituto de Materiais (iMATUS), Universidade de Santiago de Compostela, Campus Vida s/n E-15782, Santiago de Compostela, Spain
[b] Facultade de Ciencias, Universidade da Coruña, Campus A Zapateira s/n E-15071, A Coruña, Spain
[c] Institute of Physical Chemistry, Polish Academy of Sciences, Kasprzaka 44/52, 01-224 Warsaw, Poland
[d] Max-Planck-Institut für Intelligente Systeme, Heisenbergstraße 3, 70569 Stuttgart, Germany
[e] IV. Institut für Theoretische Physik, Universität Stuttgart, Pfaffenwaldring 57, 70569 Stuttgart, Germany

ARTICLE INFO

Article history:
Received 16 January 2022
Revised 8 March 2022
Accepted 15 March 2022
Available online 19 March 2022

DOI: https://doi.org/10.1016/j.molliq.2022.118955

Part III

Conclusions

USC
UNIVERSIDADE DE SANTIAGO DE COMPOSTELA

USC
UNIVERSIDADE
DE SANTIAGO
DE COMPOSTELA

11- Conclusions and Future Perspectives

11.1 Conclusions

The main conclusions derived from this thesis are:

1. MD simulations with large simulation boxes and atomic resolutions can be now easily performed by using simulations with CG force fields to obtain the initial configurations. The Gaddle Maps algorithm, developed during the first stages of this thesis, allows performing automatically the change between force fields in a simulation. This opens the door to perform simulations in multiple time and size scales, while having always access to the atomic resolution to study the properties in a more detailed way. In this sense, simulations with IL crystals (which have very slow dynamics and form mesoscopic structures) or large nanostructures dispersed in ILs are now more accessible.

2. Regarding solvation properties of ILs, the addition of molecular cosolvents does not change the ionic distribution around the solute independently of the charge of the dissolved particles. This was reported in the neighbourhood of small spherical particles by means of simulations of a PIL in the presence of small amounts of water. The same was observed in the surroundings of planar interfaces in the presence of an AIL in mixtures with different molecular cosolvents such as water or short chained alcohols.

3. It is reported by means of MD simulations of salts with cations of different sizes and charges that the ionic structure around them is completely determined by the electric field at their surface. In addition, the structure around the solutes, which is mainly determined by the electrostatic interaction, is directly related to other

USC UNIVERSIDADE DE SANTIAGO DE COMPOSTELA

macroscopic properties such as the enthalpy of solvation of the solutes.

4. The water-like properties of the EAN IL were analysed and understood by means of high precision calorimetric measures and MD simulations. The latter showed that the solutes present very similar coordination numbers in both media. Moreover, the anions in the IL and also water molecules in the first solvation shell, point their oxygen atoms towards the solute metal cation. The results for the solvation enthalpies together with the results from the simulations, showed that the electrostatic interactions are the main contribution to the energetics of the solvation process. The van der Waals and excluded volume interactions are only relevant in the solvation shell around the cation with the highest charge density (Mg^{2+}), i.e. the most electrostrictive one.

5. The properties of a proton conductor based on a heteropolyacid were shown to be tunable by adding water and imidazolium, precursors of ILs. It has been shown how simulations allow accessing the information about the adsorption sites and orientation of the different species around complex atomic structures. In addition, DFT calculations allow a better understanding of the proton transfer routes and why they are favoured with the addition of these species. There is a perfect agreement between the experimental and computational data, the latter yielding a very detailed microscopic picture of the physics behind it.

6. Using computer simulations of a PIL between two neutral interfaces, it has been analysed how the macroscopic properties of an IL under nanoconfinement conditions can be tuned by adjusting the slit size. A strong competition between electrostatic and excluded volume interactions is observed in that scenario. Maxima in the total density and minima in the numbers of hydrogen bonds are observed when the distance between interfaces allows a perfect ionic layering.

USC
UNIVERSIDADE DE SANTIAGO DE COMPOSTELA

7. With these simulations and a simple theoretical formalism, a framework was built to quantitatively determine the range of the effect of the interfaces. In case of EAN, the effect of the interfaces extends around the equivalent of 2-3 ionic layers around them.

8. The presence of interfaces not only alters the structure of the ionic media in the perpendicular direction, but also in the parallel one. This change gives rise to patterns in the lateral distribution of the ions in the first layers. These patterns are determined by the charge density in the neighbourhood of the interface, which can be tuned by changing the charge of the interface or adding molecular cosolvents. This structure propagates to the subsequent 2-3 ionic layers. This 3D structure of the electric double layer opens the door to the existence of routes with lower potential energy barriers than those calculated only with the axial structure, which could allow a better transport of compounds like lithium at these interfaces.

9. The addition of small amounts of molecular cosolvents does not significantly change the structure of ILs, but it does significantly change the dynamics. This is further studied by testing the pseudo-lattice random-alloy theoretical framework and analysing the dependence of the conductivity on solvent concentration. The model perfectly recreates the phenomenology and offers a new insight on the micro- and macroscopic relationship of dynamics. With this theory, we have a solid framework to understand the dynamics of these complex charged fluids that serve as media for different nanostructures.

11.2 Future Perspectives

The work presented in this thesis offers a very detailed fundamental understanding of the solvation and dynamic properties of ILs and their

USC UNIVERSIDADE DE SANTIAGO DE COMPOSTELA

mixtures with molecular cosolvents. To carry out these studies, we have mainly used approaches where either very large or very small solutes were studied. A tool that facilitates the simulation of intermediate structures was also developed. That said, after the completion of this thesis, the following research lines will be addressed:

1. Characterize by means of simulations, the dynamics and structure of dispersions of different nanostructures (e.g. nanotubes, nanowires...) with photonic or electrochemical interest in ionic liquids.

2. Carry out self-assembly simulations of structures using ionic liquid crystals and understand how the addition of salts or other solvents affects the stability of these structures.

3. Simulate ILs immersed in nanostructured matrices formed by long-chain polymers or other materials such as silicon. With this, a microscopic image of what happens in ionogels, materials with special interest for their applications in electrochemical devices, would be obtained.

4. Perform studies to better understand electron transfer between ILs and different nanostructures, e.g. gold nanoparticles, with special interest in photonics.

USC
UNIVERSIDADE DE SANTIAGO DE COMPOSTELA

B- Supplementary Information

In the following pages we include the Supplementary information for the following articles:

- Enthalpy of solvation of alkali metal salts in a protic ionic liquid: Effect of cation charge and size
- A New Solid State Proton Conductor: The Salt Hydrate Based on Imidazolium and 12-Tungstophosphate
- 3D Structure of the Electric Double Layer of Ionic Liquid-Alcohol Mixtures at the Electrochemical Interface
- Nanoconfined Ionic Liquids: A Computational Study
- Structure Dynamics and Conductivities of Ionic Liquid-Alcohol Mixtures

USC
UNIVERSIDADE DE SANTIAGO DE COMPOSTELA

USC
UNIVERSIDADE
DE SANTIAGO
DE COMPOSTELA

SUPPORTING INFORMATION

Solvation enthalpy of alkali metal salts in a protic ionic liquid: Effect of cation charge and size

Juan J. Parajó[1,2], José M. Otero-Mato[2], Ana I.M.C.L. Lobo Ferreira[1], Luis M. Varela[2], Luis M.N.B.F. Santos[1]

[1] CIQUP, Institute of Molecular Sciences (IMS) - Departamento de Química e Bioquímica, Faculdade de Ciências da Universidade do Porto, Rua do Campo Alegre, P-4169-007 Porto, Portugal

[2] Grupo de Nanomateriais, Fotónica e Materia Branda, Departamento de Física de Partículas, Universidade de Santiago de Compostela, Campus Vida s/n E-15782, Santiago de Compostela, Spain

Tables

Table S1 Enthalpy of the solution of THAM(cr) in 0.100 mol·dm^{-3} of HCl(aq), at 298.15 K.

Table S2 Mass of alkaline metal nitrate salts and EAN(l) used for the different molalities of the compound mixtures. *Not fully soluble.

Table S3 Simulation parameters of the used alkali metal cations. σ and ε are the Lennard-Jones parameters used for the short-range interactions.

Table S4 Mass sample and enthalpy of solution (in 100 cm3 of water or previously solution with EAN in the case of the metal nitrates) of EAN(l), $LiNO_3$(cr), KNO_3(cr), $RbNO_3$(cr), $CsNO_3$(cr), $Mg(NO_3)_2{\cdot}6H_2O$(cr) and $Ca(NO_3)_2{\cdot}4H_2O$(cr) at 298.15 K.

Table S5 Values of the measured enthalpies of solution for the EAN/salt mixtures at different salt concentrations ($\Delta_s H_3$) and molar solution enthalpy ($\Delta_s H_m^{\infty}$) for all the studied EAN plus salt mixtures at different molalities in water at 298.15 K.

Table S6 Values enthalpy of solvation of the metal cations in water ($\Delta_{hyd}H_m$) and in EAN ($\Delta_s H_m^{\infty *}$).

Table S7 Coordination numbers of water molecules and nitrate anions around alkali metal cations in both solvents (water and EAN). The numbers for the nitrate were obtained from our simulations while the ones for water were extracted from the literature.

USC UNIVERSIDADE DE SANTIAGO DE COMPOSTELA

Table S1

Enthalpy of the solution of THAM(cr) in 0.100 mol·dm^{-3} of HCl(aq), at 298.15 K.

m_{THAM} / g	$\Delta_s H_{THAM}$ / kJ·mol^{-1}
0.37731	29.56
0.34853	29.66
0.32075	29.66
0.33704	29.82
0.31757	29.81
Average	29.70 ± 0.10

Uncertainty calculated as twice the standard error of the mean (95%)

USC
UNIVERSIDADE DE SANTIAGO DE COMPOSTELA

Table S2

Mass of alkaline metal nitrate salts and EAN(l) used for the different molalities of the compound mixtures. *Not fully soluble.

Compound /mixtures	M_{IL} / g	m_{salt} / g	molality / mol·kg^{-1}
EAN(l) + $LiNO_3$(cr)	1.758	0.014	0.113
	1.518	0.025	0.242
	0.976	0.033	0.492
	1.519	0.091	0.867
	0.739	0.053	1.031
	1.514	0.157	1.502
	1.399	0.191	1.976
EAN(l) + $NaNO_3$(cr)	0.938	0.005	0.059*
	0.843	0.016	0.222*
EAN(l) + KNO_3(cr)	0.905	0.007	0.078
	5.135	0.051	0.099
	1.162	0.015	0.128
	0.980	0.015	0.149
	5.033	0.090	0.177
	0.914	0.023	0.245*
	0.833	0.018	0.215*
EAN(l) + $RbNO_3$(cr)	1.626	0.023	0.097
	1.116	0.020	0.119
	1.220	0.026	0.143
	1.129	0.029	0.175
	1.104	0.032	0.199
	1.141	0.043	0.253*
EAN(l) + $CsNO_3$(cr)	1.050	0.015	0.071
	1.006	0.016	0.081
	0.936	0.022	0.120
	0.863	0.023	0.138
	1.483	0.050	0.173*
	1.136	0.044	0.199*
EAN(l) + $Mg(NO_3)_2 \cdot 6H_2O$(cr)	1.170	0.029	0.096
	0.893	0.045	0.196
	0.641	0.065	0.397
	1.011	0.205	0.789
	0.938	0.438	1.823
EAN(l) + $Ca(NO_3)_2 \cdot 4H_2O$(cr)	1.256	0.083	0.279
	1.475	0.188	0.538
	1.250	0.187	0.635
	1.188	0.222	0.793
	1.439	0.334	0.983
EAN(l) + $Sr(NO_3)_2$(cr)	0.946	0.015	0.073*
	1.112	0.031	0.132*
EAN(l) + $Ba(NO_3)_2$(cr)	4.265	0.015	0.014*
	1.293	0.035	0.103*
	1.035	0.001	0.004

USC UNIVERSIDADE DE SANTIAGO DE COMPOSTELA

Table S3
Simulation parameters of the used alkali metal cations. σ and ε are the Lennard-Jones parameters used for the short-range interactions.

Metal	Atom-type	σ (nm)	ε (kJ/mol)	Charge (e)	Mass (a.u.)
Li	opls_406	0.213	0.0765	+1	6.9
Na	opls_407	0.333	0.0116	+1	23.0
K	opls_408	0.493	0.001237	+1	39.1
Rb	opls_409	0.562	0.000715	+1	85.47
Cs	opls_410	0.672	0.000339	+1	132.9
Mg	opls_411	0.164	3.66	+2	24.3
Ca	opls_412	0.241	1.88	+2	40.0
Sr	opls_413	0.310	0.485	+2	87.6
Ba	opls_414	0.382	0.197	+2	137.3

Table S4

Mass sample and enthalpy of solution (in 100 cm^3 of water or previously solution with EAN in the case of the metal nitrates) of EAN(l), $LiNO_3$(cr), KNO_3(cr), $RbNO_3$(cr), $CsNO_3$(cr), $Mg(NO_3)_2 \cdot 6H_2O$(cr) and $Ca(NO_3)_2 \cdot 4H_2O$(cr) at 298.15 K.

Compound	m / g	$\Delta_s H$ / kJ·mol^{-1}
EAN(l)	0.12820	4.962
	0.24720	4.961
	0.24398	4.970
	0.24640	4.960
	0.25546	4.929
$LiNO_3$(cr)	0.03180	-2.077
	0.05492	-2.046
	0.05846	-2.170
	0.05651	-2.105
	0.05607	-2.133
KNO_3(cr)	0.02822	35.276
	0.01706	35.212
	0.04590	35.106
	0.03746	35.162
$RbNO_3$(cr)	0.16146	36.540
	0.04414	36.694
$CsNO_3$(cr)	0.05458	39.982
	0.12346	40.232
$Mg(NO_3)_2 \cdot 6H_2O$(cr)	0.04845	19.081
	0.05783	18.976
$Ca(NO_3)_2 \cdot 4H_2O$(cr)	0.04867	32.051
	0.03315	32.196

USC UNIVERSIDADE DE SANTIAGO DE COMPOSTELA

Table S5

Values of the measured enthalpies of solution for the EAN/salt mixtures at different salt concentrations ($\Delta_s H_3$) and molar solution enthalpy ($\Delta_s H_m^\infty$) for all the studied EAN plus salt mixtures at different molalities in water at 298.15 K.

Compound	Molality	γ	$\Delta_s H_3$	$\Delta_s H_m^\infty$
EAN:γ$LiNO_3$(l)	0.113	0.010	4.825 ± 0.035	–0.115 ± 0.038
	0.242	0.026	4.478 ± 0.048	–0.247± 0.039
	0.492	0.053	4.255 ± 0.045	–0.500 ± 0.039
	0.867	0.094	3.953 ± 0.007	–0.881 ± 0.039
	1.031	0.111	3.789 ± 0.0	–1.047 ± 0.040
	1.502	0.162	3.167 ± 0.016	–1.526 ± 0.041
	1.976	0.214	2.36 ± 0.089	–2.009 ± 0.043
EAN:γKNO_3(l)	0.078	0.008	5.212 ± 0.0	–0.028 ± 0.043
	0.099	0.011	5.319 ± 0.017	–0.036 ± 0.044
	0.128	0.014	5.389 ± 0.025	–0.046 ± 0.046
	0.149	0.016	5.483 ± 0.0	–0.054 ± 0.047
	0.177	0.019	5.559 ± 0.03	–0.064 ± 0.049
EAN:γ$RbNO_3$(l)	0.097	0.010	5.262 ± 0.016	–0.048 ± 0.048
	0.119	0.013	5.352 ± 0.008	–0.058 ± 0.050
	0.143	0.015	5.436 ± 0.041	–0.070 ± 0.052
	0.175	0.019	5.581 ± 0.039	–0.086 ± 0.055
	0.199	0.021	5.668 ± 0.011	–0.097 ± 0.057
EAN:γ$CsNO_3$(l)	0.071	0.008	5.296 ± 0.013	0.022 ± 0.052
	0.081	0.009	5.358 ± 0.006	0.025 ± 0.054
	0.120	0.013	5.511 ± 0.005	0.037 ± 0.060
	0.138	0.015	5.577 ± 0.004	0.043 ± 0.062
EAN:γ$Mg(NO_3)_2$(l)	0.096	0.010	4.61 ± 0.038	–0.759 ± 0.042
	0.196	0.021	3.725 ± 0.0	–1.553 ± 0.046
	0.397	0.043	2.976 ± 0.021	–3.150 ± 0.053
	0.789	0.085	0.356 ± 0.226	–6.264 ± 0.065
	1.823	0.197	-6.732 ± 0.005	–14.473 ± 0.089
EAN:γ$Ca(NO_3)_2$(l)	0.279	0.030	4.888 ± 0.104	–1.127 ± 0.061
	0.538	0.058	4.735 ± 0.041	–2.172 ± 0.077
	0.635	0.068	4.618 ± 0.026	–2.561 ± 0.082
	0.793	0.086	4.532 ± 0.0	–3.207 ± 0.089
	0.983	0.106	4.254 ± 0.016	–3.965 ± 0.098

The uncertainties of the molality and γ were calculated considering the balance ($2 \cdot 10^{-4}$ %) and the measuring mass ($5 \cdot 10^{-2}$ %) errors, shown in Table S1. $\Delta_s H_m^\infty$ errors were calculated as the sum of the uncertainties of solution enthalpy of Eq. (3). as the expanded uncertainties for confidence level = 0.95, k≈2. The values for $\Delta_s H_3$ are the result of averaging all the measures for that concentration and the uncertainty is the standard deviation of the data (an uncertainty of 0 means there is only one measure for that concentration).

USC
UNIVERSIDADE DE SANTIAGO DE COMPOSTELA

Table S6

Values enthalpy of solvation of the metal cations in water ($\Delta_{hyd}H_m$) and in EAN ($\Delta_s H_m^{\infty *}$).

Cation	$\Delta_{hyd}H_m$ (kJ·mol^{-1})*	$\Delta_s H_m^{\infty *}$ (kJ·mol^{-1})
Li^+	-519	-505.71 ± 42
K^+	-322	-339.34 ± 62
Rb^+	-293	-312.23 ± 40
Cs^+	-264	-288.9 ± 1.0
Mg^{2+}	-1921	-1762.2 ± 1.9
Ca^{2+}	-1571	-1506.9 ± 2.2

*Ref. [1]

Table S7

Coordination numbers of water molecules and nitrate anions around alkali metal cations in both solvents (water and EAN). The numbers for the nitrate were obtained from our simulations while the ones for water were extracted from the.

Cation	CN_{H_2O}	CN_{NO_3}
Li^+	4[a]	4
K^+	6[b]	6
Rb^+	6[b]	5.9
Cs^+	8[b]	6.2
Mg^{2+}	6[c]	5.9
Ca^{2+}	7.3[c]	6.9

[a] ref. [2]; [b] ref. [3]; [c] ref. [4]

USC
UNIVERSIDADE DE SANTIAGO DE COMPOSTELA

Figures

Fig. S1 NMR spectra of dried nitrate salt solutions in EAN. The insets show the peaks associated to water which were only appreciable for mixtures with lithium and magnesium.

Fig. S2 Dependence of the anhydrous salt enthalpy of solution in EAN with the ionic density in the crystal phase.

Fig. S3 Spatial distribution functions of the simulated monovalent alkali metals around nitrate anions (top) and ethylammonium cations (bottom). The regions of the space coloured in green and blue around anions represent regions where it is 25 and 65 times more probable, respectively, of finding a metal compared with a homogeneous distribution. This numbers are 5 and 6 for distributions around the cation. The numbers in above the mid dashed line are the quotient between the metal valence and the square of its exclusion radius in the simulations.

Fig. S4 Same as Fig. S3 but for divalent salts.

USC
UNIVERSIDADE DE SANTIAGO DE COMPOSTELA

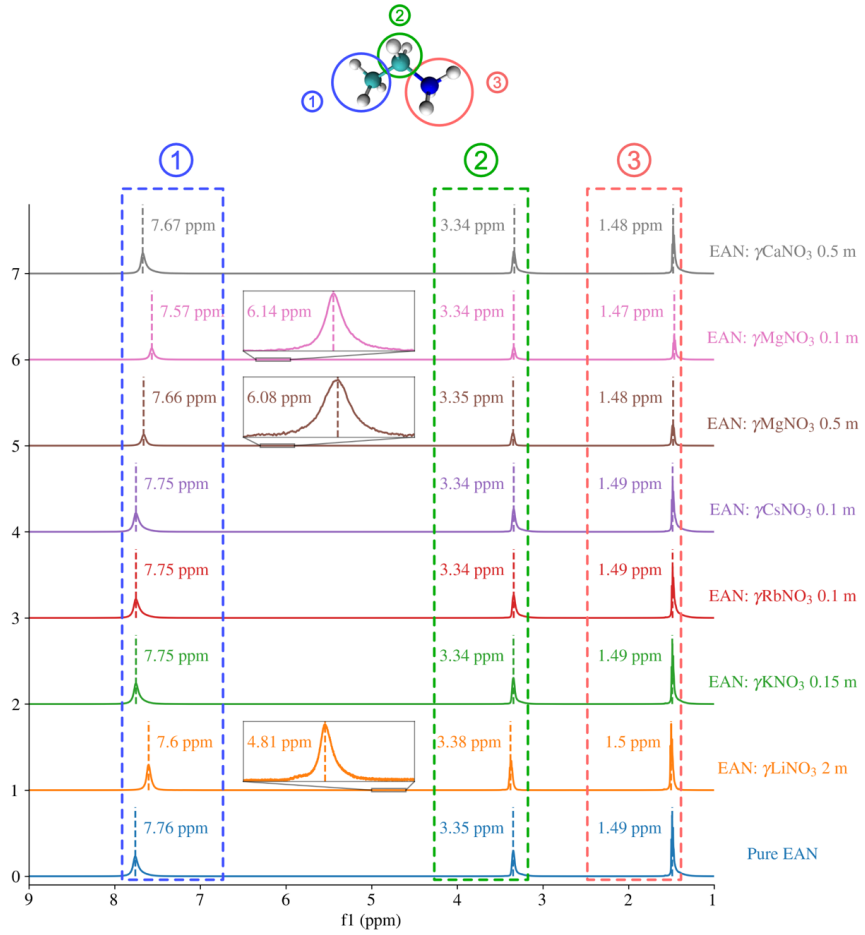

Fig. S1. NMR spectra of dried nitrate salt solutions in EAN. The insets show the peaks associated to water which were only appreciable for mixtures with lithium and magnesium.

USC
UNIVERSIDADE DE SANTIAGO DE COMPOSTELA

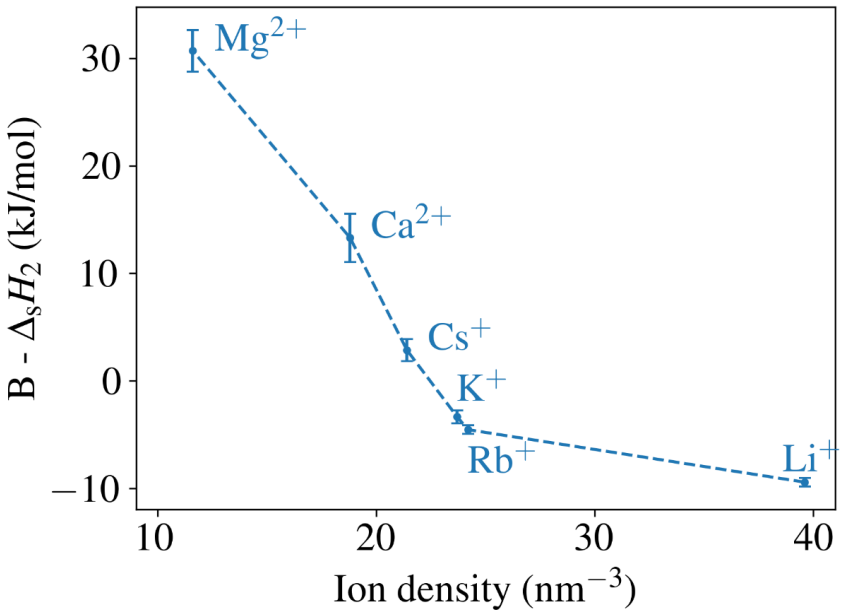

Fig. S2. Dependence of the anhydrous salt enthalpy of solution in EAN with the ionic density in the crystal phase.

USC
UNIVERSIDADE DE SANTIAGO DE COMPOSTELA

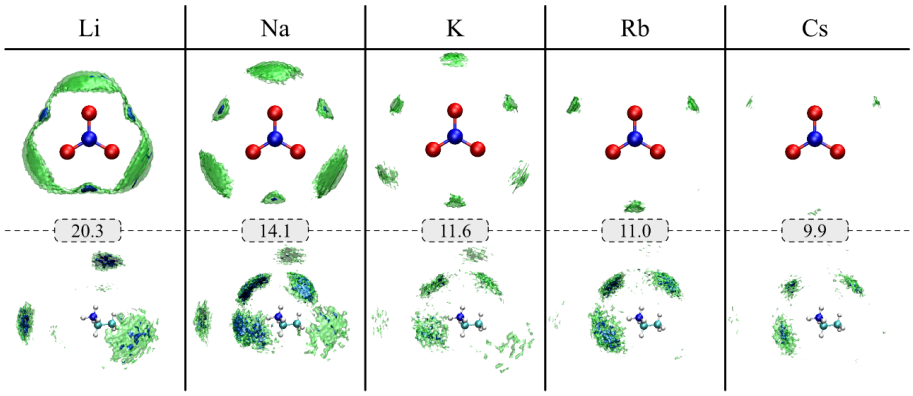

Fig. S3. Spatial distribution functions of the simulated monovalent alkali metals around nitrate anions (top) and ethylammonium cations (bottom). The regions of the space coloured in green and blue around anions represent regions where it is 25 and 65 times more probable, respectively, of finding a metal compared with a homogeneous distribution. This numbers are 5 and 6 for distributions around the cation. The numbers in above the mid dashed line are the quotient between the metal valence and the square of its exclusion radius in the simulations.

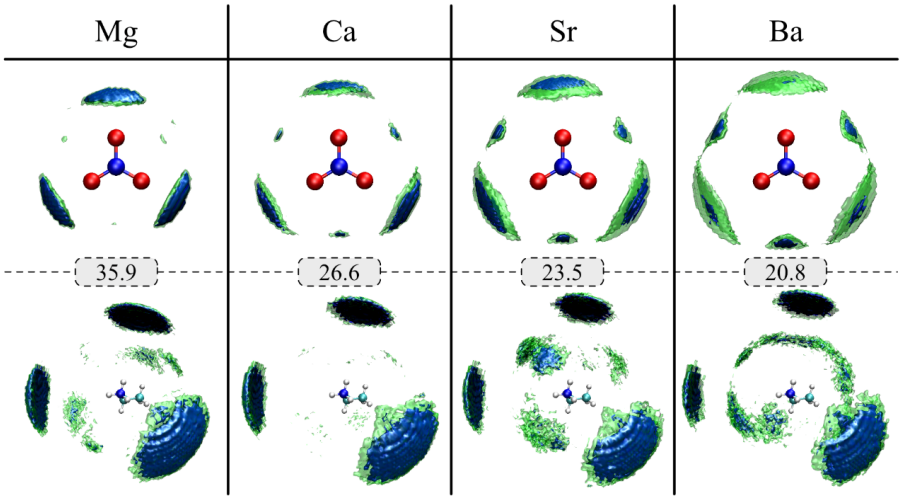

Fig. S4. Same as Fig. S3 but for divalent salts.

USC
UNIVERSIDADE DE SANTIAGO DE COMPOSTELA

References

[1] D.W. Smith, Ionic hydration enthalpies, J. Chem. Educ. 54 (1977) 540.

[2] S. Varma, S.B. Rempe, Coordination numbers of alkali metal ions in aqueous solutions. Biophys. Chem. 124(3) (2006) 192-199.

[3] P. R. Smirnov, V.N. Trostin, Structures of the nearest surroundings of the K+, Rb+, and Cs+ ions in aqueous solutions of their salts. Russ. J. Gen. Chem. 77(12) (2007) 2101-2107.

[4] D. Jiao, C. King, A. Grossfield, T.A. Darden, P. Ren, Simulation of Ca^{2+} and Mg^{2+} solvation using polarizable atomic multipole potential. J. Phys. Chem. B, 110(37), (2006) 18553-18559.

USC
UNIVERSIDADE DE SANTIAGO DE COMPOSTELA

USC
UNIVERSIDADE
DE SANTIAGO
DE COMPOSTELA

SUPPORTING INFORMATION

A New Solid State Proton Conductor: The Salt Hydrate Based on Imidazolium and 12-Tungstophosphate†

Anna Martinelli,[a*] José M. Otero-Mato,[b] Mounesha N. Garaga,[c] Khalid Elamin,[a] Seikh Mohammad Habibur Rahman,[a] Josef W. Zwanziger,[c] Ulrike Werner-Zwanziger,[c] and Luis M. Varela[b]

[a] Department of Chemistry and Chemical Engineering, Chalmers University of Technology, Gothenburg, Sweden
* E-mail: anna.martinelli@chalmers.se (corresponding author)
[b] Department of Physics, University of Santiago de Compostela, Santiago de Compostela, Spain
[c] Department of Chemistry, Dalhousie University, Halifax, Canada

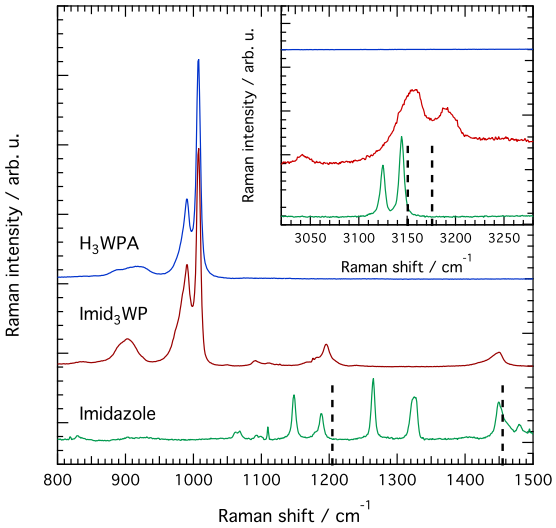

Figure S1. Raman spectra collected at room temperature for H_3WPA, $Imid_3WP$ and neutral (un-protonated) imidazole. The high-frequency range of the spectra, where $C^{2,4,5}$–H stretch modes appear, is shown in the inset. The vertical dashed lines indicate the frequency of vibrational modes calculated for the imidazolium cation. [1]

References

1 Majoube, M. and Henry, M. and Chinsky, L. and Turpin, P.Y. Preresonance Raman spectra for imidazole and imidazolium ion: interpretation of the intensity enhancement from a precise assignment of normal modes. *Chemical Physics*, **1993**, *169*(2), 231–241.

USC UNIVERSIDADE DE SANTIAGO DE COMPOSTELA

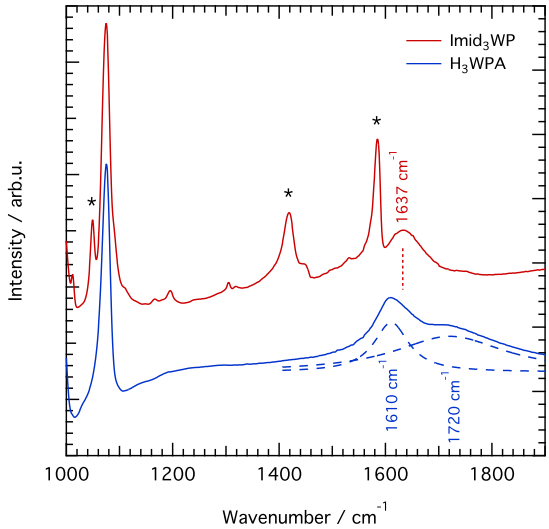

Figure S2. Infrared spectra collected at room temperature for the $Imid_3WP$ and the H_3WPA hydrates, in the region of the H-O-H bending modes. Asterisks indicate vibrational modes arising from the imidazolium cation.

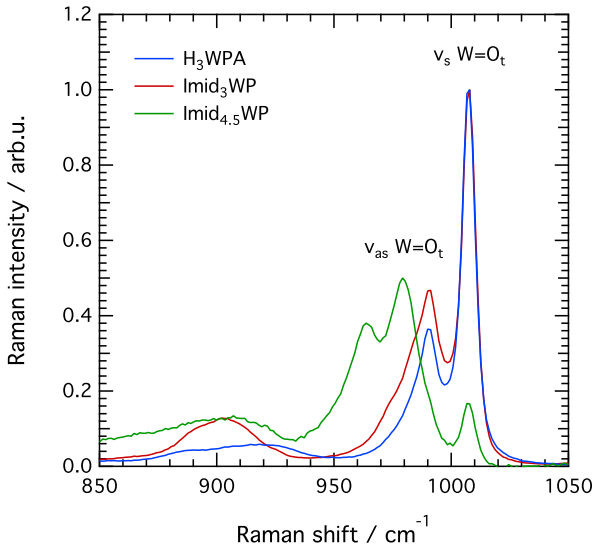

Figure S3. Raman spectra recorded at room temperature for $Imid_xWP$ salt hydrates where x is equal to 0 (i.e. the reference H_3WP salt), 3 (acidic environment of the Keggin ion) and 4.5 (basic environment of the Keggin ion).

USC
UNIVERSIDADE DE SANTIAGO DE COMPOSTELA

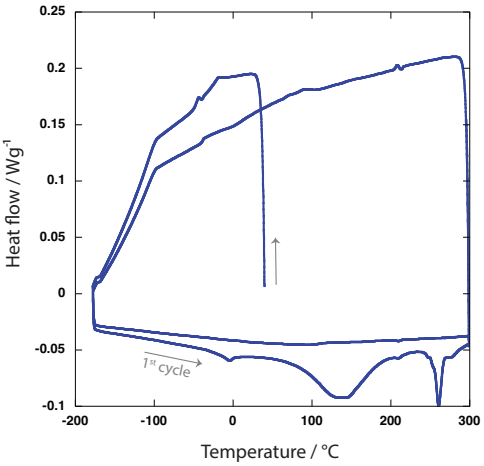

Figure S4. DSC traces recorded for the $Imid_3WP$ salt hydrate, showing the first and second cooling/heating cycles.

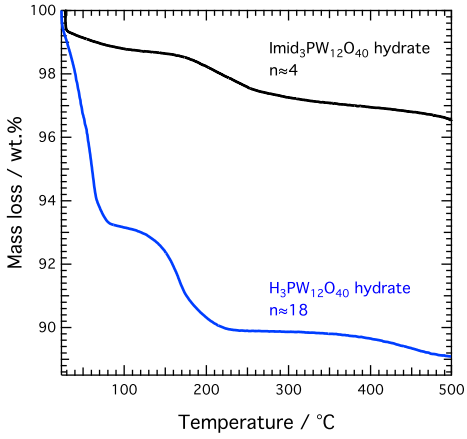

Figure S5. TGA curves recorded for the reference compound H_3WPA (blue trace) and the salt hydrate $Imid_3WP$ (black trace).

USC
UNIVERSIDADE DE SANTIAGO DE COMPOSTELA

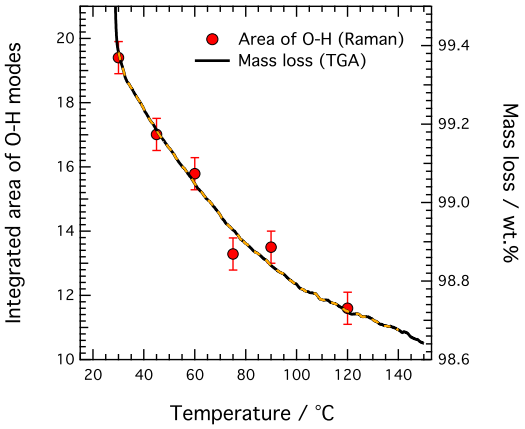

Figure S6. Integrated area of the vibrational modes attributed to O-H stretching, i.e. to water (Raman), and mass loss (TGA) as a function of increased temperature.

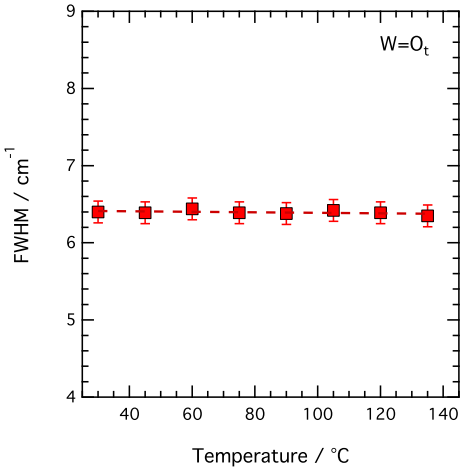

Figure S7. Full Width at Half Maxmimum (FWHM) of the W=O$_t$ symmetric stretching mode as a function of increased temperature, and thus dehydration of the Imid$_3$WP hydrate.

USC
UNIVERSIDADE DE SANTIAGO DE COMPOSTELA

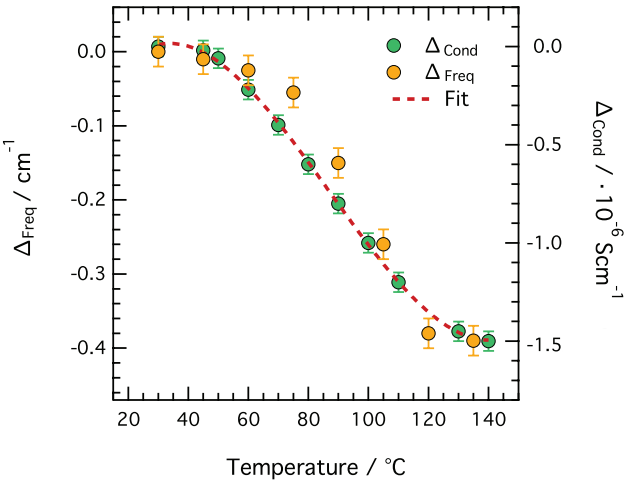

Figure S8. Deviation from the case of thermal effects only of the frequency of the W=O_t symmetric stretching mode (yellow symbols) and the deviation of proton conductivity from the case of no dehydration (green symbols), for the $Imid_3WPA{\cdot}nH_2O$ hydrate and as a function of temperature.

USC
UNIVERSIDADE DE SANTIAGO DE COMPOSTELA

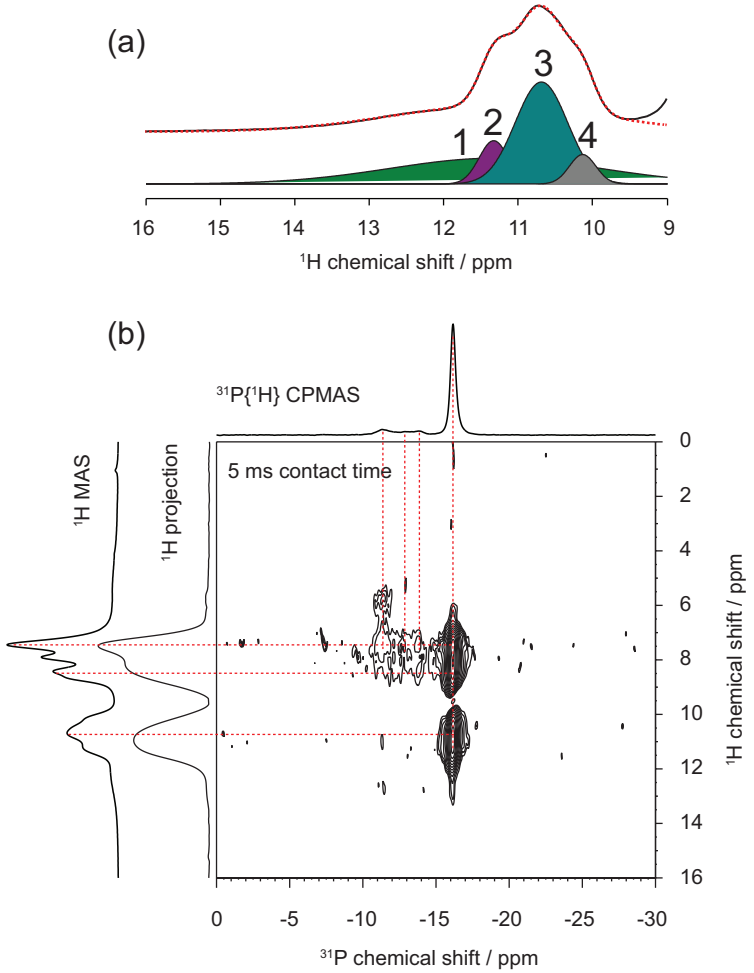

Figure S9. (a) Deconvolution of the 1D ^{1}H MAS NMR spectrum (NH region) fitted using the DMFIT software [Ref: Massiot et al., Magnetic resonance in chemistry, vol. 40, pp70-76 (2002)], highlighting the presence of different NH species. (b) 2D ^{31}P^{1}H HETCOR NMR spectrum collected on a 400 MHz Bruker NMR spectrometer with the contact time set to 5 ms.

USC
UNIVERSIDADE DE SANTIAGO DE COMPOSTELA

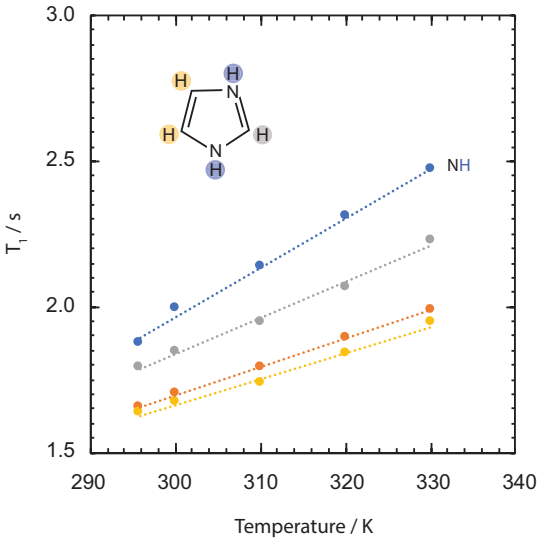

Figure S10. ^{1}H spin-lattice relaxation time (T1) measured as a function of temperature (23 °C – 57 °C) on a 400 MHz spectrometer by using a saturation recovery pulse sequence. The ^{1}H signal was collected over 16 increments with the delay, which allow for spins to relax, varied up to 15 s. The sample was spun at 20 kHz MAS.

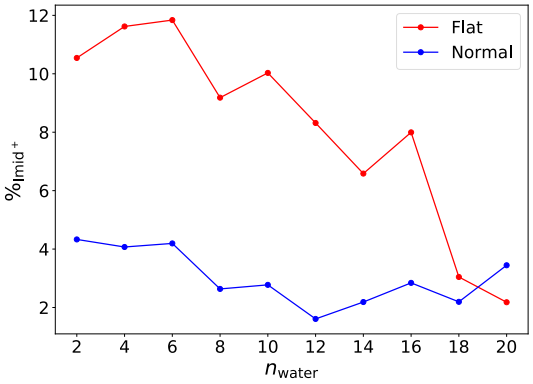

Figure S11. Fraction of imidazolium cations oriented flat or normal with respect to the surface of the Keggin anion, for all the simulated hydration levels.

USC
UNIVERSIDADE DE SANTIAGO DE COMPOSTELA

USC
UNIVERSIDADE
DE SANTIAGO
DE COMPOSTELA

Electronic Supplementary Information for PCCP article:

3D Structure of the Electric Double Layer of Ionic Liquid-Alcohol Mixtures at the Electrochemical Interface

José M. Otero-Mato,[1] Hadrián Montes-Campos,[1] Oscar Cabeza,[2] Diddo Diddens,[3] Alina Ciach,[4] Luis J. Gallego,[1] and Luis M. Varela[1, a)]

[1)] *Grupo de Nanomateriais, Fotónica e Materia Branda, Departamento de Física de Partículas, Universidade de Santiago de Compostela, Campus Vida s/n E-15782, Santiago de Compostela, Spain*

[2)] *Facultade de Ciencias, Universidade da Coruña, Campus A Zapateira s/n E-15008, A Coruña, Spain*

[3)] *Helmholtz-Institute Münster (HI MS), Ionics in Energy Storage, Forschungszentrum Jülich GmbH, Corrensstraße 46, 48149 Münster, Germany*

[4)] *Institute of Physical Chemistry, Polish Academy of Sciences, Kasprzaka 44/52, 01-224 Warszawa, Poland*

[a)] Electronic mail: luismiguel.varela@usc.es

USC UNIVERSIDADE DE SANTIAGO DE COMPOSTELA

I. IONIC POSITIONS FLUCTUATIONS: THEORETICAL DESCRIPTION

Let's suppose a situation where the ions are forming a two-dimensional triangular lattice in an ionic layer close to the electrodes. In a first approximation, we can calculate the probability of finding a given ion out of its equilibrium position at $\Delta\vec{r} = (\epsilon_x, \epsilon_y)$ (see Fig. A). This probability will be governed by the Boltzmann distribution. In our problem, the electrostatic potential energy plays a dominant role, so we can approximate this energy for the considered ion by the contributions of its first neighbours:

$$E_p = \frac{q^2}{4\pi\epsilon_r}\left(\frac{1}{\sqrt{\epsilon_x^2+(\epsilon_y-a)^2}} + \frac{1}{\sqrt{\epsilon_x^2+(\epsilon_y+a)^2}} + \frac{1}{\sqrt{\left(\epsilon_x-\frac{\sqrt{3}}{2}a\right)^2+(\epsilon_y-\frac{1}{2}a)^2}} + \frac{1}{\sqrt{\left(\epsilon_x-\frac{\sqrt{3}}{2}a\right)^2+(\epsilon_y+\frac{1}{2}a)^2}} + \frac{1}{\sqrt{\left(\epsilon_x+\frac{\sqrt{3}}{2}a\right)^2+(\epsilon_y-\frac{1}{2}a)^2}} + \frac{1}{\sqrt{\left(\epsilon_x+\frac{\sqrt{3}}{2}a\right)^2+(\epsilon_y+\frac{1}{2}a)^2}}\right), \tag{1}$$

where q is the charge of the ions, ϵ_r the electric permitivity of the medium and a the lattice parameter of the model. It is straightforward to see that, since $(0,0)$ is a minimum of the potential, this expression can be approximated to the lowest order by:

$$E_p \approx \frac{3q^2}{2\pi\epsilon a} + \frac{9q^2(\epsilon_x^2+\epsilon_y^2)}{8\pi\epsilon a^3} + O(\epsilon_x^4, \epsilon_y^4). \tag{2}$$

Using this approximation of the energy together with the Boltzmann distribution, the probability of finding an ion out of its equilibrium position can be approximated by:

$$p(\epsilon_x, \epsilon_y) = \frac{1}{Z}e^{-\frac{E_p}{k_BT}} \approx \frac{1}{Z}e^{-\frac{q^2}{k_BT\pi\epsilon a}}e^{-\frac{3q^2(\epsilon_x^2+\epsilon_y^2)}{4\pi\epsilon a^3 k_BT}}, \tag{3}$$

where Z is the partition function, k_B the Boltzmann constant and T the temperature. As it can be seen, the probability of fluctuation in the positions of the ions is described by a Gaussian distribution function with the standard deviation

$$s_p = \frac{a^2}{q}\sqrt{\frac{2\pi\epsilon k_BT}{3a}} \propto \frac{\sqrt{T\epsilon}}{\sigma}, \tag{4}$$

where $\sigma = q/a^2$ is the surface charge density.

USC
UNIVERSIDADE DE SANTIAGO DE COMPOSTELA

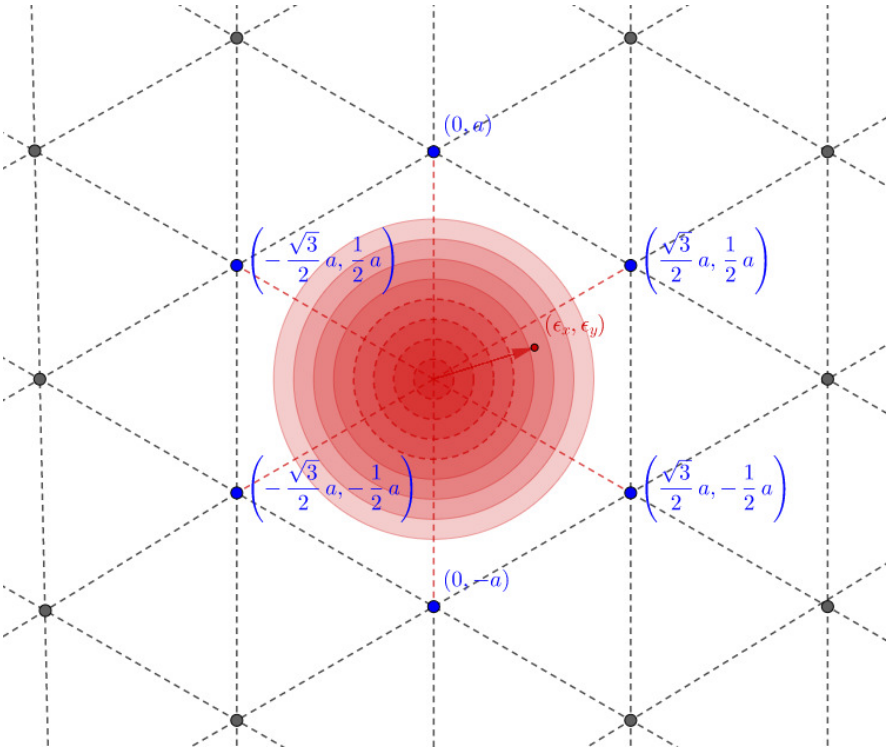

FIG. A: Scheme of the considered model for the calculation of the dispersion in the ionic position. The dots represents the ions positions, being a the lattice parameter. The considered ions for the energy calculation are those in blue.

USC
UNIVERSIDADE DE SANTIAGO DE COMPOSTELA

USC
UNIVERSIDADE
DE SANTIAGO
DE COMPOSTELA

Supplementary Information for: "Nanoconfined Ionic Liquids: A Computational Study"

José M. Otero-Mato[a], Hadrián Montes-Campos[a], Oscar Cabeza[b], Luis J. Gallego[a], Luis M. Varela[a,*]

[a] *Grupo de Nanomateriais, Fotónica e Materia Branda, Departamento de Física de Partículas, Universidade de Santiago de Compostela, Campus Vida s/n E-15782, Santiago de Compostela, Spain*
[b] *Facultade de Ciencias, Universidade da Coruña, Campus A Zapateira s/n E-15008, A Coruña, Spain*

1. EAN topology file

Listing 1: Example of EAN topology file used for the MD simulations

```
#include "opls_aa/forcefield.itp"

[ moleculetype ]
EA                      3

[ atoms ]
 1       opls_287     1         EA        N1      1      -0.627
 2       opls_290     1         EA        H2      2       0.397
 3       opls_290     1         EA        H3      3       0.392
 4       opls_290     1         EA        H4      4       0.392
 5       opls_292     1         EA        C5      5      -0.131
 6       opls_140     1         EA        H6      6       0.214
 7       opls_140     1         EA        H7      7       0.214
 8       opls_135     1         EA        C8      8      -0.377
 9       opls_140     1         EA        H9      9       0.161
```

*Corresponding author
Email address: luismiguel.varela@usc.es (Luis M. Varela)

USC UNIVERSIDADE DE SANTIAGO DE COMPOSTELA

```
10       opls_140    1         EA        H10     10      0.161
11       opls_140    1         EA        H11     11      0.204

[ bonds ]
1         2       1
1         3       1
1         4       1
1         5       1
5         6       1
5         7       1
5         8       1
8         9       1
8        10       1
8        11       1

[ angles ]
1         5       8        1
1         5       7        1
1         5       6        1
2         1       5        1
2         1       4        1
2         1       3        1
3         1       5        1
3         1       4        1
4         1       5        1
5         8       11       1
5         8       10       1
5         8       9        1
6         5       8        1
6         5       7        1
7         5       8        1
9         8       11       1
9         8       10       1
```


USC UNIVERSIDADE DE SANTIAGO DE COMPOSTELA

```
10        8       11       1

[ dihedrals ]
4     1     5     8     3
3     1     5     8     3
2     1     5     8     3
4     1     5     7     3
3     1     5     7     3
2     1     5     7     3
4     1     5     6     3
3     1     5     6     3
2     1     5     6     3
1     5     8     11    3
7     5     8     11    3
6     5     8     11    3
1     5     8     10    3
7     5     8     10    3
6     5     8     10    3
1     5     8     9     3
7     5     8     9     3
6     5     8     9     3

[ pairs ]
8     4     1
8     3     1
8     2     1
7     4     1
7     3     1
7     2     1
6     4     1
6     3     1
6     2     1
11    1     1
```


USC UNIVERSIDADE DE SANTIAGO DE COMPOSTELA

```
11    7     1
11    6     1
10    1     1
10    7     1
10    6     1
9     1     1
9     7     1
9     6     1

[ atomtypes ]
DNO3         DNO3    0     20.6683      0.000        A     0.00000e+00
0.00000e+00
v_opls_787   N       7      0.000      0.794       V     3.49600e-01
7.11280e-01
v_opls_788   O       8      0.000     -0.598       V     3.17500e-01
8.78640e-01

[ moleculetype ]
NO3                      3

[ atoms ]
1         DNO3           1     NO3       A12       12       0.
2         DNO3           1     NO3       A13       13       0.
3         DNO3           1     NO3       A14       14       0.
4         v_opls_787     1     NO3       N15       15       0.794
5         v_opls_788     1     NO3       O16       16      -0.598
6         v_opls_788     1     NO3       O17       17      -0.598
7         v_opls_788     1     NO3       O18       18      -0.598

[ constraints ]
1     2     1     0.187
1     3     1     0.187
2     3     1     0.187
```


USC UNIVERSIDADE DE SANTIAGO DE COMPOSTELA

```
[ virtual_sites3 ]
4         1       2       3     1     0.3333333333333     0.3333333333
5         1       2       3     1    -0.0455271207692    -0.0455271207692
6         1       2       3     1     1.09105424154      -0.0455271207692
7         1       2       3     1    -0.0455271207692     1.09105424154

[exclusions]
4 5 6 7
5 6 7 4
6 7 5 4
7 4 5 6

[ system ]
ILconf

[ molecules ]
EA                1562
NO3               1562
```

2. Simulation parameters

In this section we are going to specify the important simulation parameters that are not mentioned in the main manuscript and how they may affect the results. The parameters that are not mentioned here were set to their default value which can be found in the Gromacs website [1].

- `rlist`: This is the cut-off distance for updating the neighbor list of the molecules for the short-range interaction calculation. The default value is 1 nm while we choose 1.2 nm. This is a very standard value in MD simulations and there are no reasons to expect special behavior in the short-range interactions in our systems.
- `coulombtype`: We used the fast smooth Particle-Mesh Ewald (SPME) for the electrostatic interactions.

USC UNIVERSIDADE DE SANTIAGO DE COMPOSTELA

- `rcoulomb`: We set this value to 1.2 nm which is also 0.2 nm larger than the default value. This value was proven to be the lowest value that guarantees a good molecular structure and good agreement with experimental results for our systems.
- `fourierspacing`: We set this to 0.1 nm following the Gromacs recommendations that state that `rcoulomb` and this parameter should be scaled in the same way to keep the accuracy of the electrostatic interactions.
- `pme_order`: We increased this parameter from 4 to 6 which is recommended by the manual when performing simulations in parallel.
- `ewald-rtol`: We also decreased this parameter to 10^{-6} to perform more accurate direct sum.
- `ewald-geometry`: We used `3dc` for this parameter as we simulated systems with periodic boundary conditions only in the XY directions.
- `vdw-type`: It was set to `cut-off`.
- `rvdw`: Also increased from its default value (1 nm) to 1.2 nm to ensure accurate short-range structure.
- `tcoupl`: `v-rescale`
- `tau_t`: 0.5 ps
- `pcoupl`: `Berendsen`
- `pcoupltype`: We used `semiisotropic` to allow only volume changes in the XY directions.
- `tau-p`: 1 ps
- `compressibility`: 10^{-6} bar^{-1} for the XY direction and 0 for the Z one.

USC
UNIVERSIDADE DE SANTIAGO DE COMPOSTELA

3. Scheme of systems superposition

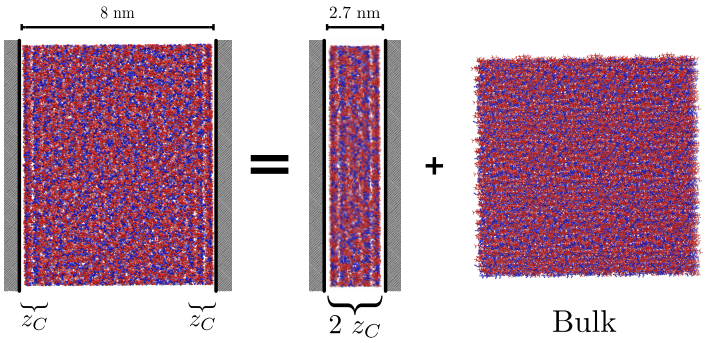

Figure S1: Schematic representation of a confined system as the superposition of a very confined IL and a bulk system.

References

[1] Gromacs mdp options, `http://manual.gromacs.org/documentation/2019/user-guide/mdp-options.html`, 2019.

USC UNIVERSIDADE DE SANTIAGO DE COMPOSTELA

USC
UNIVERSIDADE
DE SANTIAGO
DE COMPOSTELA

Supplementary Information for: "Structure, dynamics and conductivities of ionic liquid-alcohol mixtures"

José M. Otero-Mato[a], Hadrián Montes-Campos[a], Víctor Gómez-González[a], Martín Montoto[a], Oscar Cabeza[b], Svyatoslav Kondrat[c,d,e], Luis M. Varela[a,*]

[a] *Grupo de Nanomateriais, Fotónica e Materia Branda, Departamento de Física de Partículas. Facultade de Física and Instituto de Materiais (iMATUS), Universidade de Santiago de Compostela, Campus Vida s/n E-15782, Santiago de Compostela, Spain*
[b] *Facultade de Ciencias, Universidade da Coruña, Campus A Zapateira s/n E-15071, A Coruña, Spain*
[c] *Institute of Physical Chemistry, Polish Academy of Sciences, Kasprzaka 44/52, 01-224 Warsaw, Poland*
[d] *Max-Planck-Institut für Intelligente Systeme, Heisenbergstraße 3, 70569 Stuttgart, Germany*
[e] *IV. Institut für Theoretische Physik, Universität Stuttgart, Pfaffenwaldring 57, 70569 Stuttgart, Germany*

*Corresponding author
Email address: luismiguel.varela@usc.es (Luis M. Varela)

USC UNIVERSIDADE DE SANTIAGO DE COMPOSTELA

Table S1: Summary of simulation parameters for mixtures of [BMIM][I] and ethanol.

x_{IL}	ϕ_{IL}	$\#_{IL}$	$\#_{Eth}$	L_{box} (nm)	ρ (g/ml)
0.03	0.10	216	6984	9.03	0.855
0.05	0.15	500	9500	10.2	0.889
0.07	0.21	216	2869	7.00	0.920
0.08	0.23	216	2484	6.74	0.935
0.09	0.25	216	2184	6.52	0.948
0.10	0.28	216	1944	6.33	0.962
0.12	0.32	216	1584	5.97	0.993
0.15	0.38	216	1224	5.70	1.021
0.20	0.47	216	864	5.33	1.069
0.25	0.54	216	648	5.07	1.110
0.30	0.60	216	504	4.89	1.145
0.40	0.70	216	324	4.64	1.200
0.50	0.78	216	216	4.48	1.242
0.60	0.84	216	144	4.37	1.275
0.75	0.92	216	72	4.26	1.313
0.90	0.97	1296	144	7.58	1.339
1.00	1.00	216	0	4.14	1.354

USC
UNIVERSIDADE DE SANTIAGO DE COMPOSTELA

Table S2: Summary of simulation parameters for mixtures of [EMIM][I] and ethanol.

x_{IL}	ϕ_{IL}	$\#_{IL}$	$\#_{Eth}$	L_{box} (nm)	ρ (g/ml)
0.05	0.13	106	2014	6.03	0.891
0.10	0.24	200	1800	6.07	0.969
0.15	0.34	285	1615	6.11	1.035
0.20	0.42	361	1444	6.14	1.092
0.25	0.49	430	1290	6.17	1.140
0.30	0.56	493	1150	6.21	1.183
0.35	0.61	550	1021	6.23	1.219
0.40	0.66	603	904	6.26	1.252
0.50	0.75	697	697	6.31	1.306
0.60	0.82	777	518	6.35	1.351
0.70	0.88	847	363	6.39	1.388
0.80	0.93	908	227	6.42	1.419
0.90	0.97	962	106	6.45	1.444
1.00	1.00	1010	0	6.49	1.463

USC
UNIVERSIDADE DE SANTIAGO DE COMPOSTELA

Table S3: Experimental ionic conductivities of mixtures of ethanol and IL at 25 ºC.

[BMIM][I]		[EMIM][I]	
$\%_{eth}$	σ (mS/cm)	$\%_{eth}$	σ (mS/cm)
100	$3.98{\cdot}10^{-4}$	100	$5.54{\cdot}10^{-4}$
95.00	2.54	94.87	3.3
89.53	4.93	90.12	5.81
80.91	8.21	79.44	11.46
70.48	12.03	69.98	16.23
60.74	14.72	60.04	20.9
49.92	16.9	50.00	25.1
39.79	17.38	39.56	27.5
30.01	15.32	29.99	27.6
19.98	11.02	19.86	22.2
0	0.522	-	-

Table S4: Experimental densities of mixtures of ethanol and IL at 20 ºC.

[BMIM][I]		[EMIM][I]	
$\%_{eth}$	ρ (g/ml)	$\%_{eth}$	ρ (g/ml)
100	0.7892	100	0.7892
95.00	0.8106	94.87	0.8079
89.53	0.8324	90.12	0.8308
80.91	0.8698	79.44	0.8828
70.48	0.9247	69.98	0.9290
60.74	0.9760	60.04	0.9966
49.92	1.0424	50.00	1.0710
39.79	1.1103	39.56	1.1533
30.01	1.1848	29.99	1.2476
19.98	1.2740	19.86	1.3546
0	1.4813	-	-

USC UNIVERSIDADE DE SANTIAGO DE COMPOSTELA

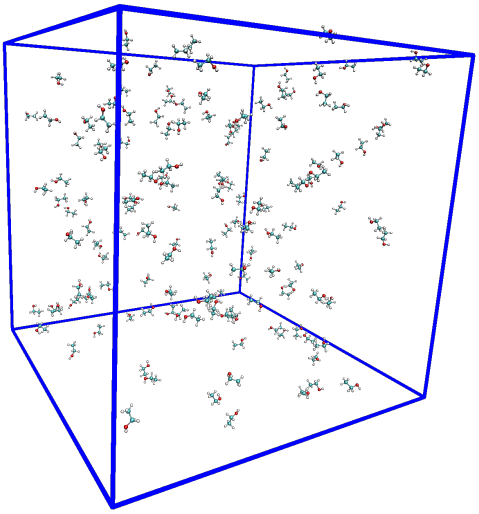

Figure S1: Snapshot of the positions of the ethanol molecules taken from the simulation with 90% of IL.

USC
UNIVERSIDADE DE SANTIAGO DE COMPOSTELA

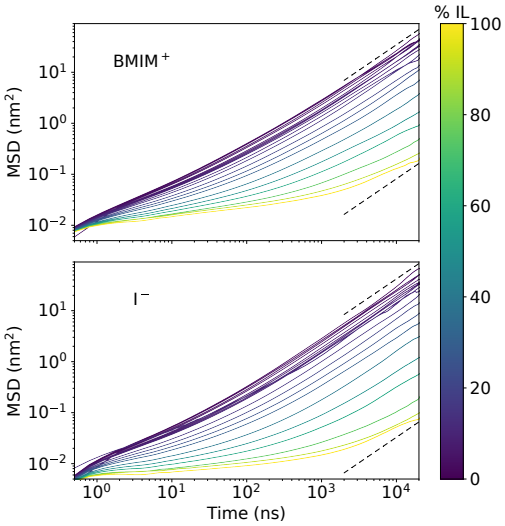

Figure S2: MSDs in log/log scale for cations and anions in the [BMIM][I]/ethanol mixtures for all the simulated concentrations. The black dashed lines of unit-slope are guides to the eye and represent the slope that the MSDs should have when entering in the diffusive regime. As it can be seen, for systems with low IL concentration the mobility is increased and the diffusive regime is reached but this is not the case for higher concentrated systems.

USC
UNIVERSIDADE DE SANTIAGO DE COMPOSTELA

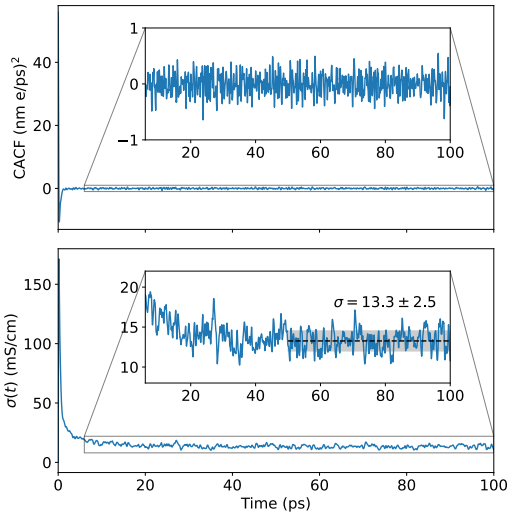

Figure S3: Current autocorrelation function (top) and the conductivity calculated using Eq. (5) changing the upper integral limit (bottom) for the simulation with 10% of IL. The final value of the conductivity is taken as the average of the cumulative function from 50 to 100 ps (black dashed line). The grey rectangle represents the region $\sigma = \bar{\sigma} \pm 2 \cdot u(\sigma)$, where $u(\sigma)$ is the standard deviation of the expected value of the conductivity in that region.

USC
UNIVERSIDADE DE SANTIAGO DE COMPOSTELA

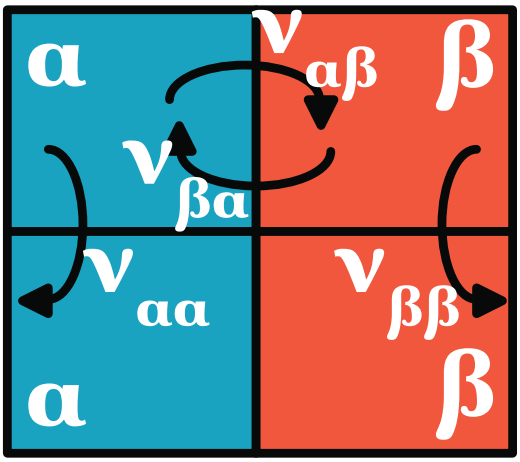

Figure S4: Schematic representation of what the different $\nu_{\gamma\epsilon}$ refer to considering two kind of cells (α and β).

USC
UNIVERSIDADE DE SANTIAGO DE COMPOSTELA

C- Information of the publications

In the following pages we include a summary of the relevant information of each publication included in this thesis as well as the authorizations of the journals to reproduce their contents here:

- GADDLE Maps: General Algorithm for Discrete object Deformations based on Local Exchange Maps
- Solvation in Ionic Liquid-Water mixtures: A Computational Study
- Enthalpy of solvation of alkali metal salts in a protic ionic liquid: Effect of cation charge and size
- A New Solid State Proton Conductor: The Salt Hydrate Based on Imidazolium and 12-Tungstophosphate
- 3D Structure of the Electric Double Layer of Ionic Liquid-Alcohol Mixtures at the Electrochemical Interface
- Nanoconfined Ionic Liquids: A Computational Study
- Structure, Dynamics and Conductivities of Ionic Liquid-Alcohol Mixtures

USC
UNIVERSIDADE DE SANTIAGO DE COMPOSTELA

USC
UNIVERSIDADE
DE SANTIAGO
DE COMPOSTELA

GADDLE Maps: General Algorithm for Discrete Object deformations Based on Local Exchange Maps

- **Authors:** José M. Otero-Mato, Hadrián Montes-Campos, Martín Calvelo, Rebeca García-Fandiño, Luis J. Gallego, Ángel Piñeiro, Luis M. Varela
- **Journal:** Journal of Chemical Theory and Computation
- **Volume (issue):** 2(14)
- **Pages:** 466-478
- **Year:** 2018
- **Journal information in 2018**:
  - **Impact factor:** 5.313
  - **Category:** Physics, Atomic, Molecular & Chemical
  - **Ranking inside category:** 6/36 (Q1)
- **Contribution of the author of this thesis:** The author of this thesis contributed to this publication, according to the CRediT contribution classification,[66;67] with: Conceptualization, Data curation, Formal Analysis, Investigation, Methodology, Software, Validation, Visualization, Writing - original draft, Writing - review & editing.

The journal has authorized the reproduction of the contents of this publication in this thesis (see bellow a snapshot of the authorization).

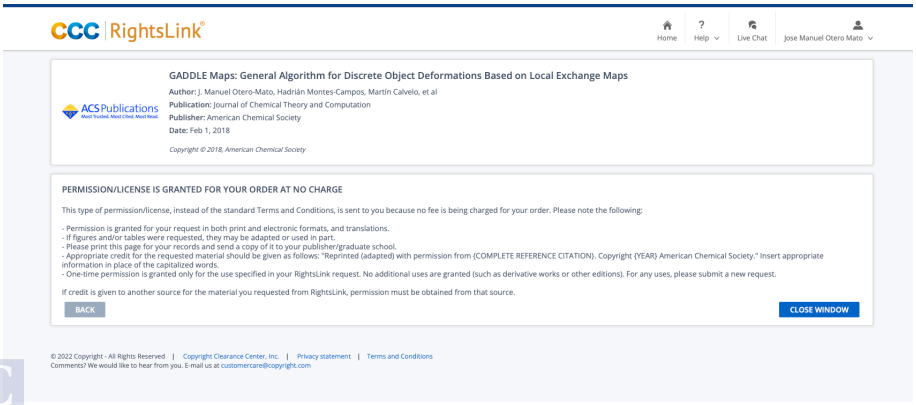

USC UNIVERSIDADE DE SANTIAGO DE COMPOSTELA

USC
UNIVERSIDADE
DE SANTIAGO
DE COMPOSTELA

Solvation in ionic liquid-water mixtures: A computational study

- **Authors:** José M. Otero-Mato, Volker Lesch, Hadrián Montes-Campos, Jens Smiatek, Diddo Diddens, Óscar Cabeza, Luis J. Gallego, Luis M. Varela
- **Journal:** Journal of Molecular Liquids
- **Volume:** 292
- **Pages:** 111273
- **Year:** 2019
- **Journal information in 2019**:
  - **Impact factor:** 5.065
  - **Category:** Physics, Atomic, Molecular & Chemical
  - **Ranking inside category:** 4/37 (Q1)
- **Contribution of the author of this thesis:** The author of this thesis contributed to this publication, according to the CRediT contribution classification,[66;67] with: Conceptualization, Data curation, Formal Analysis, Investigation, Methodology, Software, Validation, Visualization, Writing - original draft, Writing - review & editing.

The journal has authorized the reproduction of the contents of this publication in this thesis (see bellow a snapshot of the authorization).

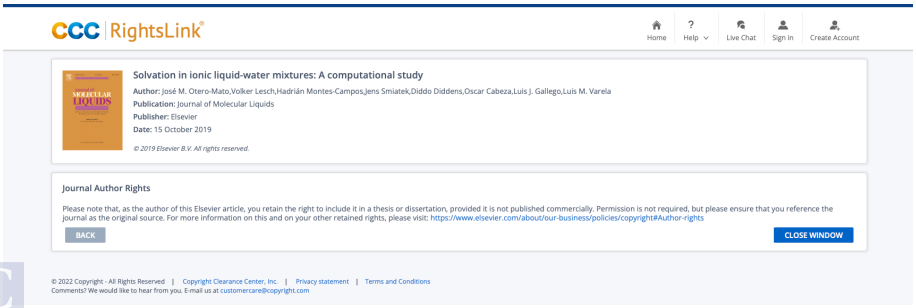

USC UNIVERSIDADE DE SANTIAGO DE COMPOSTELA

USC
UNIVERSIDADE
DE SANTIAGO
DE COMPOSTELA

Enthalpy of solvation of alkali metal salts in a protic ionic liquid: Effect of cation charge and size

- **Authors:** Juan J. Parajó, José M. Otero-Mato, Ana I. M. C. L. Lobo Ferreira, Luis M. Varela, Luis M. N. B. F. Santos
- **Journal:** Journal of Molecular Liquids
- **Volume:** 360
- **Pages:** 119228
- **Year:** 2022
- **Journal information in 2020**:
  - **Impact factor:** 6.165
  - **Category:** Physics, Atomic, Molecular & Chemical
  - **Ranking inside category:** 4/37 (Q1)
- **Contribution of the author of this thesis:** The author of this thesis contributed to this publication, according to the CRediT contribution classification,[66;67] with: Conceptualization, Methodology, Software, Validation, Formal Analysis, Investigation, Data Curation, Writing - Original Draft, Writing - Review & Editing, Visualization.

The journal has authorized the reproduction of the contents of this publication in this thesis (see bellow a snapshot of the authorization).

USC UNIVERSIDADE DE SANTIAGO DE COMPOSTELA

USC
UNIVERSIDADE
DE SANTIAGO
DE COMPOSTELA

A New Solid-State Proton Conductor: The Salt Hydrate Based on Imidazolium and 12-Tungstophosphate

- **Authors:** Anna Martinelli, José M. Otero-Mato, Mounesha N. Garaga, Khalid Elamin, Seikh Mohammad Habibur Rahman, Josef W. Zwanziger, Ulrike Werner-Zwanziger, Luis M. Varela
- **Journal:** Journal of the American Chemical Society
- **Volume (issue):** 34(143)
- **Pages:** 13895-13907
- **Year:** 2021
- **Journal information in 2020**:
  - **Impact factor:** 15.419
  - **Category:** Chemistry, Multidisciplinary
  - **Ranking inside category:** 15/178 (Q1)
- **Contribution of the author of this thesis:** The author of this thesis contributed to this publication specially with the computational part. The experiments have been carried out by the rest of the coauthors in their facilities. In terms of the CRediT contribution classification,[66;67] the author contributed to the computational part with: Data curation, Formal Analysis, Investigation, Methodology, Software, Validation, Visualization, Writing - original draft, Writing - review & editing.

The journal has authorized the reproduction of the contents of this publication in this thesis (see bellow a snapshot of the authorization).

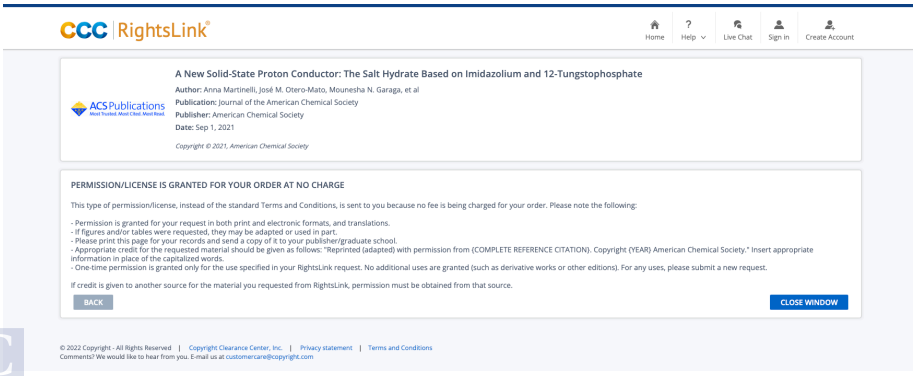

USC UNIVERSIDADE DE SANTIAGO DE COMPOSTELA

USC
UNIVERSIDADE
DE SANTIAGO
DE COMPOSTELA

3D structure of the electric double layer of ionic liquid-alcohol mixtures at the electrochemical interface

- **Authors:** José M. Otero-Mato, Hadrián Montes-Campos, Óscar Cabeza, Diddo Diddens, Alina Ciach, Luis J. Gallego, Luis M. Varela
- **Journal:** Physical Chemistry Chemical Physics
- **Volume (issue):** 48(20)
- **Pages:** 30412-30427
- **Year:** 2018
- **Journal information in 2018**:
  - **Impact factor:** 3.567
  - **Category:** Physics, Atomic, Molecular & Chemical
  - **Ranking inside category:** 9/36 (Q1)
- **Contribution of the author of this thesis:** The author of this thesis contributed to this publication, according to the CRediT contribution classification,[66;67] with: Conceptualization, Data curation, Formal Analysis, Investigation, Methodology, Software, Validation, Visualization, Writing - original draft, Writing - review & editing.

The journal has authorized the reproduction of the contents of this publication in this thesis (see bellow a snapshot of the authorization).

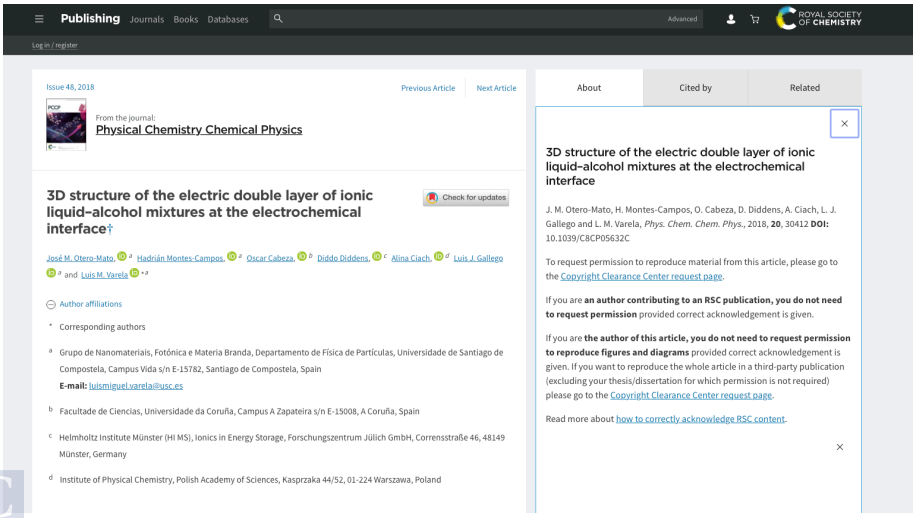

USC UNIVERSIDADE DE SANTIAGO DE COMPOSTELA

USC
UNIVERSIDADE
DE SANTIAGO
DE COMPOSTELA

Nanoconfined ionic liquids: A computational study

- **Authors:** José M. Otero-Mato, Hadrián Montes-Campos, Óscar Cabeza, Luis J. Gallego, Luis M. Varela
- **Journal:** Journal of Molecular Liquids
- **Volume:** 320
- **Pages:** 114446
- **Year:** 2020
- **Journal information in 2020**:
  - **Impact factor:** 6.165
  - **Category:** Physics, Atomic, Molecular & Chemical
  - **Ranking inside category:** 4/37 (Q1)
- **Contribution of the author of this thesis:** The author of this thesis contributed to this publication, according to the CRediT contribution classification,[66;67] with: Conceptualization, Data curation, Formal Analysis, Investigation, Methodology, Software, Validation, Visualization, Writing - original draft, Writing - review & editing.

The journal has authorized the reproduction of the contents of this publication in this thesis (see bellow a snapshot of the authorization).

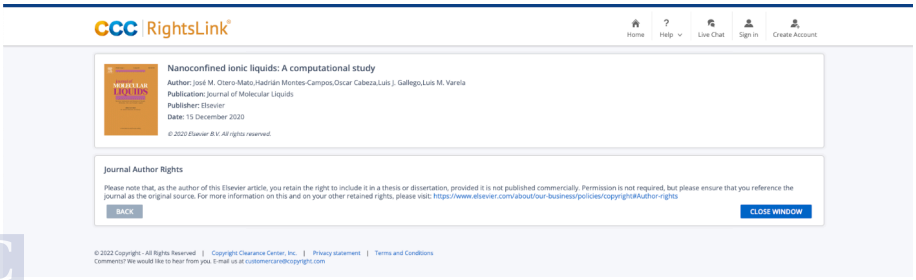

USC
UNIVERSIDADE DE SANTIAGO DE COMPOSTELA

USC
UNIVERSIDADE
DE SANTIAGO
DE COMPOSTELA

Structure, Dynamics and Conductivities of Ionic Liquid-Alcohol Mixtures

- **Authors:** José M. Otero-Mato, Hadrián Montes- Campos, Víctor Gómez-González, Martín Montoto, Óscar Cabeza, Svyatoslav Kondrat, Luis M. Varela
- **Journal:** Journal of Molecular Liquids
- **Volume:** 360
- **Pages:** 119228
- **Year:** 2022
- **Journal information in 2020**:
  - **Impact factor:** 6.165
  - **Category:** Physics, Atomic, Molecular & Chemical
  - **Ranking inside category:** 4/37 (Q1)
- **Contribution of the author of this thesis:** The author of this thesis contributed to this publication, according to the CRediT contribution classification,[66;67] with: Conceptualization, Methodology, Software, Validation, Formal Analysis, Investigation, Data Curation, Writing - original draft, Writing - review & editing, Visualization.

The journal has authorized the reproduction of the contents of this publication in this thesis (see bellow a snapshot of the authorization).

USC UNIVERSIDADE DE SANTIAGO DE COMPOSTELA

USC
UNIVERSIDADE
DE SANTIAGO
DE COMPOSTELA

Bibliography

[1] James F. Wishart. Energy applications of ionic liquids. *Energy & Environmental Science*, 2(9):956–961, 2009.

[2] Julie M. Rieland and Brian J. Love. Ionic liquids: A milestone on the pathway to greener recycling of cellulose from biomass. *Resources, Conservation and Recycling*, 155:104678, 2020.

[3] Guillaume Zante, Arthur Braun, Abderrazak Masmoudi, Rémi Barillon, Dominique Trebouet, and Maria Boltoeva. Solvent extraction fractionation of manganese, cobalt, nickel and lithium using ionic liquids and deep eutectic solvents. *Miner. Eng.*, 156: 106512, 2020.

[4] Marcelo P. Stracke, Günter Ebeling, Renato Cataluña, and Jairton Dupont. Hydrogen-storage materials based on imidazolium ionic liquids. *Energy & fuels*, 21(3):1695–1698, 2007.

[5] Zhiqi He and Paschalis Alexandridis. Ionic liquid and nanoparticle hybrid systems: Emerging applications. *Adv. Colloid Interfac*, 244:54–70, 2017.

[6] Battery 2030+ roadmap, (2020). `https://battery2030.eu/`, .

[7] Philippe Hapiot and Corinne Lagrost. Electrochemical reactivity in room-temperature ionic liquids. *Chem. Rev.*, 108(7):2238–2264, 2008.

[8] Paul Walden. Molecular weights and electrical conductivity of several fused salts. *Bull. Acad. Imper. Sci.(St. Petersburg)*, 1800, 1914.

[9] Koen Binnemans. Ionic liquid crystals. *Chem. Rev.*, 105(11): 4148–4204, 2005.

[10] Tamar L. Greaves and Calum J. Drummond. Protic ionic liquids: properties and applications. *Chem. Rev.*, 108(1):206–237, 2008.

USC UNIVERSIDADE DE SANTIAGO DE COMPOSTELA

[11] Vitaly V. Chaban, Iuliia V. Voroshylova, Oleg N. Kalugin, and Oleg V. Prezhdo. Acetonitrile Boosts Conductivity of Imidazolium Ionic Liquids. *J. Phys. Chem. B*, 116(26):7719–7727, jul 2012. ISSN 1520-6106.

[12] John D. Holbrey and K. R. Seddon. Ionic liquids. *Clean products and processes*, 1(4):223–236, 1999.

[13] Ortrud Aschenbrenner, Somsak Supasitmongkol, Marie Taylor, and Peter Styring. Measurement of vapour pressures of ionic liquids and other low vapour pressure solvents. *Green Chem.*, 11 (8):1217–1221, 2009.

[14] H. A. Øye, M. Jagtoyen, T. Oksefjell, and J. S. Wilkes. Vapour pressure and thermodynamics of the system 1-methyl-3-ethylimidazolium chloride-aluminium chloride. In *Materials Science Forum*, volume 73, pages 183–190. Trans Tech Publ, 1991.

[15] Martyn J. Earle, José M. S. S. Esperança, Manuela A. Gilea, José N. Canongia Lopes, Luís P. N. Rebelo, Joseph W. Magee, Kenneth R. Seddon, and Jason A. Widegren. The distillation and volatility of ionic liquids. *Nature*, 439(7078):831–834, 2006.

[16] Banqiu Wu, Ramana G. Reddy, and Robin D. Rogers. Novel ionic liquid thermal storage for solar thermal electric power systems. In *International Solar Energy Conference*, volume 16702, pages 445–451. American Society of Mechanical Engineers, 2001.

[17] Pierre Bonhote, Ana-Paula Dias, Nicholas Papageorgiou, Kuppuswamy Kalyanasundaram, and Michael Grätzel. Hydrophobic, highly conductive ambient-temperature molten salts. *Inorg. Chem.*, 35(5):1168–1178, 1996.

[18] Alessandro Bagno, Craig Butts, Cinzia Chiappe, Fabio D'Amico, Jason C. D. Lord, Daniela Pieraccini, and Federico Rastrelli. The effect of the anion on the physical properties of trihalide-based n, n-dialkylimidazolium ionic liquids. *Organic & biomolecular chemistry*, 3(9):1624–1630, 2005.

USC
UNIVERSIDADE DE SANTIAGO DE COMPOSTELA

[19] Ichiro Minami. Ionic liquids in tribology. *Molecules*, 14(6):2286–2305, 2009.

[20] Matthew W. Thompson, Ray Matsumoto, Robert L. Sacci, Nicolette C. Sanders, and Peter T. Cummings. Scalable screening of soft matter: A case study of mixtures of ionic liquids and organic solvents. *J. Phys. Chem. B*, 123(6):1340–1347, feb 2019. ISSN 1520-6106.

[21] Douglas R. Macfarlane, Pavla Meakin, Jiazeng Sun, Nahid Amini, and Maria Forsyth. Pyrrolidinium imides: a new family of molten salts and conductive plastic crystal phases. *J. Phys. Chem. B*, 103(20):4164–4170, 1999.

[22] Rika Hagiwara and Je Seung Lee. Ionic liquids for electrochemical devices. *Electrochemistry*, 75(1):23–34, 2007.

[23] Martyn J. Earle and Kenneth R. Seddon. Ionic liquids. green solvents for the future. *Pure Appl. Chem.*, 72(7):1391–1398, 2000.

[24] A. A. H. Pádua, M. F. Costa Gomes, and J. N. A. Canongia-Lopes. Molecular solutes in ionic liquids: A structural perspective. *Acc. Chem. Res.*, 40(11):1087–1096, 2007.

[25] Hadrián Montes-Campos, José M. Otero-Mato, Trinidad Méndez-Morales, Elena López-Lago, Olga Russina, Oscar Cabeza, Luis J. Gallego, and Luis M. Varela. Nanostructured solvation in mixtures of protic ionic liquids and long-chained alcohols. *J. Chem. Phys.*, 146(12):124503, mar 2017. ISSN 0021-9606.

[26] Shengdong Zhu, Yuanxin Wu, Qiming Chen, Ziniu Yu, Cunwen Wang, Shiwei Jin, Yigang Ding, and Gang Wu. Dissolution of cellulose with ionic liquids and its application: a mini-review. *Green Chem.*, 8(4):325–327, 2006.

USC UNIVERSIDADE DE SANTIAGO DE COMPOSTELA

[27] Suzie Su Yin Tan and Douglas R. MacFarlane. Ionic liquids in biomass processing. *Top. Curr. Chem.*, pages 311–339, 2009.

[28] Cristina Prudêncio, Mónica Vieira, Seppe Van der Auweraer, and Ricardo Ferraz. Recycling old antibiotics with ionic liquids. *Antibiotics*, 9(9):578, 2020.

[29] Mark James Abraham, Teemu Murtola, Roland Schulz, Szilárd Páll, Jeremy C. Smith, Berk Hess, and Erik Lindahl. Gromacs: High performance molecular simulations through multi-level parallelism from laptops to supercomputers. *SoftwareX*, 1:19–25, 2015.

[30] B. Hess, C. Kutzner, D. V. D. Spoel, and E. Lindahl. GROMACS 4: Algorithms for highly efficient, load-balanced, and scalable molecular simulation. *J. Chem. Theory Comput.*, 4(3):435–447, 2008.

[31] A. P. Thompson, H. M. Aktulga, R. Berger, D. S. Bolintineanu, W. M. Brown, P. S. Crozier, P. J. in 't Veld, A. Kohlmeyer, S. G. Moore, T. D. Nguyen, R. Shan, M. J. Stevens, J. Tranchida, C. Trott, and S. J. Plimpton. LAMMPS - a flexible simulation tool for particle-based materials modeling at the atomic, meso, and continuum scales. *Comp. Phys. Comm.*, 271:108171, 2022. doi: 10.1016/j.cpc.2021.108171.

[32] Leandro Martínez, Ricardo Andrade, Ernesto G. Birgin, and José Mario Martínez. Packmol: a package for building initial configurations for molecular dynamics simulations. *J. Comput. Chem.*, 30(13):2157–2164, 2009.

[33] José M. Otero-Mato, Alejandro Rivera-Pousa, Hadrián Montes-Campos, Oscar Cabeza, A. Heuer, D. Diddens, and Luis M. Varela. Computational study of the structure of ternary ionic liquid/salt/polymer electrolytes based on protic ionic liquids. *J. Mol. Liq.*, 333:115883, 2021.

USC
UNIVERSIDADE DE SANTIAGO DE COMPOSTELA

[34] William L. Jorgensen and Julian Tirado-Rives. The opls [optimized potentials for liquid simulations] potential functions for proteins, energy minimizations for crystals of cyclic peptides and crambin. *J. Am. Chem. Soc.*, 110(6):1657–1666, 1988.

[35] William L. Jorgensen, David S. Maxwell, and Julian Tirado-Rives. Development and testing of the opls all-atom force field on conformational energetics and properties of organic liquids. *J. Am. Chem. Soc.*, 118(45):11225–11236, 1996.

[36] José N. Canongia Lopes, Johnny Deschamps, and Agílio A. H. Pádua. Modeling ionic liquids using a systematic all-atom force field. *J. Phys. Chem. B*, 108(6):2038–2047, 2004.

[37] Oleg Borodin. Polarizable force field development and molecular dynamics simulations of ionic liquids. *J. Phys. Chem. B*, 113(33): 11463–11478, 2009.

[38] Walter R. P. Scott, Philippe H. Hünenberger, Ilario G. Tironi, Alan E. Mark, Salomon R. Billeter, Jens Fennen, Andrew E. Torda, Thomas Huber, Peter Krüger, and Wilfred F. van Gunsteren. The gromos biomolecular simulation program package. *J. Phys. Chem. A*, 103(19):3596–3607, 1999.

[39] Wendy D. Cornell, Piotr Cieplak, Christopher I. Bayly, Ian R. Gould, Kenneth M. Merz, David M. Ferguson, David C. Spellmeyer, Thomas Fox, James W. Caldwell, and Peter A. Kollman. A second generation force field for the simulation of proteins, nucleic acids, and organic molecules. *J. Am. Chem. Soc.*, 117 (19):5179–5197, 1995.

[40] Alex D. MacKerell Jr, Donald Bashford, M. L. D. R. Bellott, Roland Leslie Dunbrack Jr, Jeffrey D. Evanseck, Martin J. Field, Stefan Fischer, Jiali Gao, H. Guo, Sookhee Ha, et al. All-atom empirical potential for molecular modeling and dynamics studies of proteins. *J. Phys. Chem. B*, 102(18):3586–3616, 1998.

USC
UNIVERSIDADE DE SANTIAGO DE COMPOSTELA

[41] Junmei Wang, Romain M. Wolf, James W. Caldwell, Peter A. Kollman, and David A. Case. Development and testing of a general amber force field. *J. Comput. Chem.*, 25(9):1157–1174, 2004.

[42] Siewert J. Marrink, H. Jelger Risselada, Serge Yefimov, D. Peter Tieleman, and Alex H. De Vries. The martini force field: coarse grained model for biomolecular simulations. *J. Phys. Chem. B*, 111(27):7812–7824, 2007.

[43] Jonathan Richard Shewchuk et al. An introduction to the conjugate gradient method without the agonizing pain, 1994.

[44] Herman J. C. Berendsen, J. P. M. van Postma, Wilfred F. Van Gunsteren, A. R. H. J. DiNola, and Jan R. Haak. Molecular dynamics with coupling to an external bath. *J. Chem. Phys.*, 81 (8):3684–3690, 1984.

[45] Giovanni Bussi, Davide Donadio, and Michele Parrinello. Canonical sampling through velocity rescaling. *J. Chem. Phys.*, 126 (1):014101, 2007.

[46] Michele Parrinello and Aneesur Rahman. Polymorphic transitions in single crystals: A new molecular dynamics method. *J. Appl. Phys.*, 52(12):7182–7190, 1981.

[47] Shūichi Nosé. A molecular dynamics method for simulations in the canonical ensemble. *Mol. Phys.*, 52(2):255–268, 1984.

[48] William G. Hoover. Canonical dynamics: Equilibrium phase-space distributions. *Phys. Rev. A*, 31(3):1695, 1985.

[49] Hadrián Montes-Campos, Jose M. Otero-Mato, Roberto Carlos Longo, Oscar Cabeza, Luis J. Gallego, and Luis M. Varela. Mixtures of lithium salts and ionic liquids at defected graphene walls. *J. Mol. Liq.*, 289:111083, 2019.

USC UNIVERSIDADE DE SANTIAGO DE COMPOSTELA

[50] Max Born and Robert Oppenheimer. Zur quantentheorie der molekeln. *Ann. Phys-Leipzig*, 389(20):457–484, 1927.

[51] Walter Kohn. Nobel lecture: Electronic structure of matter—wave functions and density functionals. *Rev. Mod. Phys.*, 71(5): 1253, 1999.

[52] Chengteh Lee, Weitao Yang, and Robert G. Parr. Development of the colle-salvetti correlation-energy formula into a functional of the electron density. *Phys. Rev. B*, 37(2):785, 1988.

[53] Richard M. Martin. *Electronic structure: basic theory and practical methods*. Cambridge university press, 2020.

[54] Hadrián Montes-Campos, Jesús Carrete, Sebastian Bichelmaier, Luis M. Varela, and Georg K. H. Madsen. A differentiable neural-network force field for ionic liquids. *J. Chem. Inf. Model.*, 2021.

[55] C. J. T. De Grotthuss. Memoir on the decomposition of water and of the bodies that it holds in solution by means of galvanic electricity. *Biochimica et Biophysica Acta (BBA)-Bioenergetics*, 1757(8):871–875, 2006.

[56] Noam Agmon. The grotthuss mechanism. *Chem. Phys. Lett.*, 244 (5-6):456–462, 1995.

[57] Martin Brehm, Henry Weber, Alfonso S. Pensado, Annegret Stark, and Barbara Kirchner. Proton transfer and polarity changes in ionic liquid–water mixtures: A perspective on hydrogen bonds from ab initio molecular dynamics at the example of 1-ethyl-3-methylimidazolium acetate–water mixtures—part 1. *Phys. Chem. Chem. Phys.*, 14(15):5030–5044, 2012.

[58] Nam H. Vu, Hieu C. Dong, My V. Nguyen, Dzung Hoang, Thuat T. Trinh, and Thang Bach Phan. Mechanism of proton transport in water clusters and the effect of electric fields: A dft study. *Curr. Appl. Phys.*, 25:62–69, 2021.

USC UNIVERSIDADE DE SANTIAGO DE COMPOSTELA

[59] Michael J. Janik, Robert J. Davis, and Matthew Neurock. Anhydrous and water-assisted proton mobility in phosphotungstic acid. *J. Am. Chem. Soc.*, 127(14):5238–5245, 2005.

[60] Volker Lesch, Andreas Heuer, Christian Holm, and Jens Smiatek. Solvent effects of 1-ethyl-3-methylimidazolium acetate: solvation and dynamic behavior of polar and apolar solutes. *Phys. Chem. Chem. Phys.*, 17(13):8480–8490, 2015.

[61] Ramesh Singh, Joshua Monk, and Francisco R. Hung. A computational study of the behavior of the ionic liquid $[BMIM^+][PF_6^-]$ confined inside multiwalled carbon nanotubes. *J. Phys. Chem. C*, 114(36):15478–15485, 2010.

[62] Quentin Berrod, Filippo Ferdeghini, Patrick Judeinstein, Nicolas Genevaz, Raphael Ramos, Adeline Fournier, Jean Dijon, Jacques Ollivier, Stephane Rols, Dehong Yu, et al. Enhanced ionic liquid mobility induced by confinement in 1d cnt membranes. *Nanoscale*, 8(15):7845–7848, 2016.

[63] Yunrui Duan, Jie Li, Tao Li, Zhichao Wang, and Hui Li. Layering and phase transition of liquid aluminum confined by different substrates. *Nato. Sc. S. Ss. Iii. C. S.*, 143:157–162, 2018.

[64] Maolin Sha, Huaze Dong, Fabao Luo, Zhongfeng Tang, Guanglai Zhu, and Guozhong Wu. Dilute or Concentrated Electrolyte Solutions? Insight from Ionic Liquid/Water Electrolytes. *J. Phys. Chem. Lett.*, 6(18):3713–3720, sep 2015.

[65] Gaddle Maps Implementation. `https://github.com/txemaotero/gaddlemaps`.

[66] Amy Brand, Liz Allen, Micah Altman, Marjorie Hlava, and Jo Scott. Beyond authorship: attribution, contribution, collaboration, and credit. *Learn. Publ.*, 28(2):151–155, 2015.

[67] Liz Allen, Alison O'Connell, and Veronique Kiermer. How can we ensure visibility and diversity in research contributions? how

USC UNIVERSIDADE DE SANTIAGO DE COMPOSTELA

the contributor role taxonomy (credit) is helping the shift from authorship to contributorship. *Learn. Publ.*, 32(1):71–74, 2019.

[68] J. Andrew McCammon, Bruce R. Gelin, and Martin Karplus. Dynamics of folded proteins. *Nature.*, 267(5612):585, 1977.

[69] Stewart A. Adcock and J. Andrew McCammon. Molecular dynamics: survey of methods for simulating the activity of proteins. *Chem. Rev.*, 106(5):1589, 2006.

[70] Jemma L. Trick, Prafulla Aryal, Stephen J. Tucker, and Mark S. P. Sansom. Molecular simulation studies of hydrophobic gating in nanopores and ion channels. *Biochem. Soc. T*, 43(2):146–150, 2015. ISSN 0300-5127. doi: 10.1042/BST20140256. URL `http://www.biochemsoctrans.org/content/43/2/146`.

[71] Andrea G. Quezada, A. Jessica Díaz-Salazar, Nallely Cabrera, Ruy Pérez-Montfort, Ángel Piñeiro, and Miguel Costas. Interplay between protein thermal flexibility and kinetic stability. *Structure.*, 25(1):167 – 179, 2017. ISSN 0969-2126. doi: http://dx.doi.org/10.1016/j.str.2016.11.018. URL `http://www.sciencedirect.com/science/article/pii/S0969212616303604`.

[72] Alan R. Fersht and Valerie Daggett. Protein folding and unfolding at atomic resolution. *Cell.*, 108(4):573–582, 2002.

[73] Siewert J. Marrink, Alex H. De Vries, and Alan E. Mark. Coarse grained model for semiquantitative lipid simulations. *J. Phys. Chem. B*, 108(2):750–760, 2004.

[74] Sebastian Kmiecik, Dominik Gront, Michal Kolinski, Lukasz Wieteska, Aleksandra Elzbieta Dawid, and Andrzej Kolinski. Coarse-grained protein models and their applications. *Chem. Rev.*, 116(14):7898–7936, 2016. doi: 10.1021/acs.chemrev.6b00163. URL `http://dx.doi.org/10.1021/acs.chemrev.6b00163`. PMID: 27333362.

USC UNIVERSIDADE DE SANTIAGO DE COMPOSTELA

[75] Chun Wu and Joan-Emma Shea. Coarse-grained models for protein aggregation. *Curr. Opin. Struct. Biol.*, 21(2):209 – 220, 2011. ISSN 0959-440X. doi: http://dx.doi.org/10.1016/j.sbi.2011.02.002. URL `http://www.sciencedirect.com/science/article/pii/S0959440X11000339`.

[76] Martini: Coarse grain forcefield for biomolecules. `http://www.cgmartini.nl`, .

[77] Tristan Bereau and Kurt Kremer. Automated parametrization of the coarse-grained martini force field for small organic molecules. *J. Chem. Theory. Comput.*, 11(6):2783–2791, 2015.

[78] James A. Graham, Jonathan W. Essex, and Syma Khalid. Pycgtool: Automated generation of coarse-grained molecular dynamics models from atomistic trajectories. *J. Chem. Inf. Model.*, 2017.

[79] Andrzej J. Rzepiela, Lars V. Schäfer, Nicolae Goga, H. Jelger Risselada, Alex H. De Vries, and Siewert J. Marrink. Reconstruction of atomistic details from coarse-grained structures. *J. Comput. Chem.*, 31(6):1333–1343, 2010.

[80] Phillip J. Stansfeld and Mark S. P. Sansom. From coarse grained to atomistic: a serial multiscale approach to membrane protein simulations. *J. Chem. Theory. Comput.*, 7(4):1157–1166, 2011.

[81] Pilar Brocos, Paola Mendoza-Espinosa, Rolando Castillo, Jaime Mas-Oliva, and Ángel Pineiro. Multiscale molecular dynamics simulations of micelles: coarse-grain for self-assembly and atomic resolution for finer details. *Soft. Matter.*, 8(34):9005–9014, 2012.

[82] Tsjerk A. Wassenaar, Kristyna Pluhackova, Rainer A. Böckmann, Siewert J. Marrink, and D. Peter Tieleman. Going backward: A flexible geometric approach to reverse transformation from coarse grained to atomistic models. *J. Chem. Theory. Comput.*,

USC UNIVERSIDADE DE SANTIAGO DE COMPOSTELA

10(2):676–690, 2014. doi: 10.1021/ct400617g. URL http://dx.doi.org/10.1021/ct400617g. PMID: 26580045.

[83] Xavier Periole, Marco Cavalli, Siewert-Jan Marrink, and Marco A. Ceruso. Combining an elastic network with a coarse-grained molecular force field: structure, dynamics, and intermolecular recognition. *J. Chem. Theory. Comput.*, 5(9):2531–2543, 2009.

[84] Marcus D. Hanwell, Donald E. Curtis, David C. Lonie, Tim Vandermeersch, Eva Zurek, and Geoffrey R. Hutchison. Avogadro: an advanced semantic chemical editor, visualization, and analysis platform. *J. Cheminform.*, 4(1):17, 2012.

[85] Martini: Dppc bilayer. http://cgmartini.nl/images/applications/bilayer/dppc_bilayer.gro, .

[86] Tsjerk A. Wassenaar, Helgi I. Ingólfsson, Rainer A. Böckmann, D. Peter Tieleman, and Siewert J. Marrink. Computational lipidomics with insane: a versatile tool for generating custom membranes for molecular simulations. *J. Chem. Theory. Comput.*, 11(5):2144–2155, 2015.

[87] Pilar Brocos, Norma Díaz-Vergara, Xavier Banquy, Silvia Pérez-Casas, Miguel Costas, and Ángel Piñeiro. Similarities and differences between cyclodextrin−sodium dodecyl sulfate host−guest complexes of different stoichiometries: Molecular dynamics simulations at several temperatures. *J. Phys. Chem. B*, 114(39):12455–12467, 2010. doi: 10.1021/jp103223u. URL http://dx.doi.org/10.1021/jp103223u. PMID: 20836518.

[88] Cesar A. López, Alex H. de Vries, and Siewert J. Marrink. Computational microscopy of cyclodextrin mediated cholesterol extraction from lipid model membranes. *Sci. Rep.*, 3:2071, 2013.

[89] Luca Monticelli, Senthil K. Kandasamy, Xavier Periole, Ronald G. Larson, D. Peter Tieleman, and Siewert-Jan Marrink. The

USC UNIVERSIDADE DE SANTIAGO DE COMPOSTELA

martini coarse-grained force field: extension to proteins. *J. Chem. Theory. Comput.*, 4(5):819–834, 2008.

[90] Djurre H. de Jong, Gurpreet Singh, W. F. Drew Bennett, Clement Arnarez, Tsjerk A. Wassenaar, Lars V. Schafer, Xavier Periole, D. Peter Tieleman, and Siewert J. Marrink. Improved parameters for the martini coarse-grained protein force field. *J. Chem. Theory. Comput.*, 9(1):687–697, 2012.

[91] Chris Oostenbrink, Alessandra Villa, Alan E. Mark, and Wilfred F. Van Gunsteren. A biomolecular force field based on the free enthalpy of hydration and solvation: the GROMOS force-field parameter sets 53a5 and 53a6. *J. Comput. Chem.*, 25(13): 1656–1676, 2004.

[92] Alpeshkumar K. Malde, Le Zuo, Matthew Breeze, Martin Stroet, David Poger, Pramod C. Nair, Chris Oostenbrink, and Alan E. Mark. An automated force field topology builder (ATB) and repository: Version 1.0. *J. Chem. Theory. Comput.*, 7(12):4026–4037, 2011. doi: 10.1021/ct200196m. URL `http://dx.doi.org/10.1021/ct200196m`. PMID: 26598349.

[93] Nathan Schmid, Andreas P. Eichenberger, Alexandra Choutko, Sereina Riniker, Moritz Winger, Alan E. Mark, and Wilfred F. van Gunsteren. Definition and testing of the GROMOS force-field versions 54A7 and 54B7. *Eur. Biophys. J*, 40(7):843, 2011.

[94] Rong Chen, David Poger, and Alan E. Mark. Effect of high pressure on fully hydrated dppc and popc bilayers. *J. Phys. Chem. B*, 115(5):1038–1044, 2010.

[95] Nora A. McDonald and William L. Jorgensen. Development of an all-atom force field for heterocycles. properties of liquid pyrrole, furan, diazoles, and oxazoles. *J. Phys. Chem. B*, 102(41):8049–8059, 1998.

USC UNIVERSIDADE DE SANTIAGO DE COMPOSTELA

[96] Robert C. Rizzo and William L. Jorgensen. Opls all-atom model for amines: resolution of the amine hydration problem. *J. Am. Chem. Soc.*, 121(20):4827–4836, 1999.

[97] Melissa L. P. Price, Dennis Ostrovsky, and William L. Jorgensen. Gas-phase and liquid-state properties of esters, nitriles, and nitro compounds with the opls-aa force field. *J. Comput. Chem.*, 22 (13):1340–1352, 2001.

[98] Edward K. Watkins and William L. Jorgensen. Perfluoroalkanes: Conformational analysis and liquid-state properties from ab initio and monte carlo calculations. *J. Phys. Chem. A*, 105(16):4118–4125, 2001.

[99] George A. Kaminski, Richard A. Friesner, Julian Tirado-Rives, and William L. Jorgensen. Evaluation and reparametrization of the opls-aa force field for proteins via comparison with accurate quantum chemical calculations on peptides. *J. Phys. Chem. B*, 105(28):6474–6487, 2001.

[100] Jakob P. Ulmschneider and Martin B. Ulmschneider. United atom lipid parameters for combination with the optimized potentials for liquid simulations all-atom force field. *J. Chem. Theory. Comput.*, 5(7):1803–1813, 2009.

[101] Kresten Lindorff-Larsen, Stefano Piana, Kim Palmo, Paul Maragakis, John L. Klepeis, Ron O. Dror, and David E. Shaw. Improved side-chain torsion potentials for the amber ff99sb protein force field. *Proteins: Struct., Funct., Bioinf.*, 78(8):1950–1958, 2010.

[102] Thomas J. Piggot, Ángel Piñeiro, and Syma Khalid. Molecular dynamics simulations of phosphatidylcholine membranes: a comparative force field study. *J. Chem. Theory Comput.*, 8(11): 4593–4609, 2012.

[103] Jan Domański, Phillip J. Stansfeld, Mark S. P. Sansom, and Oliver Beckstein. Lipidbook: a public repository for force-field

USC UNIVERSIDADE DE SANTIAGO DE COMPOSTELA

parameters used in membrane simulations. *J. Membrane Biol.*, 236(3):255–258, 2010. doi: 10.1007/s00232-010-9296-8. URL `http://lipidbook.bioch.ox.ac.uk`.

[104] Gideon Goldstein, Margrit Scheid, Ulrich Hammerling, D. H. Schlesinger, H. D. Niall, and E. A. Boyse. Isolation of a polypeptide that has lymphocyte-differentiating properties and is probably represented universally in living cells. *Proc. Natl. Acad. Sci.*, 72(1):11–15, 1975.

[105] Cecile M. Pickart and Michael J. Eddins. Ubiquitin: structures, functions, mechanisms. *BBA-Mol. Cell. Res.*, 1695(1):55–72, 2004.

[106] Senadhi Vijay-Kumar, Charles E. Bugg, and William J. Cook. Structure of ubiquitin refined at 1.8 åresolution. *J. Mol. Biol.*, 194(3):531–544, 1987.

[107] Gabriel Cornilescu, John L. Marquardt, Marcel Ottiger, and Ad Bax. Validation of protein structure from anisotropic carbonyl chemical shifts in a dilute liquid crystalline phase. *J. Am. Chem. Soc.*, 120(27):6836–6837, 1998.

[108] David B. Kony, Philippe H. Hünenberger, and Wilfred F. van Gunsteren. Molecular dynamics simulations of the native and partially folded states of ubiquitin: Influence of methanol co-solvent, ph, and temperature on the protein structure and dynamics. *Protein. Sci.*, 16(6):1101–1118, 2007.

[109] Erez Koren and Vladimir P. Torchilin. Cell-penetrating peptides: breaking through to the other side. *Trends. Mol. Med.*, 18(7): 385–393, 2012.

[110] Iria Louzao, Rebeca Garcia-Fandino, and Javier Montenegro. Hydrazone-modulated peptides for efficient gene transfection. *J. Mater. Chem. B*, 5:4426–4434, 2017.

USC UNIVERSIDADE DE SANTIAGO DE COMPOSTELA

[111] Athanassios Stavrakoudis, Ioannis G. Tsoulos, Zakhar O. Shenkarev, and Tatiana V. Ovchinnikova. Molecular dynamics simulation of antimicrobial peptide arenicin-2: β-hairpin stabilization by noncovalent interactions. *Pept. Sci.*, 92(3):143–155, 2009.

[112] M. Reza Ghadiri, Juan R. Granja, Ronald A. Milligan, Duncan E. McRee, and Nina Khazanovich. Self-assembling organic nanotubes based on a cyclic peptide architecture. *Nature.*, 366(6453): 324, 1993.

[113] Rebeca Garcia-Fandiño, Ángel Piñeiro, Jemma L. Trick, and Mark S. P. Sansom. Lipid bilayer membrane perturbation by embedded nanopores: A simulation study. *ACS Nano.*, 10(3):3693–3701, 2016. doi: 10.1021/acsnano.6b00202. URL `http://dx.doi.org/10.1021/acsnano.6b00202`. PMID: 26943498.

[114] M. Reza Ghadiri, Juan R. Granja, and Lukas K. Buehler. Artificial transmembrane ion channels from self-assembling peptide nanotubes. *Nature.*, 369(6478):301, 1994.

[115] Jorge Sánchez-Quesada, Markus P. Isler, and M. Reza Ghadiri. Modulating ion channel properties of transmembrane peptide nanotubes through heteromeric supramolecular assemblies. *J. Am. Chem. Soc.*, 124(34):10004–10005, 2002.

[116] Javier Montenegro, M. Reza Ghadiri, and Juan R. Granja. Ion channel models based on self-assembling cyclic peptide nanotubes. *Accounts. Chem. Res.*, 46(12):2955–2965, 2013. doi: 10.1021/ar400061d. URL `http://dx.doi.org/10.1021/ar400061d`. PMID: 23898935.

[117] Sara Fernandez-Lopez, Hui-Sun Kim, Ellen C. Choi, Mercedes Delgado, Juan R. Granja, Alisher Khasanov, Karin Kraehenbuehl, Georgina Long, Dana A. Weinberger, Keith M. Wilcoxen, et al. Antibacterial agents based on the cyclic d, l-α-peptide architecture. *Nature.*, 412(6845):452–455, 2001.

USC UNIVERSIDADE DE SANTIAGO DE COMPOSTELA

[118] Shabnam Ain, Babita Kumar, and Kamla Pathak. Cyclodextrins: versatile carrier in drug formulations and delivery systems. *Int. J. Pharm. Chem. Biol. Sci*, 5:583–598, 2015.

[119] Lingxiang Jiang, Yu Peng, Yun Yan, and Jianbin Huang. Aqueous self-assembly of sds@ 2 β-cd complexes: lamellae and vesicles. *Soft. Matter.*, 7(5):1726–1731, 2011.

[120] Baghali G. Mathapa and Vesselin N. Paunov. Cyclodextrin stabilised emulsions and cyclodextrinosomes. *Phys. Chem. Chem. Phys.*, 15(41):17903–17914, 2013.

[121] Alexey Ryzhakov, Thao Do Thi, Jef Stappaerts, Laura Bertoletti, Kristof Kimpe, André Rodrigues Sá Couto, Phennapha Saokham, Guy Van den Mooter, Patrick Augustijns, Govert W. Somsen, et al. Self-assembly of cyclodextrins and their complexes in aqueous solutions. *J. Pharm. Sci-Us.*, 105(9):2556–2569, 2016.

[122] Edgar Mixcoha, José Campos-Terán, and Ángel Piñeiro. Surface adsorption and bulk aggregation of cyclodextrins by computational molecular dynamics simulations as a function of temperature: α-CD vs β-CD. *J. Phys. Chem. B*, 118(25):6999–7011, 2014.

[123] Jorge Hernandez-Pascacio, Ángel Piñeiro, Juan M. Ruso, Natalia Hassan, Richard A. Campbell, José Campos-Terán, and Miguel Costas. Complex behavior of aqueous α-cyclodextrin solutions. interfacial morphologies resulting from bulk aggregation. *Langmuir.*, 32(26):6682–6690, 2016.

[124] Niel M. Henriksen and Michael K. Gilson. Evaluating force field performance in thermodynamic calculations of cyclodextrin host-guest binding: water models, partial charges, and host force field parameters. *J. Chem. Theory. Comput.*, 2017. doi: 10.1021/acs.jctc.7b00359. URL `http://dx.doi.org/10.1021/acs.jctc.7b00359`. DOI: 10.1021/acs.jctc.7b00359.

USC UNIVERSIDADE DE SANTIAGO DE COMPOSTELA

[125] Lisa Sercombe, Tejaswi Veerati, Fatemeh Moheimani, Sherry Y. Wu, Anil K. Sood, and Susan Hua. Advances and challenges of liposome assisted drug delivery. *Front. Pharmacol.*, 6:286, 2015.

[126] Christiana M. Neophytou and Andreas I. Constantinou. Drug delivery innovations for enhancing the anticancer potential of vitamin e isoforms and their derivatives. *Biomed. Res. Int.*, 2015, 2015.

[127] S. Zhang, N. Sun, X. He, X. Lu, and X. Zhang. Physical properties of ionic liquids: Database and evaluation. *J. Phys. Chem. Ref. Data.*, 35(4):1475–1517, 2006.

[128] M. Freemantle. *An Introduction to Ionic Liquids*. RSC Publishing, 2009.

[129] P. Wasserscheid and T. Welton. *Ionic liquids in synthesis*. Wiley Online Library, 2003.

[130] Li Li Zhang and X. S. Zhao. Carbon-based materials as supercapacitor electrodes. *Chem. Soc. Rev.*, 38(9):2520–2531, 2009.

[131] Robert Hayes, Gregory G. Warr, and Rob Atkin. Structure and nanostructure in ionic liquids. *Chem. Rev.*, 115(13):6357–6426, 2015. doi: 10.1021/cr500411q.

[132] Vincent Zoete, Michel A. Cuendet, Aurélien Grosdidier, and Olivier Michielin. Swissparam: A fast force field generation tool for small organic molecules. *J. Comput. Chem.*, 32(11):2359–2368, 2011. ISSN 1096-987X. doi: 10.1002/jcc.21816. URL `http://dx.doi.org/10.1002/jcc.21816`.

[133] Leela S. Dodda, Israel Cabeza de Vaca, Julian Tirado-Rives, and William L. Jorgensen. Ligpargen web server: an automatic opls-aa parameter generator for organic ligands. *Nucleic. Acids. Res.*, 45(W1):W331–W336, 2017. doi: 10.1093/nar/gkx312. URL `+http://dx.doi.org/10.1093/nar/gkx312`.

USC UNIVERSIDADE DE SANTIAGO DE COMPOSTELA

[134] John D. Holbrey, W. Matthew Reichert, Scott K. Spear, Richard P. Swatloski, Megan B. Turner, and Ann E. Visser. Ionic liquids as green solvents: progress and prospects. In *ACS symposium series*, volume 856. American Chemical Society, 2003.

[135] Christian Reichardt and Thomas Welton. *Solvents and solvent effects in organic chemistry*. John Wiley & Sons, 2011.

[136] M. Galiński, A. Lewandowski, and I. Stepniak. Ionic liquids as electrolytes. *Electrochim. Acta*, 51(26):5567–5580, 2006.

[137] Aleksandar Matic and Bruno Scrosati. Ionic liquids for energy applications. *MRS Bullet.*, 38(07):533–537, 7 2013. ISSN 1938-1425.

[138] Tomohiro Yasuda and Masayoshi Watanabe. Protic ionic liquids: Fuel cell applications. *MRS Bullet.*, 38:560–566, 7 2013. ISSN 1938-1425.

[139] Hermann Weingärtner. Understanding ionic liquids at the molecular level: facts, problems, and controversies. *Angew. Chem. Int. Ed.*, 47(4):654–670, 2008.

[140] Kenneth R. Seddon, Annegret Stark, and María-José Torres. Influence of chloride, water, and organic solvents on the physical properties of ionic liquids. *Pure Appl. Chem.*, 72(12):2275–2287, 2000.

[141] L. Cammarata, S. G. Kazarian, P. A. Salter, and T. Welton. Molecular states of water in room temperature ionic liquids. *Phys. Chem. Chem. Phys.*, 3(23):5192–5200, 2001.

[142] Jennifer L. Anthony, Edward J. Maginn, and Joan F. Brennecke. Solution thermodynamics of imidazolium-based ionic liquids and water. *J. Phys. Chem. B*, 105(44):10942–10949, 2001.

[143] Selimar Rivera-Rubero and Steven Baldelli. Influence of water on the surface of hydrophilic and hydrophobic room-temperature ionic liquids. *J. Am. Chem. Soc.*, 126(38):11788–11789, 2004.

USC UNIVERSIDADE DE SANTIAGO DE COMPOSTELA

[144] R. M. Lynden-Bell, Jorge Kohanoff, and M. G. Del Popolo. Simulation of interfaces between room temperature ionic liquids and other liquids. *Farad. Discuss.*, 129:57–67, 2005.

[145] Wei Jiang, Yanting Wang, and Gregory A. Voth. Molecular dynamics simulation of nanostructural organization in ionic liquid/water mixtures. *Synthesis*, 4(18):6, 2007.

[146] B. L. Bhargava, Yoshiro Yasaka, and Michael L. Klein. Computational studies of room temperature ionic liquid–water mixtures. *Chem. Commun.*, 47(22):6228–6241, 2011.

[147] Trinidad Mendez-Morales, Jesus Carrete, Oscar Cabeza, Luis J. Gallego, and Luis M. Varela. Molecular dynamics simulation of the structure and dynamics of water–1-alkyl-3-methylimidazolium ionic liquid mixtures. *J. Phys. Chem. B*, 115 (21):6995–7008, 2011.

[148] Robert Hayes, Silvia Imberti, Gregory G. Warr, and Rob Atkin. How water dissolves in protic ionic liquids. *Angew. Chem. Int. Ed.*, 51(30):7468–7471, 2012.

[149] Katie A. Maerzke, George S. Goff, Wolfgang H. Runde, William F. Schneider, and Edward J. Maginn. Structure and dynamics of uranyl (vi) and plutonyl (vi) cations in ionic liquid/water mixtures via molecular dynamics simulations. *J. Phys. Chem. B*, 117(37):10852–10868, 2013.

[150] Guang Feng, Xikai Jiang, Rui Qiao, and Alexei A. Kornyshev. Water in ionic liquids at electrified interfaces: The anatomy of electrosorption. *ACS Nano*, 8(11):11685–11694, 2014.

[151] Joshua E. S. J. Reid, Adam J. Walker, and Seishi Shimizu. Residual water in ionic liquids: clustered or dissociated? *Phys. Chem. Chem. Phys.*, 17(22):14710–14718, 2015.

[152] Joshua E. S. J. Reid, Richard J. Gammons, John M. Slattery, Adam J. Walker, and Seishi Shimizu. Interactions in water–ionic

USC UNIVERSIDADE DE SANTIAGO DE COMPOSTELA

liquid mixtures: Comparing protic and aprotic systems. *J. Phys. Chem. B*, 121:599–609, 2017.

[153] Liumin Suo, Oleg Borodin, Tao Gao, Marco Olguin, Janet Ho, Xiulin Fan, Chao Luo, Chunsheng Wang, and Kang Xu. "water-in-salt" electrolyte enables high-voltage aqueous lithium-ion chemistries. *Science*, 350(6263):938–943, 2015.

[154] Aoife M. O'Mahony, Debbie S. Silvester, Leigh Aldous, Christopher Hardacre, and Richard G. Compton. Effect of water on the electrochemical window and potential limits of room-temperature ionic liquids. *J. Chem. Eng. Data*, 53(12):2884–2891, 2008.

[155] Borja Docampo-Álvarez, Victor Gómez-González, Hadrián Montes-Campos, José M. Otero-Mato, Trinidad Méndez-Morales, Oscar Cabeza, L. J. Gallego, Ruth M. Lynden-Bell, Vladislav B. Ivaništšev, Maxim V. Fedorov, et al. Molecular dynamics simulation of the behaviour of water in nano-confined ionic liquid–water mixtures. *J. Phys. Condens. Matter*, 28(46): 464001, 2016.

[156] Hsiu-Wei Cheng, Philipp Stock, Boaz Moeremans, Theodoros Baimpos, Xavier Banquy, Frank Uwe Renner, and Markus Valtiner. Characterizing the influence of water on charging and layering at electrified ionic-liquid/solid interfaces. *Adv. Mater. Interfaces*, 2(12):1500159, 2015.

[157] Kenta Motobayashi and Masatoshi Osawa. Potential-dependent condensation of water at the interface between ionic liquid [BMIM][TFSA] and an Au electrode. *Electrochem. Commun.*, 65:14–17, 2016.

[158] Tong Cui, Abhishek Lahiri, Timo Carstens, Natalia Borisenko, Giridhar Pulletikurthi, Chantal Kuhl, and Frank Endres. Influence of water on the electrified ionic liquid/solid interface: a direct observation of the transition from a multilayered structure to

USC UNIVERSIDADE DE SANTIAGO DE COMPOSTELA

a double-layer structure. *J. Phys. Chem. C*, 120(17):9341–9349, 2016.

[159] Andrew R. Porter, Steven Y. Liem, and Paul L. A. Popelier. Room temperature ionic liquids containing low water concentrations—a molecular dynamics study. *Phys. Chem. Chem. Phys.*, 10(29): 4240–4248, 2008.

[160] S. Feng and G. A. Voth. Molecular dynamics simulations of imidazolium-based ionic liquid/water mixtures: Alkyl side chain length and anion effects. *Fluid Phase Equilib.*, 294(1–2):148–156, 2010.

[161] Takeshi Kobayashi, Joshua E. S. J. Reid, Seishi Shimizu, Maria Fyta, and Jens Smiatek. The properties of residual water molecules in ionic liquids: a comparison between direct and inverse kirkwood–buff approaches. *Phys. Chem. Chem. Phys.*, 19(29): 18924–18937, 2017.

[162] C. Schröder, T. Rudas, G. Neumayr, Siegfried Benkner, and O. Steinhauser. On the collective network of ionic liquid/water mixtures. I. orientational structure. *J. Chem. Phys.*, 127(23): 234503, 2007.

[163] Michael Haberler, Christian Schröder, and Othmar Steinhauser. Hydrated ionic liquids with and without solute: The influence of water content and protein solutes. *J. Chem. Theo. Comput.*, 8(10): 3911–3928, 2012.

[164] Michael Haberler and Othmar Steinhauser. On the influence of of hydrated ionic liquids on the dynamical structure of model proteins: a computational study. *Phys. Chem. Chem. Phys.*, 13(40): 17994–18004, 2011.

[165] Jonathan G. Huddleston, Ann E. Visser, W. Matthew Reichert, Heather D. Willauer, Grant A. Broker, and Robin D. Rogers. Characterization and comparison of hydrophilic and hydrophobic

USC UNIVERSIDADE DE SANTIAGO DE COMPOSTELA

room temperature ionic liquids incorporating the imidazolium cation. *Green Chem.*, 3(4):156–164, 2001.

[166] José N. Canongia Lopes, Margarida F. Costa Gomes, and Agílio A. H. Pádua. Nonpolar, polar, and associating solutes in ionic liquids. *J. Phys. Chem. B*, 110(34):16816–16818, 2006.

[167] Amrish Menjoge, JaNeille Dixon, Joan F. Brennecke, Edward J. Maginn, and Sergey Vasenkov. Influence of water on diffusion in imidazolium-based ionic liquids: A pulsed field gradient nmr study. *J. Phys. Chem. B*, 113(18):6353–6359, 2009.

[168] Esther Rilo, Juan Vila, José Pico, Sandra García-Garabal, Luisa Segade, Luis M. Varela, and Oscar Cabeza. Electrical conductivity and viscosity of aqueous binary mixtures of 1-alkyl-3-methyl imidazolium tetrafluoroborate at four temperatures. *J. Chem. Eng. Data*, 55(2):639–644, 2009.

[169] E. Rilo, J. Vila, S. García-Garabal, L. M. Varela, and O. Cabeza. Electrical conductivity of seven binary systems containing 1-Ethyl-3-methyl imidazolium alkyl sulfate ionic liquids with water or ethanol at four temperatures. *J. Phys. Chem. B*, 117(5):1411–1418, 2013.

[170] Manish S. Kelkar and Edward J. Maginn. Effect of temperature and water content on the shear viscosity of the ionic liquid 1-ethyl-3-methylimidazolium bis (trifluoromethanesulfonyl) imide as studied by atomistic simulations. *J. Phys. Chem. B*, 111(18): 4867–4876, 2007.

[171] Imran Khan, Mohamed Taha, Paulo Ribeiro-Claro, Simão P. Pinho, and João A. P. Coutinho. Effect of the cation on the interactions between alkyl methyl imidazolium chloride ionic liquids and water. *J. Phys. Chem. B*, 118(35):10503–10514, 2014.

[172] Hua Zhao. Protein stabilization and enzyme activation in ionic liquids: specific ion effects. *J. Chem. Technol. Biotechnol.*, 91: 25–50, 2015.

USC
UNIVERSIDADE DE SANTIAGO DE COMPOSTELA

[173] Hsin-Ju Tung and Jim Pfaendtner. Kinetics and mechanism of ionic-liquid induced protein unfolding: application to the model protein hp35. *Mol. Syst. Des. Eng.*, 1(4):382–390, 2016.

[174] Christian Schröder. Proteins in ionic liquids: Current status of experiments and simulations. *Top. Curr. Chem.*, 375(2):25, 2017.

[175] Jens Smiatek. Aqueous ionic liquids and their effects on protein structures: an overview on recent theoretical and experimental results. *J. Phys.: Condens. Matter*, 29(23):233001, 2017.

[176] Diana Constantinescu, Hermann Weingärtner, and Christian Herrmann. Protein denaturation by ionic liquids and the hofmeister series: a case study of aqueous solutions of ribonuclease a. *Angew. Chem. Int. Ed.*, 46(46):8887–8889, 2007.

[177] Zhen Yang. Hofmeister effects: an explanation for the impact of ionic liquids on biocatalysis. *J. Biotechnol.*, 144(1):12–22, 2009.

[178] Zhen Yang, Xiu-Ju Liu, Chao Chen, and Peter J. Halling. Hofmeister effects on activity and stability of alkaline phosphatase. *Biochim. Biophys. Acta*, 1804(4):821–828, 2010.

[179] Awanish Kumar and Pannuru Venkatesu. A comparative study of myoglobin stability in the presence of hofmeister anions of ionic liquids and ionic salts. *Process Biochem.*, 49(12):2158–2169, 2014.

[180] Michael Senske, Diana Constantinescu Aruxandei, Martina Havenith, Hermann Weingärtner, Christian Herrmann, and Simon Ebbinghaus. Thermodynamic fingerprints of the hofmeister series-protein interactions with ionic liquids. *Biophys. J.*, 110(3): 212a, 2016.

[181] Michael Senske, Diana Constantinescu-Aruxandei, Martina Havenith, Christian Herrmann, Hermann Weingärtner, and Simon Ebbinghaus. The temperature dependence of the hofmeister

USC UNIVERSIDADE DE SANTIAGO DE COMPOSTELA

series: thermodynamic fingerprints of cosolute–protein interactions. *Phys. Chem. Chem. Phys.*, 18(43):29698–29708, 2016.

[182] Tristan G. A. Youngs, John D. Holbrey, Maggel Deetlefs, Mark Nieuwenhuyzen, Margarida F. Costa Gomes, and Christopher Hardacre. A molecular dynamics study of glucose solvation in the ionic liquid 1, 3-dimethylimidazolium chloride. *Chem. Phys. Chem.*, 7(11):2279–2281, 2006.

[183] T. G. A. Youngs, C. Hardacre, and J. D. Holbrey. Glucose solvation by the ionic liquid 1, 3-dimethylimidazolium chloride: A simulation study. *J. Phys. Chem. B*, 111(49):13765–13774, 2007.

[184] Christopher Hardacre, John D. Holbrey, Mark Nieuwenhuyzen, and Tristan G. A. Youngs. Structure and solvation in ionic liquids. *Acc. Chem. Res.*, 40(11):1146–1155, 2007.

[185] C. G. Hanke, N. A. Atamas, and R. M. Lynden-Bell. Solvation of small molecules in imidazolium ionic liquids: a simulation study. *Green Chem.*, 4(2):107–111, 2002.

[186] Jennifer L. Anthony, Jessica L. Anderson, Edward J. Maginn, and Joan F. Brennecke. Anion effects on gas solubility in ionic liquids. *J. Phys. Chem. B*, 109(13):6366–6374, 2005.

[187] Lorna Crowhurst, Philip R. Mawdsley, Juan M. Perez-Arlandis, Paul A. Salter, and Thomas Welton. Solvent–solute interactions in ionic liquids. *Phys. Chem. Chem. Phys.*, 5(13):2790–2794, 2003.

[188] Sérgio M. Urahata and Mauro C. C. Ribeiro. Structure of ionic liquids of 1-alkyl-3-methylimidazolium cations: A systematic computer simulation study. *J. Chem. Phys.*, 120(4):1855–1863, 2004.

[189] Volker Lesch, Andreas Heuer, Christian Holm, and Jens Smiatek. Properties of apolar solutes in alkyl imidazolium-based ionic li-

USC UNIVERSIDADE DE SANTIAGO DE COMPOSTELA

quids: The importance of local interactions. *Chem. Phys. Chem.*, 17(3):387–394, 2016.

[190] Andrea Mele, Chieu D. Tran, and Silvia H. De Paoli Lacerda. The structure of a room-temperature ionic liquid with and without trace amounts of water: The role of C-H...O and C-H...F interactions in 1-n-butyl-3-methylimidazolium tetrafluoroborate. *Angew. Chem-Ger Edit.*, 115(36):4500–4502, 2003.

[191] Chieu D. Tran, Silvia H. De Paoli Lacerda, and Daniel Oliveira. Absorption of water by room-temperature ionic liquids: effect of anions on concentration and state of water. *Appl. Spectrosc.*, 57 (2):152–157, 2003.

[192] Y. Danten, M. I. Cabaço, and M. Besnard. Interaction of water diluted in 1-butyl-3-methyl imidazolium ionic liquids by vibrational spectroscopy modeling. *J. Mol. Liq.*, 153(1):57–66, 2010.

[193] YingJie Xu, Yan Gao, LiQun Zhang, Jia Yao, CongMin Wang, and HaoRan Li. Microscopic structures of ionic liquids 1-ethyl-3-methylimidazolium tetrafluoroborate in water probed by the relative chemical shift. *Sci. China Chem.*, 53(7):1561–1565, 2010.

[194] C. G. Hanke and R. M. Lynden-Bell. A simulation study of water-dialkylimidazolium ionic liquid mixtures. *J. Phys. Chem. B*, 107 (39):10873–10878, 2003.

[195] José N. A. Canongia Lopes and Agílio A. H. Pádua. Nanostructural organization in ionic liquids. *J. Phys. Chem. B*, 110(7): 3330–3335, 2006.

[196] Ruth M. Lynden-Bell, Mario G. Del Popolo, Tristan G. A. Youngs, Jorge Kohanoff, Christof G. Hanke, Jason B. Harper, and Carlos C. Pinilla. Simulations of ionic liquids, solutions, and surfaces. *Accounts Chem. Res.*, 40(11):1138–1145, 2007.

USC UNIVERSIDADE DE SANTIAGO DE COMPOSTELA

[197] Marco Klähn, Claudia Stüber, Abirami Seduraman, and Ping Wu. What determines the miscibility of ionic liquids with water? identification of the underlying factors to enable a straightforward prediction. *J. Phys. Chem. B*, 114(8):2856–2868, 2010.

[198] Amir A. Niazi, Brooks D. Rabideau, and Ahmed E. Ismail. Effects of water concentration on the structural and diffusion properties of imidazolium-based ionic liquid–water mixtures. *J. Phys. Chem. B*, 117(5):1378–1388, 2013.

[199] Takeshi Kobayashi, Andre Kemna, Maria Fyta, Björn Braunschweig, and Jens Smiatek. Aqueous mixtures of room-temperature ionic liquids: Entropy-driven accumulation of water molecules at interfaces. *J. Phys. Chem. C*, page DOI: 10.1021/acs.jpcc.9b04098, 2019.

[200] Hanbin Liu, Kenneth L. Sale, Blake A. Simmons, and Seema Singh. Molecular dynamics study of polysaccharides in binary solvent mixtures of an ionic liquid and water. *J. Phys. Chem. B*, 115(34):10251–10258, 2011.

[201] Adam S. Gross, Alexis T. Bell, and Jhih-Wei Chu. Thermodynamics of cellulose solvation in water and the ionic liquid 1-butyl-3-methylimidazolim chloride. *J. Phys. Chem. B*, 115(46):13433–13440, 2011.

[202] Barmak Mostofian, Xiaolin Cheng, and Jeremy C. Smith. Replica-exchange molecular dynamics simulations of cellulose solvated in water and in the ionic liquid 1-butyl-3-methylimidazolium chloride. *J. Phys. Chem. B*, 118(38):11037–11049, 2014.

[203] Jens Smiatek. Osmolyte effects: Impact on the aqueous solution around charged and neutral spheres. *J. Phys. Chem. B*, 118(3):771–782, 2014.

USC UNIVERSIDADE DE SANTIAGO DE COMPOSTELA

[204] David Van Der Spoel, Erik Lindahl, Berk Hess, Gerrit Groenhof, Alan E. Mark, and Herman J. C. Berendsen. Gromacs: fast, flexible, and free. *J. Comput. Chem.*, 26(16):1701–1718, 2005.

[205] J. N. Canongia-Lopes and A. A. H. Pádua. Molecular force field for ionic liquids composed of triflate or bistriflylimide anions. *J. Phys. Chem. B*, 108(43):16893–16898, 2004.

[206] José N. Canongia Lopes, Agílio A. H. Pádua, and Karina Shimizu. Molecular force field for ionic liquids iv: Trialkylimidazolium and alkoxycarbonyl-imidazolium cations; alkylsulfonate and alkylsulfate anions. *J. Phys. Chem. B*, 112(16):5039–5046, 2008.

[207] William L. Jorgensen, Jayaraman Chandrasekhar, Jeffry D. Madura, Roger W. Impey, and Michael L. Klein. Comparison of simple potential functions for simulating liquid water. *J. Chem. Phys.*, 79(2):926–935, 1983.

[208] Mariusz Makowski, Cezary Czaplewski, Adam Liwo, and Harold A. Scheraga. Potential of mean force of association of large hydrophobic particles: Toward the nanoscale limit. *J. Phys. Chem. B*, 114(2):993–1003, 2009.

[209] Alexei A. Kornyshev. Double-layer in ionic liquids: Paradigm change? *J. Phys. Chem. B*, 111(20):5545–5557, 2007.

[210] Víctor Gómez-González, Borja Docampo-Álvarez, Trinidad Méndez-Morales, Oscar Cabeza, Vladislav B. Ivaništšev, Maxim V. Fedorov, Luis J. Gallego, and Luis M. Varela. Molecular dynamics simulation of the structure and interfacial free energy barriers of mixtures of ionic liquids and divalent salts near a graphene wall. *Phys. Chem. Chem. Phys.*, 19(1):846–853, 2017.

[211] Y. Shim, M. Y. Choi, and Hyung J. Kim. A molecular dynamics computer simulation study of room-temperature ionic liquids. i. equilibrium solvation structure and free energetics. *J. Chem. Phys.*, 122(4):044510, 2005.

USC
UNIVERSIDADE DE SANTIAGO DE COMPOSTELA

[212] José M. Otero-Mato, Hadrián Montes-Campos, Oscar Cabeza, Diddo Diddens, Alina Ciach, Luis J. Gallego, and Luis M. Varela. 3d structure of the electric double layer of ionic liquid–alcohol mixtures at the electrochemical interface. *Phys. Chem. Chem. Phys.*, 20(48):30412–30427, 2018.

[213] O. Borodin. Molecular dynamics simulations of ionic liquids: Influence of polarization on IL structure and ion transport. *Mater. Res. Soc. Proc.*, 1082:Q06–04, 2008.

[214] José N. Canongia Lopes and Agílio A. H. Pádua. CL&P: A generic and systematic force field for ionic liquids modeling. *Theor. Chem. Acc.*, 131(3):1129, 2012.

[215] Florian Dommert, Katharina Wendler, Robert Berger, Luigi Delle Site, and Christian Holm. Force fields for studying the structure and dynamics of ionic liquids: a critical review of recent developments. *Chem. Phys. Chem.*, 13(7):1625–1637, 2012.

[216] Mathieu Salanne. Simulations of room temperature ionic liquids: from polarizable to coarse-grained force fields. *Phys. Chem. Chem. Phys.*, 17(22):14270–14279, 2015.

[217] T. Yan, C. J. Burnham, M. G. Del Pópolo, and G. A. Voth. Molecular dynamics simulation of ionic liquids: The effect of electronic polarizability. *J. Phys. Chem. B*, 108(32):11877–11881, 2004.

[218] Johan Jacquemin, Pascale Husson, Agilio A. H. Padua, and Vladimir Majer. Density and viscosity of several pure and water-saturated ionic liquids. *Green Chem.*, 8(2):172–180, 2006.

[219] Craig A. Hall, Kim A. Le, Cyrielle Rudaz, Asanah Radhi, Christopher S. Lovell, Robin A. Damion, Tatiana Budtova, and Michael E. Ries. Macroscopic and microscopic study of 1-ethyl-3-methyl-imidazolium acetate–water mixtures. *J. Phys. Chem. B*, 116(42):12810–12818, 2012.

USC UNIVERSIDADE DE SANTIAGO DE COMPOSTELA

[220] Sebastian Fendt, Sasisanker Padmanabhan, Harvey W. Blanch, and John M. Prausnitz. Viscosities of acetate or chloride-based ionic liquids and some of their mixtures with water or other common solvents. *J. Chem. Eng. Data*, 56(1):31–34, 2010.

[221] Suojiang Zhang, Jian Sun, Xiaochun Zhang, Jiayu Xin, Qingqing Miao, and Jianji Wang. Ionic liquid-based green processes for energy production. *Chem. Soc. Rev.*, 43(22):7838–7869, 2014.

[222] Catarina M. S. S. Neves, Teresa B. V. Dinis, Pedro J. Carvalho, Bernd Schröder, Luís M. N. B. F. Santos, Mara G. Freire, and João A. P. Coutinho. Binary mixtures of ionic liquids in aqueous solution: Towards an understanding of their salting-in/salting-out phenomena. *J. Solution Chem.*, 48(7):983–991, 2019.

[223] Tânia E. Sintra, Miguel Vilas, Margarida Martins, Sónia P. M. Ventura, Ana I. M. C. Lobo Ferreira, Luís M. N. B. F. Santos, Fernando J. M. Gonçalves, Emília Tojo, and João A. P. Coutinho. Synthesis and characterization of surface-active ionic liquids used in the disruption of escherichia coli cells. *Chem. Phys. Chem.*, 20(5):727–735, 2019.

[224] Maxim V. Fedorov and Alexei A. Kornyshev. Ionic liquids at electrified interfaces. *Chem. Rev.*, 114(5):2978–3036, 2014.

[225] L. M. Varela, T. Méndez-Morales, J. Carrete, V. Gómez-González, B. Docampo-Álvarez, L. J. Gallego, O. Cabeza, and O. Russina. Solvation of molecular cosolvents and inorganic salts in ionic liquids: a review of molecular dynamics simulations. *J. Mol. Liq.*, 210:178–188, 2015.

[226] Anna Martinelli, Aleksandar Matic, Per Jacobsson, Lars Borjesson, Alessandra Fernicola, and Bruno Scrosati. Phase behavior and ionic conductivity in lithium bis (trifluoromethanesulfonyl) imide-doped ionic liquids of the pyrrolidinium cation and bis (trifluoromethanesulfonyl) imide anion. *J. Phys. Chem. B*, 113(32):11247–11251, 2009.

USC
UNIVERSIDADE DE SANTIAGO DE COMPOSTELA

[227] J. Salgado, J. J. Parajó, M. Villanueva, J. R. Rodríguez, O. Cabeza, and L. M. Varela. Liquid range of ionic liquid–metal salt mixtures for electrochemical applications. *J. Chem. Thermodyn*, 134:164–174, 2019.

[228] Juan J. Parajo, María Villanueva, Ines Otero, Josefa Fernández, and Josefa Salgado. Thermal stability of aprotic ionic liquids as potential lubricants. comparison with synthetic oil bases. *J. Chem. Thermodyn*, 116:185–196, 2018.

[229] J. J. Parajó, M. Villanueva, P. B. Sánchez, and J. Salgado. Liquid window of some biologically-active ionic liquids. *J. Chem. Thermodyn*, 126:1–10, 2018.

[230] Josefa Salgado, Tamara Teijeira, Juan José Parajó, Josefa Fernández, and Jacobo Troncoso. Isobaric heat capacity of nanostructured liquids with potential use as lubricants. *J. Chem. Thermodyn*, 123:107–116, 2018.

[231] Trinidad Méndez-Morales, Jesús Carrete, Julio R. Rodriguez, Oscar Cabeza, Luis J. Gallego, Olga Russina, and Luis M. Varela. Nanostructure of mixtures of protic ionic liquids and lithium salts: effect of alkyl chain length. *Phys. Chem. Chem. Phys.*, 17(7): 5298–5307, 2015.

[232] O. Russina, R. Caminiti, T. Méndez-Morales, J. Carrete, O. Cabeza, L. J. Gallego, L. M. Varela, and A. Triolo. How does lithium nitrate dissolve in a protic ionic liquid? *J. Mol. Liq.*, 205: 16–21, 2015.

[233] D. Fennell Evans, Shaw-Horng Chen, George W. Schriver, and Edward M. Arnett. Thermodynamics of solution of nonpolar gases in a fused salt. hydrophobic bonding behavior in a non-aqueous system. *J. Am. Chem. Soc.*, 103(2):481–482, 1981.

[234] Dorota Warmińska and Iwona Cichowska-Kopczyńska. Thermodynamic study of binary mixtures of toluene with ionic liquids,

USC UNIVERSIDADE DE SANTIAGO DE COMPOSTELA

1-butyl-1-methylpyrrolidinium bis (trifluoromethylsulfonyl) imide, 1-hexyl-1-methylpyrrolidinium bis (trifluoromethylsulfonyl) imide and 1-butylpyridinium bis (trifluoromethylsulfonyl) imide. *J. Mol. Liq.*, 304:112754, 2020.

[235] Yingjun Cai, Nicolas von Solms, Suojiang Zhang, and Kaj Thomsen. Density, viscosity, and conductivity of [VAIM][TFSI] in mixtures for lithium-ion battery electrolytes. *J. Chem. Eng. Data*, 65(2):495–502, 2020.

[236] Juan José Parajó, Pablo Vallet, Luis Miguel Varela, María Villanueva, and Josefa Salgado. Ecotoxicity of binary mixtures of ils and inorganic salts of electrochemical interest. *Environ Sci. Pollut. R.*, 29(17):24983–24994, 2022.

[237] Y. Marcus. Ions and their properties. *Ions in solution and their solvation*, pages 10–62, 2015.

[238] M. F. Gautreaux Jr and Jesse Coates. Activity coefficients at infinite dilution. *AIChE Journal*, 1(4):496–500, 1955.

[239] Donald G. Archer, Jason A. Widegren, Duane R. Kirklin, and Joseph W. Magee. Enthalpy of solution of 1-octyl-3-methylimidazolium tetrafluoroborate in water and in aqueous sodium fluoride. *J. Chem. Eng. Data*, 50(4):1484–1491, 2005.

[240] Wei Guan, Heng Wang, Lei Li, Qing-Guo Zhang, and Jia-Zhen Yang. Enthalpy of solution of the ionic liquid bmibf4 in water. *Thermochim Acta*, 437(1-2):196–197, 2005.

[241] Mikhail A. Varfolomeev, Artashes A. Khachatrian, Bulat S. Akhmadeev, Boris N. Solomonov, Andrei V. Yermalayeu, and Sergey P. Verevkin. Enthalpies of solution and enthalpies of solvation in water: the anion effect in ionic liquids with common 1-ethyl-3-methyl-imidazolium cation. *J. Solution Chem.*, 44(3): 811–823, 2015.

USC UNIVERSIDADE DE SANTIAGO DE COMPOSTELA

[242] Frank E. Young. Heats of formation of $Mg(NO_2)_2$, $Mg(NO_3)_2 \cdot 6H_2O$, $Ca(NO_3)_2$, $Ca(NO_3)_2 \cdot 4H_2O$ and $Ba(NO_3)_2$. *J. Am. Chem. Soc.*, 66(5):773–777, 1944.

[243] Hermenegild Arved Flaschka. *EDTA titrations: an introduction to theory and practice*. Elsevier, 2013.

[244] Vladimir V. Matveev, Alexandr V. Ievlev, Mikhail A. Vovk, Oscar Cabeza, Josefa Salgado-Carballo, Juan J. Parajo, Julio R. Rodriguez, Raul de la Fuente, Erkki Lähderanta, and Luis M. Varela. NMR investigation of the structure and single-particle dynamics of inorganic salt solutions in a protic ionic liquid. *J. Mol. Liq.*, 278:239–246, 2019.

[245] Manuel A. V. Ribeiro da Silva, Luís M. N. B. F. Santos, and Edward Giera. Standard molar enthalpies of formation of nickel (II) β-diketonates and monothio-β-diketonates. *J. Chem. Thermodyn*, 39(3):361–370, 2007.

[246] L. M. N. B. F. Santos, M. Silva, B. Schröder, and L. Gomes. Labtermo: methodologies for the calculation of the corrected temperature rise in isoperibol calorimetry. *J. Therm. Anal. Calorim*, 89 (1):175–180, 2007.

[247] R. J. Irving and I. Wadsö. Use of tris (hydroxymethyl) aminomethane as a test substance in reaction calorimetry. *Acta. Chem. Scand*, 18:195–201, 1964.

[248] Michael W. Mahoney and William L. Jorgensen. A five-site model for liquid water and the reproduction of the density anomaly by rigid, nonpolarizable potential functions. *J. Chem. Phys.*, 112(20):8910–8922, 2000.

[249] Tom Darden, Darrin York, and Lee Pedersen. Particle mesh Ewald: An N·log(N) method for Ewald sums in large systems. *J. Chem. Phys.*, 98(12):10089–10092, 1993.

USC UNIVERSIDADE DE SANTIAGO DE COMPOSTELA

[250] Ulrich Essmann, Lalith Perera, Max L. Berkowitz, Tom Darden, Hsing Lee, and Lee G. Pedersen. A smooth particle mesh Ewald method. *J. Chem. Phys.*, 103(19):8577–8593, 1995.

[251] William Humphrey, Andrew Dalke, and Klaus Schulten. VMD – Visual Molecular Dynamics. *J. Mol. Graphics.*, 14:33–38, 1996.

[252] A. Podgorsek, J. Jacquemin, A. A. H. Pádua, and M. F. Costa Gomes. Mixing enthalpy for binary mixtures containing ionic liquids. *Chem. Rev.*, 116(10):6075–6106, 2016.

[253] Stanislav Pandelov, Jasper C. Werhahn, Bert M. Pilles, Sotiris S. Xantheas, and Hristo Iglev. An empirical correlation between the enthalpy of solution of aqueous salts and their ability to form hydrates. *J. Phys. Chem. A*, 114(38):10454–10457, 2010.

[254] G. Wolf, V. Vacek, and V. Pekarek. Enthalpies of solution and of crystallization of lithium nitrate and of lithium nitrate trihydrate in water at 25°C. *J. Solution Chem.*, 19(10):1029–1039, 1990.

[255] H. D. B. Jenkins and T. C. Waddington. Enthalpy of formation, $\Delta H°_f NO_3^-(g)$ and solvation, $\delta H°_{solv} NO_3^-(g)$ of the gaseous nitrate ion charge distribution in the NO_3^- ion and lattice energies of $LiNO_3$, $NaNO_3$ and KNO_3. *Journal of Inorganic and Nuclear Chemistry*, 34(8):2465–2473, 1972.

[256] Bartłomiej Pałecz, Jolanta Barczyńska, and Stefania Taniewska-Osińska. Enthalpies of solution of some nitrates in aqueous methanol solutions at 298.15 k. *Thermochim Acta*, 150(1):121–123, 1989.

[257] Hanen Jendoubi, Dalila Hellali, Hmida Zamali, and Jacques Rogez. Mixing enthalpies of solid solutions $(Cs_{1-x},Rb_x)NO_3$ at, t = (298.15 and 473.15)K. *J. Chem. Thermodyn*, 79:215–223, 2014. ISSN 0021-9614. doi: https://doi.org/10.1016/j.jct.2014.07.024. URL `https://www.sciencedirect.com/science/article/pii/S0021961414002444`.

USC UNIVERSIDADE DE SANTIAGO DE COMPOSTELA

[258] Robert Weintraub, Alexander Apelblat, and Abraham Tamir. Enthalpy of solution of rubidium nitrate in water. *J. Chem. Thermodyn*, 16(5):419–422, 1984.

[259] P. A. G. O'Hare and Juliana Boerio. Cesium nitrate. standard enthalpies of solution and formation and the standard entropy at 298.15 K. *J. Chem. Thermodyn*, 7(10):937–941, 1975.

[260] Warren W. Ewing, Ernst Klinger, and John D. Brandner. Studies on the vapor pressure—temperature relations and on the heats of hydration, solution and dilution of the binary system magnesium nitrate—water. *J. Am. Chem. Soc.*, 56(5):1053–1057, 1934.

[261] Warren W. Ewing, Alfred N. Rogers, John Z. Miller, and Edward McGovern. Calcium nitrate. III. heats of hydration and of solution of the binary system calcium nitrate-water. *J. Am. Chem. Soc.*, 54 (4):1335–1343, 1932.

[262] Warren W. Ewing and Alfred N. Rogers. Calcium nitrate. IV. heats of dilution of solutions of calcium nitrate in water. *J. Am. Chem. Soc.*, 55(9):3603–3609, 1933.

[263] Juliana Boerio and P. A. G. O'Hare. Standard enthalpies of solution and formation at 298.15 K of anhydrous magnesium and calcium nitrates. *J. Chem. Thermodyn*, 8(8):725–729, 1976.

[264] Donald D. Wagman, William H. Evans, Vivian B. Parker, Richard H. Schumm, and Iva Halow. The NBS tables of chemical thermodynamic properties. selected values for inorganic and C1 and C2 organic substances in SI units. Technical report, National Standard Reference Data System, 1982.

[265] Anubhav Jain, Shyue Ping Ong, Geoffroy Hautier, Wei Chen, William Davidson Richards, Stephen Dacek, Shreyas Cholia, Dan Gunter, David Skinner, Gerbrand Ceder, et al. Commentary: The materials project: A materials genome approach to accelerating materials innovation. *APL materials*, 1(1):011002, 2013.

USC
UNIVERSIDADE DE SANTIAGO DE COMPOSTELA

[266] M. W. Chase Jr, C. A. Davies, J. R. Downey Jr, D. J. Frurip, R. A. McDonald, and A. N. Syverud. JANAF thermochemical tables: II: Cr-Zr. *J. Phys. Chem. Ref. Data*, 14:927–1856, 1985.

[267] Martin Allen, D. Fennell Evans, and Rufus Lumry. Thermodynamic properties of the ethylammonium nitrate+water system: Partial molar volumes, heat capacities, and expansivities. *J. Solution Chem.*, 14(8):549–560, 1985.

[268] Robert Hayes, Silvia Imberti, Gregory G. Warr, and Rob Atkin. Amphiphilicity determines nanostructure in protic ionic liquids. *Phys. Chem. Chem. Phys.*, 13(8):3237–3247, 2011.

[269] Derek W. Smith. Ionic hydration enthalpies. *J. Chem. Educ.*, 54 (9):540, 1977.

[270] José M. Otero-Mato, Volker Lesch, Hadrián Montes-Campos, Jens Smiatek, Diddo Diddens, Oscar Cabeza, Luis J. Gallego, and Luis M. Varela. Solvation in ionic liquid-water mixtures: A computational study. *J. Mol. Liq.*, 292:111273, 2019.

[271] Solvation Interpolator. `https://github.com/txemaotero/solvation_interpolator`, .

[272] Song-Song Bao, Kazuya Otsubo, Jared M. Taylor, Zheng Jiang, Li-Min Zheng, and Hiroshi Kitagawa. Enhancing proton conduction in 2D Co–La coordination frameworks by solid-state phase transition. *J. Am. Chem. Soc.*, 136(26):9292–9295, 2014.

[273] M. Vijayakumar, Alex D. Bain, and Gillian R. Goward. Investigations of proton conduction in the monoclinic phase of RbH2PO4 using multinuclear solid-state NMR. *J. Phys. Chem. C*, 113(41): 17950–17957, 2009.

[274] Osamu Nakamura, Teruo Kodama, Isao Ogino, and Yoshizo Miyake. High-conductivity solid proton conductors: Dodecamolybdophosphoric acid and dodecatungstophosphoric acid crystals. *Chem. Lett.*, 8(1):17–18, 1979.

USC UNIVERSIDADE DE SANTIAGO DE COMPOSTELA

[275] Daniil I. Kolokolov, Maxim S. Kazantsev, Mikhail V. Luzgin, Hervé Jobic, and Alexander G. Stepanov. Direct 2H NMR observation of the proton mobility of the acidic sites of anhydrous 12-tungstophosphoric acid. *Chem. Phys. Chem.*, 14(9):1783–1786, 2013.

[276] N. Tjapkin, M. Davidović, Ph Colomban, and U. Mioč. Complex dielectric permittivity, bulk and surface conductivity of 12-tungstophosphoric acid hexahydrate and its dehydrated forms. *Solid State Ionics*, 61(1-3):179–185, 1993.

[277] U. Mioč, Ph Colomban, and Aleksander Novak. Infrared and raman study of some heteropolyacid hydrates. *J. Mol. Struct.*, 218:123–128, 1990.

[278] I. Holclajtner-Antunović, Ubavka B. Mioč, M. Todorović, Z. Jovanović, M. Davidović, D. Bajuk-Bogdanović, and Zoran Laušević. Characterization of potassium salts of 12-tungstophosphoric acid. *Mater. Res. Bull.*, 45(11):1679–1684, 2010.

[279] U. B. Mioe, Marija R. Todorović, S. M. Uskoković-Marković, M. Davidović, A. Kremenović, Anne Spasojević-de Bire, T. Čajkovski, V. Likar-Smiljanić, and R. Biljić. Structure and proton conductivity in a magnesium salt of 12-tungstophosphoric acid. *Solid State Ionics*, 162:217–223, 2003.

[280] M. Davidović, T. Čajkovski, D. Čajkovski, V. Likar-Smiljanić, R. Biljić, Ubavka B. Mioč, and Zoran Nedić. Dielectric relaxation and conductivity in barium salt of 12-tungstophosphoric acid hydrate. *Solid State Ionics*, 147(1-2):123–128, 2002.

[281] Alexander Igorevich Chikin, Alexander Vladimirovich Chernyak, Zhao Jin, Yulia Sergeevna Naumova, Alexander Evgenevich Ukshe, Nina Vladimirovna Smirnova, Vitaliy Ivanovich Volkov, and Yury Anatolevich Dobrovolsky.

USC UNIVERSIDADE DE SANTIAGO DE COMPOSTELA

Mobility of protons in 12-phosphotungstic acid and its acid and neutral salts. *J. Solid State Electr.*, 16(8):2767–2775, 2012.

[282] Yuhua Zhou, Jing Yang, Haibin Su, Jie Zeng, San Ping Jiang, and William A. Goddard. Insight into proton transfer in phosphotungstic acid functionalized mesoporous silica-based proton exchange membrane fuel cells. *J. Am. Chem. Soc.*, 136(13):4954–4964, 2014.

[283] James L. Horan, Anitha Lingutla, Hui Ren, Mei-Chen Kuo, Sonny Sachdeva, Yuan Yang, Soenke Seifert, Lauren F. Greenlee, Michael A. Yandrasits, Steven J. Hamrock, et al. Fast proton conduction facilitated by minimum water in a series of divinylsilyl-11-silicotungstic acid-co-butyl acrylate-co-hexanediol diacrylate polymers. *J. Phys. Chem. C*, 118(1):135–144, 2014.

[284] John C. MacDonald, Pieter C. Dorrestein, and Malissa M. Pilley. Design of supramolecular layers via self-assembly of imidazole and carboxylic acids. *Crystal Growth & Design*, 1(1): 29–38, 2001.

[285] Elliott P. Barrett, Leslie G. Joyner, and Paul P. Halenda. The determination of pore volume and area distributions in porous substances. I. computations from nitrogen isotherms. *J. Am. Chem. Soc.*, 73(1):373–380, 1951.

[286] Stephen Brunauer, Paul Hugh Emmett, and Edward Teller. Adsorption of gases in multimolecular layers. *J. Am. Chem. Soc.*, 60 (2):309–319, 1938.

[287] Somisetti V. Sambasivarao and Orlando Acevedo. Development of OPLS-AA force field parameters for 68 unique ionic liquids. *J. Chem. Theory Comput.*, 5(4):1038–1050, 2009.

[288] Borja Docampo-Álvarez, Victor Gomez-Gonzalez, Oscar Cabeza, Vladislav B. Ivaništšev, Luis J. Gallego, and Luis M. Varela. Molecular dynamics simulations of novel electrolytes

USC UNIVERSIDADE DE SANTIAGO DE COMPOSTELA

based on mixtures of protic and aprotic ionic liquids at the electrochemical interface: Structure and capacitance of the electric double layer. *Electrochim Acta*, 305:223–231, 2019.

[289] Curt M. Breneman and Kenneth B. Wiberg. Determining atom-centered monopoles from molecular electrostatic potentials. the need for high sampling density in formamide conformational analysis. *J. Comput. Chem.*, 11(3):361–373, 1990.

[290] M. J. Frisch, G. W. Trucks, H. B. Schlegel, G. E. Scuseria, M. A. Robb, J. R. Cheeseman, G. Scalmani, V. Barone, G. A. Petersson, H. Nakatsuji, X. Li, M. Caricato, A. V. Marenich, J. Bloino, B. G. Janesko, R. Gomperts, B. Mennucci, H. P. Hratchian, J. V. Ortiz, A. F. Izmaylov, J. L. Sonnenberg, D. Williams-Young, F. Ding, F. Lipparini, F. Egidi, J. Goings, B. Peng, A. Petrone, T. Henderson, D. Ranasinghe, V. G. Zakrzewski, J. Gao, N. Rega, G. Zheng, W. Liang, M. Hada, M. Ehara, K. Toyota, R. Fukuda, J. Hasegawa, M. Ishida, T. Nakajima, Y. Honda, O. Kitao, H. Nakai, T. Vreven, K. Throssell, J. A. Montgomery, Jr., J. E. Peralta, F. Ogliaro, M. J. Bearpark, J. J. Heyd, E. N. Brothers, K. N. Kudin, V. N. Staroverov, T. A. Keith, R. Kobayashi, J. Normand, K. Raghavachari, A. P. Rendell, J. C. Burant, S. S. Iyengar, J. Tomasi, M. Cossi, J. M. Millam, M. Klene, C. Adamo, R. Cammi, J. W. Ochterski, R. L. Martin, K. Morokuma, O. Farkas, J. B. Foresman, and D. J. Fox. Gaussian 16 Revision C.01, 2016. Gaussian Inc. Wallingford CT.

[291] A. D. McLean and G. S. Chandler. Contracted Gaussian basis sets for molecular calculations. I. Second row atoms, z = 11–18. *J. Chem. Phys.*, 72(10):5639–5648, 1980.

[292] R. B. J. S. Krishnan, J. Stephen Binkley, Rolf Seeger, and John A. Pople. Self-consistent molecular orbital methods. xx. a basis set for correlated wave functions. *J. Chem. Phys.*, 72(1):650–654, 1980.

USC
UNIVERSIDADE DE SANTIAGO DE COMPOSTELA

[293] Axel D. Becke. A new mixing of hartree–fock and local density-functional theories. *J. Chem. Phys.*, 98(2):1372–1377, 1993.

[294] Xavier Lopez, Carlos Nieto-Draghi, Carles Bo, Josep Bonet Avalos, and Josep M. Poblet. Polyoxometalates in solution: molecular dynamics simulations on the α-PW12O403-Keggin anion in aqueous media. *J. Phys. Chem. A*, 109(6):1216–1222, 2005.

[295] L. Ts Kazanskij. Molecular and electronic structure of heteropolycomplexes. *Izvestiya Akademii Nauk SSSR, Seriya Khimicheskaya*, pages 274–278, 1978.

[296] Rene Thouvenot, Michel Fournier, Raymonde Franck, and Claude Rocchiccioli-Deltcheff. Vibrational investigations of polyoxometalates. 3. isomerism in molybdenum (vi) and tungsten (vi) compounds related to the keggin structure. *Inorg. Chem.*, 23 (5):598–605, 1984.

[297] Ivanka Holclajtner-Antunović, Danica Bajuk-Bogdanović, Alexandru Popa, and Snežana Uskoković-Marković. Spectroscopic identification of molecular species of 12-tungstophosphoric acid in methanol/water solutions. *Inorg. Chim. Acta*, 383:26–32, 2012.

[298] D. H. Bonsor, B. Borah, R. L. Dean, and J. L. Wood. Complex hydrogen bonded cations. The imdazole/imidazolium complex cation. *Can. J. Chemistry*, 54(15):2458–2464, 1976.

[299] M. Majoube, M. Henry, L. Chinsky, and P. Y. Turpin. Prereson-ance raman spectra for imidazole and imidazolium ion: interpretation of the intensity enhancement from a precise assignment of normal modes. *Chem. Phys.*, 169(2):231–241, 1993.

[300] Robert C. T. Slade, Ian M. Thompson, Richard C. Ward, and Christiane Poinsignon. Resolution of dynamic processes in proton-conducting 12-tungstophosphoric acid 14-hydrate by a combination of quasielastic neutron-scattering and nmr techniques. *J. Chem. Soc., Chem. Commun.*, 10:726–727, 1987.

USC
UNIVERSIDADE DE SANTIAGO DE COMPOSTELA

[301] U. Mioč, Milorad Davidović, Nikola Tjapkin, Ph Colomban, and A. Novak. Equilibrium of the protonic species in hydrates of some heteropolyacids at elevated temperatures. *Solid State Ionics*, 46(1-2):103–109, 1991.

[302] Marcos de Oliveira Jr, Ubirajara Pereira Rodrigues-Filho, and J. Schneider. Thermal transformations and proton species in 12-phosphotungstic acid hexahydrate studied by 1H and 31P solid-state nuclear magnetic resonance. *J. Phys. Chem. C*, 118(22): 11573–11583, 2014.

[303] Toshio Okuhara and Yuichi Kamiya. Oxide catalysts in solid-state chemistry. *Encyclopedia of Inorganic and Bioinorganic Chemistry*, 2011.

[304] Paola Gilli, Loretta Pretto, Valerio Bertolasi, and Gastone Gilli. Predicting hydrogen-bond strengths from acid-base molecular properties. the pK_a slide rule: toward the solution of a long-lasting problem. *Accounts Chem. Res.*, 42(1):33–44, 2009.

[305] A. Piecha, R. Jakubas, A. Pietraszko, J. Baran, W. Medycki, and D. Kruk. Structural characterization, thermal, dielectric, vibrational properties and molecular motions in [c3n2h5] 6 [bi4br18]. *J. Solid State Chem.*, 182(11):2949–2960, 2009.

[306] J. Demaison, Michel Herman, and Jacques Liévin. The equilibrium oh bond length. *Int. Rev. Phys. Chem.*, 26(3):391–420, 2007.

[307] Sjors Bakels, Marie-Pierre Gaigeot, and Anouk M. Rijs. Gas-phase infrared spectroscopy of neutral peptides: Insights from the far-ir and thz domain. *Chem. Rev.*, 120(7):3233–3260, 2020.

[308] Noam Agmon. Hydrogen bonds, water rotation and proton mobility. *J. chim. Phys. Phys.-Chim. Biol.*, 93:1714–1736, 1996.

[309] Soohaeng Yoo Willow, Michael A. Salim, Kwang S. Kim, and So Hirata. Ab initio molecular dynamics of liquid water using

USC UNIVERSIDADE DE SANTIAGO DE COMPOSTELA

embedded-fragment second-order many-body perturbation theory towards its accurate property prediction. *Sci. Rep.*, 5(1):1–14, 2015.

[310] Myong Yong Choi and Roger E. Miller. Infrared laser spectroscopy of imidazole complexes in helium nanodroplets: Monomer, dimer, and binary water complexes. *J. Phys. Chem. A*, 110(30):9344–9351, 2006.

[311] Zhengbo Han, Guoyou Luan, and Enbo Wang. Synthesis, properties and crystal structure of a novel organic–inorganic hybrid constructed from tungstophosphoric acid and benzotriazole. *Transit Metal Chem.*, 28(1):63–68, 2003.

[312] Josefine Schnee and Eric M. Gaigneaux. Elucidating and exploiting the chemistry of keggin heteropolyacids in the methanol-todme conversion: enabling the bulk reaction thanks to operando raman. *Catalysis Science & Technology*, 7(4):817–830, 2017.

[313] A. Kremenović, A. Spasojević-de Biré, R. Dimitrijević, P. Sciau, U. B. Mioč, and Ph Colomban. Keggin's ion structural modification and expansion of dodecatungstophosphoric acid hexahydrate induced by temperature treatment: In situ x-ray powder diffraction and raman investigations. *Solid State Ionics*, 132(1-2):39–53, 2000.

[314] Silvana Raquel Matkovic, Laura Estefanía Briand, and Miguel Ángel Bañares. Investigation of the thermal stability of phosphotungstic wells-dawson heteropoly-acid through in situ raman spectroscopy. *Mater. Res. Bull.*, 46(11):1946–1948, 2011.

[315] K. D. Kreuer, A. Fuchs, M. Ise, Maier Spaeth, and J. Maier. Imidazole and pyrazole-based proton conducting polymers and liquids. *Electrochim Acta*, 43(10-11):1281–1288, 1998.

USC UNIVERSIDADE DE SANTIAGO DE COMPOSTELA

[316] A. Kawada, A. R. McGhie, and M. M. Labes. Protonic conductivity in imidazole single crystal. *J. Chem. Phys.*, 52(6):3121–3125, 1970.

[317] Masanobu Nakayama, Yasuyuki Sugiura, Tomokatsu Hayakawa, and Masayuki Nogami. A novel proton conductor of imidazole–aluminium phosphate hybrids in the solid state. *Phys. Chem. Chem. Phys.*, 13(20):9439–9444, 2011.

[318] Paweł Ławniczak, Katarzyna Pogorzelec-Glaser, Adam Pietraszko, and Bożena Hilczer. Impedance spectroscopy studies of proton conductivity in imidazolium malonate. *Solid State Ionics*, 306:25–30, 2017.

[319] Sylwia Zięba, Alina T. Dubis, Andrzej K. Gzella, Paweł Ławniczak, Katarzyna Pogorzelec-Glaser, and Andrzej Łapiński. Toward a new type of proton conductor based on imidazole and aromatic acids. *Phys. Chem. Chem. Phys.*, 21(31):17152–17162, 2019.

[320] Yuqing Meng, Jun Gao, Zeyu Zhao, Jake Amoroso, Jianhua Tong, and Kyle S. Brinkman. Recent progress in low-temperature proton-conducting ceramics. *J. Mater. Sci.*, 54(13):9291–9312, 2019.

[321] Qingfeng Li, David Aili, Robert F. Savinell, and Jens Oluf Jensen. Acid–base chemistry and proton conductivity. In *High Temperature Polymer Electrolyte Membrane Fuel Cells*, pages 37–57. Springer, 2016.

[322] Adam Rachocki, Katarzyna Pogorzelec-Glaser, Adam Pietraszko, and Jadwiga Tritt-Goc. The structural dynamics in the proton-conducting imidazolium oxalate. *J. Phys. Condens. Matter*, 20(50):505101, 2008.

[323] Alain Chaumont and Georges Wipff. Do keggin anions repulse each other in solution? the effect of solvent, counterions and ion

USC UNIVERSIDADE DE SANTIAGO DE COMPOSTELA

representation investigated by free energy (pmf) simulations. *Cr. Chim.*, 15(2-3):107–117, 2012.

[324] Ferhan Tümer, Muhammet Köse, and Mehmet Tümer. Synthesis, crystal structure and spectroscopic properties of ethanol solvated α-keggin heteropolymolybdate. *J. Mol. Struct.*, 1147:622–628, 2017.

[325] Yuan Mei, Wei Huang, Zhen Yang, Jun Wang, and Xiaoning Yang. Ion-pairing and aggregation of ionic liquid-neutralized polyoxometalate salts in aqueous solutions. *Fluid Phase Equilibr*, 425:31–39, 2016.

[326] Ville R. I. Kaila and Gerhard Hummer. Energetics and dynamics of proton transfer reactions along short water wires. *Phys. Chem. Chem. Phys.*, 13(29):13207–13215, 2011.

[327] Yu-Guo Guo, Jin-Song Hu, and Li-Jun Wan. Nanostructured materials for electrochemical energy conversion and storage devices. *Adv. Mater.*, 20(15):2878–2887, 2008.

[328] Antonino Salvatore Arico, Peter Bruce, Bruno Scrosati, Jean-Marie Tarascon, and Walter Van Schalkwijk. Nanostructured materials for advanced energy conversion and storage devices. *Nat. Mater.*, 4(5):366, 2005.

[329] Jenel Vatamanu, Zongzhi Hu, Dmitry Bedrov, Carlos Perez, and Yury Gogotsi. Increasing energy storage in electrochemical capacitors with ionic liquid electrolytes and nanostructured carbon electrodes. *J. Phys. Chem. Lett.*, 4(17):2829–2837, 2013.

[330] Martyn Earle, Alain Forestièr, Hélène Olivier-Bourbigou, and Peter Wasserscheid. *Organic synthesis*. Wiley Online Library, 2003.

[331] Hiroyuki Ohno. *Electrochemical aspects of ionic liquids*. John Wiley & Sons, 2005.

USC UNIVERSIDADE DE SANTIAGO DE COMPOSTELA

[332] M. Armand, F. Endres, D. R. MacFarlane, H. Ohno, and B. Scrosati. Ionic-liquid materials for the electrochemical challenges of the future. *Nat. Mater.*, 8(8):621–629, 2009.

[333] Natalia V. Plechkova and Kenneth R. Seddon. Applications of ionic liquids in the chemical industry. *Chem. Soc. Rev.*, 37(1): 123–150, 2008.

[334] Hua Zhao and Sanjay V. Malhotra. Applications of ionic liquids in organic synthesis. *Aldrichim Acta*, 2002.

[335] R. D. Rogers and K. R. Seddon. *Ionic Liquids: Industrial Applications for Green Chemistry*. American Chemical Society, 2002.

[336] Yunpu Zhai, Yuqian Dou, Dongyuan Zhao, Pasquale F. Fulvio, Richard T. Mayes, and Sheng Dai. Carbon materials for chemical capacitive energy storage. *Adv. Mater.*, 23(42):4828–4850, 2011.

[337] Patrice Simon and Y. Gogotsi. Capacitive energy storage in nanostructured carbon–electrolyte systems. *Accounts. Chem. Res.*, 46 (5):1094–1103, 2012.

[338] François Béguin, Volker Presser, Andrea Balducci, and Elzbieta Frackowiak. Carbons and electrolytes for advanced supercapacitors. *Adv. Mater.*, 26(14):2219–2251, 2014.

[339] Christian Schröder. Comparing reduced partial charge models with polarizable simulations of ionic liquids. *Phys. Chem. Chem. Phys.*, 14(9):3089–3102, 2012.

[340] Volker Lesch, Hadrián Montes-Campos, Trinidad Méndez-Morales, Luis Javier Gallego, Andreas Heuer, Christian Schröder, and Luis M. Varela. Molecular dynamics analysis of the effect of electronic polarization on the structure and single-particle dynamics of mixtures of ionic liquids and lithium salts. *J. Chem. Phys.*, 145(20):204507, 2016.

USC UNIVERSIDADE DE SANTIAGO DE COMPOSTELA

[341] Markus Mezger, Sebastian Schramm, Heiko Schröder, Harald Reichert, Moshe Deutsch, Emerson J. De Souza, John S. Okasinski, Benjamin M. Ocko, Veijo Honkimäki, and Helmut Dosch. Layering of $[BMIM]^+$-based ionic liquids at a charged sapphire interface. *J. Chem. Phys.*, 131(9):094701, 2009.

[342] Sergey A. Kislenko, Igor S. Samoylov, and Ravil H. Amirov. Molecular dynamics simulation of the electrochemical interface between a graphite surface and the ionic liquid [BMIM][PF_6]. *Phys. Chem. Chem. Phys.*, 11(27):5584–5590, 2009.

[343] Céline Merlet, David T. Limmer, Mathieu Salanne, René Van Roij, Paul A. Madden, David Chandler, and Benjamin Rotenberg. The electric double layer has a life of its own. *J. Phys. Chem. C*, 118(32):18291–18298, 2014.

[344] Benjamin Rotenberg and Mathieu Salanne. Structural transitions at ionic liquid interfaces. *J. Phys. Chem. Lett.*, 6(24):4978–4985, 2015.

[345] Yu-Zhuan Su, Yong-Chun Fu, Jia-Wei Yan, Zhao-Bin Chen, and Bing-Wei Mao. Double layer of au (100)/ionic liquid interface and its stability in imidazolium-based ionic liquids. *Angew. Chem.*, 121(28):5250–5253, 2009.

[346] Yu-Zhuan Su, Yong-Chun Fu, Yi-Min Wei, Jia-Wei Yan, and Bing-Wei Mao. The electrode/ionic liquid interface: electric double layer and metal electrodeposition. *Chem. Phys. Chem.*, 11(13):2764–2778, 2010.

[347] Ge-Bo Pan and Werner Freyland. 2d phase transition of pf6 adlayers at the electrified ionic liquid/au (1 1 1) interface. *Chem. Phys. Lett.*, 427(1-3):96–100, 2006.

[348] Ge-Bo Pan and Werner Freyland. In situ STM investigation of spinodal decomposition and surface alloying during underpotential deposition of Cd on Au (111) from an ionic liquid. *Phys. Chem. Chem. Phys.*, 9(25):3286–3290, 2007.

USC
UNIVERSIDADE DE SANTIAGO DE COMPOSTELA

[349] Trinidad Méndez-Morales, Jesús Carrete, Martín Pérez-Rodríguez, Óscar Cabeza, Luis J. Gallego, Ruth M. Lynden-Bell, and Luis M. Varela. Molecular dynamics simulations of the structure of the graphene–ionic liquid/alkali salt mixtures interface. *Phys. Chem. Chem. Phys.*, 16(26):13271–13278, 2014.

[350] Hadrián Montes-Campos, José M. Otero-Mato, Trinidad Méndez-Morales, Oscar Cabeza, Luis J. Gallego, Alina Ciach, and Luis M. Varela. Two-dimensional pattern formation in ionic liquids confined between graphene walls. *Phys. Chem. Chem. Phys.*, 2017.

[351] Inês C. M. Vaz, Margarida Bastos, Carlos E. S. Bernardes, José N. Canongia Lopes, and Luís M. N. B. F. Santos. Solvation of alcohols in ionic liquids–understanding the effect of the anion and cation. *Phys. Chem. Chem. Phys.*, 2018.

[352] Borja Docampo-Álvarez, Víctor Gómez-González, Trinidad Méndez-Morales, Jesús Carrete, Julio R. Rodríguez, Óscar Cabeza, Luis J. Gallego, and Luis M. Varela. Mixtures of protic ionic liquids and molecular cosolvents: A molecular dynamics simulation. *J. Chem. Phys.*, 140(21):214502, 2014.

[353] Oleg Borodin, David L. Price, Bachir Aoun, Miguel A. González, Justin B. Hooper, Maiko Kofu, Shinji Kohara, Osamu Yamamuro, and Marie-Louise Saboungi. Effect of water on the structure of a prototype ionic liquid. *Phys. Chem. Chem. Phys.*, 18(34):23474–23481, 2016.

[354] Olga Russina, Alessio Sferrazza, Ruggero Caminiti, and Alessandro Triolo. Amphiphile meets amphiphile: Beyond the polar–apolar dualism in ionic liquid/alcohol mixtures. *J. Phys. Chem. Lett.*, 5(10):1738–1742, 2014.

[355] Iuliia V. Voroshylova, Sergei R. Smaga, Elena V. Lukinova, Vitaly V. Chaban, and Oleg N. Kalugin. Conductivity and associ-

USC UNIVERSIDADE DE SANTIAGO DE COMPOSTELA

ation of imidazolium and pyridinium based ionic liquids in methanol. *J. Mol. Liquids*, 203:7–15, 2015.

[356] Herman J. C. Berendsen, David van der Spoel, and Rudi van Drunen. Gromacs: a message-passing parallel molecular dynamics implementation. *Comput. Phys. Commun.*, 91(1-3):43–56, 1995.

[357] Peter Debye. Näherungsformeln für die zylinderfunktionen für große werte des arguments und unbeschränkt veränderliche werte des index. *Math. Ann.*, 67(4):535–558, 1909.

[358] Nuno M. Micaelo, António M. Baptista, and Cláudio M. Soares. Parametrization of 1-butyl-3-methylimidazolium hexafluorophosphate/nitrate ionic liquid for the gromos force field. *J. Phys. Chem. B*, 110(29):14444–14451, 2006.

[359] Daan Frenkel and Berend Smit. *Understanding molecular simulation: from algorithms to applications*, volume 1. Elsevier (formerly published by Academic Press), 2002.

[360] In-Chul Yeh and Max L. Berkowitz. Ewald summation for systems with slab geometry. *J. Chem. Phys.*, 111(7):3155–3162, 1999.

[361] Yaodong Liu, Yi Zhang, Guozhong Wu, and Jun Hu. Coexistence of liquid and solid phases of Bmim-PF_6 ionic liquid on mica surfaces at room temperature. *J. Am. Chem. Soc.*, 128(23):7456–7457, 2006.

[362] Daniel Ebeling, Stephan Bradler, Bernhard Roling, and André Schirmeisen. 3-dimensional structure of a prototypical ionic liquid–solid interface: Ionic crystal-like behavior induced by molecule–substrate interactions. *J. Phys. Chem. C*, 120(22): 11947–11955, 2016.

[363] Maxym Dudka, Svyatoslav Kondrat, Alexei Kornyshev, and Gleb Oshanin. Phase behaviour and structure of a superionic liquid

USC UNIVERSIDADE DE SANTIAGO DE COMPOSTELA

in nonpolarized nanoconfinement. *J. Phys. Condens. Matter*, 28 (46):464007, 2016.

[364] David T. Limmer. Interfacial ordering and accompanying divergent capacitance at ionic liquid-metal interfaces. *Phys. Rev. Lett.*, 115(25):256102, 2015.

[365] Paulo Schmitz, Martin Kolek, Diddo Diddens, Marian Cristian Stan, Kirsi Jalkanen, Martin Winter, and Peter Bieker. Counterintuitive trends of the wetting behavior of ionic liquid-based electrolytes on modified lithium electrodes. *Phys. Chem. Chem. Phys.*, 19(29):19178–19187, 2017.

[366] N. G. Almarza, J. Pękalski, and A. Ciach. Periodic ordering of clusters and stripes in a two-dimensional lattice model. II. results of monte carlo simulation. *J. Chem. Phys.*, 140(16):164708, 2014.

[367] J. Pękalski, A. Ciach, and N. G. Almarza. Periodic ordering of clusters and stripes in a two-dimensional lattice model. I. ground state, mean-field phase diagram and structure of the disordered phases. *J. Chem. Phys.*, 140(11):114701, 2014.

[368] Nobuyuki Otsu. A threshold selection method from gray-level histograms. *Automatica.*, 11(285-296):23–27, 1975.

[369] Kathleen Kirchner, Tom Kirchner, V. Ivaništšev, and Maxim V. Fedorov. Electrical double layer in ionic liquids: Structural transitions from multilayer to monolayer structure at the interface. *Electrochim. Acta.*, 110:762–771, 2013.

[370] K. R. Mecke. Morphological characterization of patterns in reaction-diffusion systems. *Phys. Rev. E*, 53(5):4794, 1996.

[371] Charles Kittel, Paul McEuen, and Paul McEuen. *Introduction to solid state physics*, volume 8. Wiley New York, 1996.

USC
UNIVERSIDADE DE SANTIAGO DE COMPOSTELA

[372] Qing Zhou, Li-Sheng Wang, and Hui-Ping Chen. Densities and viscosities of 1-butyl-3-methylimidazolium tetrafluoroborate+H_2O binary mixtures from (303.15 to 353.15) K. *J. Chem. Eng. Data*, 51(3):905–908, 2006.

[373] Esther Rilo, Juan Vila, Manuel García, Luis M. Varela, and Oscar Cabeza. Viscosity and electrical conductivity of binary mixtures of C_nMIM-BF_4 with ethanol at 288 K, 298 K, 308 K, and 318 K. *J. Chem. Eng. Data*, 55(11):5156–5163, 2010.

[374] Alina Ciach. Simple theory for oscillatory charge profile in ionic liquids near a charged wall. *arXiv preprint arXiv:1705.10551*, 2017.

[375] Phil Attard. Asymptotic analysis of primitive model electrolytes and the electrical double layer. *Phys. Rev. E*, 48(5):3604, 1993.

[376] Ludwik Leibler. Theory of microphase separation in block copolymers. *Macromolecules.*, 13(6):1602–1617, 1980.

[377] G. Gommper and M. Schick. Self-assembling amphiphilic systems, vol. 16 of phase transitions and critical phenomena, 1994.

[378] A. Ciach, J. Pękalski, and W. T. Góźdź. Origin of similarity of phase diagrams in amphiphilic and colloidal systems with competing interactions. *Soft. Matter.*, 9(27):6301–6308, 2013.

[379] Jia Le Ma, Qiangqiang Meng, and Jun Fan. Charge driven lateral structural evolution of ions in electric double layer capacitors strongly correlates with differential capacitance. *Phys. Chem. Chem. Phys.*, 20(12):8054–8063, 2018.

[380] A. Ciach and W. T. Góźdź. Mesoscopic description of network-forming clusters of weakly charged colloids. *Condens. Matter. Phys.*, 2010.

[381] R. M. Lynden-Bell. Gas—liquid interfaces of room temperature ionic liquids. *Mol. Phys.*, 101(16):2625–2633, 2003.

USC UNIVERSIDADE DE SANTIAGO DE COMPOSTELA

[382] Tianying Yan, Shu Li, Wei Jiang, Xueping Gao, Bing Xiang, and Gregory A. Voth. Structure of the liquid- vacuum interface of room-temperature ionic liquids: A molecular dynamics study. *J. Phys. Chem. B*, 110(4):1800–1806, 2006.

[383] Maxim V. Fedorov and R. M. Lynden-Bell. Probing the neutral graphene–ionic liquid interface: insights from molecular dynamics simulations. *Phys. Chem. Chem. Phys.*, 14(8):2552–2556, 2012.

[384] Céline Merlet, Benjamin Rotenberg, Paul A. Madden, and Mathieu Salanne. Computer simulations of ionic liquids at electrochemical interfaces. *Phys. Chem. Chem. Phys.*, 15(38):15781–15792, 2013.

[385] Shiguo Zhang, Jiaheng Zhang, Yan Zhang, and Youquan Deng. Nanoconfined ionic liquids. *Chem. Rev.*, 117(10):6755–6833, 2017.

[386] Anna Martinelli and Lars Nordstierna. An investigation of the sol–gel process in ionic liquid–silica gels by time resolved raman and 1 H NMR spectroscopy. *Phys. Chem. Chem. Phys.*, 14(38): 13216–13223, 2012.

[387] Moheb Nayeri, Matthew T. Aronson, Diana Bernin, Bradley F. Chmelka, and Anna Martinelli. Surface effects on the structure and mobility of the ionic liquid C_6C_1ImTFSI in silica gels. *Soft Matter*, 10(30):5618–5627, 2014.

[388] Shimou Chen, Keita Kobayashi, Yasumitsu Miyata, Naoki Imazu, Takeshi Saito, Ryo Kitaura, and Hisanori Shinohara. Morphology and melting behavior of ionic liquids inside single-walled carbon nanotubes. *J. Am. Chem. Soc.*, 131(41):14850–14856, 2009.

[389] Wei Shi and Dan C. Sorescu. Molecular simulations of CO_2 and H_2 sorption into ionic liquid 1-n-hexyl-3-methylimidazolium bis

USC UNIVERSIDADE DE SANTIAGO DE COMPOSTELA

(trifluoromethylsulfonyl) amide ([hmim][Tf2N]) confined in carbon nanotubes. *J. Phys. Chem. B*, 114(46):15029–15041, 2010.

[390] José Leobardo Bañuelos, Guang Feng, Pasquale F. Fulvio, Song Li, Gernot Rother, Nikolas Arend, Antonio Faraone, Sheng Dai, Peter T. Cummings, and David J. Wesolowski. The influence of a hierarchical porous carbon network on the coherent dynamics of a nanoconfined room temperature ionic liquid: A neutron spin echo and atomistic simulation investigation. *Carbon*, 78:415–427, 2014.

[391] Kozo Matsumoto and Takeshi Endo. Confinement of ionic liquid by networked polymers based on multifunctional epoxy resins. *Macromolecules*, 41(19):6981–6986, 2008.

[392] Jing Yang, Sébastien Pruvost, Sébastien Livi, and Jannick Duchet-Rumeau. Understanding of versatile and tunable nanostructuration of ionic liquids on fluorinated copolymer. *Macromolecules*, 48(13):4581–4590, 2015.

[393] André Vioux, Lydie Viau, Sabrina Volland, and Jean Le Bideau. Use of ionic liquids in sol-gel; ionogels and applications. *Cr. Chim.*, 13(1-2):242–255, 2010.

[394] Jean Le Bideau, Lydie Viau, and André Vioux. Ionogels, ionic liquid based hybrid materials. *Chem. Soc. Rev.*, 40(2):907–925, 2011.

[395] Víctor Gómez-González, Borja Docampo-Álvarez, J. Manuel Otero-Mato, Oscar Cabeza, Luis J. Gallego, and Luis M. Varela. Molecular dynamics simulations of the structure of mixtures of protic ionic liquids and monovalent and divalent salts at the electrochemical interface. *Phys. Chem. Chem. Phys.*, 20(18):12767–12776, 2018.

[396] Víctor Gómez-González, Borja Docampo-Álvarez, Hadrián Montes-Campos, Juan Carlos Otero, Elena López Lago, Oscar

USC UNIVERSIDADE DE SANTIAGO DE COMPOSTELA

Cabeza, Luis J. Gallego, and Luis M. Varela. Solvation of Al^{3+} cations in bulk and confined protic ionic liquids: a computational study. *Phys. Chem. Chem. Phys.*, 20(28):19071–19081, 2018.

[397] Kun Dong, Guohui Zhou, Xiaomin Liu, Xiaoqian Yao, Suojiang Zhang, and Alexander Lyubartsev. Structural evidence for the ordered crystallites of ionic liquid in confined carbon nanotubes. *J. Phys. Chem. C*, 113(23):10013–10020, 2009.

[398] Youngseon Shim and Hyung J. Kim. Solvation of carbon nanotubes in a room-temperature ionic liquid. *ACS Nano*, 3(7):1693–1702, 2009.

[399] Shu Wang, Shu Li, Zhen Cao, and Tianying Yan. Molecular dynamic simulations of ionic liquids at graphite surface. *J. Phys. Chem. C*, 114(2):990–995, 2010.

[400] Yong-Lei Wang, Aatto Laaksonen, and Zhong-Yuan Lu. Influence of ionic liquid film thickness on ion pair distributions and orientations at graphene and vacuum interfaces. *Phys. Chem. Chem. Phys.*, 15(32):13559–13569, 2013.

[401] Mahtab Alibalazadeh and Masumeh Foroutan. Specific distributions of anions and cations of an ionic liquid through confinement between graphene sheets. *J. Mol. Model.*, 21(7):168, 2015.

[402] Siti Aminah Mohd Noor, P. M. Bayley, Maria Forsyth, and Douglas Robert Macfarlane. Ionogels based on ionic liquids as potential highly conductive solid state electrolytes. *Electrochim Acta*, 91:219–226, 2013.

[403] Djamel Aidoud, Delphine Guy-Bouyssou, Dominique Guyomard, Jean Le Bideau, and Bernard Lestriez. Photopolymerized organic host network of ionogels for lithium batteries: effects of mesh size and of ethylene oxide content. *J. Electrochem Soc.*, 165(13):A3179–A3185, 2018.

USC
UNIVERSIDADE DE SANTIAGO DE COMPOSTELA

[404] Vitaly V. Chaban and Oleg V. Prezhdo. Nanoscale carbon greatly enhances mobility of a highly viscous ionic liquid. *ACS Nano*, 8 (8):8190–8197, 2014.

[405] Yadong He, Rui Qiao, Jenel Vatamanu, Oleg Borodin, Dmitry Bedrov, Jingsong Huang, and Bobby G. Sumpter. Importance of ion packing on the dynamics of ionic liquids during micropore charging. *J. Phys. Chem. Lett.*, 7(1):36–42, 2016.

[406] Ramesh Singh, Joshua Monk, and Francisco R. Hung. Heterogeneity in the dynamics of the ionic liquid $[BMIM^+][PF_6^-]$ confined in a slit nanopore. *J. Phys. Chem. C*, 115(33):16544–16554, 2011.

[407] Nav Nidhi Rajput, Joshua Monk, Ramesh Singh, and Francisco R. Hung. On the influence of pore size and pore loading on structural and dynamical heterogeneities of an ionic liquid confined in a slit nanopore. *J. Phys. Chem. C*, 116(8):5169–5181, 2012.

[408] Zhongyang Dai, Lili Shi, Linghong Lu, Yunhao Sun, and Xiaohua Lu. Unique structures and vibrational spectra of protic ionic liquids confined in TiO2 slits: the role of interfacial hydrogen bonds. *Langmuir*, 34(44):13449–13458, 2018.

[409] Víctor Gómez-González, J. Manuel Otero-Mato, Hadrián Montes-Campos, Xabier García-Andrade, Amador García-Fuente, Andrés Vega, Jesús Carrete, Oscar Cabeza, Luis J. Gallego, and Luis M. Varela. Borophene vs. graphene interfaces: Tuning the electric double layer in ionic liquids. *J. Mol. Liq.*, page 112647, 2020.

[410] Kenneth W. Desmond and Eric R. Weeks. Random close packing of disks and spheres in confined geometries. *Phys. Rev. E*, 80(5): 051305, 2009.

[411] Hamed Akbarzadeh, Mohsen Abbaspour, Sirous Salemi, and Somayeh Abdollahzadeh. Investigation of the melting of ionic

USC UNIVERSIDADE DE SANTIAGO DE COMPOSTELA

liquid [EMIM][PF_6] confined inside carbon nanotubes using molecular dynamics simulations. *RSC Adv.*, 5(5):3868–3874, 2015.

[412] Yusheng Liu, Yuxiao Wang, and Jing Li. Molecular dynamics study of confined ionic liquids in au nanopore. *Ionics*, 22(9): 1681–1686, 2016.

[413] Douglas S. Martin, Martin B. Forstner, and Josef A. Käs. Apparent subdiffusion inherent to single particle tracking. *Biophys J.*, 83(4):2109–2117, 2002.

[414] Sirous Salemi, Hamed Akbarzadeh, and Somayeh Abdollahzadeh. Nano-confined ionic liquid [EMIM][PF_6] between graphite sheets: a molecular dynamics study. *J. Mol. Liq.*, 215:512–519, 2016.

[415] In-Chul Yeh and Gerhard Hummer. System-size dependence of diffusion coefficients and viscosities from molecular dynamics simulations with periodic boundary conditions. *J. Phys. Chem. B*, 108(40):15873–15879, 2004.

[416] Sonja Gabl, Christian Schröder, and Othmar Steinhauser. Computational studies of ionic liquids: Size does matter and time too. *J. Chem. Phys.*, 137(9):094501, 2012.

[417] Gota Kikugawa, Shotaro Ando, Jo Suzuki, Yoichi Naruke, Takeo Nakano, and Taku Ohara. Effect of the computational domain size and shape on the self-diffusion coefficient in a lennard-jones liquid. *J. Chem. Phys.*, 142(2):024503, 2015.

[418] Alexandru Botan, Virginie Marry, and Benjamin Rotenberg. Diffusion in bulk liquids: finite-size effects in anisotropic systems. *Mol. Phys.*, 113(17-18):2674–2679, 2015.

[419] Pauline Simonnin, Benoît Noetinger, Carlos Nieto-Draghi, Virginie Marry, and Benjamin Rotenberg. Diffusion under confinement: Hydrodynamic finite-size effects in simulation. *J. Chem. Theory Comput.*, 13(6):2881–2889, 2017.

USC UNIVERSIDADE DE SANTIAGO DE COMPOSTELA

[420] Song Li, Kee Sung Han, Guang Feng, Edward W. Hagaman, Lukas Vlcek, and Peter T. Cummings. Dynamic and structural properties of room-temperature ionic liquids near silica and carbon surfaces. *Langmuir*, 29(31):9744–9749, 2013.

[421] Suojiang Zhang, Xingmei Lu, Qing Zhou, Xiaohua Li, Xiangping Zhang, and Shucai Li. *Ionic Liquids: Physicochemical Properties*. Elsevier, 2009.

[422] R. D. Rogers and K. R. Seddon. Ionic liquids–solvents of the future? *Science*, 302(5646):792–793, 2003.

[423] P. Debye, E. Hückel, and I. I. Zur Theorie der Elektrolyte. Das grenzgesetz für die elektrische leitfähigkeit. *Phys. Z.*, 24:305–325, 1923.

[424] L. W. Bahe. Structure in concentrated solutions of electrolytes. Field-dielectric-gradient forces and energies. *J. Phys. Chem.*, 76 (7):1062–1071, 1972.

[425] L. M. Varela, M. Garcia, F. Sarmiento, D. Attwood, and V. Mosquera. Pseudolattice theory of strong electrolyte solutions. *J. Chem. Phys.*, 107(16):6415–6419, 1997.

[426] Hadrián Montes-Campos, Svyatoslav Kondrat, Esther Rilo, Oscar Cabeza, and Luis M. Varela. Random-alloy model for the conductivity of ionic Liquid–Solvent mixtures. *J. Phys. Chem. C*, 124(22):11754–11759, 2020.

[427] Borja Docampo-Álvarez, Víctor Gómez-González, Trinidad Méndez-Morales, Julio R. Rodríguez, Elena López-Lago, Oscar Cabeza, Luis J. Gallego, and Luis M. Varela. Molecular dynamics simulations of mixtures of protic and aprotic ionic liquids. *Phys. Chem. Chem. Phys.*, 18(34):23932–23943, 2016.

[428] Borja Docampo-Álvarez, Víctor Gómez-González, Trinidad Méndez-Morales, Julio R. Rodríguez, Oscar Cabeza, Mireille

USC UNIVERSIDADE DE SANTIAGO DE COMPOSTELA

Turmine, Luis J. Gallego, and Luis M. Varela. The effect of alkyl chain length on the structure and thermodynamics of Protic–Aprotic ionic liquid mixtures: A molecular dynamics study. *Phys. Chem. Chem. Phys.*, 20(15):9938–9949, 2018.

[429] T. Méndez-Morales, J. Carrete, O. Cabeza, L. J. Gallego, and L. M. Varela. Molecular dynamics simulations of the structural and thermodynamic properties of imidazolium-based ionic liquid mixtures. *J. Phys. Chem. B*, 115(38):11170–11182, 2011.

[430] C. Schröder, M. Haberler, and O. Steinhauser. On the computation and contribution of conductivity in molecular ionic liquids. *J. Chem. Phys.*, 128(13):134501, 2008.

[431] Christian Schröder and Othmar Steinhauser. On the dielectric conductivity of molecular ionic liquids. *J. Chem. Phys.*, 131(11): 114504, 2009.

[432] Jesse G. McDaniel and Chang Yun Son. Ion correlation and collective dynamics in BMIM/BF4-based organic electrolytes: From dilute solutions to the ionic liquid limit. *J. Phys. Chem. B*, 122(28):7154–7169, 2018.

[433] Box Gep and G. C. Tiao. Bayesian inference in statistical analysis. *Reading: Addison-Wesley*, 1973.

[434] John Salvatier, Thomas V. Wiecki, and Christopher Fonnesbeck. Probabilistic programming in Python using PyMC3. *PeerJ Comput. Sci.*, 2:e55, apr 2016. ISSN 2376-5992.

[435] Oscar Nordness and Joan F. Brennecke. Ion dissociation in ionic liquids and ionic liquid solutions. *Chem. Rev.*, 120(23):12873–12902, 2020.

[436] Naveen Michaud-Agrawal, Elizabeth J. Denning, Thomas B. Woolf, and Oliver Beckstein. MDAnalysis: A toolkit for the analysis of molecular dynamics simulations. *J. Comput. Chem.*, 32 (10):2319–2327, 2011.

USC
UNIVERSIDADE DE SANTIAGO DE COMPOSTELA

[437] Richard J. Gowers, Max Linke, Jonathan Barnoud, Tyler J. E. Reddy, Manuel N. Melo, Sean L. Seyler, Jan DomaÅski, David L. Dotson, SÃ©bastien Buchoux, Ian M. Kenney, and Oliver Beckstein. MDAnalysis: A python package for the rapid analysis of molecular dynamics simulations. In Sebastian Benthall and Scott Rostrup, editors, *Proceedings of the 15th Python in Science Conference*, pages 98–105, 2016.

USC
UNIVERSIDADE DE SANTIAGO DE COMPOSTELA

USC
UNIVERSIDADE
DE SANTIAGO
DE COMPOSTELA

This thesis presents an exhaustive study of the properties of ionic liquids and their mixtures in the presence of interfaces or solutes with different sizes, topologies and materials. The main objective of this work is to lay a solid foundation on which to understand and characterize more complex systems of special interest in electrochemistry or photonics. To carry out this task, results from simulations, experiments and theoretical analysis are reported, where the focus is on the structure, effect of nanoconfinement, dynamics and even proton transport in these densely ionic fluids. In addition, a tool that considerably shortens the simulation times of larger systems is presented, which opens the door to study dispersions of larger nanostructures in these media.